Synthesis and characterisation of novel polypeptide materials by the polymerisation of N-carboxyanhydrides

Gibson, Matthew Ian

SYNTHESIS AND CHARACTERISATION OF NOVEL POLYPEPTIDE MATERIALS BY THE POLYMERISATION OF *N*-CARBOXYANHYDRIDES

BY

MATTHEW IAN GIBSON

Synthesis and Characterisation of Novel Polypeptide Materials by the Polymerisation of *N*-Carboxyanhydrides

Thesis submitted for the degree of:

"Doctor of Philosophy", PhD

From work conducted in the Interdisciplinary Research Centre in Polymer Science and Technology, within the Department of Chemistry at the University of Durham

The work was funded by the Engineering and Physical Sciences Research Council, UK, by a doctoral training account (DTA) award.

Further financial support was generously provided by:

Collingwood College at the University of Durham

IRC in Polymer Science and Technology

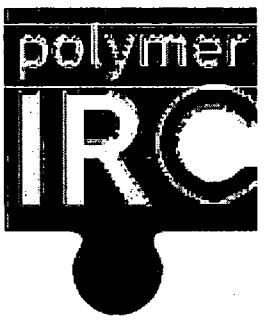

Royal Society of Chemistry

RSC | Advancing the Chemical Sciences

STATEMENT OF COPYRIGHT

DECLARATION

The work reported in this thesis was carried out in the Department of Chemistry at the University of Durham between October 2003 and December 2006. All the work was carried out by the author unless otherwise stated, and has not previously been submitted for a degree at this or any other university.

ACKNOWLEDGEMENTS

After three and a bit years of toil, tears and laughter it seems that the hardest part of this work is to ensure that everyone who has been on this journey with me receives the credit they are due. Firstly I must express my deepest gratitude to Dr Neil Cameron. From a scientific point of view he has always been on hand to guide and discuss, and allowing me to attend a huge array of meetings and conferences, feeding my interest in the field. On a personal level I can not thank him enough for showing compassion and understanding during the most difficult of times.

Dr's Oliver Largrille and Fransico-Fernadez Trillo (Paco) are both thanked for sharing their apparently bottomless wells of knowledge and technical skills with me, freely and without condition. Without their input, this project would have strayed and floundered at any number of occasions.

Dr Lian Hutchings is thanked for all his discussions regarding GPC, and for setting me on this path during my Masters project. I am also grateful to Dr Sharon Cooper for allowing me the use of her equipment, and offering advice with regard to the black art of crystal growth and modification.

I would like to thank Dr Richard Thompson for trusting me with the AFM, Douglass Carswell for attempting so many DSCs and Dr A Kenright and Ms C Heffernan for assisting me with the interpretation of the NMR data.

Working in Lab 169 is an experience, which should be open to anyone who has the will! The white board moments shared with Wee Mike, the river of PVA glue held in check by Big Mike, the assorted dyes and piles of washing up from the Johnson and if only there were words to describe 'Egon' Albertin's short stay.

Special mention should be made to Seb, Jon and Paco for providing me with friendship and encouragement which makes even weekend chemistry fun! Dr Ross Carnachan is thanked for providing the only constant presence during my stay, and for all the afternoons and evenings in the New Inn willingly watching the mighty Man Utd. Sorry to those who there is simply not room to write about, but who I can at least thank by name: Tom, Francoise, Alex, Greg, Geraldine, Helen, Sue, Emily and any who I forgotten. You were all part my experience.

For the time spent outside of the lab, the CNM gang all know who you are, but not how much I will miss you all. Tom, Dan, Ruth, Victoria, Jamie and Greg have my gratitude for coming along on the ski trips which have provided me with so many memories. Finally Sandy and Sarah: just for being there.

In science one tries to tell people, in such as way as to be understood by everyone, something that no on ever knew before. But in poetry, it's the exact opposite.

Paul Dirac

All shall be well, and all shall be well, and all manner of things shall be well.

Julian of Norwich

ABSTRACT

Advances in controlled polymerisation strategies over the last decade have allowed chemists to create materials of defined structure and architecture to probe and mimic the greatest chemist of them all – mother nature. In this work poly-peptides have been synthesised by the polymerisation of amino acid *N*-carboxy anhydrides without the need for transition metal catalysts. Application of stringent reaction conditions and high-purity monomers allowed control to be imposed on the system and a series of novel homo- and block co-polypeptides to be synthesised and characterised fully. Their ability to assemble into nano- and micro-structures, apparently directed by β-sheet stacking has been investigated in the solid state by WAXS, electron microscopy and AFM. Organo-gelation was also observed and studied in dilute concentrations of the block-co-poly-peptides.

A new and improved synthesis for *N*-carboxy anhydrides bearing carbohydrate motifs was developed without the need for extensive protecting group manipulation or toxic mercury compounds, which were used previously.

Finally the possibility of using water soluble polypeptides and vinyl derived polymers as mimics of antifreeze glyco-proteins in the inhibition of the recrystallisation of ice has been evaluated. This showed that not all of the complex structural features present in the native protein are required to retain at least some activity.

Matthew I. Gibson, Durham, December 2006

AIMS AND OBJECTIVES

The initial aim of this project is to investigate if comparatively simple polymers could be used as mimics to study the activity of antifreeze glyocoproteins, which have an extremely regular structure relative to the antifreeze proteins. In order to probe this activity it was decided to use the polymerisation of *N*-carboxy anhydrides (NCAs) to produce synthetic polypeptides, which do not bear the precise primary or tertiary structures of native proteins, but can exhibit secondary structures and side group functionality. The first objective is thus to synthesis and polymerise a range of NCAs which will result in a variety of side chain functionality allowing the effect of the water solublising group on antifreeze activity to be probed. This can then be compared to the activity of vinyl derived polymers, which do not posses rigid amide bonds. Importantly this allows, for the first time, the effect of backbone structure on antifreeze activity to be studied. Additionally a series of glycosylated NCAs will be synthesised to allow access to glycopeptide structures.

TABLE OF CONTENTS

ABBREVIATIONS

^{13}C-NMR	Carbon-13 nuclear magnetic resonance
^{1}H-NMR	Proton nuclear magnetic resonance
AFGP	Antifreeze glycoprotein
AFM	Atomic force microscopy
AFP	Antifreeze protein
ATRP	Atom transfer radical polymerisation
AUC	Analytical ultracentrifugation
BOC	Tert-butoxycarbonyl
CD	Circular Dichroism
CRP	Controlled radical polymerisation
DCC	*N,N'*-Dicyclohexylcarbodiimide
DCHA	Dicyclohexylamine
DCM	Dichloromethane
DLS	Dynamic light scattering
DMAc	*N,N'*-Dimethyl acetamide
DMF	*N,N'*-Dimethyl formamide
DSC	Differential scanning calorimetry
EPO	Erythroprotein
ESEM	Environmental scanning electron microscope
ESI-MS	Electrospray ionization mass spectrometry
EtOAc	Ethyl Acetate
EtOH	Ethanol

FDA	Food and drug admistration
FMOC	Fluorenylmethyloxycarbonyl
FTIR	Fourier-transform infrared
GPC	Gel-permeation chromatography
IFN	Interferon
IR	Infrared
LCST	Lower critical solution temperature
MADIX	Macromolecular design via interchange of Xanthates
MALDI-TOF MS	Matrix assisted laser desorption ionisation time of flight mass spectrometry
MeOH	Methanol
NCA	*N*-carboxyanhydride
NMP	Nitroxide mediated polymerisation
PEG	Poly(ethylene glycol)
PEO	Poly(ethylene oxide)
PVA	Poly(vinyl alcohol)
PVAc	Poly(vinyl acetate)
PyBOP	(Benzotriazol-1-yloxy)tripyrrolidinophosphonium hexafluophosphate
RAFT	Reversible addition-fragmentation chain transfer
RALS	Right angle light scattering
RI	Refractive Index
SAXS	Small-angle X-ray scattering
SEM	Scanning electron microscope

SPPS	Solid phase peptide synthesis
SPR	Surface plasmon resonance
TCE	1,1,1,2 Tetrachloroethane
TEA	Triethylamine
TEM	Transmission electron microscope
TFA	Trifluoroacetic acid
TH	Thermal hysteresis
THF	Tetrahydrofuran
TMS	Trimethyl silyl (protecting group)
TMS	Tetramethyl silane (NMR reference)
UCST	Upper critical solution temperature
UV	Ultraviolet
UV/VIS	Ultraviolet/visible spectroscopy
WAXS	Wide-angle X-ray scattering

CHAPTER 1

INTRODUCTION

1.1 BIO-INSPIRED MATERIALS

The terms biopolymers and biomaterials can be broadly defined as being those which can be interfaced with biological systems to evaluate, enhance, treat or replace tissue and functions within the body[1]. Examples include the synthesis of scaffolds for cell growth ex-vivo in the name of tissue engineering, sutures for improved wound healing and lightweight joint replacement therapy[2,3]. There is also a desire to understand the underlying mechanisms which govern biological processes through the synthesis of new materials with systematic absences or inclusions. From this, new materials can be developed which incorporate the most desirable features with (ideally) improved activity, reduced immuogenicity (using recombinant human insulin in place of porcine insulin for example) and toxicity (shielding low molecular weight drugs). The synthesis of these new materials is also essential for establishing a route for the large scale production of new bioactive species, which may not be available in sufficient scale from biological sources (an excellent example are the fish antifreeze proteins covered in section 1.4). In terms of peptidic biomaterials the closest relatives available to the synthetic chemist are polymers. The search for systems where synthetic macromolecules can replace or augment their natural cousins is of great importance. Perhaps obviously, but it should be mentioned, is that the source of inspiration for these materials is always nature itself, which produces a wide array of diversity of both structure and function using very simple starting materials and under aqueous conditions and in response to environmental changes in: temperature, altitude, gas concentration, pressure, light and feedstuffs to name a few.

1.2 HYBRID PEPTIDE-BASED MATERIALS

Peptides and proteins being natures own materials are a logical choice for design and synthesis of new biomaterials[4]. Through macromolecular self-assembly they produce nanometre and larger, structures whose properties are strongly dependant on not only their chemical reactivity, but their 3-dimensional spatial alignment. These elegant assemblies act as catalysts, recognition domains, provide structure and much more[5]. When producing new proteinic materials it is difficult to predict their biocompatibility, toxicity, immunogenicity and degradation characteristics due to their innate complexity.

The synthesis of these materials remains difficult despite the many advances in solid phase peptide synthesis, mainly due to the inevitable truncations which occur over a large number of coupling steps and the subsequent purification and characterisation. It is thus unsurprising that synthetic polymers which share the characteristics of high molecular weight and side group functionality are attractive substitutes. Contrary to peptides the properties of polymers are characterised in terms of their inhomogeneity: even the most precise polymerisation methods gives rise to polydispersity, where as others have variability in backbone and end-group compositions. Synthetic polymers are capable of undergoing self-assembly, but is typically driven by the chemical incompatibility of two or more blocks or the formation of liquid crystalline phases, in both solution and solid states[6-9]. Recent advances in controlled radical polymerisation allow access to protein-polymer conjugates[10] through either addition of a suitable initiator[11,12] (grafting from) or reaction between peptide and end group functionality on the polymer[13] (grafting to). These materials have been coined as peptide-synthetic "hybrid" materials[14] or "molecular chimeras"[15]. The synthesis and

characterisation of new materials based upon, and containing, peptide sequences and their incorporation with synthetic macromolecules is of great interest for both academic and practical applications and has been the subject of numerous review articles[14-18].

1.2.1 DRUG DELIVERY

Perhaps the most extensively studied synthetic polymer for biological applications is poly(ethyleneglycol), PEG (often referred to as poly(ethylene oxide), PEO). PEG is both non-toxic and non-immunogenic, along with being water soluble at physiological temperature and pH. Conjugation of PEG to therapeutically relevant peptides results in an increase in molecular weight and corresponding increase in hydrodynamic volume which is a pharmacologically useful property. Removal of low molecular weight compounds from the blood stream occurs rapidly due to glomerular filtration in the kidneys. Above a certain molecular weight (or more specifically hydrodynamic radius) filtration is reduced or prevented, thus these peptide(drug)-polymer conjugates have increased blood circulation times relative to the free peptide. This field (which is dominated by but not limited to PEG[19]) is termed polymer therpaeutics[20,21] and is particularly appealing for cancer therapy where through a process known as the EPR (enhanced permeation and retention) effect, macromolecules preferentially accumulate in cancerous tissue. As an example, dendrimers bearing two 10kDa PEG chains were cleared from the blood within 5 hours of administration, whereas 20 % of a dendrimer with eight 20 kDa PEG chains remained in circulation after 50 hours[22]. When implanted into mice a single dose of these dendrimers was capable of curing mice with colon cancer, whilst shielding the

body from the harmful side-effects of the drug[23]. The second benefit is the steric protection afforded by the presence a bulky polymeric chain. Enzymes, such as peptidases, are present in the blood serum which readily degrade polypeptide based pharmaceuticals. The steric hindrance of the conjugated polymer chain prevents enzymes from approaching the drug. The third property is the process of opsonisation, whereby proteins absorb onto foreign particles, which eventually leads to removal by the immune system, is also reduced by applying a surface coating of PEG[24].

Kochendorfer *et al.* have conjugated branched PEG to an EPO (erythropoiesis protein) mimetic (coined as SEP). This does not significantly reduce the activity of EPO, but results in vastly increased blood residency times and as such less of the active peptide has to be injected to achieve an equivalent therapeutic effect over an extended period of time[25]. In order to create a single chemical entity, which is required for regulatory bodies, site specific ligation of the polymer was necessary. This was achieved by PEGylating small fragments of the peptide, which are easier to synthesise, and then assembling in such a manner which ensures the correct folding pattern is achieve thus maintaining the activity of the peptide, with the polymer chains in their desired locations (Figure 1).

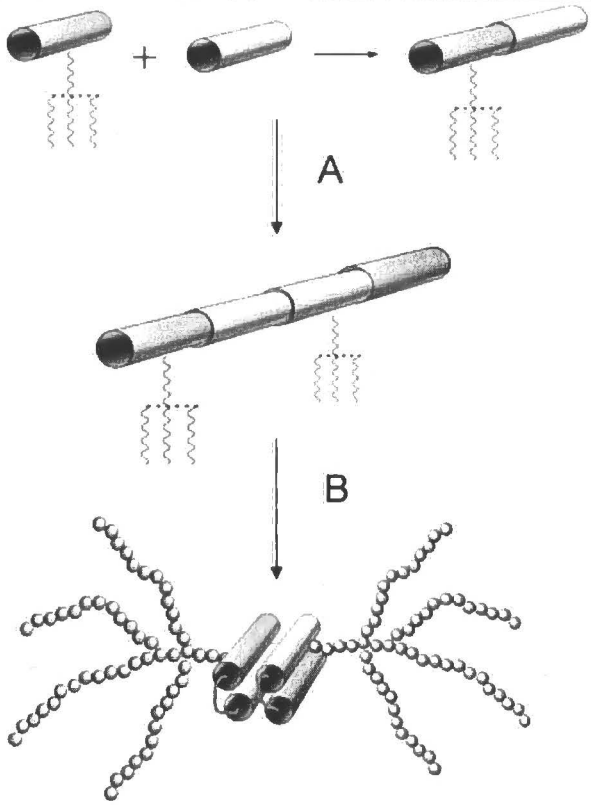

Figure 1 – Schematic of SEP synthesis[25]; A, Linear assembly of peptide subunits which have been site-specifically modified with branched PEG chains; B, Folding of peptide subunits to give the desired, active, tertiary structure.

Brocchini and coworkers have recently developed a simple method to insert a PEG chain between native disulfide bonds in proteins[26]. The therapeutically useful interferon α-2b (IFN, hepatitis C treatment) was conjugated with a single 10 or 20kDa PEG chain. There was a small reduction in biological activity (which was offset by a vastly superior blood residency time) which is attributable to the steric hindrance of the polymer chain, rather than a change in the tertiary structure of the protein. The efficiency and general applicability of this strategy was extended to glutathione, somatostatin and L-asparaginase[27]. This method is particularly advantageous in that the native peptides do not require the insertion of an addition amino acid (normally cysteine) in the primary sequence as an 'anchor' point for conjugation. There exists a

huge range of strategies for the coupling of PEG to peptides. These are too numerous to be described here and have been extensively reviewed[28-30].

Block copolymers of PEG and poly(L-lysine) spontaneously form micelle-like structures in the presence of DNA (due to co-operative electrostatic binding of anionic DNA, and cationic lysine residues). These nanostructures have enhanced circulation times, and with the appropriate surface ligands can deliver the genetic materials *in vitro*, followed by protein expression[31,32]. The poly(peptide) segment is readily degraded allowing clearance of the foreign polymers post-delivery, with non-toxic side products.

1.2.2 STIMULI-RESPONSIVE MATERIALS

Attachment of a stimuli-responsive (eg. that displaying either LCST, or USCT behaviour) synthetic polymer to a protein imparts a further level of complexity on the protein allowing modulation of the properties, when appropriate binding points are chosen[33]. Hoffman and co-workers attached poly(*N*-isopropylacrylamide) in a site-specific fashion near the biotin binding pocket of strepavidin[34]. Below the LCST the protein-biotin binding proceeded as with the wild-type. Upon increasing the temperature above the LCST the binding potential was reduced to less than 20%. This was attributed to the collapse of the polymer, effectively blocking the binding site. Increasing the distance of the polymer (in this case poly(*N,N*-diethylacrylamide) from the binding pocket resulted in the opposite behaviour: below the LCST the polymer is in its extended conformation which can block the active sites, whereas increasing the temperature induces contraction of the chain, exposing the binding pocket[35]. Similar results have been obtained with polymers whose solubility characteristics change with

the wavelength of light irradiation used[36]. Selective isolation of proteins from complex mixtures using protein-thermoresponsive polymer conjugates has been demonstrated. First the protein of interest interacts specifically with the polymer-protein conjugate and then upon addition of the stimuli the conjugate, along with bound substrate, is precipitated specifically. A similar strategy can be employed to recover enzymes from reaction solutions. The degree of substitution by the polymer can hugely influence the utility of these systems, with too much polymer preventing the recognition events or too little reducing the efficiency of precipitation[37].

1.2.3 PEPTIDE DRIVEN SELF ASSEMBLY

The specific self assembly of peptides, resulting from their precise primary structure, can be maintained following conjugation to a synthetic polymer allowing higher order structures to be formed, which could not be accessed simply by the phase separation of incompatible blocks.

In 1998 Meredith *et al.* used the central domain of a β-amyloid protein conjugated at the C-terminus with PEG to investigate their aggregation behaviour[38,39]. The aggregation of these proteins is responsible for Alzheimer's disease *via* the formation of insoluble fibrils. The addition of a soluble polymer allowed the individual steps of fibrillogenesis to be characterised[40]. The initial steps in fibrillogenesis were shown to be thermodynamically reversible, but limited in the natural system by precipitation of the insoluble aggregates. The steric shielding and addition solubility associated with the PEG block allowed this to be observed.

Interest in this, and other β-sheet forming peptides, has resulted in many systems being studied for applications in (bio)nanotechnology[17,41].

A particular problem with the well documented (and desirable) physical properties of spider silk is that it suffers from considerable shrinkage and onset of rubber-like properties upon exposure to moisture[42] (which is beneficial in nature as it allows spiders to re-shape their webs). A commercial high performance fibre must have consistent properties across a range of environmental conditions. The strength giving region of silk from *N*-clavipes is poly(L-alanine) which assembles into crystalline regions though the lateral alignment of β-sheets. A simple analogue of this was made by combining a short poly(L-alanine) core as the B block in an ABA triblock copolymer with flanking PEG chains, which mimic the amorphous regions contributing to the elongation properties[43]. Crucially the lengths of the PEG chains were limited to prevent formation of a polymeric crystalline domain. In this system the β-sheet domain directed the solid state organisation as occurs with the natural material. Van Hest *et al.* used a modified silk-based peptide sequence [(alanine-glycine)$_3$glutamic acid-glycine]$_{10}$ with flanking PEG chains to direct self assembly of fibres shown in Figure 2[44]. An interesting variation of this strategy was to incorporate a single repeat unit of the β-sheet peptide as a methacylic monomer. An A-B-A block copolymer was synthesised where the A block represents the amorphous regions (poly(methylmethacrylate)) and the B block the crystalline β-sheet domain[45].

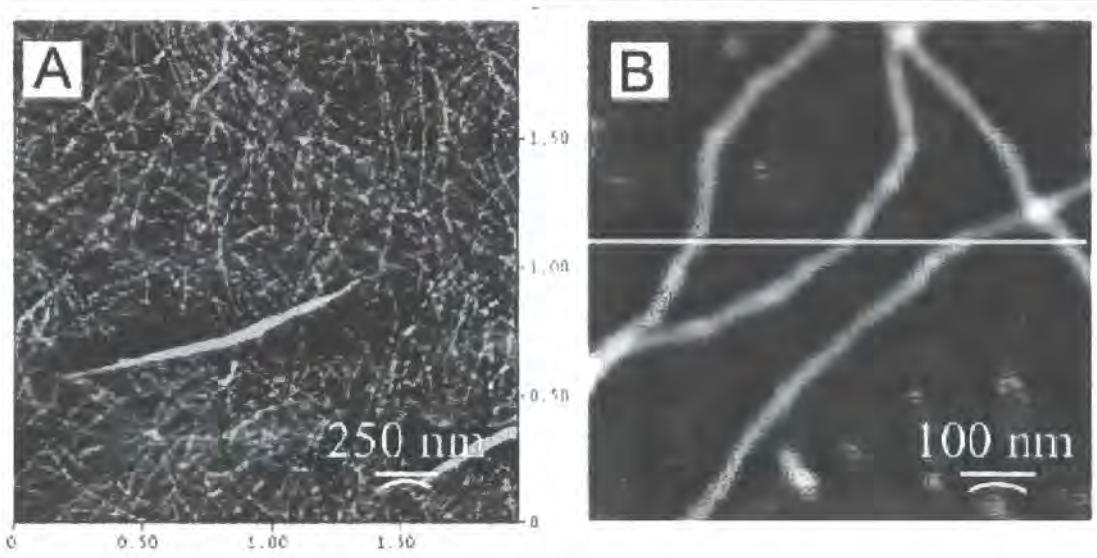

Figure 2 – AFM height images of silk-like peptide-PEG_{2000} triblock copolymer of van Hest *et al*[44].

By utilising ATRP the length of each block could be controlled and the amount of peptide synthesis minimised. IR analysis confirmed that the peptide assumed a β-sheet in the solid state. This side-chain approach has also been applied to peptides derived from the elastin sequence fragment $[VPGVG]_n$ (valine-proline-glycine-valine-proline) which displays LCST due to the aggregation of the chains with the entropically driven expulsion of water[46]. An ABA polymer in which a PEG chain was flanked with two units of poly(VPGVG-methacrylate) displayed an LCST which could be tuned from 20 to 60°C by varying the chain lengths of the peptide containing segment[47]. Similarly polymers and dendrimers[48] bearing fragments from the leucine zipper protein[49] have been incorporated into self assembling, stimuli responsive materials[50].

A different class of assembling proteins are coiled-coils. These comprise of 2-5 alpha helical protein strands, which assemble into a left handed 'super helix' and are estimated to form in 2-3% of all protein residues[51-53]. Whereas β-sheet peptides direct the formation of lateral stacks, the coiled-coil forming proteins form discrete

nano-structures which are almost uniform in size. Following conjugation of a polymer to a single terminus of these peptides the self-assembly behaviour is retained, as shown by AUC and CD observations. A core of coiled peptides is surrounded by a corona of the synthetic polymer (Figure 3) retaining the same pH and temperature dependency of the original proteins[54,55]. If the peptide is also therapeutically active then the system potentially behaves as a stimuli responsive (peptide) drug delivery vehicle.

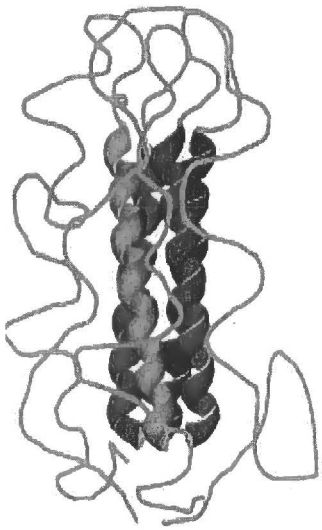

Figure 3 – Model for the self organisation of peptide-block-PEG block copolymer directed by coiled-coil formation[56].

Nolte *et al.* suggested in 2001 the idea of creating a "giant amphiphile" from a polar protein head group and a lipid-like polymer chain. Strepavidin (a 60 kDa hydrophilic protein) was used as the head-group though association with biotin-terminated polystyrene and its surface activity studied as with a low molecular weight surfactant[57]. The enzyme horseradish peroxidase was conjugated with a 9000 Da poly(styrene) chain to give a giant amphiphile which formed vesicles in aqueous solution, as shown in the TEM images in Figure 4, and the ability to internalise a

water soluble dye[58]. Interestingly the enzyme retained some, albeit much reduced, of its catalytic activity in this form.

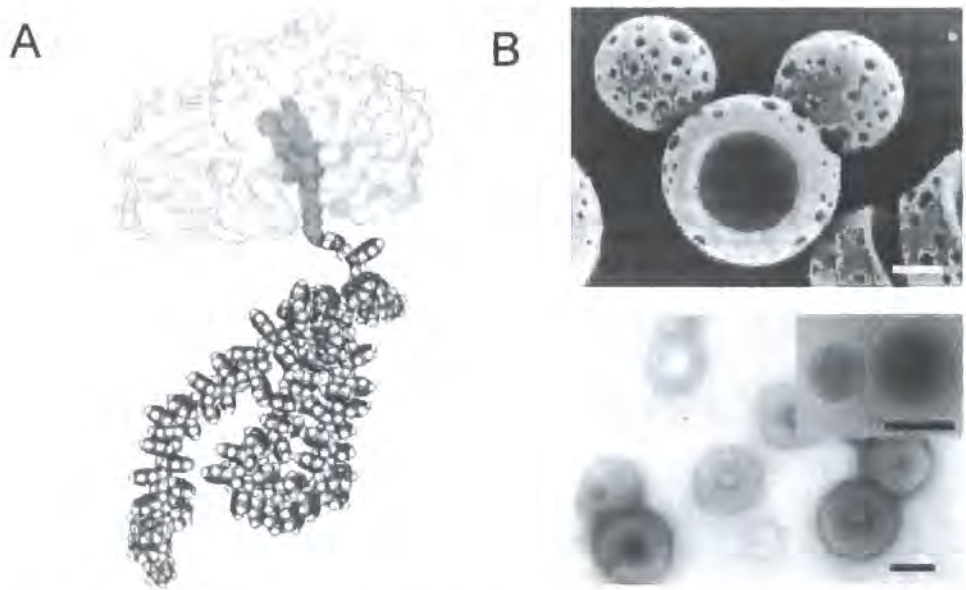

Figure 4 – Horseradish peroxidase-block-poly(styrene)$_{90}$.[58]; A, Computer generated image of the the conjugate; B, SEM (top) and cryoTEM (bottom) images of the aggregates formed in water showing the vesicular nature. Scale bar = 200nm.

Other groups have made related amphiphiles by either coupling the reactive end group of a polymer, or an initiator for controlled radical polymerisation to the protein. Recently Haddleton *et al.* utilised a protected maleimido functionalised ATRP initiator to give well defined polymers bearing alkyne groups in the side[13]. Free cysteine residues present in the commercial protein BSA (bovine serum albumin) were then allowed to react with the maleimide group in aqueous solution to give a water soluble polymer-protein conjugate. By making use of the highly efficient [3 + 2] dipolar cycloaddition[59,60] (Scheme 1), "click" reaction between an azide and the pendant alkynes it was possible to increase the hydrophobicity of the polymer chain to

give a hydrophobic "giant amphiphile" which could self assemble into micelles with the protein head group at the periphery (Figure 5).

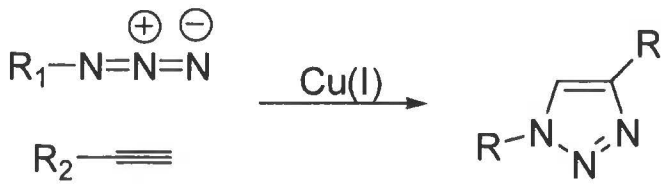

Scheme 1 – Huisgen's [3 + 2] cycloaddition, or "click" reaction between an azide and an alkyne to give a disubstituted triazole.

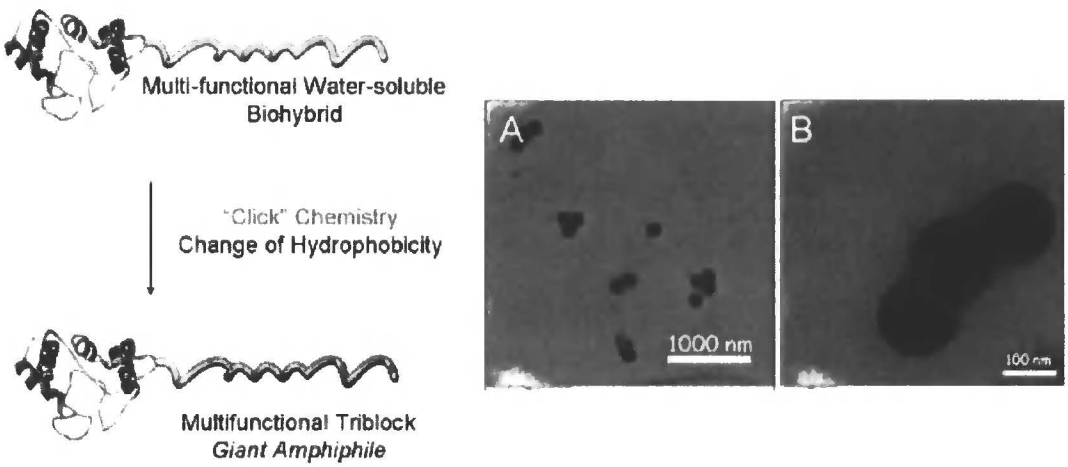

Figure 5 – Left, BSA-hydrophilic conjugate, functionalisation by "click" chemistry to give giant amphiphile; Right, TEM images of micelles formed by the hydrophobic conjugate in water[13].

Rather than using complex peptide fragments, homo(poly amino acids) can also be incorporated as the bio-inspired block[15,61]. The chemical composition of the synthetic block in this case is far more varied than has been achieved with the protein based hybrids. Gallott and co-workers showed in the 1970's that copolymers of poly(styrene) or poly(butadiene) with poly(γ-benzyl-L-glutamate) or poly(ε-benzyloxycarbonyl-L-lysine) phase separated in the solid state to give lamellar structures[62]. They deduced that there was no dependence on the block copolymer composition on the structures formed. This was later re-investigated by Schlaad *et al.* using modern X-ray scattering techniques[63,64]. They deduced that the length of the

peptidic block was important in the formation of new phases. Different lamellar structures were found depending on the secondary structure of the individual peptide segments. Poly(butadiene)$_{85}$-*block*-poly(L-glutamic acid)$_{55}$ diblock copolymers were shown to form vesicles in aqueous solution. Interestingly the peptidic block showed a pH dependant coil-helix transition without any associated change in the size or structure of the vesicle. PB_{27}-*b*-$PLGA_{64}$ resulted in spherical micelle formation but PB_{40}-b-$PLGA_{100}$ formed vesicles. Polystyrene-block-poly(L-lysine), where the polystyrene was varied from 8-10 units formed, instead of micelles, cylindrical assemblies irrespective of the poly(L-lysine) block length[65]. These subtle differences in chemical composition strongly affect the morphology and structure of assembled aggregates. Chécot *et al.* also showed that poly(butadiene)-*block*-poly(L-glutamic acid) vesicles exhibited pH dependant hydrodynamic radius[66]. At high pH the acids were fully ionised and the polypeptide in a random coil, but at lower pHs the polypeptide were protonated giving rise to an α-helical conformation, which being a rigid rod led to expansion of the vesicle. Block copolymers containing a biodegradable polymer conjugated to homo(polypeptide), such as poly(lactic acid) and poly(ε-caprolactone), have been synthesised[67]. The dependency of micelle size with pH, resulting from electrostatic interactions of a poly(aspartic acid) block, showed that larger micelles form in basic conditions when the carboxyl groups are fully deprotonated[68]. These smart nano-objects[9] have been suggested for drug delivery applications by the solubilisation of hydrophobic drugs in micelles or hydrophilic drugs in vesicles[21].

1.3 GLYCOPOLYMERS

Polysaccharides are amongst the most abundant organic molecules on earth. They have a variety of functions from providing structure (cellulose, chitin, collagen), energy storage (starch, glycogen), blood coagulation (heparin) and joint lubrication (hyaluran). A key feature of carbohydrates which allows for this diverse array of functionality is their huge potential for structural variety. For proteins and oligonucleotides the structure varies in the sequence of amino acids or nucleotide bases. For sugars there is not only sequence information, but also positional and stereochemical variability. This huge potential for information density is often referred to as the 'glycocode'. For instance 20 carbohydrate letters can combine to form $1.14x10^{15}$ different words[69]. Glycopolymers[70-72] as a general term refer to any polymeric material based upon carbohydrates whether naturally occurring or manmade. However, synthetic polymer chemists tend to interpret this in a narrower context as a polymer backbone with pendant carbohydrate groups. The incorporation of these biological markers into polymers allows many important cell-cell, ligand-cell, virus-cell and bacterial-cell interactions to be probed[73]. Carbohydrate recognition is involved in such diverse biological process[74-76] as inflammation, gamete fertilization, immune defence, endothelial barrier crossing and viral infection which are all key research areas of glycomics and glycobiology[77]. The limiting step in preparing these materials is the inherent complexity of carbohydrate synthesis, requiring orthogonal protecting group strategies with multistep synthesis. Modern synthetic strategies and precise polymerise methodology are now allowing the traditional fields of organic and polymer chemistry to merge[78].

1.3.1 MULTIVALENCY: THE CLUSTER GLYCOSIDE EFFECT

It was observed as far back as 1888 that red blood cells agglutinated upon the addition of an oil extract from caster beans. It has since been determined that this was due to a binding event between a protein and the cell surface carbohydrates resulting in cross linking and hence precipitation. This protein was later identified as being a member of the Lectin family[79,80]: proteins which bind carbohydrates, which are not enzymes or antibodies. Lectins display high selectivity for specific carbohydrates and this property was instrumental in the assignment of blood groups according to their surface sugar decoration. The binding of a single sugar molecule to a lectin is in itself a very weak process[81]. However, in biological systems multiple copies of the same carbohydrates are displayed. For instance red blood cells displace many copes of sialic acid which are recognised by the cell surface proteins on the influenza virus[74]. These recognition and binding events eventually lead to cell endoytosis by the virus particle resulting in infection. This specific binding can be used detect or even remove influenza virus by the addition of synthetic compounds presenting multiple copies of the sialic acid residue[82]. Assuming all the carbohydrates bind with equal strength, one would expect that an excess of the competitive, inhibiting, compound would be required. This is not the case however, due to the cluster glycoside effect: defined as being " the enhancement in the activity of a multivalent ligand beyond what would be expected due to the increase in local sugar concentration"[83]. Polyvalent carbohydrate ligands display increased binding affinity per sugar unit than the free sugar and hence preferential binding. (It should be made clear that Lectins are not unique in binding carbohydrates, and many antibodies display this high specificity, along with proteins and small molecules[73,84]). Many complex carbohydrates and glycopeptides have been

identified in cellular recognition processes. These have not been incorporated into polymers probably due to complex multistep synthesis required to isolated even small quantities of the carbohydrates[85-87].

The relative strength of the binding increases with the length of the polymer chain and hence an increase in the number of repeated carbohydrate groups. Kiesseling *et al.* have investigated the effect of architecture on the interaction between multivalent compounds and Concanavalin A (a mannose specific lectin) which suggested that well-defined linear polymers were more effective inhibitors (ie. binding preferentially to the free sugar) than polydisperse polymers or those bearing a lower density of the carbohydrate moieties[88]. Similarly, multivalent deindrimers have been investigated and shown to have increased binding affinities compared to the free sugar[89-91]. The interaction between peanut nut agglutinin and a β-D-galactose bearing polymer was shown to be 50 times greater than the parent carbohydrate[92] and similar values have been obtained for lectins specific to other sugars showing the generality of this increased affinity[93]. Finally, the effect of the linker between the polymer and the carbohydrate has been investigated. The results suggest that increasing the linker length and hydrophobicity of the linker may increase the binding[94].

1.3.2 GLYCOPOLYMER SYNTHESIS

One of the first reports of a synthetic glycopolymers was made by Horejsi *et al.* in 1978[95] (Scheme 2). They copolymerised acrylamide with various allyl glycosides to give high molecular weight water soluble polymers by free radical methods and investigated their interaction with plant lectins (Section 1.3.2).

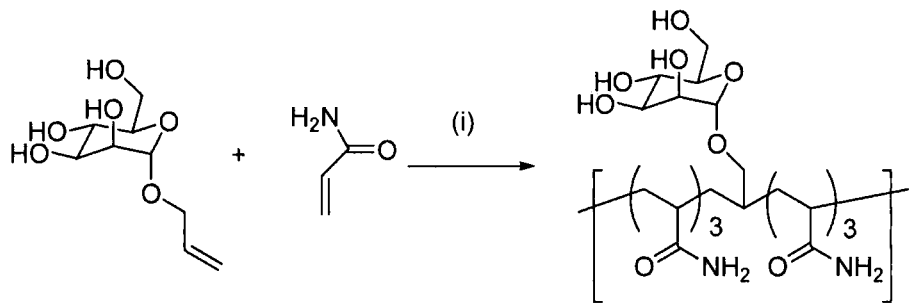

Scheme 2 – Copolymerisation of acrylamide and allyl-mannoside. Conditions; (i) TMEDA, ammonium pesulfate,H_2O, 100°C 10 mins.

It is no surprise that attempts have since been made to utilise controlled polymerisation techniques to give control over the degree of polymerisation, chain end functionality and to reduce the polydispersity values. Initial work focused on ionic polymerisation methods[96,97] (cationic and anionic). This approach is limited by the requirements of stringent reaction conditions with the rigorous exclusion of all moisture and oxygen[98]. Furthermore it was necessary to fully protect all the monomers which would otherwise lead to side reactions. The well defined ruthenium based catalysts introduced by the Grubbs[99] for Ring Opening Metathesis Polymerisation (ROMP) have been exploited for glycopolymers synthesis using both protected[100] and unprotected[101] carbohydrate based monomers owing to the catalyst's excellent tolerance of functionality. However, the catalyst must be thoroughly removed prior to biological evaluations and the unsaturated backbone can potentially undergo further reactions.

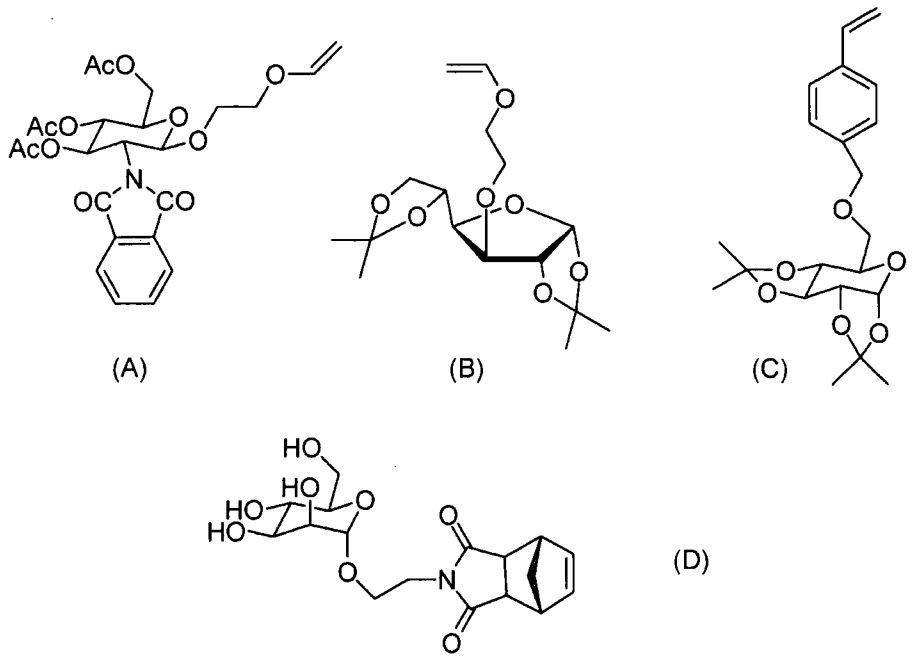

Figure 6 – Examples of monomers used for glycopolymers synthesis by various methods; (A) cationic, 2,4,6-tri-o-acetyl-2-deoxy-2-phtalimido-1-(2-vinyloxy ethyl)-D-glucopyranose; (B) cationic 1,2:5,6-Di-isopropylidene-3-(2-vinyloxy ethyl)-D-glucofuranose; (C) anionic, *m*-(1,2:3,4-di-*O*-isopropylidine-α-D-glucopyranose-6-oxymethyl)styrene; (D) ROMP, 1-*O*-α-D-mannopyranoside-7-oxanorbornene derivative.

The introduction of controlled radical polymerisation has allowed polymer chemists to create a vast range of new polymers (and architectures) owing to high functional group tolerance and the choice of numerous systems for mediating the polymerisation. When radical methods are utilised it is possible to conduct the polymerisation in aqueous solution using monomers with no protecting groups. This results in homogenous materials rather than a mixture of products which can be found following deprotection[102]. Nitroxide Mediated Polymerisation (NMP) has been used to polymerise protected sugars[103,104], but only a single example of the use of unprotected sugars has been shown, giving low conversions and no polymerisation when high the targeted DP was above 100[105]. Side reactions due to the high temperature employed in NMP (>100°C commonly) and transfer of the propagating chain to a hydroxyl group are to responsible for the reduced control. Atom Transfer

Radical Polymerisation (ATRP) is more versatile than NMP and can be conducted at ambient temperatures[106]. Narrain and Armes demonstrated that unprotected monomer 2-gluconamido-ethyl methacrylate (GAMA) could be polymerised at ambient temperature in MeOH/H_2O and also thermoresponsive block copolymers poly(propylene oxide)[107,108]. Perhaps the most versatile CRP technique with respect to its tolerance of a range of monomer types is Reversible Addition-Fragmentation chain Transfer (RAFT) polymerisation[109] (Figure 7). The first RAFT glycopolymer synthesis was by Lowe *et al.* in 2003[110], by the polymerisation of glucosyl methacrylate under basic aqueous conditions. Using appropriate RAFT agents and solvent combinations complex architectures can be synthesised such as block copolymers[111], star-branched polymers[112,113], surface immobilised polymer brushes[114,115] and glycosylated metal colloids[116].

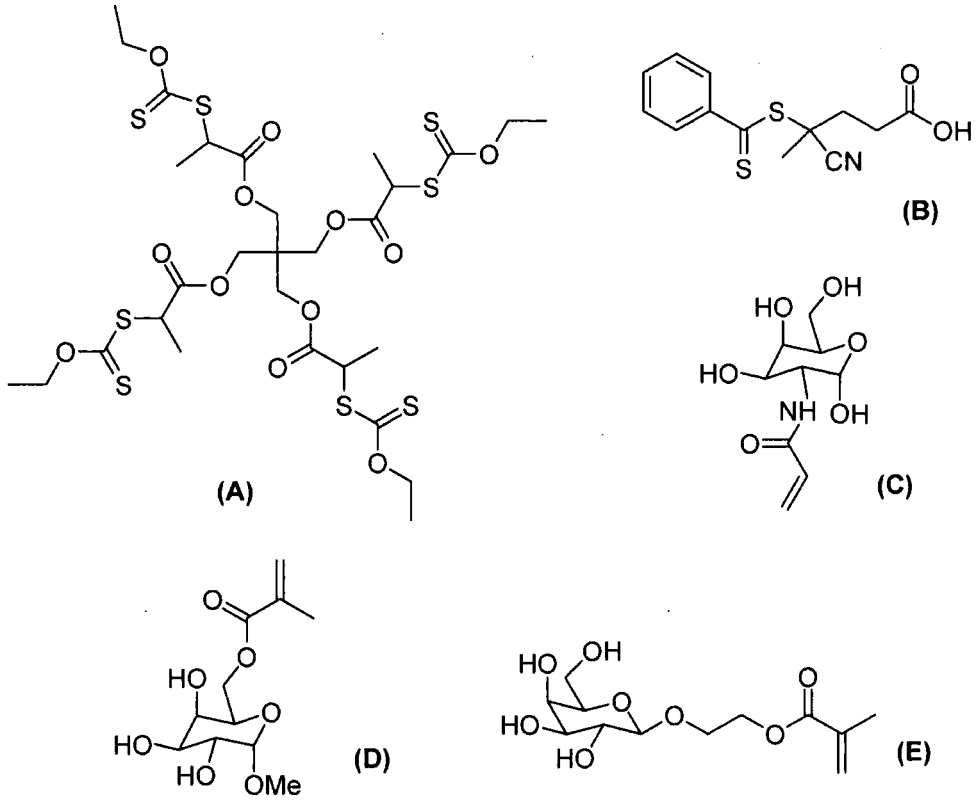

Figure 7 – Monomers and initiators used for RAFT glycopolymer synthesis; (A) tetrafunctonal Xanthate; (B) (4-cyano-pentanoic acid)-4-dithiobenzoate; (C) α-D-galactopyranosyl-2-deoxy-2-amethacrylamide, (D) (1-*O*-methyl-α-D-galactopryanosyl-6-O-methaacylate; (E) 2-(β-D-galactosyloxy)ethyl methacrylate

Post-polymerisation glycosylation offers an alternative route to glycopolymers[72]. Indeed nature produces glycopeptides by post-translational modification of peptides. For the synthetic chemist this removes the requirement for multistep monomer synthesis and can reduce the protecting group considerations. Poly(vinyl alcohol) was glycosylated with glycosyl oxazolines by Takasu *et al.*[117] The degree of substitution of the hydroxyl groups was less than 40 %. This is in part is limited by the solubility of PVA in organic solvents, but mostly attributable to the steric hindrance of adding a large (acylated) carbohydrate moiety so close to the polymer backbone. Whitesides *et al.*[118] used copolymers of acrylamide and *N*-hydroxysuccinimide (Scheme 3, A) which were then substituted with sialic acid

residues to give polymers which could effectively bind to the Influenza virus. Müller *et al.*[119] demonstrated that *N*-methacryloxysuccinimide can be polymerised by ATRP using Cu(I)/bipy in DMSO (owing to its low solubility in other organic solvents) to give narrow molecular weight reactive precursors[120], which were converted to their corresponding glycoconjugate polyacrylamides by addition of galactose- and glucosamine[121] (Scheme 3, B).

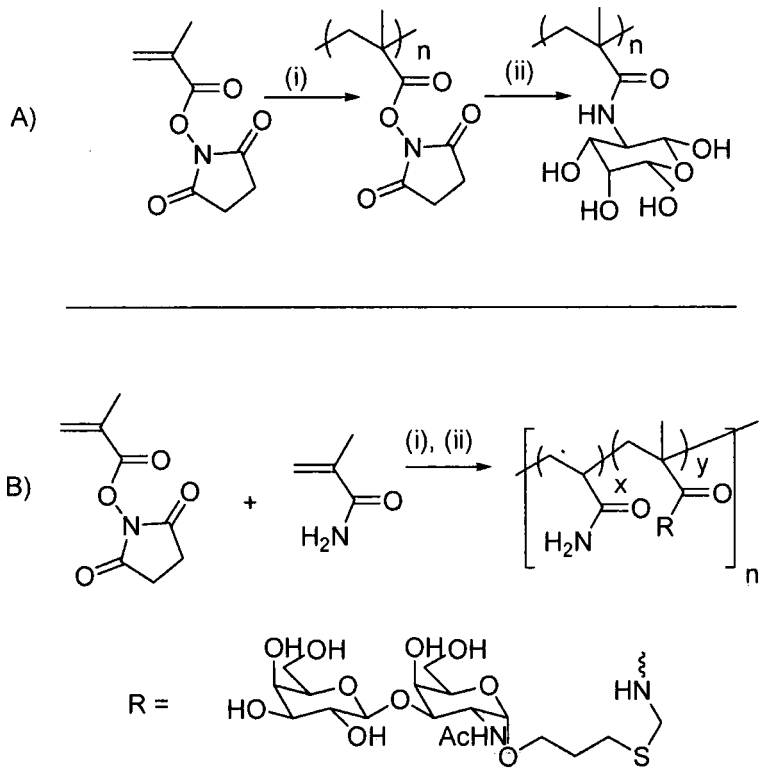

Scheme 3 – Glycopolymer synthesis by post-polymerisation modification of *N*-hydroxy succinimide active esters; (A) (i) 2-hydroxyethyl-2-bromoisobutyrate, CuBr/bipy, 80°C; (ii) Galactosamine/NEt_3 (1:2), DMF; (B) (i) AIBN, (10 mol%) THF, 50°C, N_2; (ii) R-H, DMSO/25°C.

Other postpolymerisation methods include poly(fluorenes) with bromo-sugars[122], poly(1,2 butadiene) with thio-sugars[123], maleic anhydride residues with amino-sugars[124,125] or pendant amines with sugar-isocyanates[126] with efficiencies of 60 to 98 %. Perhaps the most significant advancement was in 2001 when Sharpeless and co-workers[59] introduced the idea of "click reactions" (Scheme 1), representing a family of high yielding, efficient reactions which require little (if any) purification and

can preferably be conducted under mild, aqueous conditions. One reaction in particular has been popularised by this: the Huisgens dipolar cycloaddition between alkynes and azides[60] (Scheme 1). Haddlteon and co-workers[127] polymerised trimethylsilyl (TMS) protected alkynes by ATRP to synthesise galactasoyl and mannosyl chain functionality from the corresponding glycosyl azides (Scheme 4, A). Near 100% functionalisation was observed. This extremely efficient reaction is ideally suited for reactions at chain-ends which display lower reactivity due to steric hindrance[128,129]. Hawker *et al.*[130] prepared asymmetric dendrimers by addition of azido-sugars to alkyne terminated dendrimers, and a single species was seen in the MALDI-tof spectrum. Riguera used the opposite strategy to couple alkyne functionalised sugars to azido terminated dendrimers[131,132] (Scheme 4, B). An interesting application of this reaction was to produce "click" glycopolymers[133], where the triazole linkage is incorporated into the polymer backbone[134]. The produced materials were thus biodegradable, but also bear a cationic charge for DNA binding.

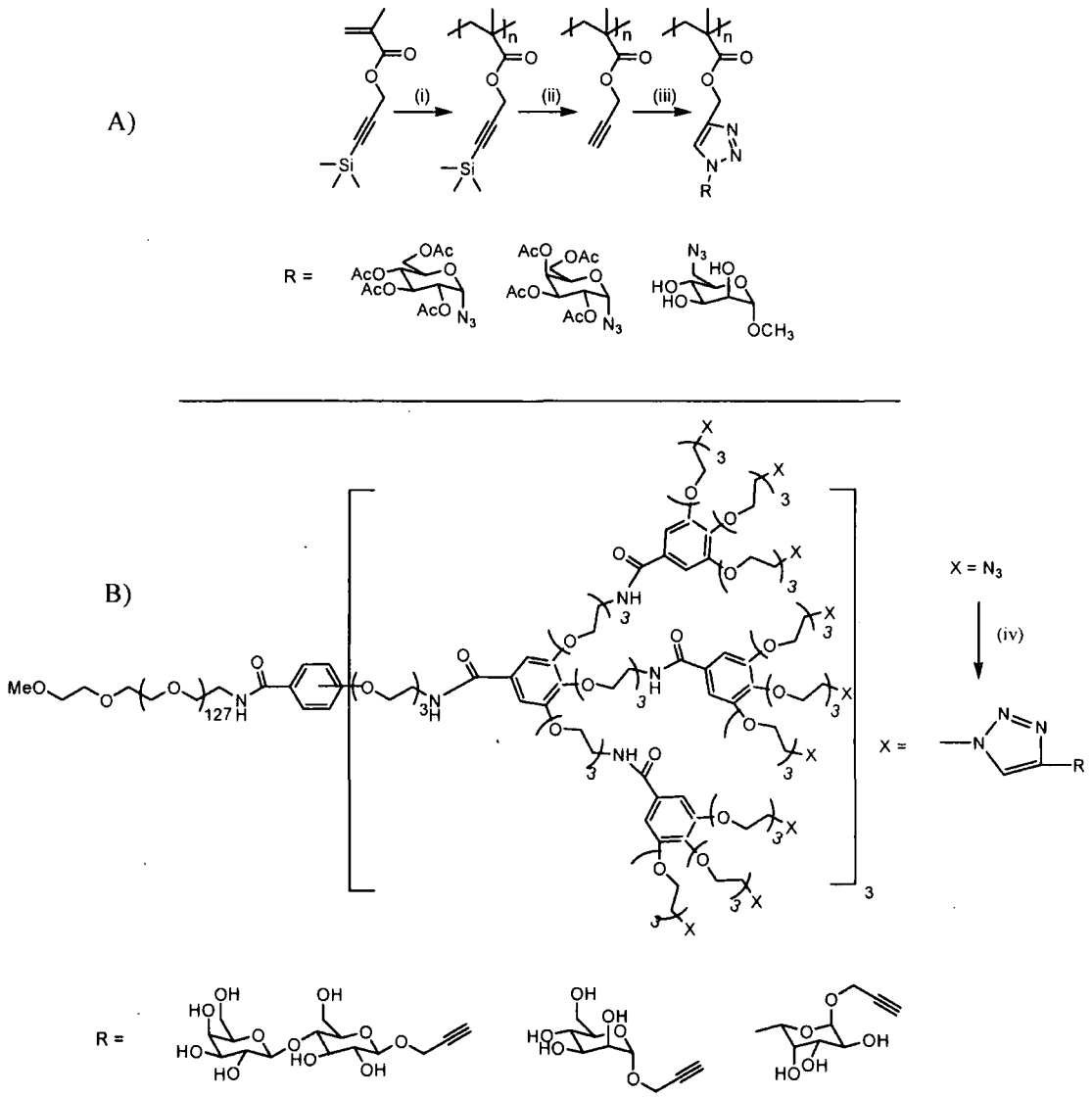

Scheme 4 – Use of the click reaction for post-polymerisation modification of linear (A) and dendritic (B) polymers; (A) (i) *N*-(n-ethyl)-2-pyridylmethanimine/CuBr, toluene, 70°C; (ii) TBAF, AcOH, THF, -20 to +25°C; (iii) RN_3, $(PPh_3)_3CuBr$, DIPEA; (B) (iv) $CuSO_4$, Sodium ascorbate, t-BuOH:H_2O (1:1)

1.3.3 APPLICATIONS OF GLYCOPOLYMERS

The importance of carbohydrates in so many biological events, along with the increased binding of multivalent carbohydrate ligands, lends glycopolymers many potential applications in glycoscience and medicine[135]. Exploitation of receptor mediated endoytosis offers a promising route for macromolecular drugs to enter cells*. Spermatoza incubated with a polymer containing an antioxidant component (α-tocopherol) and β-D-galactose residues were shown to increase their viability following storage, shown to be due to the protective effects of the polymer. An equivalent polymer without the galactose residues showed no improvement in cell viability[137]. Self-assembled block copolymer micelles containing a DNA core, were decorated with lactose and also show an increase in cellular uptake by endocytosis[31]. Other self assembled systems have been indicated as potential drug delivery vectors; including glycosomes[123] (carbohydrate decorated vesicles) and micelles where the hydrophilic block is a glycopolymer[123]. Silica functionalised with 1st generation glycosylated dendrimers have been made for affinity chromatography of carbohydrate specific proteins such as the afore mentioned lectins. The multivalent architecture resulted in higher purity proteins than the corresponding monovalently functionalised silica following chromatography[138].

Incorporation of a fluorophore into an influenza-inhibiting glycopolymer can be used for detecting the presence of viruses which bind to the selected carbohydrate[139]. Poly(allyl glucoside) immobilised on a porous membrane was shown to be able to absorb lipase onto the surface by non-specific hydrophilic interactions[140]. Even following 10 cycles of catalysing hydrolysis and washing the enzyme remained

* This uptake is distinct from the enhanced uptake of macromolecules by tumour cells by the "enhanced permeability and retention effect" (EPR) due to increase rates of extravasation, which has been exploited for drug delivery to cancerous tissue[20,136].

82% efficient, indicating a strong binding to the surface. Glycopolymers bearing biotin end-groups have been immobilised by the highly specific binding a to streptavidin coated gold slides to create functionalised surfaces[141]. The binding of proteins to the surface can be monitored non-invasively by shifts in the surface plasmon resonance band. Similarly glycopolymers immobilised onto the surface of metallic nano-particles (particularly gold and silver) can be used to monitor biological recognition events *in situ*. Magnetic glyco-nanoparticles can be utilised for MRI contrast reagents or targeted delivery[116,142].

A glycosylated dendrimer, decorated with mannose residues has been shown to mimic the glycoalyx surface of cells, which reduces bio-fouling by blood-borne proteins, by minimising non-specific adhesion and maximising entropic repulsion[143]. The advantage of using a glycosylated structure here over conventional antifouling polymers, such as PEG, is the lack of temperature dependant aggregation (LCST).

A surprising non-biological application of glycopolymers was shown by Ye *et al.*, who used glycopolymers amphiphiles as solublising agents in supercritical CO_2, a "green" solvent which many compounds are insoluble in[144].

1.4 ANTIFREEZE GLYCOPROTEINS: AFGPs

The annual sea temperature at McMurdo Sound, Antarctica is -1.87°C just above its freezing point of -1.9°C[145,146], which is low enough to freeze the blood serum of most terrestrial species. However, life is found to flourish despite the inhospitable environment[147]. Marine mammals survive by virtue of being warm blooded: generating body heat and insulation provided by thick blubber. Cold blooded species, particularly fish, require other mechanisms to survive. In 1969 Wohlschlag and DeVries[148] observed that the freezing point of three species of fish *Trematonus borchgrevinki*, *Trematonus hansoni* and *Trematonus bernacchii* was approximately -2.0°C. Less than half of this depression was attributable to the dissolved sodium chloride, in comparison to that of temperate fish where 80% of the serum freezing point depression is due to dissolved salts. Raised levels of other solutes including sugars and proteins contributed to some of the remaining freezing point depression. It was found that a set of glycoproteins were responsible for the remaining 30% of this depression, far more than would be expected on the basis of colligative arguments. These proteins were coined as being antifreeze glycoproteins, or AFGPs for simplicity. The AFGPs require significantly lower molar concentrations to give an equivalent freezing point depression to NaCl therefore reducing the osmotic pressure, which can lead to cell leakage or rupture. The freezing point depression activity of AFGPs was later shown to actually be a thermal hysteresis: That is the freezing point was depressed but the equilibrium melting point remained unchanged. An ice crystal held in a solution of AFGP in this thermal hysteresis gap will not melt until the temperature is raised above the equilibrium melting point, even though it is above its freezing point. Ice crystals held in this manner will also tend to form pyramidal

crystals rather than circular[149] (Figure 8, A). More recently proteins have been isolated from both animal[150] and plant kingdoms[151] including amongst many, insects[152,153], grasses[154], carrots[155] and bacteria[156]. These are commonly referred to as antifreeze proteins or AFPs. The effect of these two classes of proteins on sub-zero water may be similar, but their structural features are not. Antifreeze proteins can take many forms, with varying size, secondary structure and degree of glycosylation, in contrast to the AFGPs which retain a large amount of structural homogeneity. (Structure shown in Figure 10)

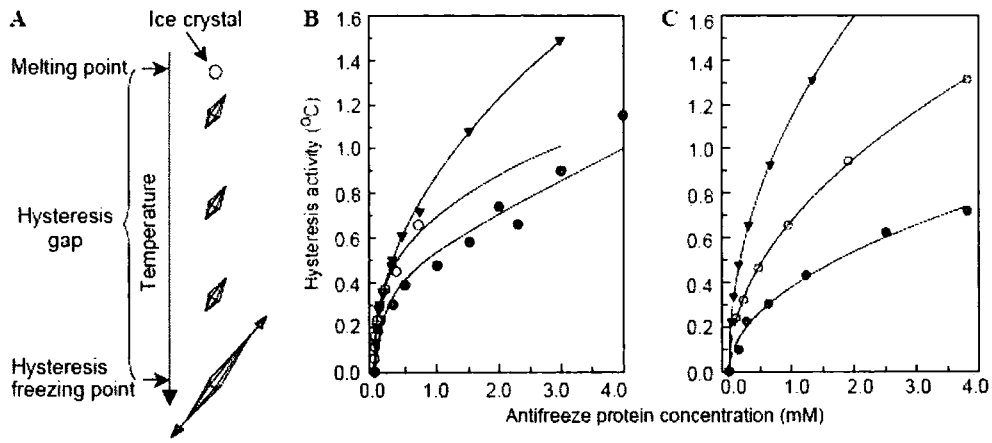

Figure 8. Antifreeze(glyco) protein activity summary[149]. A) Dynamic ice shaping in the hysteresis gap; B) Antifreeze proteins from various sources; C) Antifreeze glycoproteins • 7.9kDa, O 10.5kDa, ▼ 28.8kDa

A rather unique feature of AFGPs is the conservation of the polypeptide structure even amongst species with no common ancestors. Each species can have a unique gene coding the same protein[157,158] making it a rare example of convergent evolution[159]. This fact in itself is enough to generate interest in this class of glycopeptide, but will not be discussed here. AFGPs comprise of a repeating tripeptide unit containing two alanines and a threonine bearing β-D-galactosyl-(1,3)-α-D-*N*-acetylgalactosamine[160,161] (Figure 10) The number of repeat units ranges from 4

to 55, giving a molecular weight range of 2.6 to 33 kDa. AFGPs are typically classified according to their size, with AFGP 8 being the shortest, and AFGP 1 the largest. These classifications are based on the initial studies where separation and identification was achieved by electrophoresis[148] as shown in Figure 9. AFGP 1-4 range from 20-30 kDA and 5 – 8 2.6 – 19 kDa.

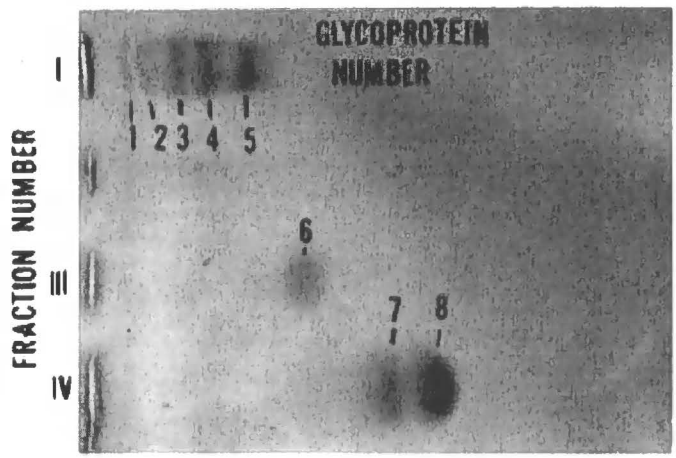

Figure 9 – Acrylamide gel electrophoresis of AFGPs isolated from the serum of *Tramatomus borchgrevinki*[146].

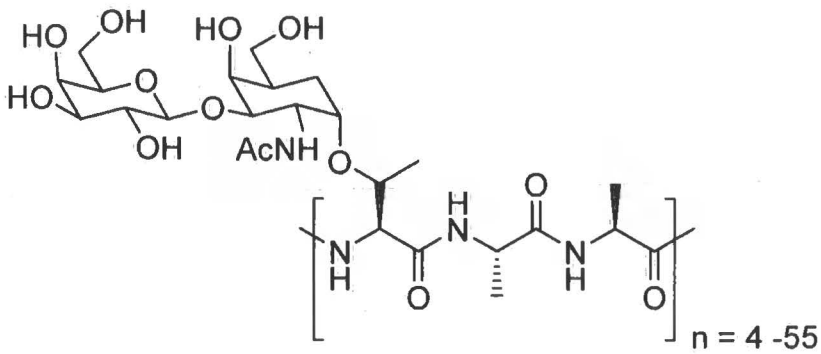

Figure 10. Native AFGP structure.

1.4.1 MODE OF ACTION

The mechanism by which AFGPs act has caused much debate since their discovery[162,163]. A key distinction to be made is that the antifreeze depressed the point at which a seed ice crystal will grow, rather than prevent its nucleation. Proteins which inhibit or promote nucleation of ice are also known to occur in nature[156]. Observations of single ice crystals grown in solutions containing AFGP showed that hexagonal bipyramidal shapes were formed as opposed to the circular crystals normally observed. This dynamic ice crystal shaping gave the important insight that the AFGPs were acting on the surface of the ice, rather than within the bulk lattice. The most commonly accepted mechanism for the activity of biological antifreezes is one of absorption-inhibition[164]. This model suggests that the antifreeze molecules absorb to the surface of the growing ice crystal. Further growth can occur in between adjacent antifreeze molecules, resulting in a large radius of curvature[165] (Figure 11).

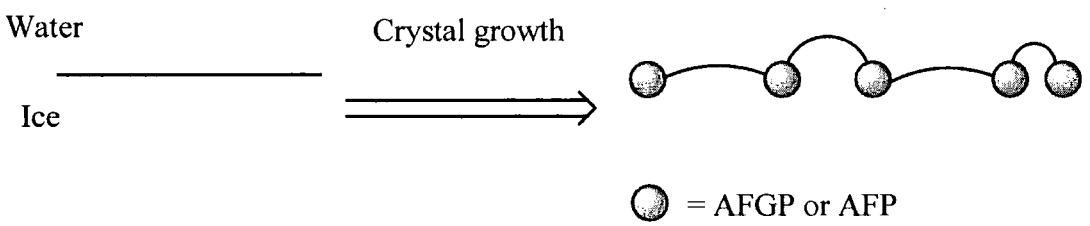

Figure 11 - Simple representation of absorption - inhibition of AF(G)Ps at ice surfaces by the mattress model

Further addition of water molecules to these curved surfaces is energetically unfavourable, due to the Kelvin effect, or also known as the Gibbs-Thompson effect when specifically related to freezing point depression[166]. This rationale fits well with the thermal hysteresis behaviour, as although addition of further water is difficult (FP depression) removal of water from the lattice is unaffected (No change in equilibrium

melting point). This mechanism is questioned by some, particularly the assumption that irreversible binding to the ice surface must be occurring. If this is so, then significant levels of absorption should be observed even at low levels of AFGP, which has not been found[163].

The binding to ice is expected to be directed by the hydrophilic hydroxyl groups of the disaccharide in one of two ways: (i) Absorption of the AFGPs to the ice by hydrogen bonds between the AFGP hydroxyl and surface water molecules (figure 12, A); (ii) Incorporation of the AFGP hydroxyls into the ice lattice Figure 12, B).

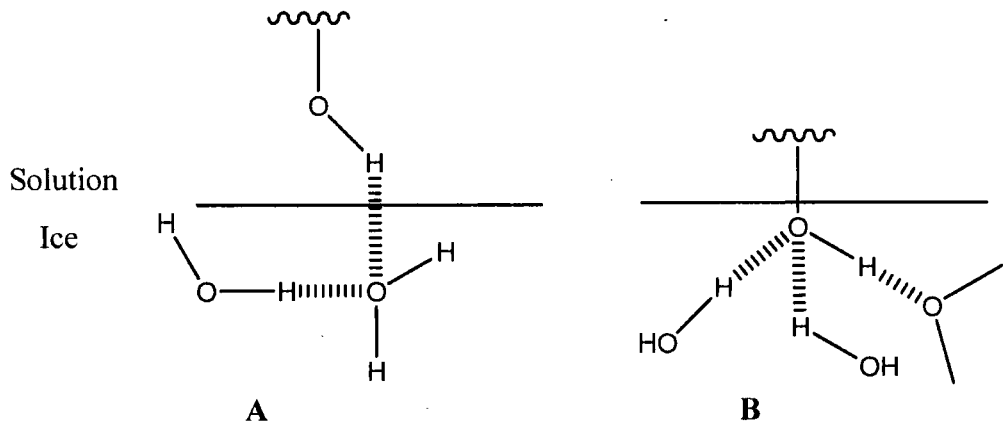

Figure 12 - Possible H-bonding interactions between AFGP and ice surface. A) Surface binding. B) Inclusion into ice lattice

Previous modelling studies have suggested that only two hydroxyls per disaccharide unit are correctly aligned to form hydrogen bonds with the ice surface[167]. In the case shown in Figure 12 A, each hydroxyl can only form one hydrogen bond to the ice, whereas when the carbohydrate hydroxyl is within the ice (Figure 12, B) three hydrogen bonds are possible[167]. Thus, for AFGP 8 (4 tripeptide repeat units) model A would allow for 8 hydrogen bonds where modal B allows for 24. Taking into account the tight biding required for adsorption-inhibition it would seem that model B would be preferential. NMR results from Knight *et al.*[167] agree with this hypothesis.

A technique known as hemispherical etching was used to determine which crystallographic faces, if any, the AFGP bound to on the ice[168,169]. Briefly a single crystal of ice is frozen onto a cold finger and immersed into a thermostated solution of antifreeze. The seed crystal begins to melt to form a thin shell around the finger, before being allowed to grow out slowly to a single crystal that is hemispherical. Due to the symmetry of the crystal formed, all possible ice faces will be exposed within each experiment. The individual faces can then be isolated and allowed to evaporate (freeze dry) at a sub zero temperature. During this period the AFGP concentration increases at the surface, appearing as etches which can be then be viewed. If no absorption occurred then no etching will be visible. This method was used to unambiguously assign the binding characteristics of AFGP.

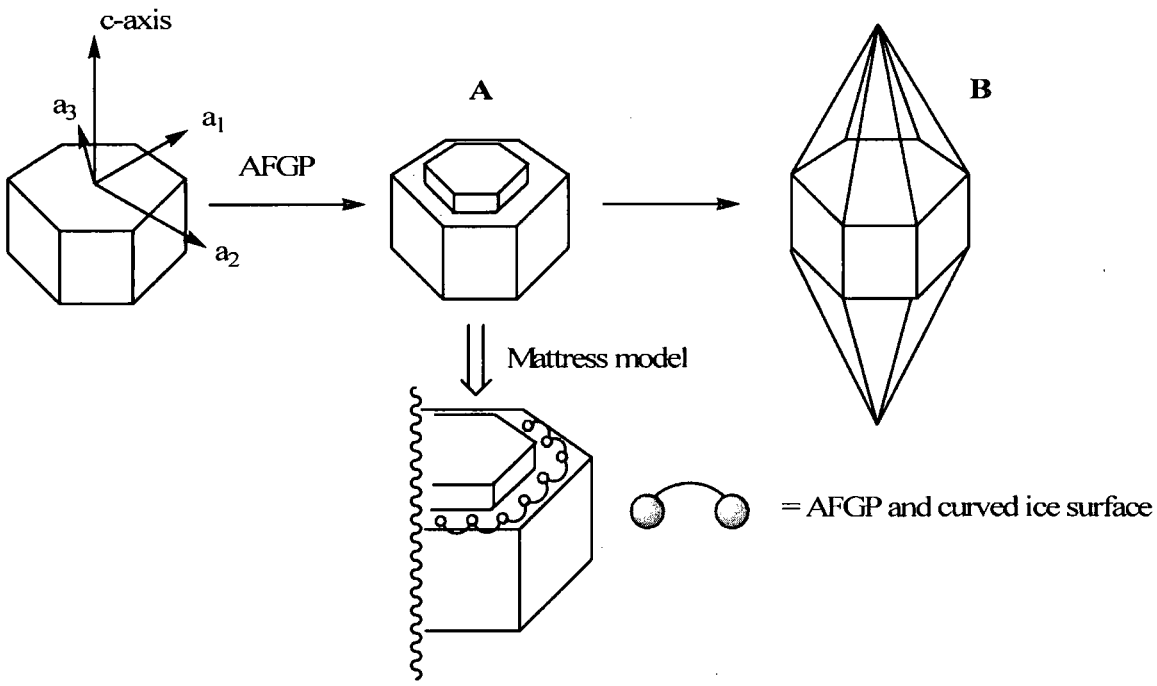

Figure 13 - Specific binding of AFGP to hexagonal ice crystal faces. A hexagonal ice crystals with steps caused by inhibition of growth at pyramidal faces by increased curvature of ice front due to AFGP B) Hexagonal bipyramidal ice crystal formed by repeated addition of AFGP onto the basal steps.

If a hexagonal (1 h) ice lattice unit is considered (Figure 13) it has two basal faces which are perpendicular to the *c*-axis, hexagonal in shape and 6 prism faces, each perpendicular to an *a*-axis and parallel to the *c*-axis. The basal faces are also referred to as the *c*-face or (0001). Normally ice crystals in the presence of pure water show limited growth on the basal face, growing at the prism faces (along *a*-axes). In the presence of AFGPs it is found that growth of the prism faces is halted completely with only slow growth along the basal plane observed at low degrees of overcooling. (ie. Just below the freezing point). As the degree of overcooling is increased to well below the freezing point explosive ice growth occurs from the basal face, to give long thin crystals. This can be explained by step pinning. Using the mattress model, described earlier one can consider a hexagonal ice crystal where the AFGP has absorbed onto a prism face, thus increasing the local degree of curvature and inhibiting the growth of ice along that face. As the system is cooled further some ice growth can occur along from the basal face, giving rise to a step, revealing another prism face, which AFGP can bind to. This process is repeated to give smaller and smaller steps until the crystal has a hexagonal bipyramid shape (Figure 14, A-C). By slowly warming and cooling the crystals, individual ridges can been viewed directly.

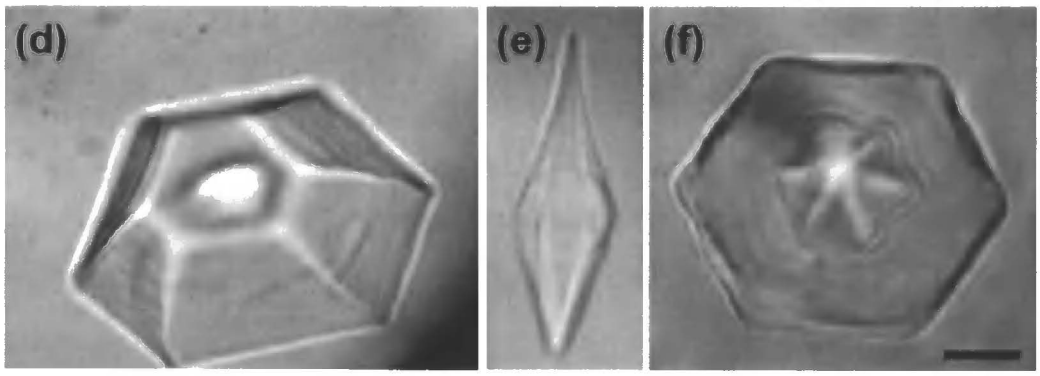

Figure 14 – Assay of antifreeze activity by ice crystal morphology[170]; (d) Adsorption of AF(G)Ps to the prism face inhibits the binding of additional water molecules, making it energetically favourable for growth in the c-axis as apposed to the basal planes; (e), At high concentrations the ice forms bipyramids with an hexagonal cross section; (f), Slow cooling and warming cycles allow visualisation of the ridges where the AF(G)P have bound.

This specificity for the prism faces is observed in some[171,172] (but not all[145]) AFP species as well as AFGPs discussed here. This would suggest that factors such as secondary structure and hydrophillicity/hydrophobicity are more important than the actual chemical composition.[173] The mechanisms of adsorption of AFP peptides to ice is well understood and has allowed detailed models to be established, which describe the binding process in terms of conformation and primary structure[174,175]. Examples of AFP structures are shown in Figure 15. This has lead to the rational design of new AFPs[176]. The effect of secondary structure on the effect of AGFPs is less clear, due to the difficulties in assigning the conformation they assume before and during ice binding[177].

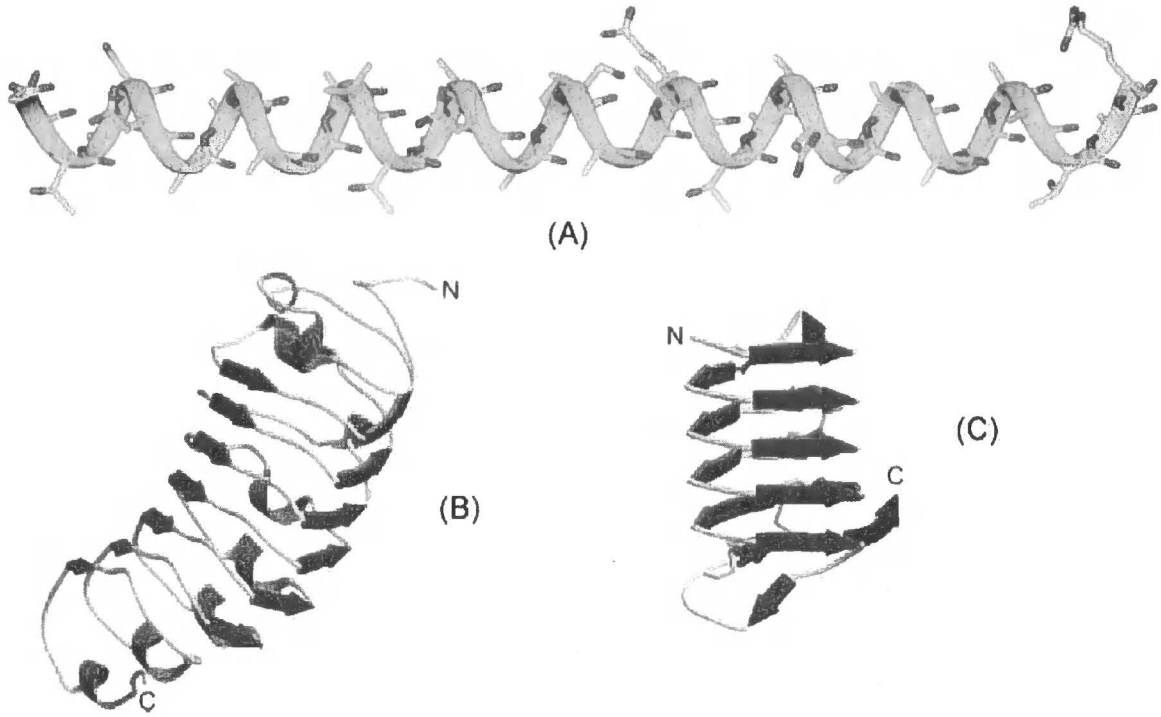

Figure 15 – X-ray structure of selected AFPs; (A) α-helical HPLC6 from winter flounder[178]; (B) β-helical AFP from *daucus carota* (carrot)[179]; (C) β-helical spruce budworm AFP[179]

Early studies on AFGP conformation concluded that they assumed a random coil, but this assignment was complicated by the fact that the CD spectra also bore a resemblance to a 3-residue-per-turn helix[180]. Light scattering and Raman spectroscopy suggest a folded structure was present. More recently high field NMR has been employed to probe the structure. In combination with molecular dynamics calculations and IR spectroscopy 1H NMR was used to show that AFGP 8 displayed no long range order, but significant local order as opposed to AFGPs 1-5 which had no long or short range order[181,182]. It would appear that the increased activity of the larger AFGPs can be attributed to their increased chain length rather than conformational changes. ^{13}C NMR suggested that a three dimensional folded conformation is formed in the presence of ice, but is also maintained once freeze dried[183]. This disagreement does suggest a high degree of conformation flexibility

which is in contrast to the rigid structures of AFPs. To date no 3-D solution structure has been published of an AFGP. Though many reports do agree that the structure involves presentation of separate hydrophilic and hydrophobic faces[163,184].

1.4.2 STRUCTURAL MOTIFS REQUIRED FOR ACTIVITY

Investigations into which features of AFGPs are essential for activity has been partially limited by the difficulty in synthesising them[163,184], compared to AFPs which have been made in reasonable quantities by solid phase synthesis[185,186] and recombinant methods in yeast[187] or plants[170].

The first structural feature on native AFGP to be modified was carbohydrate degradation[160]. A series of structural modifications are shown in Figure 16. Unsurprisingly peracetylation of the hydroxyls removed all activity, most likely giving a water insoluble material. The selective oxidation of the C-6 hydroxyls to the aldehyde resulted in no loss of hysteresis activity, agreeing with the modelling data which suggested only certain hydroxyls bind directly to the ice. Further oxidation of the C-6 position to the bisulfite or carboxylic acid completely removed all activity. Introducing a negative charge at the C-4 and C-3 positions by addition of sodium borate resulted in reversible removal of activity, until the borate was displaced by a change in pH. This implies that the individual OH groups are not essential for at least some antifreeze effect, but that negatively charged species are not tolerated at any position.

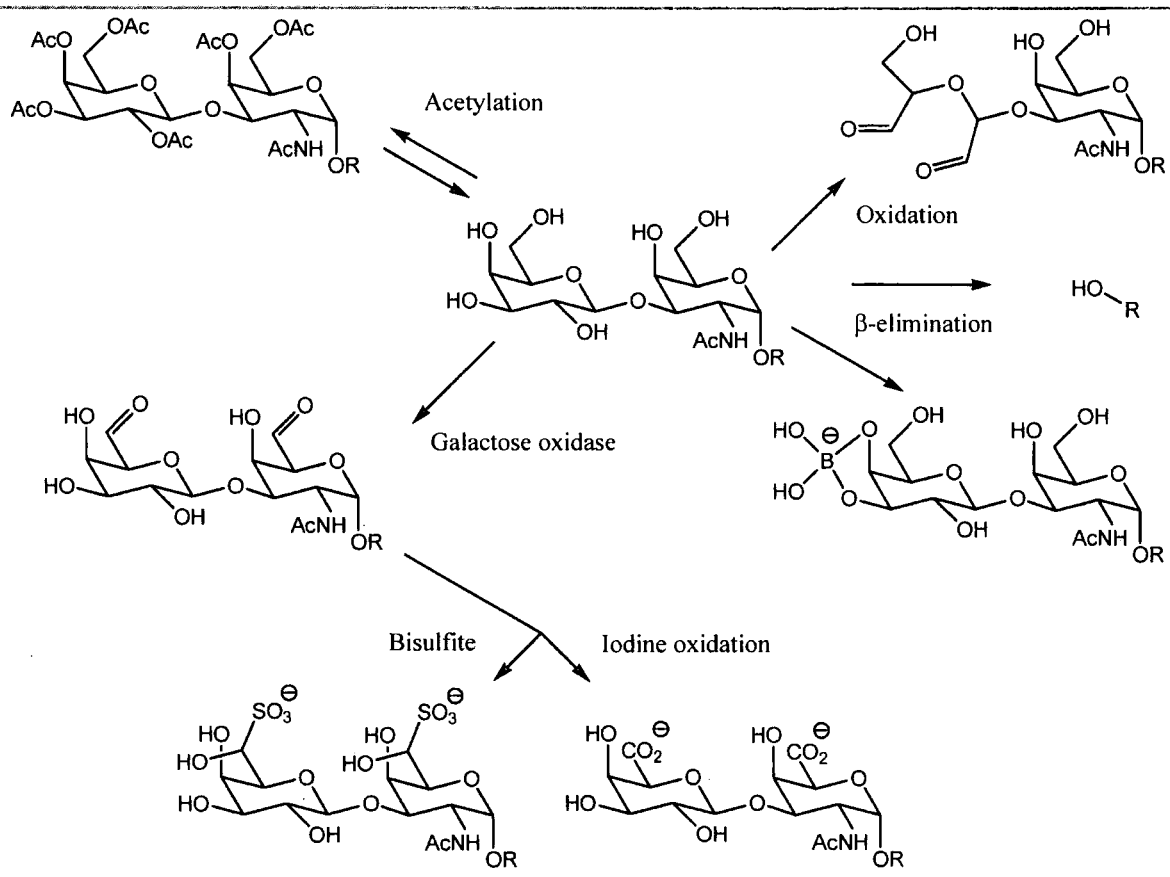

Figure 16 - AFGP carbohydrate degradation products which have been analysed for thermal hysteresis activity. R = thr-al-al tripeptide

The most complete study to date on the effect of individual structural motifs on thermal hysteresis and ice shaping ability was undertaken by Nishimura *et al.*[188-190] (Figure 17). The number of repeat tripeptide units was varied along with the systematic replacement of various regions of the carbohydrate moiety. Increasing the chain length showed a corresponding increase in thermal hysteresis activity between 2 and 5 tripeptide units (1257 – 3082 Da) at equal mass concentrations. At 6 and 7 repeat units there was little change in the TH activity, though in molar rather than mass terms they are more active. All apart from the dimer showed significant ice crystal shaping. A peptide synthesised without any carbohydrate groups displayed no

activity, indicating that a carbohydrate moiety of some description is necessary. The sialylated analogue (Figure 17, B) displayed no activity, agreeing with earlier work that the introduction of negatively charged groups removes antifreeze activity. No thermal hysteresis was seen when lactose and galactose were substituted, but there was some reduced (relative to native AFGP) thermal hysteresis for LacNAc (Figure 17, D) and GalNAc (Figure 17, C) indicating for the first time the importance of the acetamide group at the 2 position. The lactose derivative did display some ice shaping effect. The β- linked equivalent of native AFGP showed no thermal hysteresis but retained the ice shaping effects. Substitution of threonine for serine resulted in no activity showing the importance of the γ-methyl. The loss or retention of activity was thus linked to the presence of the acetamide group and the conformation restrictions it places. All analogues containing an acetamide displayed similar CD spectra to that of native AFGP, assuming it has a poly (proline) type helix. It was thus surmised that conformation is of utmost importance for TH activity.

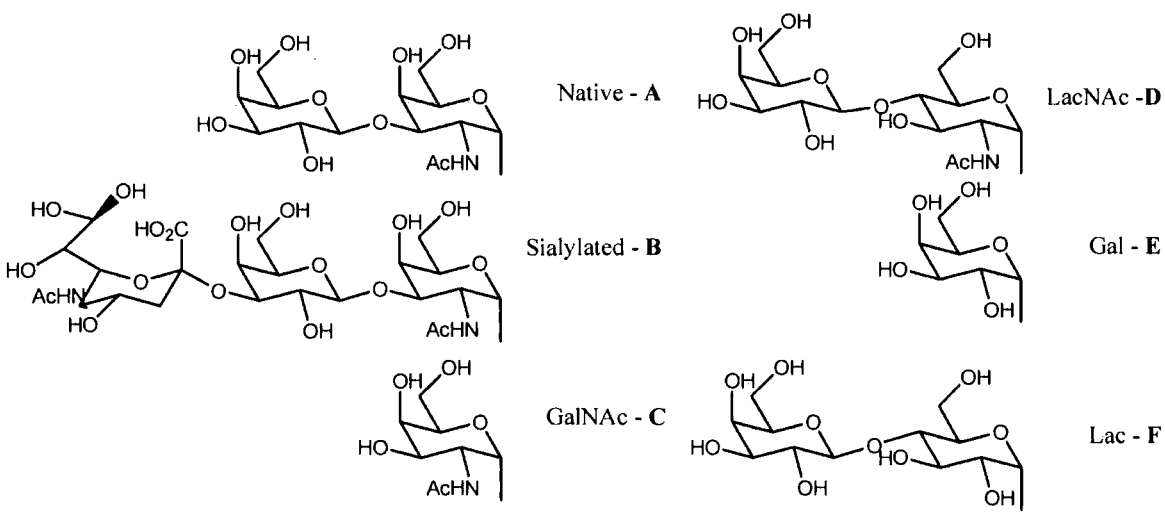

Figure 17 – Carbohydrate moieties studied by Nishimura *et al.* on the native AFGP backbone[188].

1.4.3 Potential Applications of AF(G)Ps and their Interactions with Biological Systems

The properties of AFGPs enable them to protect living cells in nature, so it is not surprising that efforts have been made to find medical applications for human use. The storage of tissues and organs is of particular interest. Currently, organs awaiting transplant are stored just above 0°C for only a few days before they are used. If the organ were cooled to liquid nitrogen temperatures (-196°C) then cellular decay would become negligible. The problem is that water leaks from the cells during freezing into the space between cells where ice crystals form and damage organ structures such as blood vessels, even in the presence of cryo-protectants like ethylene glycol[191]. Protection of spermatozoa by freezing has been possible for some time however[192]. Thus it is not surprising that AF(G)Ps have been investigated for their usefulness in these applications[193]. Ovine embryos, porcine oocytes and bovine oocytes have been vitrified in the presence of fish AFGP, resulting in improved storage[194].

A somewhat counterintuitive application of AF(G)Ps is in cryosurgery[195]: the process whereby disease tissue is killed by application of cryoscopic temperatures. In the presence of AF(G)Ps, below a critical temperature, bipyramidal crystals form resulting in long thing ice crystals. These can pierce the cell membrane resulting in cell death at the locations where cryoscopic temperatures are applied, which is desirable for anti-cancer therapy. Solutions of 10mg.mL^{-1} of AFP injected into tumours in mice, followed by slow cooling resulted in 100% cell death, specifically at the tumour[196]. This effect is important when considering cell preservation applications, as it could lead to negative effects during freezing. The investigation into the effect of a synthetic AFGP analogue, (bearing a monosaccharide α-D-galactose, in

place of the native disaccharide) on the thawing of Islet cells following cryostorage showed two effects[197]. At low concentrations (500 $\mu g.mL^{-1}$) cell death was reduced from 46% to 12%, attributable to the inhibition of recrystallisation during warming. At 3000 $\mu l.mL^{-1}$, cell death was increased to 50% because of the formation of spiracles which can pierce the cell membranes. High concentrations (> 1 $mg.mL^{-1}$) of the low molecular weight native AFGP-8 is toxic to human kidney and liver cells. A C-linked analogue, which does not show any thermal hysteresis activity,but retains the recrystallisation inhibition properties, shows none of this toxicity[198] (Figure 18). Interestingly, non mammalian cells (fish gill endothelium) were not affected even at high concentrations.

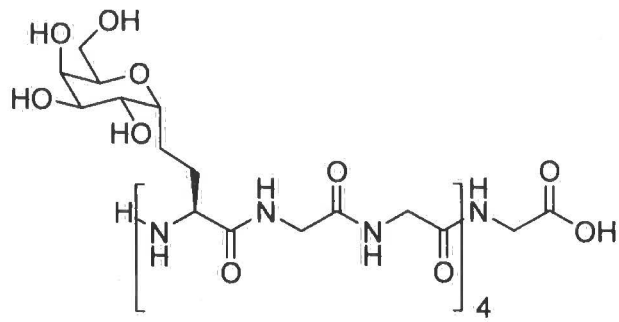

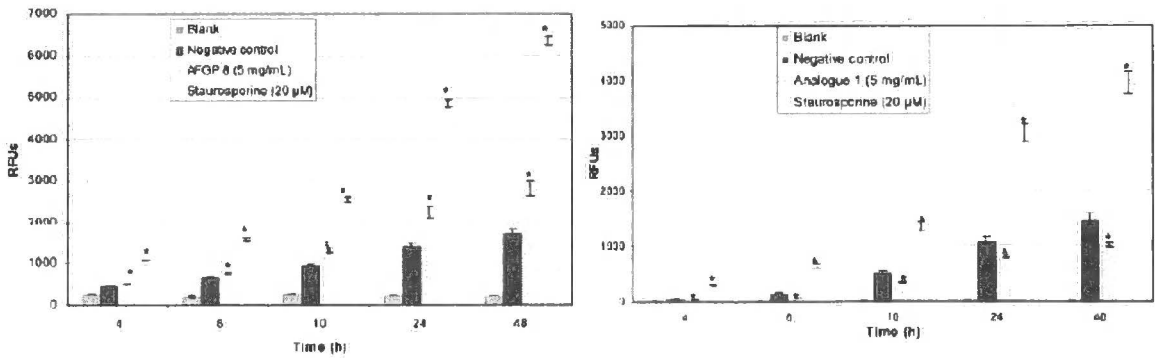

Figure 18. Toxicity evaluation of C-linked AFGP by the caspase-3/7 assay on human kidney cells. Increase RFU (fluorescence) values represent increased cell death. Above, structure of C-linked AFGP analogue tested here[198].

The final effect of AF(G)Ps on cellular protection is their interaction with cell membranes. During cooling of cells significant cell leakage often occurs due to the change in osmotic potential associated with extra-cellular ice formation which increases the concentration of dissolved salts. During the storage of pig oocytes at 4°C their membrane potentials were monitored[199]. The presence of AFGP (1→8) prevented any leakage of ions, probably due to blocking of the potassium and calcium ion channels during cooling[200]. Similar results are found with bull spermatozoa[201]. Blood platelets when cooled below 20°C loose membrane stability, thus they must be stored at raised (~22°C) temperatures which limits their 'shelf life' to 5 days. In the presence of AFGPs, platelets can be stored at 4°C for 21 days without losing their function[202]. Conversely, addition of AFGPs to isolated rat hearts which were then stored at hypothermic temperatures resulted in increased damage at all AFGP concentrations[203]. The interaction between various lipid membranes with AFGPs were investigated to draw insight into these processes[204]. Dielaidoylphosphatidylcholine (DEPC) liposomes were incubated with AFGP 8 down to 0°C. Without the AFGPs, cooling the liposomes resulted in leakage of 50% of their contents, whereas this was completely halted upon addition of up to 10 $mg.mL^{-1}$ AFGP, with the higher molecular weight fractions showing a stronger effect[205] (Figure 19). The leakage events were attributed to the membranes passing through their liquid-crystalline to gel phase transition, T_m, increasing their permeability. It is proposed that the interaction of the proteins with the membrane alters its Tm sufficiently to reduce/prevent leakage[206]. Those cells whose T_m's are unaffected such as galactolipids in plant thylakoids (or raised) by addition of AFGP suffer negative effects during cooling[207]. A comprehensive list of cell types stored with AF(G)Ps at low temperatures has been collated[208].

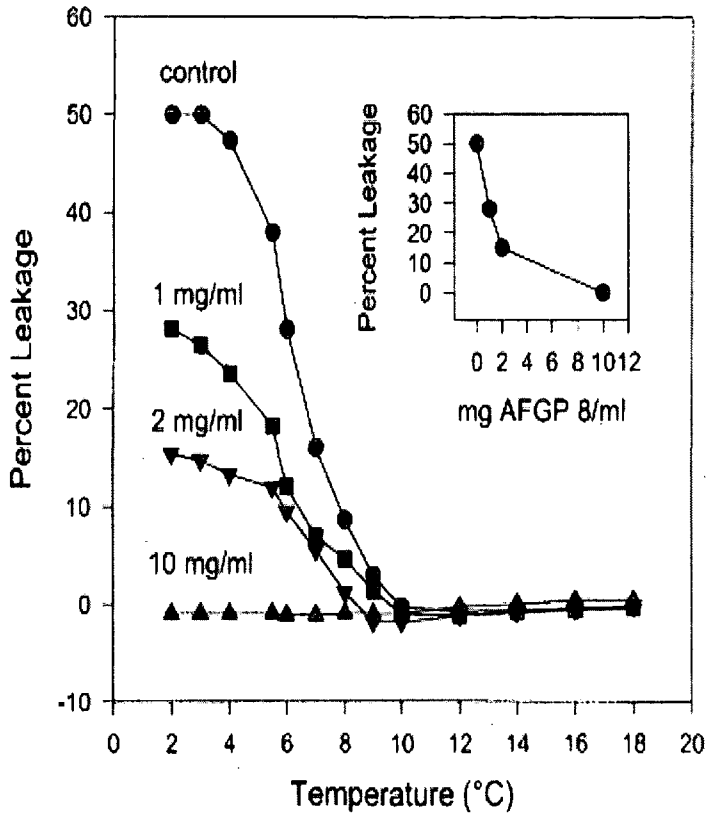

Figure 19. Leakage of a dye (carboxyfluorescin) from DEPC liposomes in the presence of differing concentrations of AFGP at various temperatures[204].

The ability to reduce the size of ice crystals by AF(G)Ps has potential applications in the frozen food industry[209]. These proteins do not appear to be toxic[210] by ingestion (despite the toxic effects when incubated with liver cells, discussed above[198]) with estimates that people living in northern climates consume up to 500 mg per day from fish and vegetation sources[211]. Reduction of the ice crystal size in frozen foods as they thaw improves the texture relative to when large crystals are present, particularly in the case of ice cream. This also allows the fat content to be reduced, as this is normally required to obtain the desired texture. A species of heat stable antifreeze proteins with strong recrystallisation inhibition has been identified for this purpose by Unilever UK[154,187,210,211], and is already added to ice cream in the USA. The effects on frozen meats have also been investigated[212]. Addition of AF(G)P

resulted in decreased size of intracellular spaces following thawing, which are caused by ice crystals, which gives a more desirable texture.

These observations indicate that although AF(G)Ps have many applications each individual effect of thermal hysteresis; dynamic ice shaping, recrystallisation inhibition and membrane interactions, must all be considered. Negative results, such as decreasing the viability of stored hearts, must not prevent the same tests being carried out on other model systems where positive results may be recorded.

These wide ranging applications have led to estimates of the total worldwide market for AF(G)Ps as high as $40 billion in 1999[213] and regularly attract media interest in specialist and popular publications[214-216].

1.4.4 SYNTHESIS OF AFGPS

Despite the wealth of potential applications of the AFGPs, outlined above, there does not yet exist any method for obtaining significant quantities of these proteins for study or application. Invariably all the methods involve solid phase peptide synthesis at one point or another. There still exists very few methods for their synthesis, and they are briefly reviewed here.

In 1988 Anderson *et al.* used a convergent approach to synthesise a close analogue of the AFGP tripeptide, with β–D-galactosyl-(1,3)-α-D-galactose in place of the native disaccharide[217], but larger polypeptides were not made. Later Filira *et al.* used stepwise solid phase synthesis using glycosylated amino acid and protected L-alanine to produce glycopolymers in a linear fashion[218] shown in Scheme 5.

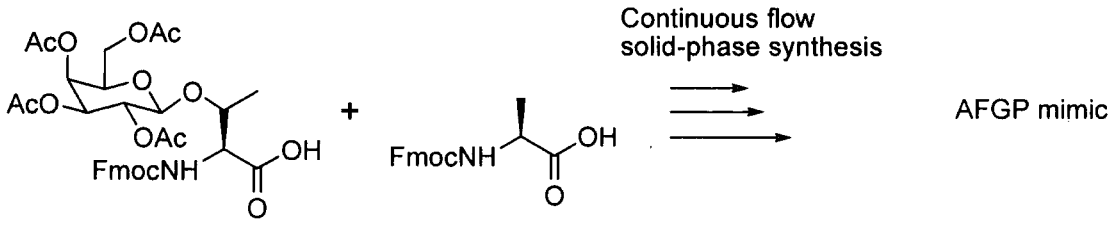

Scheme 5. Linear solid-phase synthesis of an AFGP mimic by Filira *et al.*[218]

These two methods were later combined by Robert Ben's group to produce glycopeptides by the stepwise peptide synthesis using tripeptide building blocks[219] (Scheme 6). This convergent approach has been used for a variety of AFGP mimcs including some with C-linked carbohohydrates which show higher enzymatic and chemical stability[220-222].

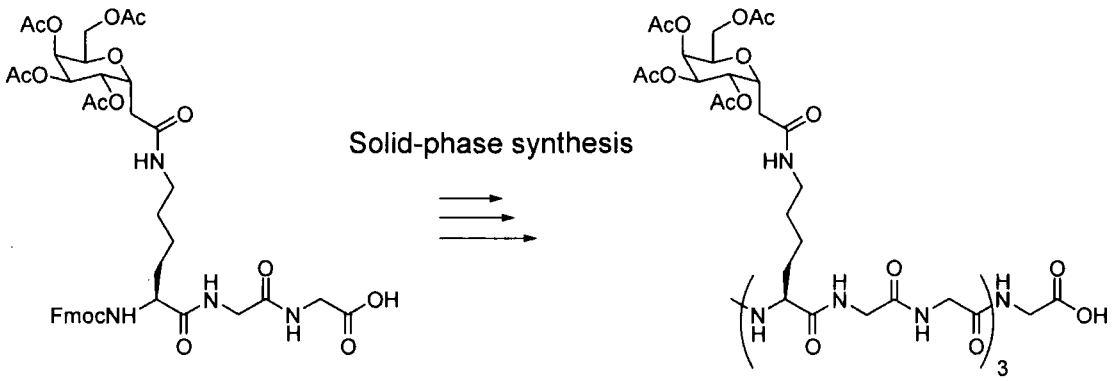

Scheme 6. Synthesis of glycopolypeptide by Ben *et al.*[220] as an AFGP analogue.

Nishimura *et al.* used conventional solid phase synthesis to create the tripeptide building block of native AFGP[223]. Following removal of all the protecting groups, this tripeptide unit was polymerised in a condensation reaction using peptide coupling agents to yield polymers with the same structure of AFGPs, but with polydisperse chain lengths[190]. This versatile strategy was extended to create a libraries of AFGP mimics with stepwise structural changes[188,189].

1.5 CONCLUDING REMARKS

Recent advances in polymer synthesis, carbohydrate chemistry and the understanding of peptide structure and function is allowing the basic mechanisms of life to be understood and exploited for biomedical applications. The weak but highly specific binding of carbohydrates with protein receptors is enhanced in nature by the presentation of multiple copies of the relevant ligands. Multivalent glycopolymers mimic this effect to allow competitive binding between polymer and natures multivalent structures present on virus and bacterium amongst others. Other polymeric structures have been created to mimic the highly specific ordering associated with polypeptide secondary (and higher order) structures, while retaining the benefits of synthetic polymers: ease of synthesis, variable architectures and a plethora of possible functionalities.

Glycoproteins present in nature have roles relating to both specific recognition *via* their carbohydrate groups and the 3-dimensional structure adopted by the peptide backbone, playing roles in catalysis, recognition and structure. There are currently few examples of synthetic materials which contain both these motifs due to the inherent difficulties their synthesis. Antifreeze glycoproteins are a particular interesting subset, in that their properties and biological importance are well understood on a micro- and macroscopic level but many questions remain regarding their solution conformation and the requirements of having the particular peptide backbone sequence and disaccharide. Recent work has suggested that both of these features are essential to maintain the thermal hysteresis and ice shaping effects but that the recrystallisation inhibition process can be retained even following major structural modification. Surprisingly, materials which are characterised as not being

antifreeze active are not screened for recrystallisation inhibition and thus the structural features necessary for this property are not understood. It is anticipated that modern polymer and carbohydrate chemistry can be combined to illuminate the mechanisms of these processes.

1.6 BIBLIOGRAPHIC REFERENCES

(1) Sakiyama-Elbert, S. E.; Hubbell, J. A. *Annu. Rev. Mater. Res.* **2001**, *31*, 183-201.

(2) Seal, B. L.; Otero, T. C.; Panitch, A. *Mat. Sci. Eng. R.* **2001**, *34*, 147-230.

(3) Wang, A.; Essner, A.; Polineni, K.; Stark, C.; Dumbleton, J. H. *Tribiology Int.* **1998**, *31*, 17-33.

(4) Mart, R. J.; Osborne, R. D.; Stevens, M. M.; Ulijn, R. V. *Soft Matter* **2006**, *2*, 822-835.

(5) Stryer, L. *Biochemistry*; 4th ed.; Freeman,, 1996.

(6) Muthukumar, M.; Ober, C. K.; Thomas, E. L. *Science* **1997**, *277*, 1225-1232.

(7) Abetz, V.; Goldacker, T. *Macromol. Rapid. Commun.* **2000**, *21*, 16-34.

(8) Ikkala, O.; ten Brinke, G. *Chem. Commun.* **2004**, 2131-2137.

(9) Rodriguez-Hernandez, J.; Checot, F.; Gnanou, Y.; Lecommandoux, S. *Prog. Polym. Sci.* **2005**, *30*, 691-724.

(10) Heredia, K. L.; Maynard, H. D. *Org. Biomol. Chem.* **2007**, *5*, 45-53.

(11) Boyer, C.; Bulmus, V.; Liu, J.; Davis, T. P.; Stenzel, M. H.; Barner-Kowollik, C. *J. Am. Chem. Soc.* **2007**, *129*, 7145-7154.

(12) Liu, J.; Bulmus, V.; Herlamband, D. L.; Barner-Kowollik, C.; Stenzel, M. H.; Davis, T. P. *Angew. Chem. Int. Ed.* **2007**, *46*, 3099-3103.

(13) Le Droumaguet, B.; Mantovani, G.; Haddleton, D. M.; Velonia, K. *J. Mater. Chem.* **2007**, *17*, 1916-1922.

(14) Klok, H.-A. *J. Pol. Sci. Part A: Pol. Chem.* **2005**, *43*, 1-17.

(15) Schlaad, H.; Antonietti, M. *Eur. Phys. J. E.* **2003**, *10*, 17-23.

(16) van Hest, J. C. M.; Tirrel, D. A. *Chem. Commun.* **2001**, 1897-1904.

(17) Zhang, S. *Nat. Biotech.* **2003**, *21*, 1171-1178.

(18) Borner, H. G.; Schlaad, H. *Soft Matter* **2007**, *3*, 394-408.

(19) Twaites, B.; de las Heras Alarcon, C.; Alexander, C. *J. Mater. Chem.* **2005**, *15*, 441-455.

(20) Duncan, R. *Nat. Rev. Drug. Disc.* **2003**, *2*, 347-360.

(21) Haag, R.; Kratz, F. *Angew. Chem. Int. Ed.* **2006**, *45*, 1198-1215.

(22) Gillies, E. R.; Dy, E.; Fréchet, J. M. J.; Szoka, F. C. *Mol. Pharm.* **2005**, *2*, 129-138.

(23) Lee, C. L.; Gillies, E. R.; Fox, M. E.; Guillaudeu, S. J.; Fréchet, J. M. J.; Dy, E.; Szoka, F. C. *Proc. Nat. Acad. Sci* **2006**, *103*, 16649-16654.

(24) Duncan, R. *Nat. Rev. Cancer.* **2006**, *6*, 688-701.

(25) Kochendoerfer, G. G.; Chen, S.-Y.; Mao, F.; Cressman, S.; Traviglia, S.; Shao, H.; Hunter, C. L.; Low, D. W.; Cagle, E. N.; Carnevali, M.; Gueriguian, V.; Keogh, P. J.; Porter, H.; Stratton, S. M.; Wiedeke, M. C.; Wilken, J.; Tang, J.; Levy, J. J.; Miranda, L. P.; Crnogorac, M. M.; Kalbag, S.; Botti, P.; Schindler-Horvat, J.; Savatski, L.; Adamson, J. W.; Kung, A.; Kent, S. B. H.; Bradburne, J. A. *Science* **2003**, *299*, 884-887.

(26) Shaunak, S.; Godwin, A.; Choi, J.-W.; Balan, S.; Pedone, E.; Vijayarangam, D.; Heidelberger, S.; Teo, I.; Zloh, M.; Brocchini, S. *Nat. Chem. Bio.* **2006**, *2*, 312-313.

(27) Balan, S.; Choi, J.-W.; Godwin, A.; Teo, I.; Laborde, C. M.; Heidelberger, S.; Zloh, M.; Shaunak, S.; Brocchini, S. *Bioconjugate Chem.* **2007**, *18*, 61-76.

(28) Roberts, M. J.; Bentley, M. D.; Harris, J. M. *Adv. Drug. Del. Rev.* **2002**, *54*, 459-476.

(29) Veronese, F. M. *Biomaterials* **2001**, *22*, 405-417.

(30) Veronese, F. M.; Harris, J. M. *Adv. Drug. Del. Rev.* **2002**, *54*, 453-456.

(31) Oishi, M.; Kataoka, K.; Nagasaki, Y. *Bioconjugate Chem.* **2006**, *17*, 677-688.

(32) Osada, K.; Kataoka, K. *Adv. Polym. Sci* **2006**, *202*, 113-153.

(33) Hoffman, A. S.; Stayton, P. S. *Macromol. Symp.* **2004**, *297*, 139-151.

(34) Stayton, P. S.; Shimoboji, T.; Long, C.; Chilkoti, A.; Chen, G.; Harris, J. M.; Hoffman, A. S. *Nature* **1995**, *378*, 472-474.

(35) Ding, Z.; Fong, R. B.; Long, C. J.; Stayton, P. S.; Hoffman, A. S. *Nature* **2001**, *411*, 59-62.

(36) Shimoboji, T.; Ding, Z.; Stayton, P. S.; Hoffman, A. S. *Bioconjugate Chem.* **2002**, *13*.

(37) Takei, Y. G.; Matsukata, M.; Aoki, T.; Sanui, K.; Ogata, N.; Kikuchi, A.; Sakurai, Y.; Okano, T. *Bioconjugate Chem.* **1994**, *5*, 577-582.

(38) Burkoth, T. S.; Benzinger, T. L. S.; Jones, D. N. M.; Hallenga, K.; Meredith, S. C.; Lynn, D. G. *J. Am. Chem. Soc.* **1998**, *120*, 7655-7656.

(39) Burkoth, T. S.; Benzinger, T. L. S.; Urban, V.; Lynn, D. G.; Meredith, S. C.; Thiyagarajan, P. *J. Am. Chem. Soc.* **1999**, *121*, 7429-7430.

(40) Thiyagarajan, P.; Burkoth, T. S.; Urban, V.; Seifert, S.; Benzinger, T. L. S.; Morgan, D. M.; Gordon, D.; Meredith, S. C.; Lynn, D. G. *J. Appl. Crystallog.* **2000**, *33*, 535-539.

(41) Waterhouse, S. H.; Gerrard, J. A. *Aust. J. Chem.* **2004**, *57*, 519-523.

(42) Zhao, H.-P.; Feng, X.-Q.; Shi, H.-J. *Mat. Sci. Eng.* **2007**, *C27*, 675-683.

(43) Rathore, O.; Sogah, D. Y. *J. Am. Chem. Soc.* **2001**, *123*, 5231-5239.

(44) Smeenk, J. M.; Schoen, P.; Otten, M. B. J.; Speller, S.; Stunnenberg, H. G.; van Hest, J. C. M. *Macromolecules* **2006**, *39*, 2989-2997.

(45) Ayres, L.; Adams, H. H. M.; Lowik, D. W. P. M.; van Hest, J. C. M. *Biomacromolecules* **2005**, *6*, 825-831.

(46) Herrero-Vanrell, R.; Rincon, A. C.; Alonso, M.; Reboto, V.; Molina-Martinez, I. T.; Rodriguez-Cabello, J. C. *J. Control. Rel.* **2005**, *102*, 113-122.

(47) Ayres, L.; Koch, K.; Adams, H. H. M.; van Hest, J. C. M. *Macromolecules* **2005**, *38*, 1699-1704.

(48) Zhou, M.; Bentley, D.; Ghosh, I. *J. Am. Chem. Soc.* **2003**, *126*, 734-735.

(49) Landschultz, W. H.; Johnson, P. F.; McKnight, S. L. *Science* **1988**, *240*, 1759-1764.

(50) Petka, W. A.; Harden, J. L.; McGrath, K. P.; Wirtz, D.; Tirrel, D. A. *Science* **1998**, *281*, 289-392.

(51) Wolf, E.; Kim, P. S.; Berger, B. *Protein. Sci.* **1997**, *6*, 1179-1189.

(52) Burkhard, P.; Stetefeld, J.; Strelkov, S. V. *Trends Cell Biol.* **2001**, *11*, 82-88.

(53) Mason, J. M. *Chem. Biol. Chem.* **2004**, *5*, 170-176.

(54) Pechar, M.; Kopeckova, P.; Joss, L.; Kopecek, J. *Macromol. Biosci.* **2002**, *2*, 199-206.

(55) Vandermeulen, G. W. M.; Tziatzios, C.; Duncan, R.; Klok, H.-A. *Macromolecules* **2005**, *38*, 761-769.

(56) Vandermeulen, G. W. M.; Hinderberger, D.; Xu, H.; Sheiko, S. S.; Jechke, G.; Klok, H.-A. *ChemPhysChem.* **2004**, *5*, 488-494.

(57) Hannik, J. M.; Cornelissen, J. J. L. M.; Farrera, J. A.; Foubert, P.; De Schryver, F. C.; Sommerdijk, N. A. J. M.; Nolte, R. J. M. *Angew. Chem. Int. Ed.* **2001**, *40*, 4732-4734.

(58) Boerakker, M. J.; Hannink, J. M.; Bomans, P. H. H.; Frederik, P. M.; Nolte, R. J. M.; Meijer, E. M.; Sommerdijk, N. A. J. M. *Angew. Chem. Int. Ed.* **2002**, *41*, 4239-4241.

(59) Kolb, H. C.; Finn, M. G.; Sharpless, K. B. *Angew. Chem. Int. Ed.* **2001**, *40*, 2004-2021.

(60) Huisgen, R. *Proc. Chem. Soc. Lond.* **1961**, 357-394.

(61) Dimitrov, I.; Kukula, H.; Colfen, H.; Schlaad, H. *Macrmol. Symp.* **2004**, *215*, 383-393.

(62) Douy, A.; Gallot, B. *Polymer* **1982**, *23*, 1039-1044.

(63) Schlaad, H.; Smarsly, B.; Below, I. *Macromolecules* **2006**, *39*, 4631-4632.

(64) Ludwigs, S.; Krausch, G.; Reiter, G.; Losik, M.; Anonietti, M.; Schlaad, H. *Macromolecules* **2005**, *38*, 7532-7535.

(65) Lubber, A.; Castelletto, V.; Hamley, I. W.; Nuhn, H.; Scholl, M.; Bourdillon, L.; Wandrey, C.; Klok, H.-A. *Langmuir.* **2005**, *21*, 6582-6589.

(66) Checot, F.; Lecommandoux, S.; Gnanou, Y.; Klok, H.-A. *Angew. Chem. Int. Ed.* **2002**, *41*, 1340-1343.

(67) Schappacher, M.; Soum, A.; Guillaume, S. M. *Biomacromolecules* **2006**, *7*, 1373-1379.

(68) Arimura, H.; Ohya, Y.; Ouchi, T. *Macromol. Rapid. Commun.* **2004**, *25*, 743-747.

(69) Laine, R. A. In *Glycosciences: Status and Perspectives*; Gabius, H. J., Gabius, S., Eds. London, 1997.

(70) Ladmiral, V.; Melia, E.; Haddleton, D. M. *Eur. Pol. J.* **2004**, *40*, 431-449.

(71) Okada, M. *Prog. Polym. Sci.* **2001**, *26*, 67-104.

(72) Spain, S. G.; Gibson, M. I.; Cameron, N. R. *J. Pol. Sci. Part A: Pol. Chem.* **2007**, *45*, 2059-2072.

(73) Kiessling, L. L.; Gestwicki, J. E.; Strong, L. E. *Angew. Chem. Int. Ed.* **2006**, *45*, 2348-2368.

(74) Mammen, M.; Choi, S.-K.; Whitesides, G. M. *Angew. Chem. Int. Ed.* **1998**, *37*, 2754-2794.

(75) Palian, M. M.; Boguslavsky, V. I.; O'Brien, D. F.; Polt, R. *J. Am. Chem. Soc.* **2003**, *125*, 5823-5831.

(76) Varki, A. *Glycobiology* **1993**, *3*, 97-130.

(77) Dwek, R. A. *Chem. Rev.* **1996**, *96*, 683-720.

(78) Hawker, C. J.; Wooley, K. L. *Science* **2005**, *309*, 1200-1205.

(79) Boyd, W. C.; Shapleigh, E. *Science* **1954**, *119*, 419.

(80) Lis, H.; Sharon, N. *Chem. Rev.* **1998**, *98*, 637-674.

(81) Dam, T. K.; Oscarson, S.; Roy, R.; Das, S. K.; Page, D.; Macaluso, F.; Brewer, C. F. *J. Biol. Chem.* **2005**, *280*, 8640-8646.

(82) Mammen, M.; Dahmann, G.; Whitesides, G. M. *J. Med. Chem* **1995**, *38*, 4179-4190.

(83) Lee, Y. C. In *Neoglycoconjugates: Preparation and Applications*; Lee, Y. C., Lee, R. T., Eds.; Academic Press: London, 1994.

(84) Komath, S. S.; Kavitha, M.; Swamy, M. J. *Org. Biomol. Chem.* **2006**, *4*, 973-988.

(85) Kunz, H. *Angew. Chem. Int. Ed.* **1987**, *26*, 294-308.

(86) Herner, H.; Reipen, T.; Schultz, M.; Kunz, H. *Chem. Rev.* **2000**, *100*, 4495-4537.

(87) Brocke, C.; Kunz, H. *Biorg. Med. Chem.* **2002**, *10*, 3085-3112.

(88) Gestwicki, J. E.; Cairo, C. W.; Strong, L. E.; Oetjen, K. A.; Kiessling, L. L. *J. Am. Chem. Soc.* **2002**, *124*, 14922-14933.

(89) Roy, R. *Trends Glycosci. Glycotechnol.* **2003**, *15*, 291-310.

(90) Mangold, S. L.; Cloninger, M. J. *Org. Biomol. Chem.* **2006**, *4*, 2458-2465.

(91) Wolfenden, M. L.; Cloninger, M. J. *Bioconjugate Chem.* **2006**, *17*, 958-966.

(92) Ambrosi, M.; Cameron, N. R.; Davis, B. G.; Stolnik, S. *Org. Biomol. Chem.* **2005**, *3*, 1476-1480.

(93) Dimik, S. M.; Powell, S. C.; McMahon, S. A.; Moothoo, D. N.; Naismith, J. H.; Toone, E. J. *J. Am. Chem. Soc.* **1999**, *121*, 10286-10296.

(94) Polizzotti, B. D.; Kiick, K. L. *Biomacromolecules* **2006**, *7*, 483-490.

(95) Horejsi, V.; Smolek, P.; Kocourek, J. *Biochem. Biophys. Acta* **1978**, *538*, 293-298.

(96) Loykulnant, S.; Hayashi, M.; Hirao, A. *Macromolecules* **1998**, *31*, 9121-9126.

(97) Yamanda, K.; Yamaoka, K.; Minoda, M.; Miyamoto, T. *J. Pol. Sci. Part A: Pol. Chem.* **1997**, *35*, 255-261.

(98) Hadjichristidis, N.; Iatrou, H.; Pispas, S.; Pitsikalis, M. *J. Pol. Sci. Part A: Pol. Chem.* **2000**, *38*, 3211-3234.

(99) Fraser, C.; Grubbs, R. H. *Macromolecules* **1995**, *28*, 7248-7255.

(100) Murphy, J. J.; Nomura, K.; Paton, R. M. *Macromolecules* **2006**, *39*, 3147-3153.

(101) Kanai, M.; Mortel, K. H.; Kiessling, L. L. *J. Am. Chem. Soc.* **1997**, *119*, 9931-9932.

(102) Ambrosi, M.; Batsanov, A. S.; Cameron, N. R.; Davis, B. G.; Howard, J. A. K.; Hunter, R. *J. Chem. Soc., Perkin Trans. 1* **2002**, 45-52.

(103) Gotz, H.; Harth, E.; Schiller, S. M.; Frank, C. W.; Knoll, W.; Hawker, C. J. *J. Pol. Sci. Part A: Pol. Chem.* **2002**, *40*, 3379-3391.

(104) Narumi, A.; Matsuda, T.; Kaga, H.; Satoh, T.; Kakuchi, T. *Polymer* **2002**, *43*, 4835-4840.

(105) Ohno, K.; Tsujii, Y.; Miyamoto, T.; Fukuda, T. *Macromolecules* **1998**, *31*, 1064-1069.

(106) Matyjaszewski, K.; Xia, J. *Chem. Rev.* **2001**, *101*, 2921-2990.

(107) Narain, R.; Armes, S. P. *Chem. Commun.* **2002**, 2776-2777.

(108) Narain, R.; Armes, S. P. *Macromolecules* **2003**, *36*, 4675-4678.

(109) Perrier, S.; Takolpuckdee, P. *J. Pol. Sci. Part A: Pol. Chem.* **2005**, *43*, 5347-5393.

(110) Lowe, A. B.; Sumerlin, B. S.; McCormick, C. L. *Polymer* **2003**, *44*, 6761-6765.

(111) Albertin, L.; Stenzel, M. H.; Barner-Kowollik, C.; Foster, L. J. R.; Davis, T. P. *Macromolecules* **2004**, *37*, 7530-7537.

(112) Bernad, J.; Favier, A.; Zhang, L.; Nilasaroya, A.; Davis, T. P.; Barner-Kowollik, C.; Stenzel, M. H. *Macromolecules* **2005**, *38*, 5475-5484.

(113) Bernard, J.; Hao, X.; Davis, T. P.; Barner-Kowollik, C.; Stenzel, M. H. *Biomacromolecules* **2006**, *7*, 232-238.

(114) Stenzel, M. H.; Zhang, L.; Huck, W. T. S. *Macromol. Rapid. Commun.* **2006**, *27*, 1121-1126.

(115) Muthukrishnan, S.; Erhard, D. P.; Mori, H.; Muller, A. H. E. *Macromolecules* **2006**, *39*, 2743-2750.

(116) Spain, S. G.; Albertin, L.; Cameron, N. R. *Chem. Commun.* **2006**, *4198-4200.*

(117) Takasu, A.; Niwa, T.; Itou, H.; Inai, Y.; Hirabayashi, T. *Macromol. Rapid. Commun.* **2000**, *21*, 764-769.

(118) Sigal, G. B.; Mammen, M.; Dahmann, G.; Whitesides, G. M. *J. Am. Chem. Soc.* **1996**, *118*, 3789-3800.

(119) Godwin, A.; Hartenstein, M.; Muller, A. H. E.; Brocchini, S. *Angew. Chem. Int. Ed.* **2001**, *40*, 594-597.

(120) Monge, S.; Haddleton, D. M. *Eur. Pol. J.* **2004**, *40*, 37-45.

(121) Hu, Z.; Liu, Y.; Hong, C.; Pan, C. *J. Appl. Polym. Sci.* **2005**, *98*, 189-194.

(122) Xue, C.; Donuru, V. R. R.; Liu, H. *Macromolecules* **2006**, *39*, 5747-5752.

(123) You, L.; Schlaad, H. *J. Am. Chem. Soc.*. **2006**, *128*, 13336-13337.

(124) Tsiourvas, D.; Paleos, C. M.; Dais, P. J. *J. Appl. Polym. Sci.* **1989**, *38*, 257-264.

(125) Schmidt, U.; Zschoche, S.; Werner, C. J. *J. Appl. Polym. Sci.* **2003**, *87*, 1255-1266.

(126) Labsky, J. *J. Eur. Polym. Mater.* **2006**, *42*, 209-212.

(127) Ladmiral, V.; Mantovani, G.; Clarkson, G. J.; Cauet, S.; Irwin, J. L.; Haddleton, D. M. *J. Am. Chem. Soc.*. **2006**, *128*, 4823-4830.

(128) Marmuse, L.; Nepogodiev, S. A.; Field, R. A. *Org. Biomol. Chem.* **2005**, *3*, 2225-2227.

(129) Gao, H.; Matyjaszewski, K. *Macromolecules* **2006**, *39*, 4960-4965.

(130) Wu, P.; Malkoch, M.; Hunt, J. N.; Vestberg, R.; Kaltgrad, E.; Finn, M. G.; Fokin, V. V.; Sharpless, K. B.; Hawker, C. J. *Chem. Commun.* **2005**, 5775-5777.

(131) Fernandez-Megia, E.; Correa, J.; Rodriguez-Meizoso, I.; Riguera, R. *Macromolecules* **2006**, *39*, 2113-2120.

(132) Fernandez-Megia, E.; Correa, J.; Riguera, R. *Biomacromolecules* **2006**, *7*, 3104-3111.

(133) Srinivasachari, S.; Liu, Y.; Zhang, G.; Prevette, L.; Reineke, T. M. *J. Am. Chem. Soc.* **2006**, *126*, 8176-8184.

(134) van Steenis, D. J. V. C.; David, O. R. P.; van Strijdonck, G. P. F.; van Maarseveen, J. H.; Reek, J. N. H. *Chem. Commun.* **2005**, 4333-4335.

(135) Roy, R. *Curr. Opin. Struct. Biol.* **1996**, *6*, 692-702.

(136) Lee, C. L.; Gillies, E. R.; Fox, M. E.; Guillaudeu, S. J.; Fréchet, J. M. J.; Dy, E. E.; Szoka, F. C. *Proc. Nat. Acad. Sci* **2006**, *103*, 16649-16654.

(137) Fleming, C.; Maldjian, A.; Da Costa, D.; Rullay, A. K.; Haddleton, D. M.; St. John, J.; Penny, P.; Noble, R. C.; Cameron, N. R.; Davis, B. G. *Nature Chem. Biol.* **2005**, *1*, 270-274.

(138) Ortega-Munoz, M.; Lopez-Jaramillo, J.; Hernandez-Mateo, F.; Santoyo-Gonzalez, F. *Adv. Synth. Catal.* **2006**, *348*, 2410-2420.

(139) Kamitakahara, H.; Suzuki, T.; Nishigori, N.; Suzuki, Y.; Kanie, O.; Wong, C.-H. *Angew. Chem. Int. Ed.* **1998**, *37*, 1524-1528.

(140) Deng, H.-T.; Xu, Z.-K.; Dai, Z.-W.; Wu, J.; Seta, P. *Enzyme. Mic. Tech.* **2005**, *36*, 996-1002.

(141) Vazquez-Dorbatt, V.; Maynard, H. D. *Biomacromolecules* **2006**, *7*, 2297-2302.

(142) de la Fuente, J. M.; Penades, S. *Biochem. Biophys. Acta* **2006**, *1760*, 636-651.

(143) Zhu, J.; Marchant, R. E. *Biomacromolecules* **2006**, *7*, 1036-1041.

(144) Ye, W.; Wells, S.; Desimone, J. M. *J. Pol. Sci. Part A: Pol. Chem.* **2001**, *39*, 3841-3849.

(145) Knight, C. A.; Cheng, C. C.; DeVries, A. L. *BioPhys. J.* **1991**, *59*, 409-418.

(146) DeVries, A. L.; Komatsu, S. K.; Feeney, R. E. *J. Biol. Chem.* **1979**, *245*, 2901-2908.

(147) Jin, Y.; DeVries, A. L. *Comp. Biochem. Phys. Part B* **2006**, *144*, 290-300.

(148) DeVries, A. L.; Wohlschlag, D. E. *Science* **1969**, *163*, 1073.

(149) Krisiansen, E.; Zachariassen, K. E. *Cryobiology* **2005**, *51*, 262-280.

(150) Graether, G. P.; Kuiper, M. J.; Gagne, S. M.; Walker, V. K.; Kia, Z.; D., S. B.; Davies, P. L. *Nature* **2000**, *406*, 325-328.

(151) Atici, O.; Nalbantoglu, B. *Phytochemistry* **2003**, *64*, 1187-1196.

(152) Duman, J. G. *Annu. Rev. Physiol.* **2001**, *63*, 327-357.

(153) Graham, L. A.; Davies, P. L. *Science* **2005**, *310*, 461.

(154) Sidebottom, C.; Buckley, S.; Pudney, P.; Twigg, S.; Jarman, C.; Holt, C.; Telford, J. *Nature* **2000**, *406*, 256.

(155) Smallwood, M.; Worral, D.; Byass, L.; Elias, L.; Ashford, D.; Doucet, C. J.; Holt, C.; Telford, J.; Lillford, P.; Bowles, D. *Biochem. J.* **1999**, *340*, 385-391.

(156) Kawahara, H. *J. Biosci. Bioeng.* **2002**, *94*, 492-496.

(157) Hsio, K.-C.; Chen, C.-H. C.; Fernandez, I. E.; Detrich, H. W.; DeVries, A. L. *Proc. Nat. Acad. Sci* **1990**, *87*, 9265-9269.

(158) Chen, L.; DeVries, A. L.; Cheng, C. H. *Proc. Nat. Acad. Sci* **1997**, *94*, 3811-3816.

(159) Chen, L.; DeVries, A. L.; Cheng, C. H. *Proc. Nat. Acad. Sci* **1997**, *94*, 3817-3822.

(160) Komatsu, S. K.; DeVries, A. L.; Feeney, R. E. *J. Biol. Chem.* **1970**, *245*, 2909-2913.

(161) Bouvet, V.; Ben, R. N. *Cell Biochem. Biophys.* **2003**, *39*, 133-144.

(162) Hederos, M.; Kondranson, P.; Borgh, A.; Liedberg, B. *J. Phys. Chem. B* **2005**, *109*, 15849-15859.

(163) Ben, R. N. *ChemBioChem* **2001**, *2*, 161-166.

(164) Wilson, P. W. *Cryo Lett.* **1993**, *14*, 31-36.

(165) Knight, C. A.; Wierzbicki, A. *Cryst. Growth. Des.* **2001**, *1*, 439-446.

(166) Sander, L. M.; Tkachenko, A. V. *Phys. Rev. Lett.* **2004**, *93*, 128102-1 - 128102-4.

(167) Knight, C. A.; Driggers, E.; DeVries, A. L. *BioPhys. J.* **1993**, *64*, 252-259.

(168) Raymond, J. A.; Wilson, P.; DeVries, A. L. *Proc. Nat. Acad. Sci* **1989**, *86*, 881-885.

(169) Knight, C. A.; Wierzbicki, A.; Laursen, R. A.; Zhang, W. *Cryst. Growth. Des.* **2001**, *1*, 429-438.

(170) Griffith, M.; Yaish, W. F. *Trends Plant Sci.* **2004**, *9*, 399-405.

(171) Chakrabartty, A.; Ananthanarayanan, V. S.; Hew, C. L. *J. Biol. Chem.* **1989**, *264*, 11307-11312.

(172) Chakrabartty, A.; Ananthanarayanan, V. S.; Hew, C. L. *J. Biol. Chem.* **1989**, *264*, 11313-11316.

(173) Sarno, D. M.; Murphy, A. V.; DiVirgilio, E. S.; Jones, W. E. J.; Ben, R. N. *Langmuir* **2003**, *19*, 4740-4744.

(174) Scotter, A. J.; Marshall, C. B.; Graham, L. A.; Gilbert, J. A.; Garnham, C. P.; Davies, P. L. *Cryobiology* **2006**, *53*, 229-239.

(175) Ewart, K. V.; Lin, Q.; Hew, C. L. *Cell. Mol. Life. Sci.* **1999**, *55*, 271-283.

(176) Kuiper, M. J.; Fecondo, J. V.; Wong, M. G. *J. Peptide. Res* **2002**, *59*, 1-8.

(177) Krishnan, V. V.; Lau, E. Y.; Tsvetkova, N. M.; Feeney, R. E.; Fink, W. H.; Yeh, Y. *J. Chem. Phys.* **2005**, *123*, 044702, 1-8.

(178) Harding, M. M.; Ward, L. G.; Haymet, A. D. J. *Eur. J. Biochem.* **1999**, *264*, 653-665.

(179) Graether, G. P.; Sykes, B. D. *Eur. J. Biochem.* **2004**, *271*, 3285-3296.

(180) DeVries, A. L.; Komath, S. K.; Feeney, R. E. *J. Biol. Chem.* **1970**, *245*, 2901-2908.

(181) Lane, A. N.; Hays, L. M.; Feeney, R. E.; Crowe, L. M.; Crowe, J. H. *Protein. Sci.* **1998**, *7*, 1555-1563.

(182) Lane, A. N.; Hays, L. M.; Tsvetkova, N. M.; Feeney, R. E.; Crowe, L. M.; Crowe, J. H. *BioPhys. J.* **2000**, *78*, 3195-3207.

(183) Tsvetkova, N. M.; Phillips, B. L.; Krishnan, V. V.; Feeney, R. E.; Fink, W. H.; Crowe, J. H.; Risbud, S. H.; Tablin, F.; Yeh, Y. *BioPhys. J.* **2002**, *82*, 464-473.

(184) Harding, M. M.; Anderberg, P. I.; Haymet, A. D. J. *Eur. J. Biochem.* **2003**, *270*, 1381-1392.

(185) Lin, Q.; Ewart, K. V.; Yang, D. S. C.; Hew, C. L. *FEBS Lett.* **1999**, *453*, 331-334.

(186) Houston, M. E.; Chao, H.; Hodges, R. S.; Sykes, B. D.; Kay, C. M.; Sonnichsen, F. D.; Loewen, M. C.; Davies, P. L. *J. Biol. Chem.* **1998**, *273*, 11714-11718.

(187) Baderschneider, B.; Crevel, R. W. R.; Earl, L. K.; Lalljie, A.; Sanders, D. J.; Sanders, I. J. *Food Chem. Tox.* **2002**, *40*, 965-978.

(188) Tachibana, Y.; Fletcher, G. L.; Fujitani, N.; Tsuda, S.; Monde, K.; Nishimura, S.-I. *Angew. Chem. Int. Ed.* **2004**, *43*, 856-862.

(189) Tachibana, Y.; Matsubara, N.; Nakajim, F.; Tsuda, T.; Tsuda, S.; Monde, K.; Nishimura, S.-I. *Tetrahedron* **2002**, *58*, 10213-10224.

(190) Tachibana, Y.; Monde, K.; Nishimura, S.-I. *Macromolecules* **2004**, *37*, 6771-6779.

(191) Kaiser, J. *Science* **2002**, *295*, 1015.

(192) Polge, C.; Smith, A. U.; Parkes, A. S. *Nature* **1949**, *164*, 666.

(193) Wang, J.-H. *Cryobiology* **2000**, *41*, 1-9.

(194) Palasz, A. T.; Mapletoft, R. J. *Biotech. Adv.* **1996**, *14*, 127-149.

(195) Rubinsky, B. *Annu. Rev. Eng.* **2000**, *2*, 157-187.

(196) Pham, L.; Dahiya, R.; Rubinsky, B. *Cryobiology* **1999**, *38*, 169-175.

(197) Matsumoto, S.; Matsusita, M.; Morita, T.; Kamachi, H.; Tsukiyama, S.; Furukawa, Y.; Koshida, S.; Tachibana, Y.; Nishimura, S.-I.; Todo, S. *Cryobiology* **2006**, *52*, 90-98.

(198) Liu, S.; Wang, W.; vonMoos, E.; Jackman, J.; Mealing, G.; Monette, R.; Ben, R. N. *Biomacromolecules* **2007**, DOI: 10.1021/bm061044o.

(199) Rubinsky, B.; Arav, A.; Mattiolo, M.; DeVries, A. L. *Biochem. Biophys. Res. Commun.* **1990**, *173*, 1369-1374.

(200) Arav, A.; Rubinsky, B.; Seren, E.; Roche, J. F.; Boland, M. P. *Theriogenology* **1994**, *41*, 107-112.

(201) Prathalingham, N. S.; Holt, W. V.; Revell, S. G.; Mirczuk, S.; Fleck, R. A.; Watson, P. F. *Theriogenology* **2006**, *66*, 1894-1900.

(202) Tablin, F.; Oliver, A. E.; Walker, N. J.; Crowe, L. M.; Crowe, J. H. *J. Cell. Physiol.* **1996**, *168*, 305-313.

(203) Wang, T. C.; Zhu, Q. Y.; Yang, X. P.; Layne, J. R.; DeVries, A. L. *Cryobiology* **1994**, *31*, 185-192.

(204) Hays, L. M.; Feeney, R. E.; Crowe, L. M.; Crowe, J. H.; Oliver, A. E. *Proc. Nat. Acad. Sci* **1996**, *93*, 6835-6840.

(205) Wu, Y.; Banoub, J.; Goddard, S. V.; Kao, M. H.; Fletcher, G. L. *Comp. Biochem. Phys. Part B* **2001**, *128*, 265-273.

(206) Tomczak, M. M.; Hincha, D. K.; Estrada, S. D.; Wolkers, W. F.; Crowe, L. M.; Feeney, R. E.; Tablin, F.; Crowe, J. H. *BioPhys. J.* **2002**, *82*, 874-881.

(207) Tomczak, M. M.; Hincha, D. K.; Estrada, S. D.; Feeney, R. E.; Crowe, J. H. *Biochem. Biophys. Acta* **2001**, *1511*, 255-263.

(208) Inglis, S. R.; Turner, J. J.; Harding, M. M. *Curr. Protein. Pep. Sci.* **2006**, *7*, 509-522.

(209) Griffith, M.; Ewart, K. V. *Biotech. Adv.* **1995**, *13*, 375-402.

(210) Hall-Manning, T.; Spurgeon, M. J.; Wolfreys, A. M.; Baldrick, A. P. *Food Chem. Tox.* **2004**, *42*, 321-33.

(211) Crevel, R. W. R.; Fedyk, J. K.; Spurgeon, M. J. *Food Chem. Tox.* **2002**, *40*, 899-903.

(212) Payne, S. R.; Sandford, D.; Harris, A.; Young, O. A. *Meat Sci.* **1994**, *37*, 429-438.

(213) Fletcher, G. L.; Goddard, S. V.; Yaling, W. *CHEMTEC* **1999**, *30*, 17-28.

(214) Ritter, S. In *Chem. Eng. News*, October 2005.

(215) Wilson, E. In *Chem. Eng. News*, February 2004.

(216) Davis, K. In *New Scientist*, October 2004.

(217) Anisuzzaman, A. K. M.; Anderson, L.; Navia, J. L. *Carb. Res.* **1988**, *174*, 265-278.

(218) Filira, F.; Bondi, L.; Scolaro, B.; Foffani, M. T.; Mammi, S.; Peggion, E.; Rocchi, R. *Int. J. Biol. Macromol.* **1990**, *12*, 41-49.

(219) Eniade, A.; Ben, R. N. *Biomacromolecules* **2001**, *2*, 557-561.

(220) Eniade, A.; Murphy, A. V.; Landreau, G.; Ben, R. N. *Bioconjugate Chem.* **2001**, *12*, 817-823.

(221) Eniade, A.; Purushotham, M.; Ben, R. N.; Wang, J. B.; Horwath, K. *Cell Biochem. Biophys.* **2003**, *38*, 115- 124.

(222) Liu, S.; Ben, R. N. *Org. Lett* **2005**, *7*, 2385-2388.

(223) Tsuda, T.; Nishimura, S.-I. *Chem. Commun.* **1996**, 2779 - 2780.

CHAPTER 2

SYNTHESIS AND CHARACTERISATION OF GLYCOSYLATED AND NON-GLYCOSYLATED *N*-CARBOXY ANHYDRIDES

2.1 INTRODUCTION

The synthesis of polypeptides is usually achieved by one of three methods: solid phase synthesis; bio-engineering[1]; or the polymerisation of *N*-carboxy anhydrides[2] (NCAs). The NCA route is the most convenient method to obtain high molecular weight homo-polypeptides.[†] The first reported synthesis of NCAs was by Leuchs[3‡] in 1906, while he was attempting the stepwise synthesis of polypeptides.

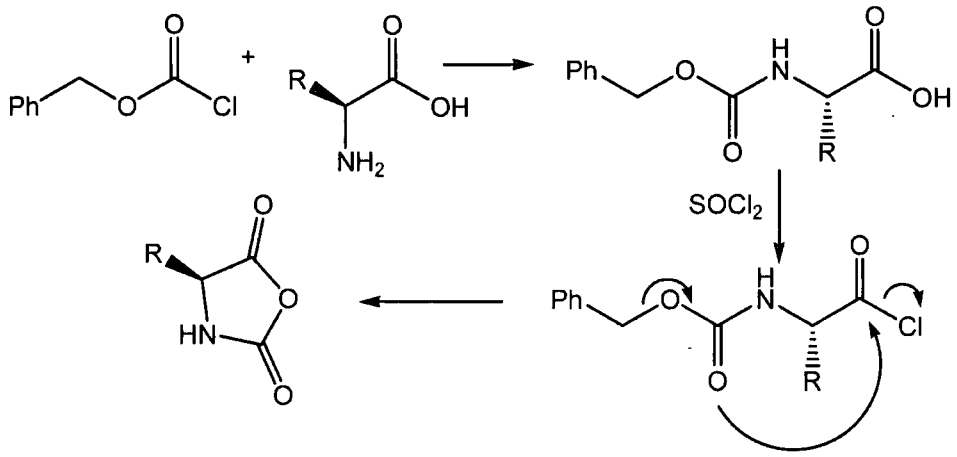

Scheme 1. Synthesis of NCAs by the Leuchs approach

Phenyl chloroformate derivatives of amino acids were used in his original synthesis, although it has also been described with methyl and ^{t}Bu equivalents. Activation of the carboxylic acid by thionyl chloride[4], then heating to reflux triggered an intramolecular cyclisation rather than intermolecular condensation give the anhydride. Although this method is now 100 years old, it is still an attractive method due to the simplicity of the alkoxyamino acid starting materials. PBr_3 and PCl_5[5,6] have also been used to activate the carboxylic acid. Apart from the toxicity and handling difficulties associated with thionyl chloride, the main difficulty with this method lies

[†] Details of the polymerisation of NCAs is covered in chapters 3 and 4 and reference [2]
[‡] NCAs are also less commonly referred to as Leuchs anhydrides, after their discoverer.

in the high temperature required for cyclisation which is close to that at which many NCAs decompose thermally.

The most common method used now for the synthesis of NCAs is the Fuchs-Farthing method[7]. It was shown that simply treating an amino acid with phosgene gas in an inert organic solvent (such as dioxane or ethyl acetate) gave the corresponding NCA in high yield (>70%) with short reaction times (<3 hours) and no racemisation (Scheme 2).

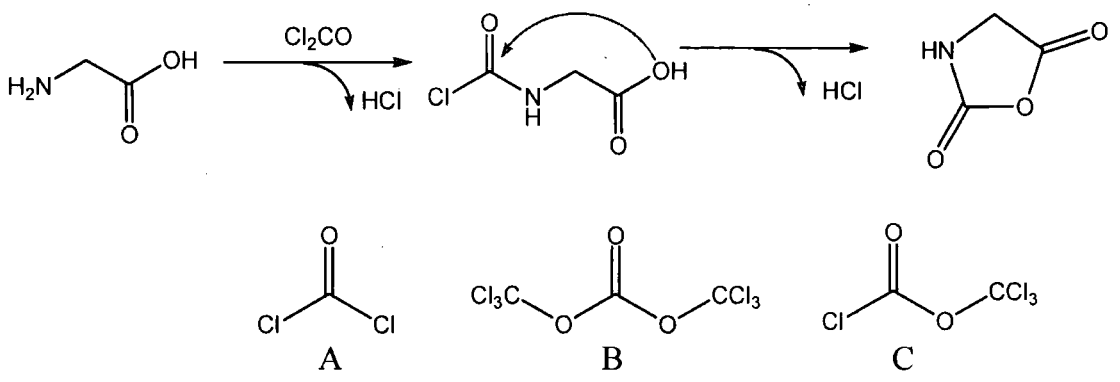

Scheme 2. Top. Fuchs-Farthing synthesis of glycine NCA using phosgene gas; below. (A) phosgene; (B) triphosgene; (C) diphosgene

In 1987 Eckert and Forster[8] showed that triphosgene (Scheme 2, B) could replace phosgene in many reactions. This is a solid at room temperature, so is far simpler and safer to handle on a laboratory scale and provides three equivalents of phosgene. Diphosgene[9] has also been used to a lesser extant, shown in Scheme 2 C. Triphosgene was soon shown to be suitable for NCA synthesis[10], and is now widely applied[11-14]. Another analogue of this is di-tert-butyltricarbonate[15] which offers the advantage of no HCl by-products but gave poor yields (25%) for less soluble amino acids.

Mobashery and Johnston[16] first used *N*-Boc protected amino acids as precursors to NCAs. By functionalising the carboxylic acid with a ^{t}Bu-dimethyl silyl ester and activation with oxalyl chloride they achieved quantitative conversion to

NCAs (Scheme 3 A). This was later improved[17] to a one-pot synthesis by removing the requirement for silyl ester synthesis. Simply treating *N*-Boc amino acids with triphosgene gave the corresponding NCA in over 70% yield, in the same fashion as Leuch's synthesis. (See above) This reaction proceeds at room temperature and the *N*-Boc group imparts greater solubility in organic solvents relative to the free amino acid (Scheme 3 B).

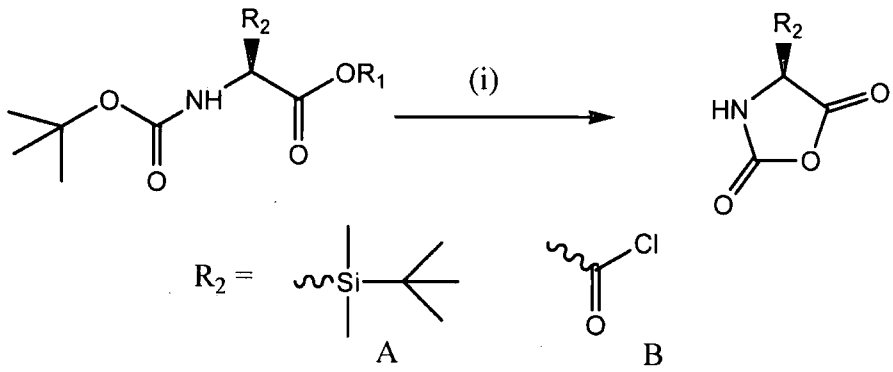

Scheme 3. Synthesis of NCAs from *N*-Boc amino acids. Where R_2 = any protected amino acid side chain. Conditions (i) When R_1 = A: oxalyl chloride, 0°C, 5 mins; R_2 = B: RT, 3 h B is introduced by triphosgene.

Some peptide coupling agents such as PyBop[18] and P_2O_5[19] induce cyclisation of *N*-Boc amino acids However, DCC[20] has been shown instead to form a symmetric anhydride. There are many more methods in the literature for NCA synthesis which can not be all be covered here including the Curtis conversion[21] which yields exclusively racemic NCA mixtures and re-arrangement of a β-lactam[22]. Perhaps the most interesting new synthesis is that of Taillades *et al*[23,24] which involves nitrosating *N*-carbamoyl amino acids, producing only H_2O and N_2 as side products. This has led to speculation that NCAs could have been involved in the prebiotic formation of peptides on Earth[25-27].

Most of the methods described above generate HCl as a side product, which can cause serious problems with NCA polymerisation[2] (see Chapter 3). Typically,

NCA purification is achieved by repeated precipitations or by judicious choice of solvent mixtures to minimise the solubility of HCl. Numerous papers and patents describe methods to reduce the HCl content by including charcoal as an absorbent[28], purging N_2 through the solution[29] and addition of alkenes[30,31] as scavengers.

In 1966 Rude and co-workers[32] demonstrated that oligo-(glyco)peptides could be synthesised by the addition of carbohydrate-functionalised NCAs to short peptide sequences.

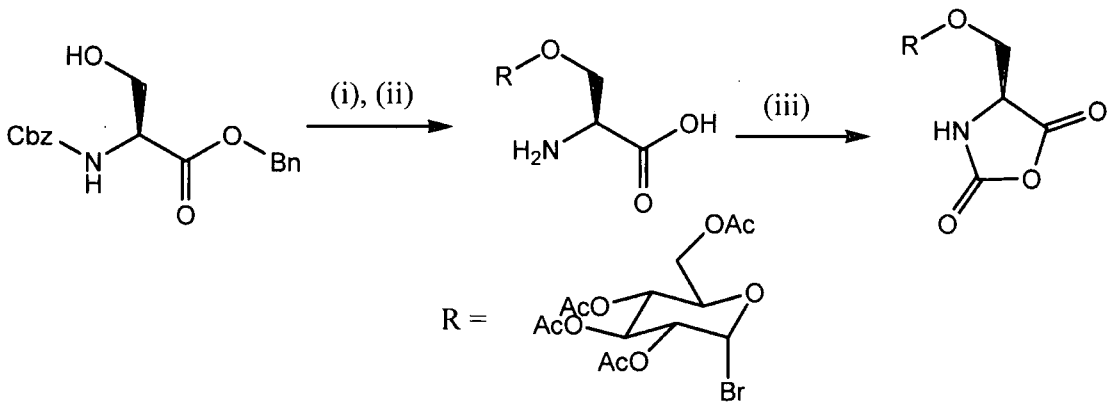

Scheme 4. Synthesis of GlycoNCA by Rude *et al.* (i) acetobromoglucose (2 equiv), $Hg(CN)_2$ (excess), dry nitromethane, 3 days; (ii) H_2/Pd, MeOH; (iii) phosgene (excess), dry dioxane, 60°C, 1 h, N_2.

The synthesis is shown in Scheme 4. The glycosylation step involves the Koenig-Knorr reaction[33] between an acetobromo sugar and a suitably protected amino acid. A promoter is required to activate the anomeric bromide and in this case an insoluble highly toxic[34] mercury salt, $Hg(CN)_2$, was used giving a reactive intermediate which can be attacked nucleophilically by the alcohol group of serine. This glycosylation promoter has been superseded by the use of less toxic Lewis acid promoters such as BF_3 and $AlCl_3$ which are tolerant of free carboxylic acid groups[35,36], thus increasing the atom efficiency of multistep syntheses. Many more strategies are available for the synthesis of glycosylated amino acids including activated cyclohexene donors[37], thioglycosides[38], enzymatic[39], and recombinant gene

expression[40] but these require more synthetic steps and are more suited to complex polysaccharide formation. Synthesis of the NCA is accomplished by taking the partially deprotected intermediate (shown in Scheme 4) and reacting it with phosgene in the Fuchs-Farthing method. This is currently the only literature method for the synthesis of NCAs, giving a final yield of less than 40% and as low as 15% for the β-D-galactose derivative[32]. Biodi *et al.*[41] did report a small modification when they used triphosgene instead of phosgene. Aoi *et al.* are the only group to have published the successful polymerisation of glycoNCAs[42], which were all derived from serine.

2.2 RESULTS AND DISCUSSION

Two different routes were employed to synthesise the glycosylated and non-glycosylated NCAs. For clarity they will be discussed separately.

2.2.1 NON-GLYCOSYLATED NCAS

The protected monomers Thr(Bzl)NCA (**1**), Glu(Bzl)NCA (**2**), Lys(Boc)NCA (**3**) and Ala NCA (**4**) were synthesised by the intramolecular cyclisation of their parent *N*-Boc protected amino acids by treatment with triphosgene and NEt_3 in dry ethyl acetate. The synthetic procedure is shown in Scheme 5. The decision to use this method was made primarily on availability of materials and minimising the number of synthetic steps. An initial investigation was undertaken to use per-trimethyl silyl protected L-threonine[43,44], which can be converted directly to the NCA. This was soon disregarded due to the difficulties encountered in purification (distillation) and lability of TMS ethers/esters/amides even under mild conditions.

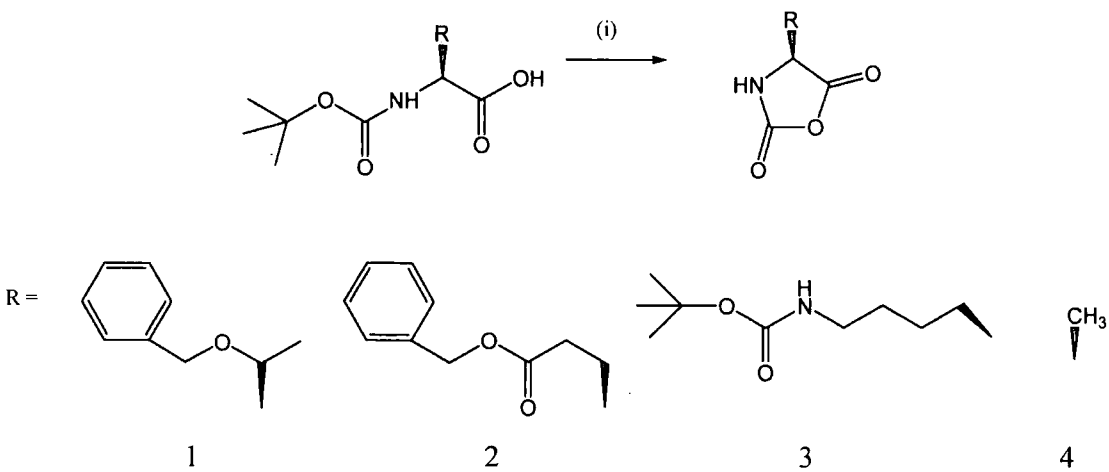

Scheme 5. Synthesis of NCAs from *N*-Boc amino acids with the R groups suitably protected. Conditions: (i) triphosgene (1/3 equiv); NEt_3 (1 equiv); dry EtOAc; under N_2; RT; 16 h.

A wide range of *N*-Boc protected amino acids with protected R groups are readily available, and the single step cyclisation expedites the process. The protecting groups also increases the solubility in organic solvents, relative to the free amino acids, which can exist as doubly charged zwitterions, leading to improved yields in some cases. This method (as with many others) is known to proceed without racemisation of the chiral centre.

The choice of ethyl acetate as solvent was important in this reaction to ensure that the NEt_3.HCl salt, which precipitates, is as sparingly soluble as possible. Reducing the temperature to –20°C prior to filtration aided its precipitation, but probably led to some precipitation of the NCA as well. During the course of the reaction excess HCl will be present, which can lead to cleavage of the Boc group and generation of the corresponding salt. These amino acid salts are insoluble in ethyl acetate and are either removed with the NEt_3.HCl by filtration or can react with triphosgene by the Fuchs-Farthing[45] route to give the same NCA product.

The formation of NCAs is traditionally confirmed by their characteristic infrared absorption bands in the carbonyl region. The unsymmetrical anhydrides give two C=O stretches in the region of 1750-1850 cm^{-1}, which are resolved from other common carbonyls such as esters and carbamates. These are summarised in Table 1.

Table 1. Infrared absorbances for NCAs synthesised[a]

		IR peaks (cm^{-1})	
NCA	**Yield**	**C_2=O**	**C_5=O**
Thr(Bzl) (1)	64 %	1860	1791
Glu(Bzl) (2)	55 %	1864	1705
Lys(Boc) (3)	65 %	1862	1769
Al (4)	68%	1861	1772

(a) Obtained from 5mg of sample prepared as a KBr disc

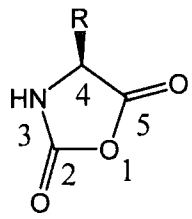

Scheme 6. Numbering scheme used for characterisation of NCAs

The ^{1}H NMR spectra of the NCAs show a peak attributable to N-**H**. Due to the labile nature of protons bound to nitrogen atoms, this peak can vary in both chemical shift and in its integral relative to C-**H** peaks. The consequences of this are discussed in some more detail in Chapter 3. There is no evidence of any residual Boc methyl groups in the ^{13}C NMR spectra for all the NCAs synthesised (Figure 1), indicating complete conversion to the NCA.

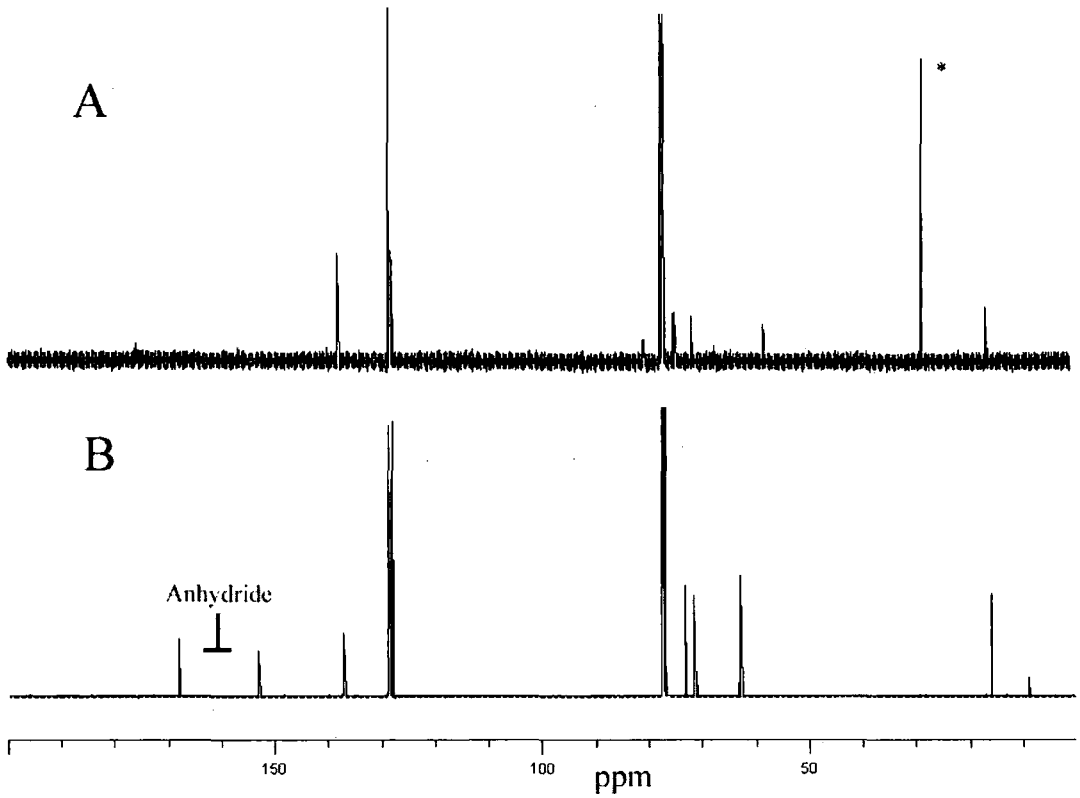

Figure 1. ^{13}C NMR spectra of A: *N*-Boc-(*O*-benzyl)-L-threonine, with methyl carbon of Boc marked*; B: *O*-benzyl-L-threonine NCA. Two carbonyl peaks arising from NCA are marked.

These monomers must be extremely pure if they are to be used in controlled polymerisation by the 'amine' mechanism. The standard methods for determination of the purity of small organic molecules are elemental analysis and/or chromatography of some type – normally GC or HPLC. NCAs will degrade to some extent during chromatography making it difficult to determine purity by this method. Similar arguments hold for elemental analysis, which is not normally conducted in a manner where all degradation pathways can be avoided. Typically NCAs are purified by repeated precipitations; however we found that this method was not sufficient to remove the NEt_3.HCl salt impurities. In order to achieve this we adopted the method of Poche *et al.*[45] The NCA solution in ethyl acetate was extracted at 0°C with an aqueous sodium bicarbonate solution. This method results in some loss of NCA due to hydrolysis (the products of which are transferred into the aqueous layer), but does

generate higher purity monomers. ^{1}H NMR of an NCA which has been extracted compared to one which has not shows no evidence of the NEt_3.HCl peaks at 3ppm (Figure 2).

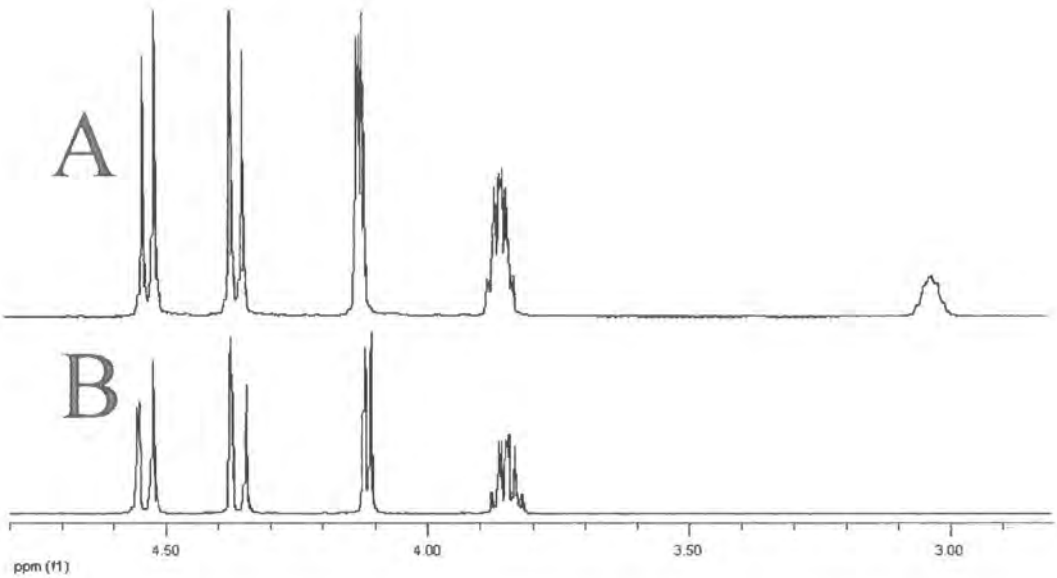

Figure 2. ^{1}H NMR spectrum of *O*-Benzyl-L-threonine NCA. A: purification by precipitation; B: purification by aqueous extraction then precipitation

Visually, it is clear that the monomers are of higher purity compared to when only recrystallisations are used (Figure 3).

Figure 3. Photograph showing NCA purified by aqueous extraction then precipitation (left) and precipitation only (right)

The purification procedures were identical for all the NCAs synthesised and the products were all isolated as powdery solids. They are soluble in THF, $CHCl_3$, DCM, EtOAc, DMF and DMAc, although alanine NCA is not soluble in $CHCl_3$ even with gentle heating.

2.2.2 GLYCOSYLATED NCAS

The acetate protected glycoNCAs BocThr(GluAc) (**7a**), BocThr(GalAc) (**7b**), BocSer(GluAc) (**7c**) and BocSer(GalAc) (**7d**), were synthesised by the Fuchs-Farthing reaction of their parent glycosylated amino acid with triphosgene. It was found that cyclisation of the *N*-Boc glycosylated amino acids to the NCA did not occur, therefore the Boc group was cleaved selectively using TFA. Iodine-mediated glycosylation of the Boc amino acids was stereospecific (β). The choice of *N*-Boc as the protecting group for the amine was made using the same considerations as for the non-glycosylated NCA synthesis: availability, ease of removal and the possibility of direct cyclisation to the NCA. The literature procedure for glycoNCA synthesis involves highly toxic mercuric cyanide as the promoter[28] which should be avoided wherever possible, and requires both amine and carboxylic acid groups to be protected meaning atom efficiency is reduced. We have utilised modern glycosylation techniques with more benign promoters which has resulted in increased yield.

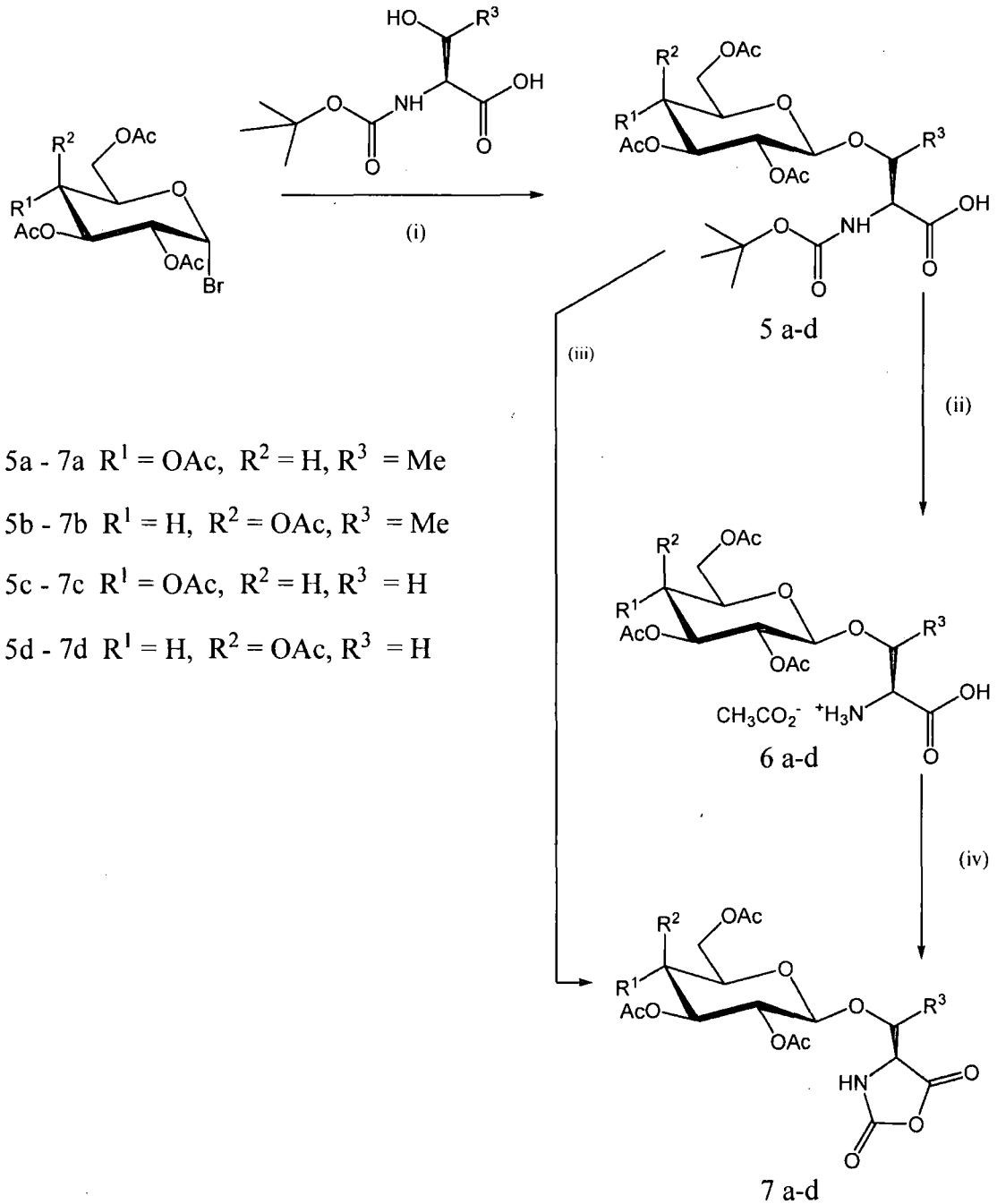

5a - 7a $R^1 = OAc$, $R^2 = H$, $R^3 = Me$

5b - 7b $R^1 = H$, $R^2 = OAc$, $R^3 = Me$

5c - 7c $R^1 = OAc$, $R^2 = H$, $R^3 = H$

5d - 7d $R^1 = H$, $R^2 = OAc$, $R^3 = H$

Scheme 7. Synthesis of glycosylated NCA monomers. Conditions: (i) *N*-Boc amino acid (2 equiv); I_2 (1.5 equiv); K_2CO_3 (1.5 equiv); MeCN; N_2; RT; 5 h; (ii) TFA (5 equiv); DCM; 1 h 0°C→ RT; (iii) triphosgene (1/3 equiv); NEt_3 (1 equiv); EtOAc; N_2; RT; 16 hrs; (iv) triphosgene (2/3 equiv); EtOAc; N_2; 20h, RT

2.2.2.1 GLYCOSYLATION OF *N*-BOC PROTECTED AMINO ACIDS

The most common amine protecting group over the last two decades in polypeptide and amino acid synthesis is the almost ubiquitous Fmoc group[46]. It is readily removed using piperidine, and is stable to strong acids and hydrogenation giving rise to desirable orthogonality. When used on the solid phase, post deprotection purification is facile and can be monitored by depletion of its fluorophore. However, in solution the liberated Fmoc cations require scavenging, which would typically be achieved by addition of a thiol[47] followed by purification.

Reports of the glycosylation of *N*-Boc amino acids in the literature are less common. To access the *N*-Boc glycoamino acids which were desired for NCA synthesis, we tested a number of different glycosyl donors and promoters. It was necessary to use protected glycosyl donors, as free OH groups are not compatible with NCAs. Acetate protected carbohydrates were chosen for their facile handing and a variety of promoting systems which they are compatible. The other common protecting group for glycosyl donors are per-benzylated derivatives, which are more active[48] ('armed'), but have associated handling difficulties.

The first system tested used β-D-glucosyl pentaacetate as the donor, under BF_3 promotion[36] (Scheme 8). This is a well known system and has been used to make carbohydrate-derivatised vinyl monomers[49].

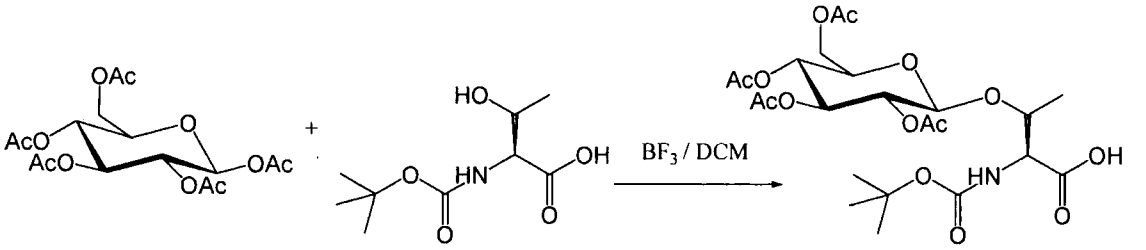

Scheme 8. Method for glycosylation of *N*-Boc L-threonine by β-D-glucosyl pentaacetate under BF_3 promotion.

Following the work up, frustratingly there was no evidence that the desired product had been synthesised. The ratio of donor to acceptor was varied from 1:2 to 2:1 and gave the same results. Changing the Lewis acid to $AlCl_3$, which has been used in the literature with Fmoc protected amino acids, again resulted in a complex mixture of products as judged by TLC.

The literature revealed that the Lewis acid $AlCl_3$[50,51] has been investigated as a reagent for *N*-Boc group removal in peptide synthesis (Scheme 9). There are reports of BF_3 cleaving a Boc group[52] and others where the Boc group it is stable under these conditions[53]. With trichloroacetimidates as the glycosyl donors, *N*-Boc amino acids can be glycosylated as only catalytic quantities of the promoter are used[54].

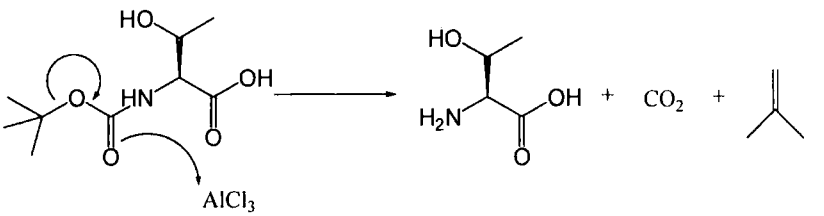

Scheme 9. Suggested mechanism for Boc group cleavage by $AlCl_3$

The primary amine formed in this reaction (Scheme 9) is far more nucleophilic than the secondary alcohol, and thus competes in the glycosylation mechanism. Side products include β and α *N*-linked glycosides, L-threonine and associated salts, along with the ortho-esters often found when carbohydrate peracetates are used. These

observations implied *N*-Boc amino acids are not compatible with glycosylation strategies involving certain Lewis acids.

A suitable method did, however, present itself in the form of iodine-promoted glycosylation, as developed by Field *et al.*[55,56] Anomeric bromides are required in place of acetates, as iodine is strongly halophilic[57], but less Lewis acidic than other promoters. The bromide is also more labile in general than acetates. This reduced Lewis acidity endows compatibility with the *N*-Boc group.

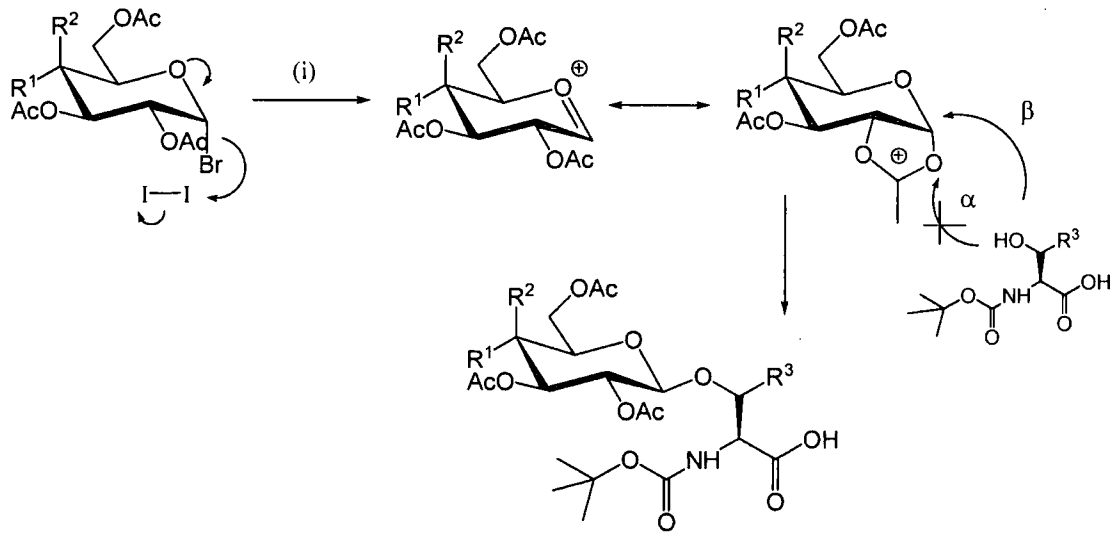

Scheme 10. Iodine mediated glycosylation of *N*-Boc amino acids with acetobromo sugars. (i) MeCN; under N_2; K_2CO_3; 5 hrs; RT. α and β indicate the product stereochemistry arising from nucleophilic attack of the oxonium intermediate at different angles.

It was necessary to have a base present, in this case insoluble K_2CO_3, to remove any HI and HBr which is evolved. The reaction was found to be complete within 5 hours by TLC measurements.

Table 2 – Results from the glycosylation of *N*-Boc amino acids under I_2 promotion. Yields quoted relative to glycosyl donor, following purification.

					Anomeric chemical shift			
	R^1	R^2	R^3	Yield	^1H	$J_{1\text{-}2}$ (Hz)	^{13}C	α/β
5(a)	OAc	H	Me	64 %	5.75	8.17	92.4	β only
5(b)	H	OAc	Me	55 %	5.73	8.26	92.9	β only
5(c)	OAc	H	H	62 %	5.75	8.13	92.0	β only
5(d)	H	OAc	H	54 %	5.73	8.21	90.0	β only

The isolated yields were reasonably high in all cases following column chromatography. For both threonine and serine derivatives it was observed that higher yields were obtained when using acetobromo glucose, than for acetobromo galactose. A rationale for this has not been proposed, but we imagine it is associated with impurities in the starting materials, rather than a significant difference in chemical reactivity. This is again our proposal for the reduced yields for serine glycosylation relative to threonine, as it would be expected that the less sterically hindered primary alcohol of serine would be more reactive than the secondary alcohol present on threonine, which is in disagreement with our observed results.

Our criteria for the glycosylation strategy stated that a single stereo isomer (or at least a large excess) be present. Acetate-protected glucose and galactose are expected only to lead to the β anomer (Scheme 10) due to neighbouring group participation. In the absence of a crystal structure, NMR is the best method to determine which anomer is present. ^{13}C NMR showed only a single peak in the region 80 – 100 ppm (where both possible configurations would be found typically) indicating a single anomeric stereoisomer (Figure 4). Evaluation of the J-couplings from the ^1H NMR spectra can provide useful information about the stereochemistry

also. A β- substitutent on a galacto- or gluco-configured sugar would result in the anomeric proton being axial, and hence trans to the axial H^2, demonstrated in Figure 5. The coupling constant for this trans situation is larger (cf trans alkenes) than for the cis configuration, when the substitutent is α. The measured values were between 8.13 and 8.26 Hz. Values below 4 Hz would be typical for α, and those above 7 Hz for β.

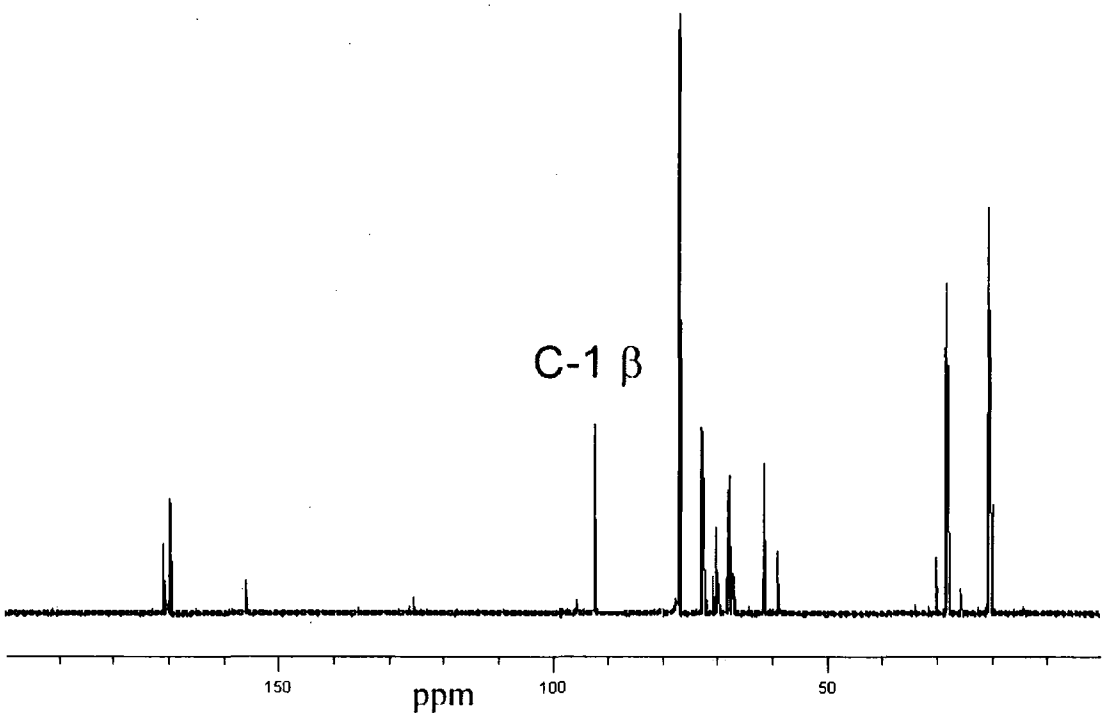

Figure 4. ^{13}C Spectra of BocThr(GluAc), 5a. Anomeric carbon = C-1

Absolute assignment of the stereochemistry was accomplished by using the NOE effect. NOESY pulse sequences allow the through-space interactions between protons to be observed. For both the carbohydrates used here the interaction between the H^3 and the H^1 protons gives the necessary information. When the substitutent is β, the H^1 proton will be axial and thus have an expected interaction with the H^3 and H^5. If the substitutent is α, then these would not been seen. This is shown more clearly in Figure 5.

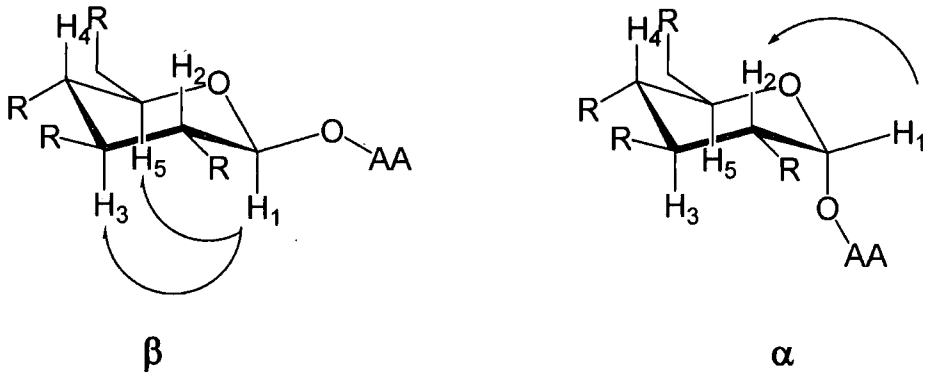

Figure 5. Predicted NOEs for β and α configurations for glucose and galactose (stereochemistry at H^4 is shown here for glucose, but characteristic NOEs for β are the same for galactose). AA = amino acid residue.

The NOESY spectra for compounds 5a, 6a, 7a and 8a show interactions between H^1 - H^3, and H^1 – H^5. Thus they were assigned as being β (Figure 6 shows the NOESY spectrum of BocThr(GluAc)).

Compounds, 5(a), 6(a), 7(a) and 8(a) were isolated as white, slightly hygroscopic powders. They were soluble in $CHCl_3$, DCM, THF, EtOAc, Et_2O, DMF, DMAc, EtOH, MeOH, CH_3CN and acetone.

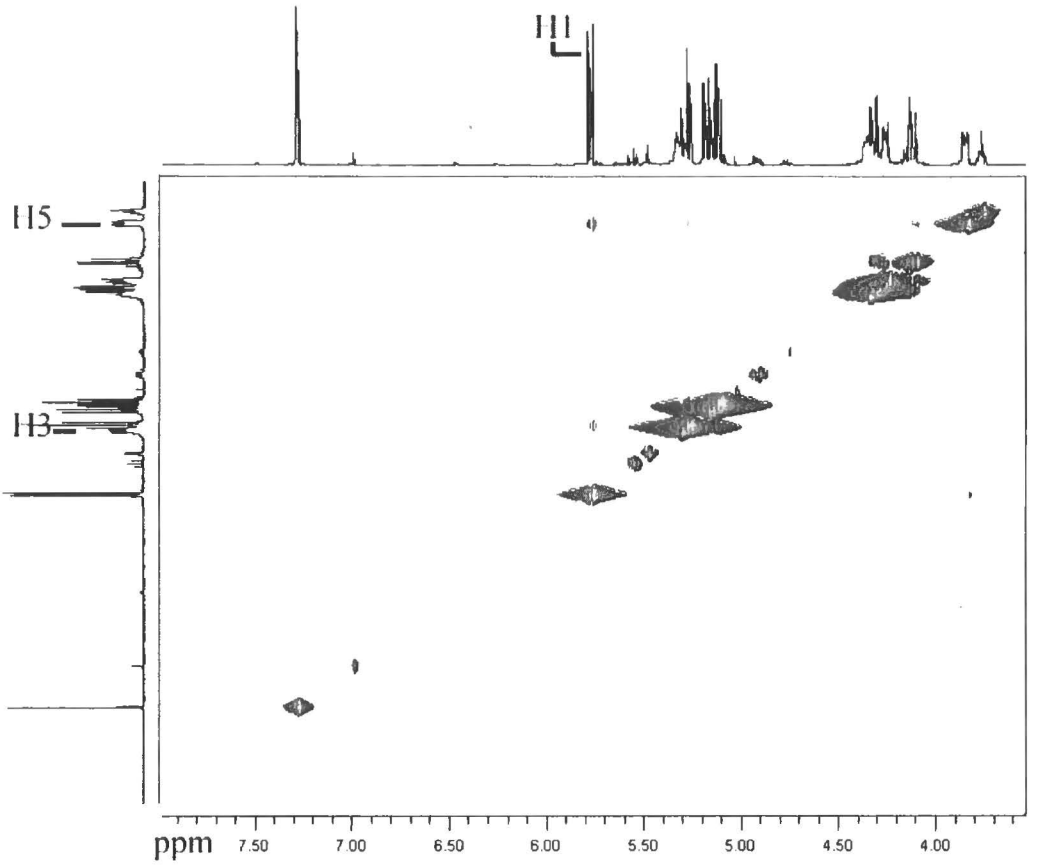

Figure 6. NOESY spectrum for BocThr(GluAc). Correlation between H^1 with H^5 and H^3 can be seen.

2.2.2.2 CYCLISATION OF BOC(GLYCO) AMINO ACIDS TO NCAS

Following the successful synthesis of a range of glycosylated *N*-Boc amino acids, the next step was to cyclise these into their respective NCAs using the same methodology as was shown to be successful for the non-glycosylated amino acids in the first section. Unfortunately, we found that no cyclisation occurred under these conditions. Different solvents were tried; (EtOAc, THF and $CHCl_3$) without success. We postulate that an intramolecular hydrogen bond between the acetate protecting groups of the carbohydrates and the N-H could be responsible. There are two possible H-bonding sites on the carbohydrate, at the 2 and 6 positions, as shown in Figure 7.

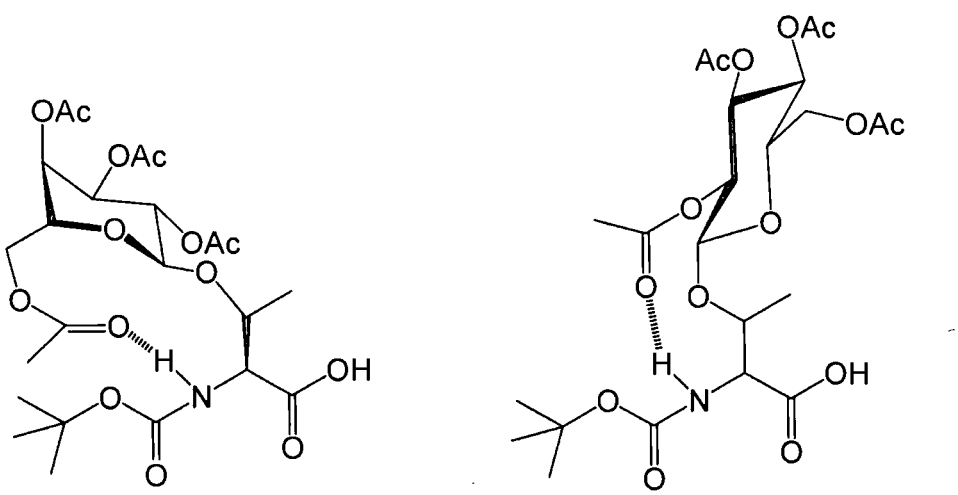

Figure 7. Proposed modes of intra-molecular H-bonding present in BocThr(GluAc)

To form the NCA, the carbonyl on the Boc group must attack nucleophilically[58] the carboxylic acid (activated by triphosgene). This would not be possible due to the H-bond 'locking' in the ring-opened conformation. Infrared analysis supported the presence of this H-bond. BocThr(Bzl) which has no H-bond donors or acceptors on its R group has an N-H stretch at 3372 cm^{-1}, compared to

BocThr(GluAc) which is at 3439 cm^{-1}. This shift to higher frequency corresponds to a lengthening of the N-H bond.

NMR analysis revealed that the starting material was recovered following the attempted synthesis. No cyclisation was possible for all the intermediates (**5a**) – (**5d**). It was thus decided that cleavage of the Boc group would have to be undertaken.

2.2.2.3 BOC GROUP CLEAVAGE

As discussed above, it was necessary to remove the *N*-Boc protecting group so that the Fuchs-Farthing (phosgenation) method could be applied. Lewis acids, which were shown to cleave partially the Boc group during glycosylation, were the first reagents tested. They offer the advantage that the glycosidic bond should not be too labile to them (or they would not be used in glycosylation reactions). It was found that they were not very efficient and only gave low yields of the cleavage products. Brønsted acids were considered instead. The strong mineral acids HCl and HBr are convenient reagents, in that they can be easily removed during the work up, and offer high reactivity. Unfortunately they tend to induce anomerisation and cleave the glycosidic bond. Considering this we chose to use TFA as it is known not to affect the glycosidic bond when it is used in moderately low concentrations and short reaction times[59]. Indeed, in our hands a 5-fold excess for 90 minutes was shown to be sufficient to give quantitative cleavage of the Boc group.

Table 3 - Results of selective cleavage of *N*-Boc group by TFA

					Anomeric chemical shift			
	R^1	**R^2**	**R^3**	**Yield**	**^1H**	**J_{1-2} (Hz)**	**^{13}C**	**α/β**
6(c)	OAc	H	Me	>95 %	5.79	8.07	93.3	β
7(c)	H	OAc	Me	>95 %	5.76	8.09	93.8	β
8(c)	OAc	H	H	>95 %	5.90	8.58	92.9	β
9(c)	H	OAc	H	>95 %	6.04	8.35	93.1	β

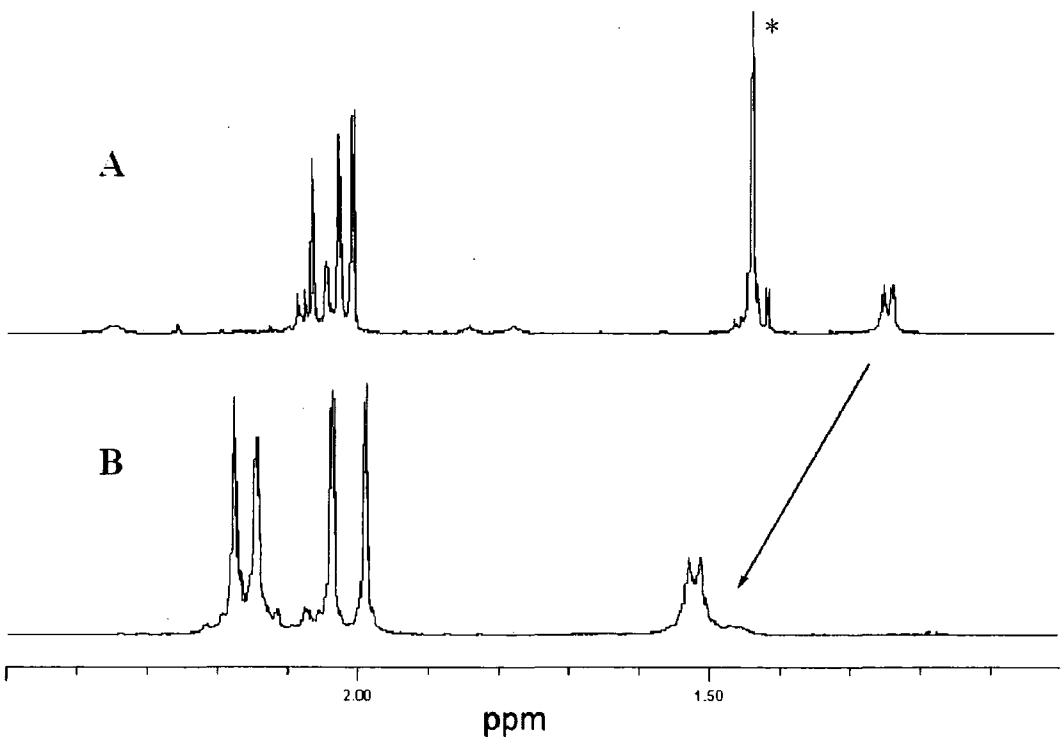

Figure 8. ^1H NMR spectra of: (A) BocThr(GluAc); (B) Thr(GluAc). Treatment with TFA/DCM removes Boc Me protons (*). β-Methyl from threonine residue shifts to lower field – arrow.

Figure 8 shows an expanded ^1H NMR spectrum of a Boc protected (A) and deprotected amino acid (B). There is no evidence of residual Boc methyl groups. The

^{13}C spectrum shows no residual ($\underline{C}H_3)_3C$ signal at 28 ppm (Figure 9). The carbonyl stretch of the Boc group in the IR spectrum can also be seen to be absent. However it is not clearly resolved from the acetate groups so was not used to quantify the degree of cleavage.

The absence of anomerisation is essential during any of the reaction steps. This is to ensure that any structure-property relationships which are later derived from the materials can be attributable to the precise structure present. A significant amount of a second anomer (in all these cases α would be the impurity) would cast doubt on any results. Evaluation of the $H^1 - H^2$ coupling constants gives values above 8 Hz, implying a trans configuration and therefore β. The proton NMR spectra also show the expected ratio between the anomeric proton and methyl of threonine (or CH_2 of serine). The carbon NMR spectra (Figure 9) show only a single peak in the anomeric region, at the same chemical shift as that assigned as β-C^1 in the Boc protected amino acid.

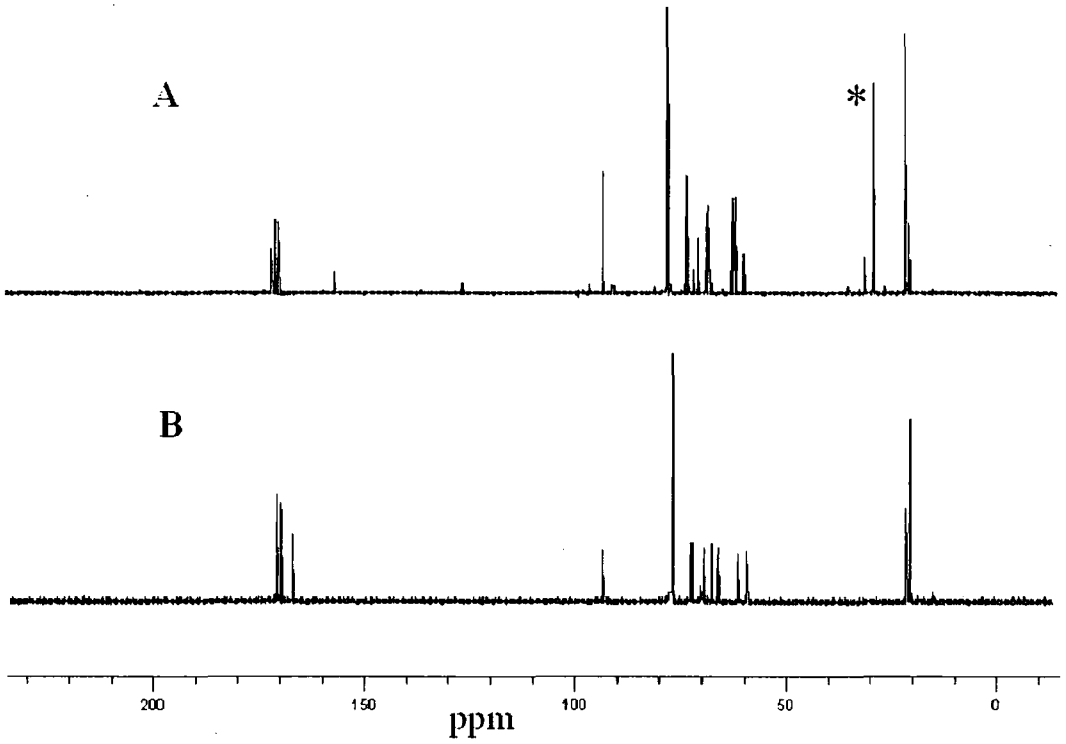

Figure 9. ^{13}C NMR Spectra for (A) BocThr(GluAc); (B) Thr(GluAc). * = ($\underline{C}H_3)_3C$ Boc

Purification of these amino acids was achieved by exchanging the TFA counterion for acetic acid. It was not possible to isolate the TFA salt as solids due to the difficulty of removing the excess TFA, even following prolonged high vacuum treatment. There was no trace of the TFA in the ^{13}C NMR spectrum following extraction of an aqueous solution containing CH_3CO_2H with hexane (expect $\underline{C}F_3CO_2H$ at ~120 ppm.). No side products were found as *N*-Boc group cleavage results in the evolution of isobutene and CO_2 which are both gaseous, allowing for facile workup. The compounds 5(b), 6(b), 7(b) and 8(b) were isolated as very hydroscopic white solids soluble in H_2O, $CHCl_3$, DCM, EtOAc, DMF, DMAc, EtOH, MeOH and CH_3COOH.

2.2.2.4 GLYCOSYLATED NCA SYNTHESIS

The Fuchs-Farthing methodology was adopted here. The amino acids were treated with triphosgene in ethyl acetate allowing for purification by aqueous extraction, as demonstrated with the non-glycosylated NCAs. Initially we wanted to conduct the reaction at room temperature to limit any decomposition which may be caused by the evolved HCl, but found that raised temperatures (60°C) were required to obtain reasonable conversion due to precipitation of the amino acid.HCl salts. This was overcome by using a 2:1 ratio of amino acid to triphosgene (triphosgene being 3 equivalents of phosgene), rather than a large excess, and adding the non basic HCl scavenger α-pinene. Terpenes such as this which contain an alkene group have been shown to be excellent reagents for this purpose in the synthesis of NCAs on a large scale.[30,31] The solution typically became clear within 90 minutes of addition of α-pinene, but if not, any remaining solids (amino acids HCl salts) were simply removed by filtration following cooling in a freezer. Repeated re-precipitations were undertaken from EtOAc to hexane to remove any residual α-pinene, or its product of reaction with HCl.

Table 4. Results for the synthesis of glycoNCAs from parent amino acids.[a]

					Anomeric chemical Shift			
	R^1	R^2	R^3	Yield (%)	^1H	J_{1-2} (Hz)	^{13}C	α/β
5(c)	OAc	H	Me	47 (73)	5.72	8.14	92.8	β
6(c)	H	OAc	Me	44 (86)	5.68	8.18	93.3	β
7(c)	OAc	H	H	43 (70)	5.75	8.00	96.1	β
8(c)	H	OAc	H	44 (82)	6.04	7.5	95.6	β

[a]Total Yield. Yield this step in parenthesises

Under these reaction conditions, no anomerisation was observed. Table 4 shows the H^1-H^2 coupling constants for all the NCAs, giving values mostly above 8Hz characteristic of β (trans) configuration. This stereochemical assignment was confirmed by NOESY. The ^{13}C NMR spectrum (Figure 10) showed only a single peak attributable to an anomeric carbon, confirming that only one stereoisomer was present.

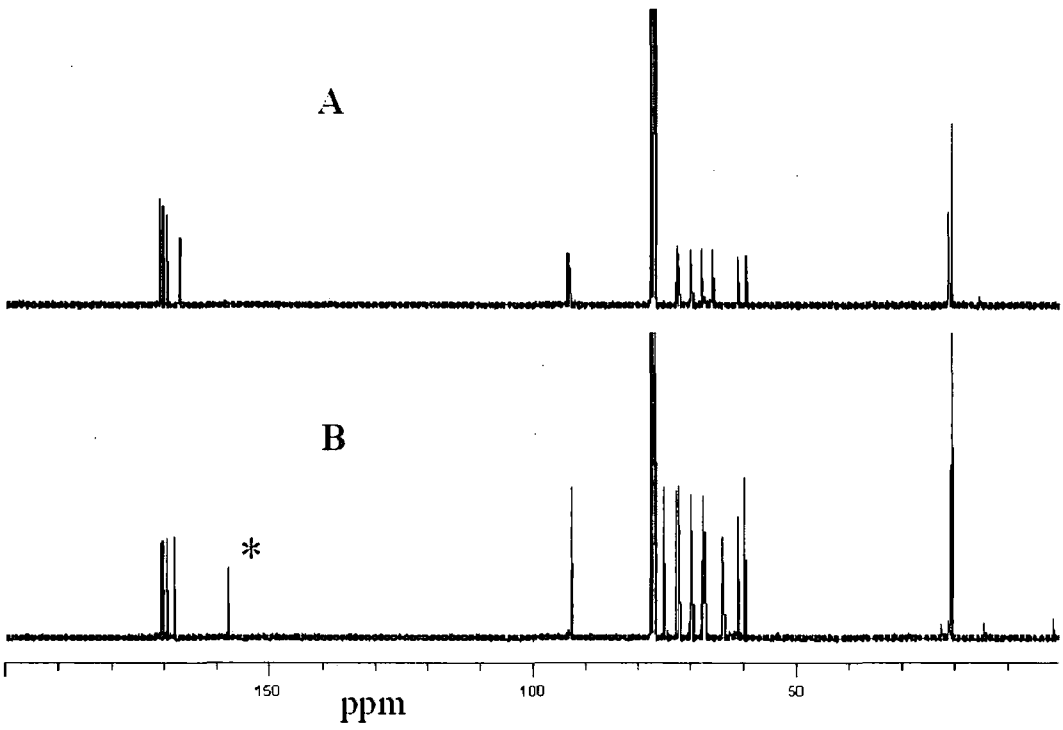

Figure 10. ^{13}C NMR spectra (A) Thr(GluAc); (B) Thr(GluAc)NCA. A single anomeric peak ~90 ppm, and characteristic C=O at 157 ppm of NCA (*), can be seen.

The proton NMR spectrum also displays an N-H peak attributable to the NCA (Figure 11), and as is expected of these it is somewhat broadened relative to other peaks, and does not show any coupling to protons on adjacent carbon atoms by COSY. Infrared analysis on these materials was not as helpful as for the non-glycosylated NCAs. The characteristic carbonyl stretches were obscured by the broad, strong absorptions attributable to the acetate protecting groups. Figure 12 shows the tentative assignments. High resolution mass spectrometry was employed to confirm the presence of NCA.

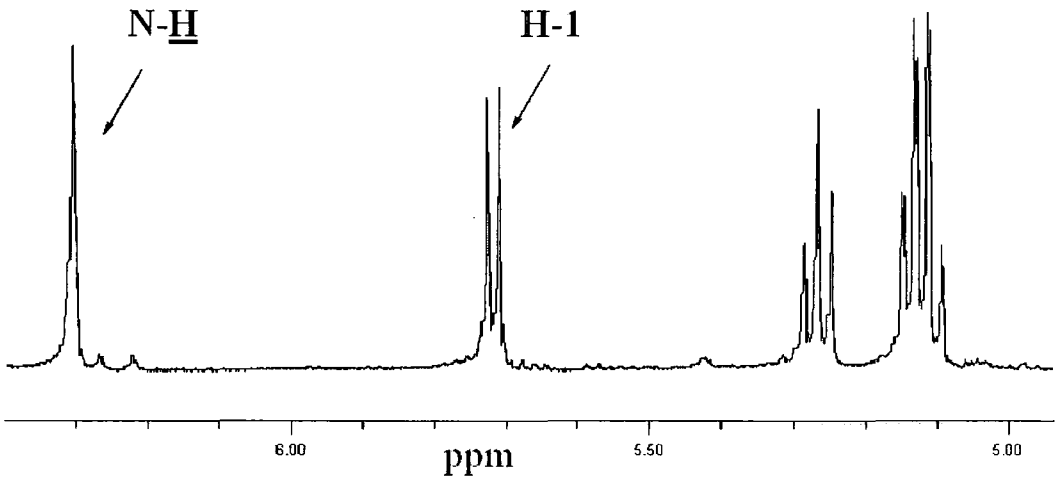

Figure 11. ^{1}H NMR spectrum of Thr(GluAc)NCA showing the N-H of the NCA and the single β anomeric peak (H-1)

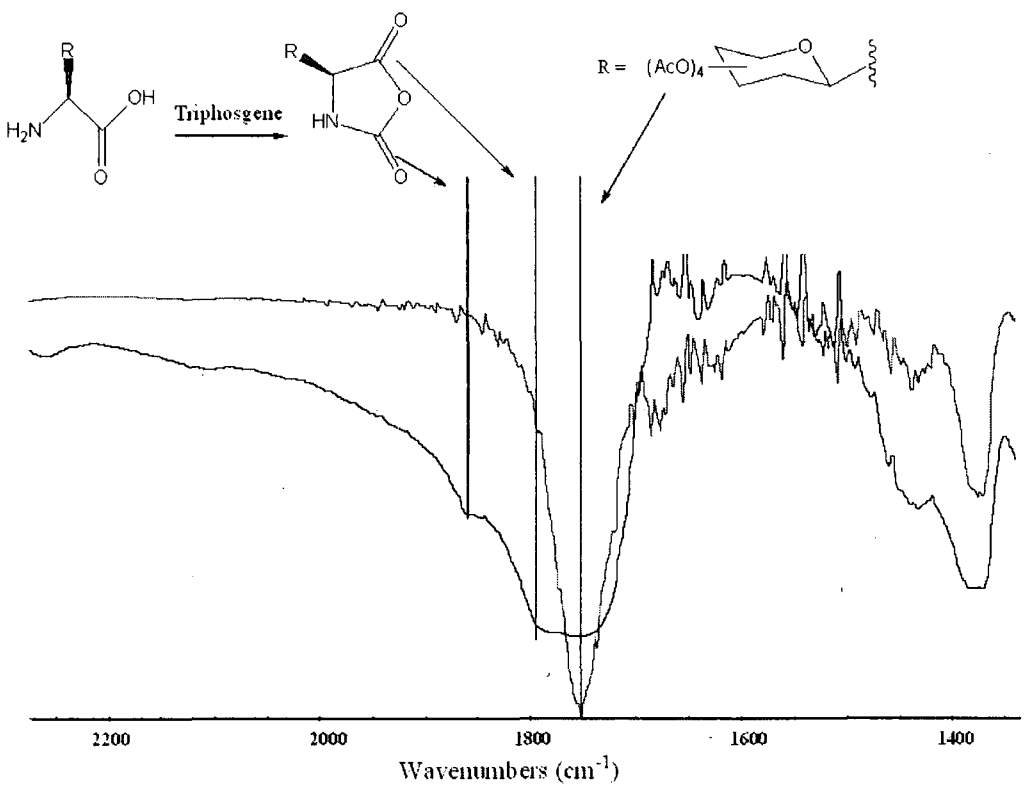

Figure 12 - Infrared analysis (5mg/KBr disc) of the conversion of glycoamino acid (red) to the corresponding NCA (blue). Arrows indicate the carbonyl stretches. Example shown is for Thr(GluAc). Peaks, cm^{-1}: 1860, 1788, 1750

The chloride content as judged by ion chromatography was below 0.01% by mass, confirming the removal of HCl related impurities.

The NCAs were soluble in $CHCl_3$, DCM, THF, EtOAc, DMF, DMAc and DMSO.

2.3 CONCLUSIONS

The synthesis of a diverse range of NCAs starting from their *N*-Boc protected amino acids in a single step has been demonstrated according to literature procedures. The extreme purification procedure was shown to be an excellent method to obtain NCAs free of acidic impurities, as judged by NMR and ion chromatography. The NCAs with functional side groups were blocked with easily cleavable protecting groups. The use of Boc L-alanine for the first time gave alanine NCA in improved yields owing to the improved solubility gained from the Boc group. This methodology was unfortunately shown to be incompatible with *N*-Boc amino acids bearing peracetate protected carbohydrate moieties. Infrared spectroscopy suggested that an intramolecular hydrogen bond between acetate and amide locked the conformation in a manner which prevented cyclisation from occurring. This problem was circumvented by selective cleavage of the *N*-Boc groups with TFA, followed by treatment with triphosgene to synthesise the glycoNCAs in improved yields over the literature method, without the need for toxic mercury salts.

We anticipate that exchanging the easy-to-handle acetosugars for the more reactive benzylated derivatives would allow the direct conversion of Boc amino acid to NCA in a single step, as there would be no hydrogen bonding sites.

2.4 EXPERIMENTAL

N-Boc (O-benzyl) L-threonine (>99%), *N*-Boc L-glutamic acid γ-benzyl ester, *N*-α,ε di-Boc L-lysine dicyclohexylammonium salt (>98%), *N*-Boc L-threonine (>98%), *N*-Boc L-serine (>98%) were purchased from Fluka. L-Alanine (99%), acetobromo-α-D-glucose (>95%), acetobromo-α-D-galactose (>95%), iodine (>99.8%), potassium carbonate (>99%), trifloroacetic acid (>98%), sulphuric acid (95-98%) and sodium carbonate (>99.5%) were purchased from Aldrich. Triphosgene (>96%) and triethylamine (>98%) were purchased from Lancaster synthesis. THF, MeCN and DCM (>99.5%) were purchased from Fischer Scientific and dried by passage through two alumina columns using an Innovative Technology Inc. solvent purification system and stored under N_2. THF was further dried over sodium/benzophenone complex with at least 3 freeze-thaw cycles, until the purple colouration persisted. Anhydrous ethyl acetate (>99.8%, <0.005% H_2O) was purchased from Aldrich. Hexane (Fischer Scientific >99%) was dried over 3A molecular sieves. 3A molecular sieves (Aldrich) were activated in an oven at 200°C before use. All other chemicals were used as received. Glass backed silica (Biotage) was used for TLC with 5wt % phosphomolybdic acid in ethanol, developed at 80°C as the visualising agent. Column chromatography was undertaken on a Biotage SP1 flash chromatography unit using UV detectors at 200 and 236nm. Gradients were calculated using the supplied software from TLC place measurements.

NMR-spectra were recorded with a Varian-Inova 500 spectrometer, operating at 500MHz (^1H) or at 125 MHz (^{13}C); results of HSQC and COSY correlation studies have been used in order to assign the observed signals to the hydrogen and carbon atoms of the compound. Alternatively ^1H and ^{13}C spectra were acquired with a Bruker

Avance-400 spectrometer operating at 400MHz and 100MHz respectively. NOESY was used to assign the configuration of carbohydrate moieties where appropriate. Mass spectra were obtained with a Micromass Platform spectrometer and with a Micromass LCT spectrometer, ionisation modes ES+ or ES-. Infrared spectroscopy was conducted on a Nicolet Nexus FT-IR as a KBr disc. Liquid samples were analysed by direct injection of the reaction medium into a liquid cell with KBr windows. Elemental analyses were conducted on an Exeter analytical E-440 elemental analyser. Digital photographs were taken using a Kodak DX6340 with a resolution of 3.1 megapixels. Images were cropped using Adobe Photoshop version 6.0.

_O_-Benzyl L-threonine _N_-carboxy anhydride – Thr(Bzl)NCA

To a stirred solution of _N_-Boc-(_O_-benzyl)-L-threonine (2.1g, 6.6mmol) in 40 mL ethyl acetate under an atmosphere of nitrogen was added triphosgene (0.65g, 2.2mmol) in one portion and stirred to dissolution. Triethylamine (0.92ml, 6.6mmol) was added dropwise *via* syringe. The reaction was stirred at 30°C under a flow of nitrogen for 16 hours. After this time the reaction flask was placed into a freezer at -20°C for 30 minutes. The hydrochloride salt of triethylamine was removed by filtration through a glass sinter.

The reaction mixture was immediately extracted with ice cold H_2O, followed by ice cold aqueous $NaHCO_3$ solution(5% w/w). The organic layer was dried over $MgSO_4$ in a refrigerator at <4°C. The organic layer was decanted from $MgSO_4$ and concentrated to $1/5^{th}$ of its original volume on a rotary evaporator under reduced pressure, with the water bath below 30°C. The concentrate was added to hexane and the precipitate recrystallised three times from ethyl acetate/hexane at -20°C. The white

solid was obtained by centrifugation following each crystallisation, and finally dried under high vacuum. Yield 1.5g; 68%.

^{1}H NMR (500MHz, $CDCl_3$) δ_{ppm}; 1.25 (3H, d, $J_{6,5}$ = 6.35Hz, H_6), 3.85 (1H, q, $J_{5,6}$ = 6.35Hz, H^5), 4.12 (1H, d, $J_{3,5}$ = 4.31Hz, H^3), 4.36 (1H, d, $J_{7a,7b}$ = 11.50Hz, H^{7a}), 4.52 (1H, d, J_{7b-7a} = 11.50Hz, H^{7b}), 6.96 (1H, s(broad), H^2), 7.18-7.28 (5H, m, H^9).

^{13}C NMR (125.7MHz, ^{1}H-decoupled, $CDCl_3$) δ_{ppm}; 15.9 (C^6), 62.9 (C^3), 71.3 (C^7), 73.0 (C^5), 127.8, 128.0, 128.5 (C^9), 136.9 (C^8), 152.9 (C^1), 167.8 (C^4).

IR (KBr disc) cm^{-1}: 3300 (N-H), 1860 (C=O amide), 1791 (C=O anhydride).

MS (ES+) m/z = 285.3 (20%) $[M+Na]^+$, 299.3 (100%) $[M+Na+MeCN]^+$, 493.3 (30%) $[2M+Na]^+$.

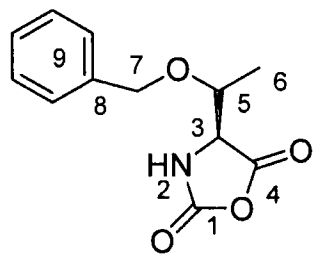

γ-Benzyl L-glutamic acid *N*-carboxy anhydride - Glu(Bzl)NCA

The same method was used as for Thr(Bzl)NCA using BocGlu(γ-Bzl) (2.0g, 5.95 mmol), triphosgene (0.58g, 1.98mmol) and Triethylamine (0.83mL, 5.95mmol). Yield 0.98g; 63%.

^{1}H NMR (500MHz, $CDCl_3$) δ_{ppm}; 2.12 (1H, m, H^{5a}), 2.26 (1H, m, H^{5b}), 2.59 (2H, t, J_{6-5} = 6.9Hz, H^6), 4.38 (1H, t, J_{3-5} = 6.1Hz, H^3), 5.13 (2H, s, H^8), 6.76 (1H, s(broad), H^2), 7.33-7.39 (5H, m, H^{10}).

^{13}C NMR (125.7MHz, ^{1}H-decoupled, $CDCl_3$) δ_{ppm}; 26.8 (C^5), 29.7 (C^6), 56.9 (C^3), 67.1 (C^8), 128.3 + 128.5 + 128.7 (C^{10}), 135.1 (C^9), 151.9 (C^1), 169.4 (C^4), 172.3 (C^7).

IR cm^{-1} (KBr disc): 1864 (C=O amide), 1785 (C=O anhydride), 1705 (C=O ester).

MS (ES^+) m/z = 286.0 (100%) $[M+Na]^+$.

Melting Point 83-84 °C.

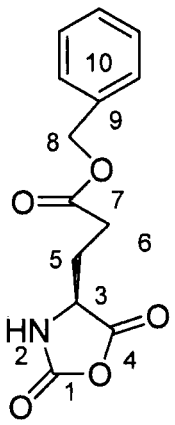

***N* (*α*,*ε*-di butoxy carbonyl) L-Lysine – (Boc_2LysOH)**

Boc_2LysOH.DCHA (5g, 9.49mmol) was suspended in 50mL of ethyl acetate at 0°C. 0.1M $H_2SO_{4(aq)}$ was added dropwise with stirring until all solids were dissolved. The reaction mixture was immediately transferred into a separating funnel and washed 3 times with brine. Following concentration and drying on a high vacuum line a white solid was obtained. Isolated yield 2.93g (89%).

^{1}H (500MHz, $CDCl_3$) δ_{ppm}; 1.42 (18H, s, H^9), 1.65 (2H, d, $J_{4\text{-}5}$ = 9.7Hz, H^4), 1.82 (2H, d, $J_{3\text{-}4}$ = 12.56Hz, H^3), 2.00 (2H, d, $J_{5\text{-}4}$ = 11.18Hz, H^5), 3.09 (2H, t, $J_{6\text{-}5}$ = 5.49Hz, H^6), 4.12 (1H, t, $J_{2\text{-}3}$ = 7.04Hz, H^2).

^{13}C NMR (125.7MHz, ^{1}H-decoupled, $CDCl_3$) δ_{ppm}; 24.9 (C_3), 28.6 (C_9), 29.3 (C_5), 32.9 (C_4), 40.5 (C_6), 54.5 (C_2), 79.5 (C_8), 156.0 (C_7), 177.0 (C_1).

IR cm^{-1} (KBr disc): 3369 (N-H), 2942 (C-H), 1705 (C=O Boc).

MS (ES^+) m/z = 369.2 (100%) $[M+Na]^+$.

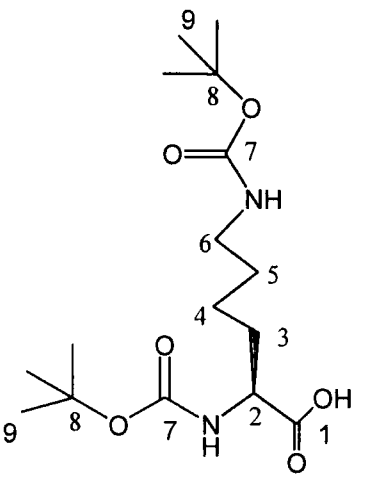

***(N*-ε-butoxy carbonyl) L-lysine *N*-carboxy anhydride - BocLysNCA**

To a stirred solution Boc_2LysOH (2.7g, 7.42mmol) in 35mL of ethyl acetate under N_2, was added triphosgene (0.73g, 2.47mmol) in one portion and stirred to dissolution. Triethyl amine (1.03ml, 7.41mmol) was added dropwise *via* syringe. The reaction was stirred at 25°C under a flow of nitrogen for 16hours. After this time the

reaction flask was placed into a freezer at -20°C for 30 minutes. The hydrochloride salt of triethyl amine was removed by filtration through a glass sinter.

The reaction mixture was immediately extracted with ice cold H_2O, followed by ice cold aqueous $NaHCO_3$ (5% w/w). The organic layer was dried over $MgSO_4$ in a refrigerator at <4°C. The organic layer was decanted from $MgSO_4$ and concentrated to ½ of its original volume on a rotary evaporator under reduced pressure, with the water bath below 30°C. The concentrate precipitated into hexane at -20°C. This was recrystalised from warm (~35°C) ethyl acetate into hexane at -20°C three times. The white solid was obtained by centrifugation following each crystallisation, and finally dried under vacuum to give a white solid. Isolated yield 1.32g. 65% yield.

^{1}H NMR (500MHz, $CDCl_3$) δ_{ppm}; 1.36 (13H, 9xH^{12}, 2xH^6, 2xH^7), 1.67 (2H, m, H^5), 2.89 (2H, q, J_1 = 6.5Hz, J_2 = 12.4Hz, H^8), 4.42 (1H, t, $J_{3\text{-}5}$ = 6.17Hz, H^3), 6.80 (1H, s, H^2) 9.08 (1H, s, H^9).

^{13}C NMR (125.7MHz, ^{1}H-decoupled, $CDCl_3$) δ_{ppm}; 22 (C_6), 28.2 (C_{12}), 28.8 (C_5), 29.8 (C_7), 40.2 (C_8), 57.1 (C_3), 77.3 (C_{11}), 152.0 (C_{10}), 155.0 (C_1), 172.4 C_4).

IR cm^{-1}: (KBr disc): 1862 (C=O amide), 1769 (C=O anhydride), 1705 (C=O ester).

MS (ES^+) m/z = 567.2 (100%) $[2M+Na]^+$.

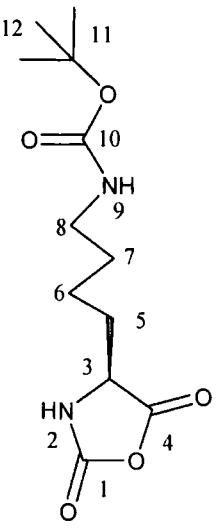

N^{α}-(Butoxy carbonyl)-3-*O*-(2, 3, 4, 6-tetra-*O*-acetyl-β-D-glucopyranosyl)-L-threonine - BocThr(GluAc) - 5(a)

N-Boc-L-threonine (3.0g, 13.6mmol), potassium carbonate (1.41g, 10.2mmol) and acetobromoglucose (2.79g, 6.8mmol) were dissolved in 40 ml of dry acetonitrile under an N_2 atmosphere with stirring for 5 minutes to ensure dissolution. Iodine (2.59g, 10.2mmol) was then added in a single portion against a flow of N_2. The vessel was sealed and allowed to stir at ambient temperature with the exclusion of light for 5 hours.

To the still-stirring solution, saturated sodium thiosulphate (aqueous) was added until the deep red colouration had gone, to leave a slightly yellow solution. The insoluble components (residual potassium carbonate) were removed by filtration and the filtrate concentrated to ¼ of its original volume under reduced pressure on a rotorary evaporator. 40 mL of dichloromethane were then added, and the solution extracted with sodium bicarbonate (aqueous 5% w/v, 50 mL) followed by brine (2 x 50mL), and the organic layer dried over magnesium sulphate. Separation by column chromatography (Hexane/THF 10:1 → 2:8) yielded the title product as a white solid. Isolated yield 2.05g; 55%.

^{1}H NMR (500MHz, $CDCl_3$) δ_{ppm}; 1.25 (3H, d, $J_{16\text{-}7}$ = 6.39Hz, H^{16}), 2.01 – 2.06 (12H, m, H^{15}), 3.82 (1H, ddd, $J_{5\text{-}6a}$ = 2.20Hz, $J_{5\text{-}6b}$ = 4.96Hz, $J_{5\text{-}4}$ = 10.07Hz, H^5), 4.09 (1H, dd, $J_{6a\text{-}5}$ = 2.19Hz, $J_{6a\text{-}6b}$ = 12.36Hz, H^{6a}), 4.23 (1H, dd, $J_{7\text{-}9}$ = 6.36Hz, $J_{7\text{-}8}$ = 9.7Hz, H^7), 4.30 (1H, dd, $J_{6b\text{-}5}$ = 5.02Hz, $J_{6b\text{-}6a}$ = 12.44Hz, H^{6b}), 4.33 (1H, m, H^8), 5.10 (1H, t, J = 9.70Hz, H^4), 5.15 (1H, dd, $J_{2\text{-}1}$ = 8.18Hz, $J_{2\text{-}3}$ = 9.60Hz, H^2), 5.26 (1H, t, J = 9.47Hz, H^3), 5.30 (1H, d, $J_{8\text{-}7}$ = 9.6Hz, H^8), 5.75 (1H, d, $J_{1\text{-}2}$ = 8.17Hz, H^1).

^{13}C NMR (125.7MHz, ^{1}H-decoupled, $CDCl_3$) δ_{ppm}; 19.9 (C^{16}), 28.2 (C^{13}), 20.5 and 20.7 (C^{15}), 58.9 (C^7), 61.3 (C^6), 67.5 (C^8), 67.8 (C^4), 70.0 (C^2), 72.5 (C^3), 72.9 (C^5), 80.1 (C^{12}), 92.4 (C^1), 156.0 (C^{11}), 169.4-167.0 (4xC^{14}), 170.9 (C^9).

IR (KBr disc) cm^{-1}: 3447, broad, (N-H), 2980 (C-H), 1757 (C=O Ac), 1718 (C=O Boc).

MS (ES+) m/z = 572.2 $[M+Na]^+$ 100%.

Elemental: (Found %); C 50.16; H 6.38; N 2.35; (Expected %); C, 50.27; H, 6.42; N, 2.55.

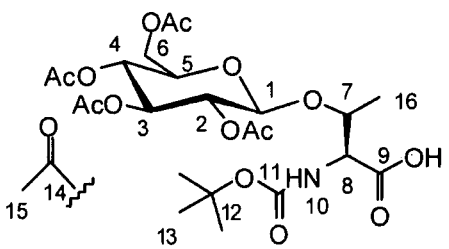

N^{α}-(Butoxy-carbonyl)-3-*O*-(2, 3, 4, 6-tetra-*O*-acetyl-β-D-galactopyranosyl)-L-threonine - BocThr(GalAc) – 5(b)

The same procedure was followed as for the glucose derivative using *N*-Boc-L-threonine (3.0g, 13.6mmol), potassium carbonate (1.41g, 10.2mmol) acetobromogalactose (2.79g, 6.8mmol) and iodine (2.59g, 10.2mmol). Separation by column chromatography (hexane/THF 10:1 → 2:8) yielded the title product as a white solid. Isolated yield 2.20g; 59%.

^{1}H NMR (500MHz, $CDCl_3$) δ_{ppm}; 1.26 (3H, d, $J_{16\text{-}7}$ = 6.38Hz, H^{16}), 1.99 – 2.06 (12H, m, H^{15}), 4.04 (1H, td, $J_{5\text{-}4}$ = 0.74Hz, $J_{5\text{-}6a}$ = $J_{5\text{-}6b}$ = 6.47Hz, H^5), 4.07 (1H, dd, $J_{6b\text{-}5}$ = 6.14Hz, $J_{6b\text{-}6a}$ = 10.89Hz, H^{6b}), 4.20 (1H, dd, $J_{6a\text{-}5}$ = 6.40Hz, $J_{6a\text{-}6b}$ = 10.86Hz, H^{6a}), 4.22 (1H, d, $J_{8\text{-}7}$ = 9.2Hz, H^8), 4.35 (1H, m, H^7), 5.08 (1H, dd, $J_{3\text{-}4}$ = 3.41Hz, $J_{3\text{-}2}$ = 10.44Hz, H^3), 5.33 (1H, dd, $J_{2\text{-}1}$ = 8.26Hz, $J_{2\text{-}3}$ = 10.44Hz, H^2), 5.42 (1H, dd, $J_{4\text{-}3}$ = 3.41Hz, $J_{4\text{-}5}$ = 0.94Hz, H^4), 5.73 (1H, d, $J_{1\text{-}2}$ = 8.26Hz, H^1).

^{13}C NMR (125.7MHz, ^{1}H-decoupled, $CDCl_3$) δ_{ppm}; 19.9 (C^{16}), 20.5-20.7 (4xC^{15}), 28.2 (C^{13}), 59.0 (C^7), 60.8 (C^6), 62.3 (C^8), 67.2 (C^4), 67.9 (C^2), 71.4 (C^3), 72.3, (C^5), 80.1 (C^{12}), 92.9 (C^1), 156.0 (C^{11}), 169.9-170.1 (4x C^{14}), 170.6 (C^9).

IR (KBr disc) cm^{-1}: 3447, broad, (N-H), 2981 (C-H), 1757 (C=O Ac), 1718 (C=O Boc).

MS (ES+) m/z = 572.2 $[M+Na]^+$ 100%.

Elemental: (Found %); C, 50.48; H, 6.54; N, 2.36; (Expected %); C, 50.27; H, 6.42; N, 2.55.

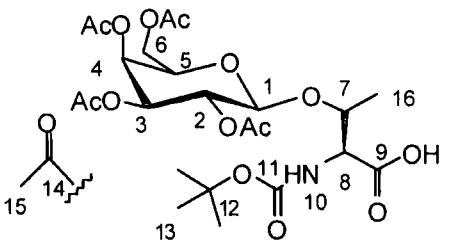

N^{α}-(Butoxy carbonyl)-3-*O*-(2, 3, 4, 6-tetra-*O*-acetyl-β-D-glucopyranosyl)-L-Serine - BocSer(GluAc) – 5(c)

The same procedure was followed as for the threonine glucose derivative using *N*-Boc-L-serine (3.01g, 14.6mmol), potassium carbonate (1.52g, 11mmol), acetobromoglucose (3.01g, 7.32mmol) and iodine (2.79g, 11mmol). Purified by column chromatography (hexane/THF 10:1 → 2:8). Isolated yield 2.19g; 56%.

^{1}H NMR (500MHz, $CDCl_3$) δ_{ppm}; 1.43 (9H, s, H^{13}), 1.99 – 2.07 (12H, m, H^{15}), 3.83 (1H, ddd, $J_{5\text{-}6a}$ = 2.15Hz, $J_{5\text{-}6b}$ = 4.65Hz, $J_{5\text{-}4}$ = 9.95Hz, H^5), 4.02 (1H, m, H^{7a}), 4.10 (1H, dd, $J_{6a\text{-}5}$ = 2.20Hz, $J_{6a\text{-}6b}$ = 12.48Hz, H^{6a}), 4.28 (1H, dd, $J_{6b\text{-}5}$ = 4.81Hz, $J_{6b\text{-}6a}$ = 12.45Hz, H^{6b}), 4.35 (1H, m, H^{7b}), 5.11 (1H, t, J = 9.90Hz , H^4), 5.14 (1H, dd, $J_{2\text{-}1}$ = 8.15Hz, $J_{2\text{-}3}$ = 9.47Hz, H^2), 5.26 (1H, t, J = 9.38Hz, H^3), 5.40 (1H, dd, $J_{8\text{-}7a}$ = 2.79Hz, $J_{8\text{-}7b}$ = 6.67Hz, H^8), 5.75 (1H, d, $J_{1\text{-}2}$ = 8.13Hz, H^1).

^{13}C NMR (125.7MHz, ^{1}H-decoupled, $CDCl_3$) δ_{ppm}; 20.5 – 20.7 (4xC^{15}), 28.0 (C^{13}), 56.2 (C^7), 61.0 (C^6), 62.3 (C^8), 67.6 (C^4), 70.0 (C^2), 71.1 (C^{12}), 72.4 (C^3), 72.8 (C^5), 92.4 (C^1), 155.1 (C^{11}), 169.2 – 170.0 (4x C^{14}), 170.8 (C^9).

IR (KBr disc) cm^{-1}: 3447, broad, (N-H), 2979 (C-H), 1753 (C=O Ac), 1717 (C=O Boc).

MS (ES+) m/z = 558.2 (100%) $[M+Na]^+$.

Elemental: (Found %); C, 49.52; H, 6.25; N, 2.10; (Expected %); C, 49.34; H, 6.21; N, 2.62

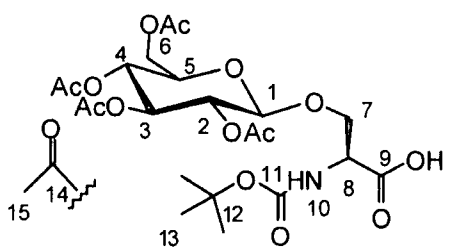

N^{α}-(Butoxy carbonyl)-3-*O*-(2, 3, 4, 6-tetra-*O*-acetyl-β-D-galactopyranosyl)-L-Serine –BocSer(GalAc) – 5(d)

The same procedure was followed as for the threonine galactose derivative using *N*-Boc-L-serine (3.06g, 14.9mmol), potassium carbonate (1.54g, 11.0mmol) and acetobromoglucose (3.07g, 7.5mmol) and iodine (2.77g, 11.0mmol). Purified by column chromatography (hexane/THF 10:1 → 2:8). Isolated yield 2.29g; 57%.

^{1}H NMR (500MHz, $CDCl_3$) δ_{ppm}; 1.43 (9H, s, H^{13}), 1.99 – 2.06 (12H, m, H^{15}), 5.08 (1H, dd, $J_{3\text{-}4}$ = 3.45Hz, $J_{3\text{-}2}$ = 10.45Hz, H^3), 5.31 (1H, dd, $J_{2\text{-}1}$ = 8.28Hz, $J_{2\text{-}3}$ = 10.43Hz, H^2), 5.46 (1H, dd, $J_{4\text{-}5}$ = 1.08Hz, $J_{4\text{-}3}$ = 3.35Hz, H^4), 5.73 (1H, d, $J_{1\text{-}2}$ = 8.21Hz, H^1).

^{13}C NMR (125.7MHz, ^{1}H-decoupled, $CDCl_3$) δ_{ppm}; 20.4 – 20.7 (4xC^{15}), 29.2 (C^{13}), 57.7 (C^7), 61.0 (C^6), 62.0 (C^8), 66.7 (C^5), 67.5 (C^3), 70.8 (C^2), 72.1 (C^4), 80.3 (C^{12}), 89.8 (C^1), 155.0 (C^{11}), 169.2 – 170.5 (4xC^{14} and C^9).

IR (KBr disc) cm^{-1}: 3411 (N-H), 2976 (C-H), 1760 (C=O Ac), 1714 (C=O Boc).

MS (ES+) m/z = 558.2 (85%) $[M+Na]^+$, 599.2 (100%) $[M+Na+CH_3CN]^+$.

Elemental: (Found %); C, 49.12 ; H, 6.30; N, 2.30; (Expected %); C, 49.34; H, 6.21; N, 2.62.

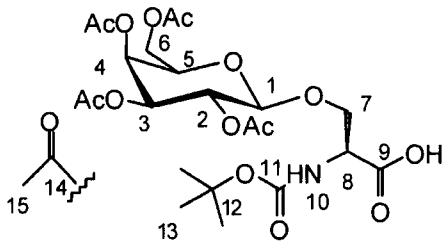

3-*O*-(2, 3, 4, 6-tetra-*O*-acetyl-β-D-glucopyranosyl)-L-threonine acetic acid salt – Thr(GluAc) – 6(a)

BocThr(GluAc) (1g, 1.82 mmol) was dissolved in 10 mL of DCM under N_2. TFA (0.7 ml, 9.11 mmol) was then added dropwise and allowed to stir at ambient temperature for 90 minutes. The solution was then concentrated under reduced pressure on a rotorary evaporator to give a thick syrup. The syrup was taken up in 20 mL of 10% w/v acetic acid(aq) solution and extracted 3 times with 20 mL portions of n-hexane. The title product was isolated as a white solid by freeze-drying. No further purification was required. Yield 0.91g; >95%.

^{1}H NMR (500MHz, $CDCl_3$) δ_{ppm}; 1.49 (3H, d, $J_{15\text{-}7}$ = 6.08Hz, H^{15}), 1.99 – 2.14 (12H, m, H^{11} + H^{13}), 4.06 (1H, d(b), J = 9.95Hz, H^5), 4.15 – 4.22 (2H, m, H^8 + H^{6b}), 4.25 (1H, dd, $J_{6a\text{-}6b}$ = 12.37Hz, $J_{6a\text{-}5}$ = 2.74Hz, H^{6a}), 4.35 (1H, q, $J_{7\text{-}8}$ = $J_{7\text{-}15}$ = 6.14Hz, H^7), 5.12 (2H, t, J = 9.24Hz, H^2 + H^4), 5.35 (1H, t, J = 9.41Hz, H^3), 6.00 (1H, d, $J_{1\text{-}2}$ = 8.12Hz, H^1).

^{13}C NMR (125.7MHz, ^{1}H-decoupled, $CDCl_3$) δ_{ppm}; 19.9-20.6 (C^{11} + C^{13}), 21.2 (C^{15}), 59.4 (C^8), 61.1 (C^6), 65.9 (C^7), 67.6 (C^4), 69.8 (C^2), 72.3 (C^3), 72.5 (C^5), 93.2 (C^1), 166.9 (C^9), 169.4-170.1 (C^{12}), 170.7 (C^{14}).

MS: (ES+) m/z = 449.9 $[M]^+$ (100%).

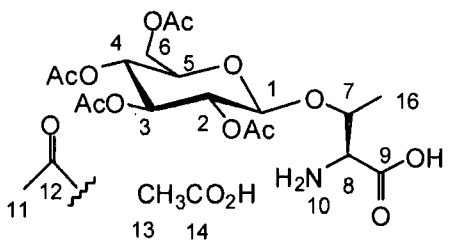

3-*O*-(2, 3, 4, 6-tetra-*O*-acetyl-β-D-galatopyranosyl)-L-threonine acetic acid salt – Thr(GalAc) – 6(b)

The same procedure as for Thr(GluAc) was followed using BocThr(GalAc) (0.9g, 1.64mmol) and TFA (0.63ml, 8.2mmol). Yield 0.83g; >95%.

^{1}H NMR (500MHz, $CDCl_3$) δ_{ppm}; 1.41 (1H, d, $J_{15\text{-}7}$ = 5.88, H^{15}), 1.95 – 2.06 (15H, m, H^{11} + H^{13}), 3.97 (1H, m, H^8), 4.08 (1H, dd, $J_{5\text{-}6a}$ = 6.62Hz, $J_{5\text{-}6b}$ = 7.88Hz) 4.13 (1H, dd, $J_{6a\text{-}6b}$ = 10.84Hz, $J_{6a\text{-}5}$ = 5.92Hz, H^{6a}), 4.19 (1H, dd, $J_{6b\text{-}6a}$ = 10.31Hz, $J_{6b\text{-}5}$ = 5.91Hz, H^{6b}), 4.39 (1H, q, $J_{7\text{-}15}$ = $J_{7\text{-}8}$ = 6.27Hz, H^7), 5.22 (1H, dd, $J_{3\text{-}2}$ = 10.44Hz, $J_{3\text{-}4}$ = 3.04Hz, H^3), 5.31 (1H, dd, $J_{2\text{-}1}$ = 8.25Hz, $J_{2\text{-}3}$ = 10.10Hz, H^2), 5.45 (1H, d, $J_{4\text{-}3}$ = 2.89Hz, H^4), 5.96 (1H, d, $J_{1\text{-}2}$ = 8.07Hz, H^1).

^{13}C NMR (125.7MHz, ^{1}H-decoupled, $CDCl_3$) δ_{ppm}; 19.5 – 20.9 (4xC^{11}, C^{13}, C^{15}), 59.2 (C^8), 60.6 (C^6), 61.9 (C^5), 65.8 (C^7), 66.6 (C^4), 67.5 (C^2), 70.3 (C^3), 71.6 (C^5), 93.7 (C^1), 166.6 (C^9), 179.8 – 171.0 (4xC^{12}), 175.6 (C^{14}).

MS (ES+) m/z = 449.9 $[M]^+$ (100%).

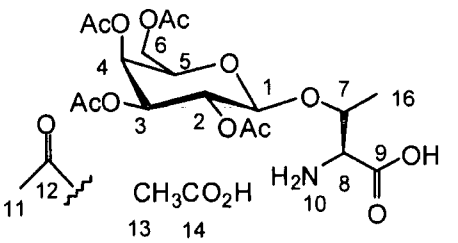

3-*O*-(2, 3, 4, 6-tetra-*O*-acetyl-β-D-glucopyranosyl)-L-serine acetic acid salt – Ser(GluAc) – 6(c)

The same procedure as for Thr(GluAc) was followed using BocSer(GalAc) (1g, 2.02mmol), TFA (0.78ml, 10.1mmol). Yield 0.93g; >95%.

^{1}H NMR (500MHz, $CDCl_3$) δ_{ppm}; 1.98- 2.18 (15H, m, H^{11}, H^{13}), 3.86 (1H, dd, $J_{7a\text{-}7b}$ = 3.63Hz, $J_{7a\text{-}8}$ = 4.43Hz, H^{7a}), 4.02-4.14 (4H, m, H^{6a}, H^{6b}, H^{7b}, H^5), 4.22 (1H, t, $J_{8\text{-}7}$ = 4.50Hz, H^8), 5.21 (1H, dd, $J_{4\text{-}5}$ = 7.45Hz, $J_{4\text{-}3}$ = 3.50Hz, H^4) 5.29 (1H, t, $J_{3\text{-}4}$ = $J_{3\text{-}2}$ = 5.00Hz, H^3), 5.33 (1H, td, $J_{2\text{-}3}$ = 2.00Hz, $J_{2\text{-}1}$ = 8.5Hz, H^2), 5.90 (1H, d, $J_{1\text{-}2}$ = 8.58Hz, H^1).

^{13}C NMR (125.7MHz, ^{1}H-decoupled, $CDCl_3$) δ_{ppm}; 18.4 - 21.4 (4xC^{11}, C^{13}), 58.9 (C^7), 59.1 (C^6), 60.3 (C^8), 66.2 (C^8), 67.4 (C^4), 69.8 (C^2), 71.0 (C^3), 72.2 (C^5), 98.9 (C^1), 166.6 - 171 (C^9, 4xC^{12}, C^{14}).

MS (ES+) m/z = 435.9 $[M]^+$ (100%).

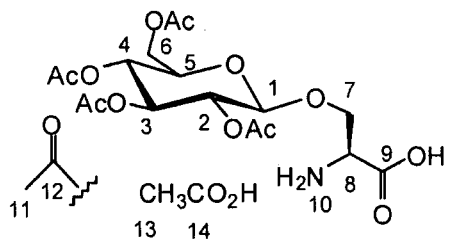

3-*O*-(2, 3, 4, 6-tetra-*O*-acetyl-β-D-galactopyranosyl)-L-serine acetic acid salt – Ser(GalAc) - 6(d)

The same procedure as for Thr(GluAc) was followed using BocSer(GalAc) (1.2g, 2.42mmol), TFA (0.94ml, 12.1 mmol). Yield 1.08g; >95%.

^{1}H NMR (500MHz, $CDCl_3$) δ_{ppm}; ; 2.05 - 2.15 (12H, m, H^{11}), 4.14 (1H, ddd, $J_{5\text{-}6a}$ = 3.00Hz, $J_{5\text{-}6b}$ = 3.60Hz, $J_{5\text{-}4}$ = 7.06Hz, H^5), 4.39 (1H, t, $J_{4\text{-}5} = J_{4\text{-}3}$ = 6.5 H^4), 4.69 (1H, dd, $J_{7a\text{-}7b}$ = 2.50Hz, $J_{7a\text{-}8}$ = 7.5Hz, H^{7a}), 4.80 (1H, m, H^{6a}), 4.91 (1H, t, J = 4.50Hz, H^2), 5.05 (1H, dd, $J_{3\text{-}4}$ = 3.5Hz, $J_{3\text{-}2}$ = 4.5Hz, H^3), 5.46 (1H, m, H^{6b}), 6.04 (1H, d, $J_{1\text{-}2}$ = 8.35Hz, H^1).

^{13}C NMR (125.7MHz, ^{1}H-decoupled, $CDCl_3$) δ_{ppm}; 20.5 - 21.2 (4xC^{11}), 59.0 (C^7), 59.3 (C^6), 60.2 (C^8), 65.2 (C^8), 69.1 (C^2), 71.0 (C^3), 72.3 (C^4), 72.6 (C^5), 99.1 (C^1), 168.2-170.6 (C^9, 4xC^{12}), 174.8 (C^{14}).

MS (ES+) : m/z = 435.1[M^+] 100%.

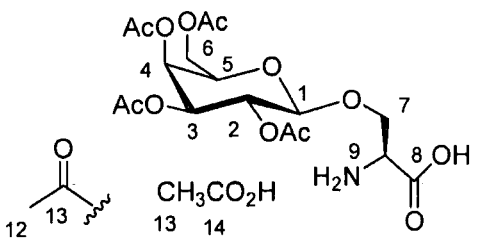

Synthesis of L-threonine ((2, 3, 4, 6-tetraacetyl)-β-D-glucopyranose)) *N*-carboxy anhydride – Thr(GluAc)NCA 7(a)

Thr(GluAc) (100mg, 0.20 mmol) was taken up in 5 mL of EtOAc under N_2. Triphosgene (39mg, 0.13 mmol) was added in a single portion, against the flow of N_2 followed by α-pinene (0.37mL, 2.34 mmol) and allowed to stir at ambient temperature for 20 hours then concentrated to ½ of its original volume on a rotary evaporator under reduced pressure, with the water bath below 30°C. The concentrate was precipitated into hexane at -20°C. The resulting solid was collected then re-precipitated from ethyl acetate into hexane at -20°C three times. The white solid was obtained by centrifugation, and finally dried under vacuum. Yield 68mg; 73%.

^{1}H NMR (500MHz, $CDCl_3$) δ_{ppm}; 1.54 (3H, d, $J_{14\text{-}7}$ = 6.24Hz, H^{14}), 1.98 – 2.10 (12H, m, H^{12}), 3.87 (1H, dd, $J_{5\text{-}4}$= 10.09Hz, $J_{5\text{-}6}$ = 2.33Hz, H^5), 4.00 (1H, d, $J_{8\text{-}7}$ = 4.85Hz, H^8), 4.09 (1H, dd, $J_{6a\text{-}6b}$ = 12.30Hz, $J_{6a\text{-}5}$ = 1.14Hz, H^{6a}), 4.28 (1H, dd, $J_{6b\text{-}6a}$ = 12.58Hz, $J_{6b\text{-}5}$ = 4.52Hz, H^{6b}), 4.76 (1H, m, H^7), 5.12 (2H, m, H^2 + H^4), 5.26 (1H, t, J = 9.41Hz, H^3), 5.72 (1H, d, $J_{1\text{-}2}$ = 8.14Hz, H^1), 6.30 (1H, s, H^9).

^{13}C NMR (125.7MHz, ^{1}H-decoupled, $CDCl_3$) δ_{ppm}; 20.5 – 21.0 (4 x C^{12} + C^{14}), 59.9 (C^8), 61.3 (C^6), 67.6 (C^4), 69.9 (C^2), 72.2 (C^3), 72.9 (C^5), 75.0 (C^7), 92.8 (C^1), 157.7 (C^{10}) 168.8 (C^{11}), 169.3 – 170.5 (4 x C^{13}).

High Resolution MS (ES+) m/z = 476.1396 $[M+Na]^+$; Expected 476.1399.

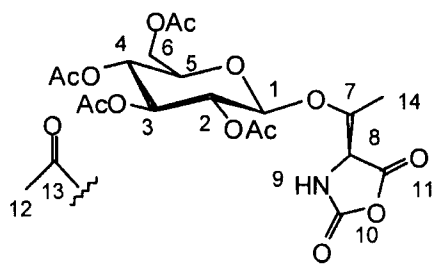

Synthesis of L-threonine ((2,3,4,6 tetraacetyl) β-D galactopyranose)) *N*-carboxy anhydride – Thr(GalAc)NCA – 7(b)

The same procedure was used as for Thr(GluAc)NCA using Thr(GalAc) (92mg, 0.18mmol), triphosgene (36mg, 0.12mmol) and α-pinene (0.34mL, 2.15mmol). Yield 73mg; 86%.

^{1}H NMR (500MHz, $CDCl_3$) δ_{ppm}; 1.55 (3H, d, $J_{14\text{-}7}$ = 6.32Hz, H^{14}), 1.96 – 2.19 (12H, m, H^{12}), 4.00 (1H, d, $J_{8\text{-}7}$ = 4.83Hz, H^{8}), 4.80 (1H, m, H^{7}), 5.11 (1H, dd, $J_{3\text{-}2}$ = 10.45Hz, $J_{3\text{-}4}$ = 3.38Hz, H^{3}), 5.29 (1H, dd, $J_{2\text{-}3}$ = 10.40Hz, $J_{2\text{-}1}$ = 8.22Hz, H^{2}), 5.43 (1H, d, $J_{4\text{-}3}$ = 2.69 Hz, H^{4}), 5.68 (1H, d, $J_{1\text{-}2}$ = 8.18Hz, H^{1}), 6.16 (1H, s, H^{9}).

^{13}C NMR (125.7MHz, ^{1}H-decoupled, $CDCl_3$) δ_{ppm}; 20.5 – 21.0 (4 x C^{12}, C^{14}), 60.2 (C^{8}), 61.1 (C^{6}), 66.8 (C^{4}), 67.9 (C^{2}), 70.5 (C^{3}), 72.2 (C^{5}), 75.4 (C^{7}), 93.3 (C^{1}), 157.9 (C^{10}), 168.0 (C^{11}), 169.8 – 170.4 (4 x C^{13}).

High Resolution MS (ES+) m/z = 498.1230 $[M+Na]^{+}$; Expected 498.1218.

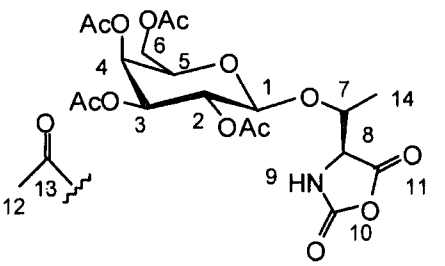

Synthesis of L-serine ((2, 3, 4, 6 tetraacetyl) β-D glucopyranose)) *N*-carboxy anhydride – Ser(GluAc)NCA - 7(c)

The same procedure was used as for Thr(GluAc)NCA using Ser(GluAc) (100mg, 0.22mmol), triphosgene (43mg, 0.14mmol) and α-pinene (0.41mL, 2.57mmol). Yield 65.1mg; 70%.

^{1}H NMR (500MHz, $CDCl_3$) δ_{ppm}; 1.99 - 2.19 (12H, m, H^{13}), 3.70 (1H, dd, J_{7a-7b} = 3.50Hz, J_{7a-8} = 4.00Hz, H^{7a}), 4.06-4.19 (4H, m, H^{6a}, H^{6b}, H^{7ba}, H^8), 4.21 (1H, t, J_{3-4} = 4.50Hz, H^3), 4.77 (1H, m, H^5), 5.11 (1H, dd, J_{4-5} = 7.50Hz, J_{4-3} = 3.00Hz, H^4), 5.25 (1H, td, J_{2-3} = 2.00Hz, J_{2-1} = 7.7Hz, H^2), 5.75 (1H, d, J_{1-2} 8.00Hz, H^1), 6.07 (1H, s, H^9).

^{13}C NMR (125.7MHz, ^{1}H-decoupled, $CDCl_3$) δ_{ppm}; 20.7 - 21.8 (4xC^{12}), 58.9 (C^7), 59.1 (C^6), 60.1 (C^8), 66.2, 67.4 (C^4), 69.8 (C^2), 71.0 (C^3), 72.2 (C^5), 98.6 (C^1), 154.1(C^{10}), 165.3(C^{11}), 168.7 -171.0 (4xC^{13}).

High Resolution MS (ES+) m/z = 484.1066 $[M+Na]^+$; Expected 484.1062.

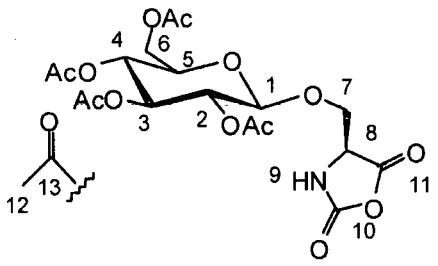

Synthesis of L-serine ((2, 3, 4, 6 tetraacetyl) β-D galactopyranose)) *N*-carboxy anhydride – Ser(GalAc)NCA - 7(d)

The same procedure was used as for Thr(GluAc)NCA using Ser(GalAc) (200mg, 0.43mmol), triphosgene (87mg, 0.28mmol) and α-pinene (0.82mL, 5.14mmol). Yield 150 mg; 82%.

^{1}H NMR (500MHz, $CDCl_3$) δ_{ppm}; 2.02 - 2.14 (H^{13}), 4.00 (1H, ddd, $J_{5\text{-}6a}$ = 3.00Hz, $J_{5\text{-}6b}$ = 3.60Hz, $J_{5\text{-}4}$ = 7.06Hz, H^5), 4.35 - 4.48 (4H, m, H^4, H^{6a}, H^{6b} H^8), 5.07 (1H, dd, $J_{2\text{-}3}$ = 3.50Hz, $J_{1\text{-}2}$ = 4.50Hz, H^2), 5.45 (1H, dd, $J_{3\text{-}2}$ 2.00Hz, $J_{3\text{-}4}$ = 3.50Hz, H^3), 6.04 (1H, d, $J_{1,2}$ = 6Hz, H^1), 6.71 (1H, s, H^9).

^{13}C NMR (125.7MHz, ^{1}H-decoupled, $CDCl_3$) δ_{ppm}; 20.5 - 21.2 (4xC^{13}), 59.0 (C^7), 59.3 (C^6), 60.4 (C^8), 69.2 (C^2), 71.0 (C^3), 72.2 (C^4), 72.6 (C^5), 99.1 (C^1), 155.8 (C^{10}), 164.7 (C^{11}), 167.2-170.1 (4xC^{13}).

High Resolution MS (ES+) m/z = 484.1061 $[M+Na]^+$; Expected 484.1062

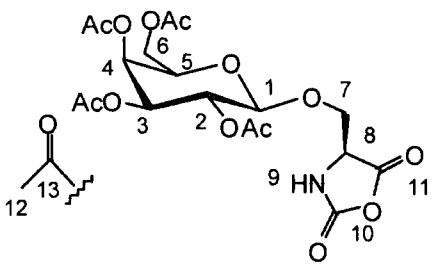

2.5 BIBLIOGRAPHICAL REFERENCES

(1) van Hest, J. C. M.; Tirrell, D. A. *Chem. Commun.* **2001**, 1897-1904.

(2) Kricheldorf, H. R. In *Alpha amino acid-N-CarboxyAnhydrides and Related Materials*; Springer-Verlag: New York, 1987.

(3) Leuchs, H. *Ber. Dtsch. Chem. Ges.* **1906**, *39*, 857-859.

(4) Farthing, A. C. *J. Am. Chem. Soc.* **1950**, 3213-3217.

(5) Kricheldorf, H. R.; Von Lossow, C.; Schwarz, G. *J. Pol. Sci. Part A: Pol. Chem.* **2005**, *43*, 5690-5698.

(6) Kricheldof, H. R.; Hull, W. E. *Macromolecules* **1980**, *13*, 87-95.

(7) Farthing, A. C.; Reynolds, R. J. W. *Nature* **1950**, *165*, 647.

(8) Eckert, H.; Forster, B. *Angew. Chem. Int. Ed.* **1987**, *26*, 894.

(9) Ramsperger, G.; Waddington, G. *J. Am. Chem. Soc.* **1933**, *55*, 214.

(10) Daly, W.; Poche, D. *Tet. Lett.* **1988**, *29*, 5859-5862.

(11) Deming, T. J.; Curtin, S. A. *J. Am. Chem. Soc.* **2000**, *122*, 5710-5717.

(12) Papadopoulos, P.; Floudas, G.; Schnell, I.; Aliferis, T.; Iatrou, H.; Hadjichristidis, N. *Biomacromolecules* **2005**, *6*, 2352-2361.

(13) Lubbert, A.; Castelletto, V.; Hamley, I. W.; Nuhn, H.; Scholl, M.; Bourdillon, L.; Wandrey, C.; Klok, H.-A. *Langmuir* **2005**, *21*, 6582-6589.

(14) Cheng, J.; Ziller, J. W.; Deming, T. J. *Org. Lett.* **2000**, *2*, 1943-1946.

(15) Nagai, A.; Sato, D.; Ishikawa, J.; Ochiai, B.; Kudo, H.; Endo, H. *Macromolecules* **2004**, *37*, 2332-2334.

(16) Mobashery, S.; Johnston, M. *J. Org. Chem.* **1985**, *50*, 2200-2202.

(17) Wilder, R.; Mobashery, S. *J. Org. Chem,* **1992**, *57*, 2755-2756.

(18) Frerot, E.; Coste, J.; Poncet, J.; Jouin, P. *Tet. Lett.* **1992**, *33*, 2815-2816.

(19) Bodanszky, M.; Klausner, Y. S.; Bodanszky, A. *J. Org. Chem.* **1975**, *40*, 1507-1508.

(20) Chen, F. M. F.; Juroda, K.; Benoiton, N. L. *Synthesis* **1978**, *78*, 928.

(21) Curtius, T.; Sieber, W. *Ber. Dtsch. Chem. Ges.* **1921**, *54*, 1430.

(22) Palomo, G.; Aizpurua, J. M.; Ganboa, I.; Maneiro, E.; Odrizola, B. *J. Chem. Soc. Chem. Commun.* **1994**, 1505-1507.

(23) Collet, H.; Bied, C.; Mion, L.; Taillades, J.; Commeyras, A. *Tet. Lett* **1996**, *37*, 9043-9046.

(24) Vayaboury, W.; Gianni, O.; Collet, H.; Commeyras, A.; Schue, F. *Amino Acids* **2004**, *27*, 161-167.

(25) Taillades, J.; Collet, H.; Garrel, L.; Beuzelin, I.; Boiteau, L.; Choukroun, H.; Commeyras, A. *J. Mol. Evol.* **1999**, *48*, 638-645.

(26) Leman, L.; Orgel, L.; Ghadiri, M. R. *Science* **2004**, *306*, 283-286.

(27) Danger, G.; Boiteau, L.; Cottet, H.; Pascal, R. *J. Am. Chem. Soc.* **2006**, *126*, 7412-7413.

(28) Rude, E.; Westphal, O.; Hurwitz, E.; Fuchs, S.; Sela, M. *Immuno. Chem.* **1966**, *3*, 137-151.

(29) Carubia, J. M.; Weaver, T. M.; Ponnusamy, E. In *PCT/US05/38836* USA, 2004.

(30) Cornille, F.; Copier, J.-L.; Senet, J.-P.; Robin, Y. In *US Patent Appl US2002/0082431* USA, 2001.

(31) Smeets, N. M. B.; van der Weide, P. l. J.; Meuldijik, J.; Vekemans, A. J. M.; Hulshof, L. A. *Org. Process. Res. Dev.* **2005**, *9*, 757-763.

(32) Rude, E.; Meyer-Delius, M. *Carb. Res.* **1968**, *8*, 219-232.

(33) Banoub, J.; Boullanger, P.; Lafont, D. *Chem. Rev.* **1992**, *92*, 1167-1195.

(34) Kartha, K. P. R.; Aloui, M.; Field, R. A. *Tet. Lett* **1996**, *37*, 5175-5178.

(35) Elofsson, M.; Walse, B.; Kihlberg, J. *Tet. Lett* **1991**, *32*, 7613-7616.

(36) Salvador, L. A.; Elofsson, M.; Kihlberg, J. *Tetrahedron* **1995**, *51*, 5643-5656.

(37) Whalen, L. J.; Halcomb, R. L. *Org. Lett.* **2004**, *6*, 3221-3224.

(38) Codee, J. D. C.; Litjens, E. J. N.; van den Bos, L. J.; Overkleeft, H. S.; van der Marel, G. A. *Chem. Soc. Rev.* **2005**, *34*, 769-782.

(39) Uzawa, H.; Nagatsuka, T.; Hiramatsu, H.; Nishida, Y. *Chem. Commun.* **2006**, 1381-1383.

(40) Zhang, Z.; Gildersleeve, J.; Yang, Y.; Xu, R.; Loo, J. A.; Uryu, S.; Wong, C.-H.; Schultz, P. G. *Science* **2004**, *303*, 371-373.

(41) Biondi, L.; Filira, F.; Gobbo, M.; Polese, A.; Scolaro, B.; Rocchi, R. Proceedings of The European Peptide Symposium, Brage, Portugal, 1994; p 723-724.

(42) Aoi, K.; Tsutsumiuchi, K.; Okada, M. *Macromolecules* **1994**, *27*, 875-877.

(43) Wies, R.; Pfaender, P. *Liebigs. Ann. Chem.* **1973**, 1269-1274.

(44) Kricheldof, H. R. *Chem. Ber.* **1971**, *104*, 87-91.

(45) Poche, D.; Moore, M. J.; Bowles, J. L. *Syn. Comm.* **1999**, *29*, 843-854.

(46) Carpino, L. A. *Acc. Chem. Res.* **1987**, *20*, 401-407.

(47) Sheppeck II, J. E.; Kar, H.; Hong, H. *Tet. Lett.* **2000**, *41*, 5329-5333.

(48) Mootoo, D. R.; Konradsson, P.; Udodong, U.; Fraser-Reid, B. *J. Am. Chem. Soc.* **1988**, *110*, 5583-5584.

(49) Ambrosi, M.; Batsanov, A.; Cameron, N. R.; Davis, B. G.; Howard, J. A. K.; Hunter, R. J. *J. Chem. Soc., Perkin Trans. 1* **2002**, 45-52.

(50) Bose, D. S.; Lakshminarayana, V. *Synthesis* **1999**, 66-68.

(51) James, D. J.; Ellington A. D *Tet. Lett.* **1998**, *39*, 175-178.

(52) Schnabel, E.; Klostermeyer, H.; Berndt, H. *Liebigs. Ann. Chem.* **1971**, *749*, 90-108.

(53) Rae, A.; Ker, J.; Tabor, A. B.; Castro, J. L.; Parsons, S. *Tet. Lett.* **1998**, *39*, 6561-6564.

(54) Saha, U. K.; Schmidt, R. R. *J. Chem. Soc., Perkin Trans. 1* **1997**, 1855-1860.

(55) Kartha, K. P. R.; Ballell, L.; Bilke, J.; McNeil, M.; Field, R. A. *J. Chem. Soc., Perkin Trans. 1* **2001**, *1*, 770-772.

(56) Stachulski, A. V. *Tet. Lett.* **2001**, *42*, 6611-6613.

(57) Kartha, K. P. R.; Aloui, M.; Field, R. A. *Tet. Lett* **1996**, *37*, 8807-8810.

(58) Curran, T. P.; Pollastri M. P; Abelleira, S. M.; Messier, R. J.; McCollum, T. A.; Rowe, C. G. *Tet. Lett.* **1994**, *35*, 5409-5412.

(59) Allen, J. R.; Harris, C. R.; Danishefsky, S. J. *J. Am. Chem. Soc.* **2001**, *123*, 1890-1897.

CHAPTER 3

L-THREONINE *N*-CARBOXY ANHYDRIDE: CONTROLLED POLYMERISATION AND CHARACTERISATION

3.1 INTRODUCTION

In the presence of an appropriate initiator, NCAs polymerise without racemisation to give high molecular weight polypeptides without the need for time consuming solid phase synthetic methods[1], although *N*-protected NCAs have also been used in stepwise peptide synthesis[2-5]. Leuchs first investigated their polymerisation in the early 20th century after observing that, in the presence of differing amounts of water, NCAs either hydrolyse or polymerise[6]. The materials produced tended to be insoluble and were difficult to characterise with the equipment available and the lack of acceptance of the idea of polymeric structures. Higher molecular weight polypeptides were successfully synthesised and characterised, by using alcohols and primary amines as initiators instead of water by workers at Courtaulds UK[7]. The homopolymers formed from NCAs allowed the identification of the famous secondary structures motifs formed by peptides[8,9], namely the α-helix and β-sheet[10] to be performed.

NCA polymerisation has historically been initiated by one of two methods[11]. Strongly nucleophilic species such as primary amines initiate by nucleophilic attack, and ring opening of the NCA. CO_2 is evolved, regenerating a primary amine end group which can continue propagation. This is referred to as the 'amine' mechanism, shown in Scheme 1.

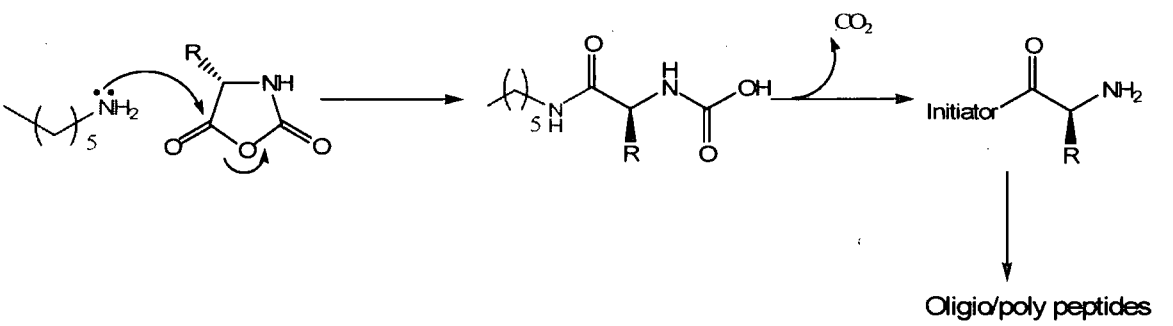

Scheme 1. NCA polymerisation by the amine mechanism using n-hexylamine as the initiator.

As the initiator is incorporated into the polymer chain, the feed ratio dictates the degree of polymerisation, in the absence of any other initiation reactions. Blout and Karlson[12] showed that, when a tertiary amine is used, the molecular weights obtained were substantially greater than with primary amines or alcohols. Bamford *et al*[13] proposed the process now known as the activated monomer (AM) mechanism to explain this (Scheme 2). Addition of base results in the formation of NCA anions by abstraction of the N-H. This can then attack nucleophilically another monomer, as with the amine mechanism. However the end group can also react with other NH_2 groups resulting in chains condensing together, thus inflating the observed molecular weight. Table 1 displays the molecular weights of poly(γ-benzyl-glutamate) (PBLG) obtained using different initiators. n-Hexylamine initiates by the amine mechanism and thus gives the lowest molecular weights, while the increasingly basic species inflate the molecular weight due to the AM mechanism.

Table 1. Molecular weights obtained by polymerisation of BLG NCA in dioxane at equal [M]:[I] ratios.[14]

Initiator	**Mol. Wt. x 10^{-3}/ Da**
n-Hexylamine	15
Diethylamine	83
Triethylamine	280
Sodium hydroxide	31
Sodium methoxide	29.5
Sodium borohydride	32.5

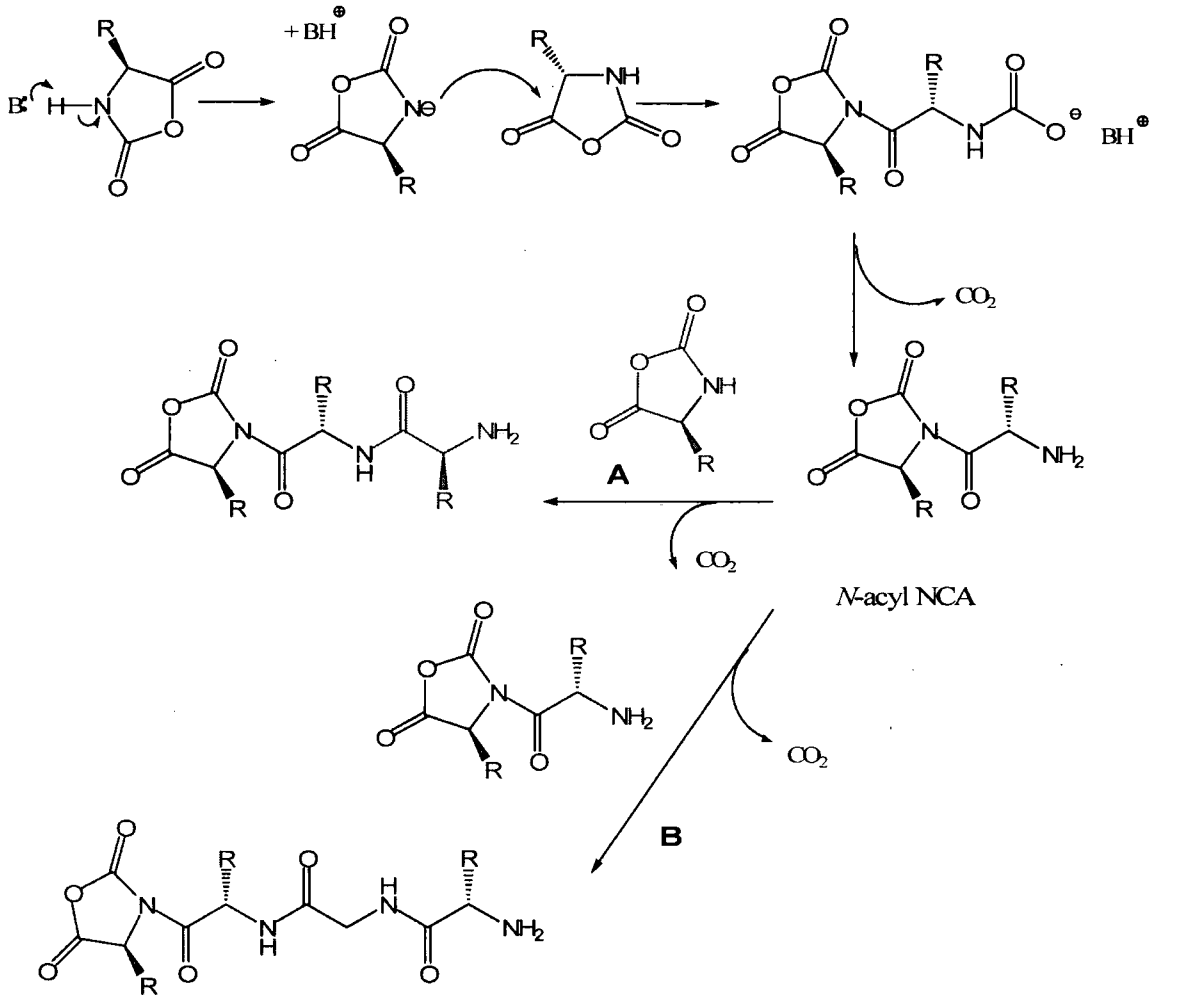

Scheme 2. NCA polymerisation by the activated monomer mechanism

Kinetic investigations into both of these mechanisms were conducted by measuring the evolution of CO_2 conductmetrically. Different groups reported conflicting findings, attributing the complex kinetics to initial and intermediate secondary structure formations, the presence of impurities and two competing mechanisms[14-17]. A common feature of NCA polymerisation through the last 50 years has been the lack of control of the molecular parameters of the final polymer[18], which have been associated with numerous side reactions involving degradation products[§] of the NCA, and the assumption that during polymerisation the mechanism switches

[§] Isocyanates have been reported, which can end-cap the amine. Hydantoic acid end groups caused by hydrolysis also terminate the chain. NCAs also degrade to their constituent amino acids in the presence of any unprotected functionality, which further complicate the process.

between the AM and amine route. The first successful procedure to overcome this was described by Deming in 1997 who exploited the previous observations[19] that various transition metal complexes polymerised NCAs although in an uncontrolled manner, and without isolation of the active species. By tuning the ligand[20] and metal it has since been shown that the best initiators are based on zero valent nickel and cobalt complexes[21,22]. Briefly the polymerisation mechanism involves[23,24] (Scheme 3) oxidative addition of the NCA across the C_5-O bond, and expulsion of CO. This generates a metallocycle which can expand to accommodate another NCA with accompanying evolution of CO_2. Proton migration releases one end of the polypeptide and re-forms the active metallocycle. A wide range of NCAs can be polymerised (including stereoselective polymerisation of racemic mixtures[25]) by this system resulting in predictable molecular weights and low polydispersity indices. Block copolymers containing up to 5 different blocks have been synthesised[26], and the method has been combined with other living polymerisations (anionic and atom transfer radical polymerisation (ATRP)) to give hybrid materials containing vinyl derived and polypeptide blocks[27,28]. Other promising organometallic initiators based on complex's between aluminium and Schiff bases have been reported[29,30].

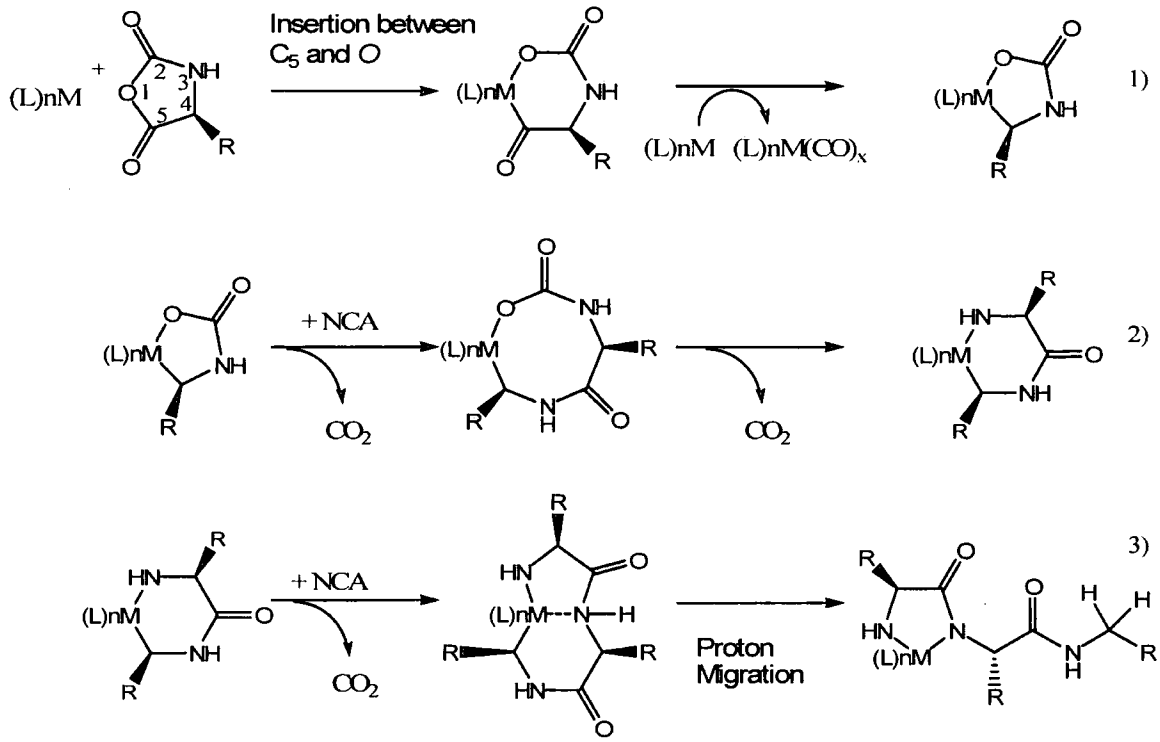

Scheme 3. Mechanism of polymerisation of NCAs by Deming type initiators.

Schlaad *et al.*[31] have proposed an alternative method involving ammonium chloride-terminated macroinitators. Polymerisation can proceed by the amine mechanism, but with reduced reactivity due to the equilibrium between the dormant ammonium and active amine species. This reduction in reactivity gives an associated increase in control and high molecular weight polypeptide blocks can be synthesised. Results using PEG-NH_3Cl however are less encouraging, producing only short polypeptide blocks (DP < 20) even with large excess of monomer and extended (over 7 days) reaction times[32].

Aoi *et al.*[33] have used ammonium salts to produce poly(sarcosine), and even claim that controlled polymerisation occurs in the presence of OH groups in the form of chitosan. No other groups have reported this behaviour, indeed the presence of any other nucleophiles has always resulted in poorly defined materials. A key feature of the ammonium mediated methods is that high purity monomers were used. These

were obtained by the aqueous extraction method of Poche *et al.*[34]. (See chapter 2) High purity NCA monomers have also been used by Hadjichristidis *et al.*[35] for controlled polymerisation. The NCAs in this method are never exposed to air during their synthesis and polymerisation. In combination with high vacuum techniques and rigorously dry solvents and initiators they showed that perfectly controlled polymerisation could be achieved to high DP (>700) while retaining the living end-groups. This has effectively settled the issue regarding whether NCA polymerisation continuously switches between the amine and activated monomer mechanisms and has indicated that poor control and side reactions were caused by impurities.

3.2 RESULTS AND DISCUSSION

3.2.1 POLYMERISATION OF NCAs PURIFIED BY STANDARD TECHNIQUES

Thr(Bzl)NCA (as described in chapter 2) was purified by the standard technique of repeated precipitations from THF into hexane. To test the utility of this monomer, which to our knowledge has not previously been polymerised, two initiating systems were used. The polymerisations were conducted under a nitrogen atmosphere using standard glassware.

1) Triethylamine, which is a strong base and poor nucleophile, initiates by the activated monomer mechanism, (Table 2).

2) n-Hexylamine, which is a weak base but strong nucleophile, initiates by the amine mechanism, (Table 3).

The results of these experiments are tabulated below.

Table 2. Polymerisation of Thr(Bzl)NCA by NEt_3

Run N°	[M]:[I]	$M_{n,SEC}$ (kDa)	DP	PDI	Modality
1[(a)]	50	11.4	60	1.34	Mono
2[(a)]	75	8.5	45	1.65	Mono
3[(a)]	100	25.9	136	1.90	Bi
4[(a)]	130	25.2	132	1.27	Mono
5[(a)]	200	30.1	158	1.86	Bi
6[(a)]	370	3,4	18	2.44	Tri
7[(a)]	520	3.7	20	1.7	Mono
8[(b)]	100	N/A	-	-	-
9[(c)]	100	N/A	-	-	-
10[(d)]	100	2.9	15	1.01[(e)]	Mono

Conditions: monomer concentration ~ 10 % (wt) under dry N_2. Solvent: (a) DCM; (b) DMF; (c) acetonitrile; (d) THF. (e) PDI value abnormally low, due to very weak signal in light scattering. Appears to be broader in RI.

Table 3. Polymerisation of Thr(Bzl)NCA by n-hexylamine.

Run N°	[M]:[I]	$M_{n,SEC}$ (kDa)	DP	PDI	Modality
1	30	2.3	12	2.02	Mono
2	50	3.9	20	1.86	Bi
3	100	24.5	128	1.90	Bi
4	100	4.3	22	1.52	Mono
5	200	<1.0	-	-	-
6	500	<1.0	-	-	-

Conditions: Monomer concentration ~ 10 % (wt) under dry N_2 in DCM

It is generally accepted that basic initiators produce higher molecular weight polypeptides than nucleophilic initiators. The results in Tables 1 and 2 clearly demonstrate this. Using NEt_3, DPs over 150 were obtained (Table 2, entry 5)

compared to the best result of 128 (Table 3, entry 3) by n-hexylamine. There are many reports of basic initiating systems giving rise to polymers with M_n's of >100 kDa[12,34] particularly in the case of γ-benzyl-L-glutamate (BLG) NCA, which is substantially greater than what is reported here. Less that 50% of the experiments conducted resulted in polymer formation.

With NEt_3 as the initiator, multimodal distributions and high molecular weight distributions were observed. There was a general trend of increasing molecular weight with increasing feed ratio as would be expected. When the feed ratio was increased above 200, then only low molecular weight species were formed. At these ratios, only a very small amount of initiating species is present, thus a lower concentration of terminating impurities are needed to prevent polymerisation. DCM was found to be a suitable solvent for the polymerisation of Thr(Bzl)NCA as it is for many other NCA monomers. Its lack of functionality prevents any unwanted interactions. The only limitation was that the reaction could not be heated above 38°C, which may have driven the polymerisation forward. DMF is probably the most commonly used solvent for NCA polymerisation[36] owing to its polarity, and ability to dissolve a wide range of peptides.** In our hands no significant polymerisation was detected when DMF was used as the solvent. Vayboury *et al.*[37] have shown that DMF can act as an end capping reagent, rendering the chain ends dead as shown in Scheme 4. DMF is also very difficult to dry, requiring fractional distillation.

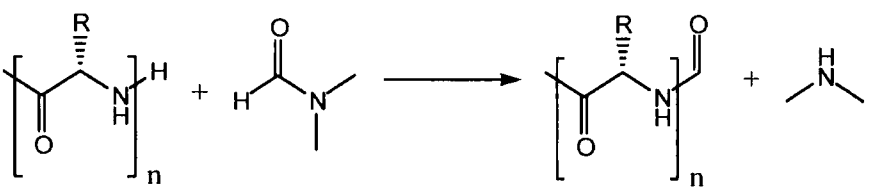

Scheme 4 - End capping of a growing polypeptide by reaction with DMF

** DMF is also commonly used in solution phase peptide synthesis.

Acetonitrile is another polar solvent, but has not been used extensively for NCA polymerisation as it is also very hygroscopic, which may explain why no polymerisation was observed when it was used, (Table 1, entry 9). With THF as the solvent, polymerisation was observed, as would be expected as its structural relative 1,4 dioxane is a commonly used solvent for NCA polymerisation and it can be easily dried over sodium. When n-hexylamine was used as the initiator, only DCM was used as the solvent and similar patterns were observed. Multimodal distributions indicate that chain termination, unequal rates of propagation or multiple initiation events are occurring.

In the early stages (0-10 hours) of the polymerisation the solutions in DCM became turbid which sometimes resulted in precipitation of oligomers and amino acid salts. This highlights the most frustrating impurity associated with NCAs, which is residual HCl from the synthetic procedure using triphosgene. The chloride ion in sufficiently high concentration can initiate polymerisation by the nucleophilic 'amine' mechanism[1], accounting for some of the multimodal distributions. More importantly the propagating amine end groups can be terminated by addition of a proton from HCl. At low DPs, the oligomers with a charged end group are less soluble in organic solvents causing precipitation. NCA decomposition products including hydantoic acids, ioscyanates and amino acid are all capable of interfering with the polymerisation.

In summary, it is clear that Thr(Bzl)NCA, which has been purified by re-precipitations, cannot be used to obtain polymers of defined molecular weight and architecture due to impurities derived from the presence of HCl. Furthermore, the failure of half of the experiments to initiate limits the application to more complex NCAs which may not be available in significant quantities.

3.2.2 POLYMERISATION OF ULTRA-PURE NCAs

To remove acidic impurities from the NCA monomer, extraction with a basic aqueous solution was conducted as an additional purification step. This extreme measure (NCAs decompose in the presence of water) leads to high purity monomers. The removal of acidic impurities should prevent deactivation of the amine initiators by an acid-base reaction. To ensure that the reaction medium remains free of impurities high vacuum techniques were used[38]. Chemicals were transferred by syringe or flask-to-flask distillation and handled under vacuum or in an inert atmosphere. THF was used as the solvent unless otherwise stated. The results of this are summarised in Table 4.

Table 4. Polymerisation of Thr(Bzl)NCA by n-hexylamine

Run N°	[M]:[I]	$M_{n,SEC}$ (kDa)	$M_{n,Theo}$ (kDa)	Conv (%)	PDI
1	25	5.1	4.5	95	1.32
2	50	4.4	5.4	57	1.25
3	50	9.6	8.6	90	1.36
4	75	10.2	12.2	85	1.25
6	100	18.9	17.6	90	1.16
5	100	21.1	19.1	95	1.12
8	150	20.4	21.5	75	1.11
7	150	30.9	27.5	95	1.4

Conditions: Monomer concentration 10 % (wt); THF distilled from Na/benzophenone; under vacuum (< 0.1mbar); 35°C; 4 days.

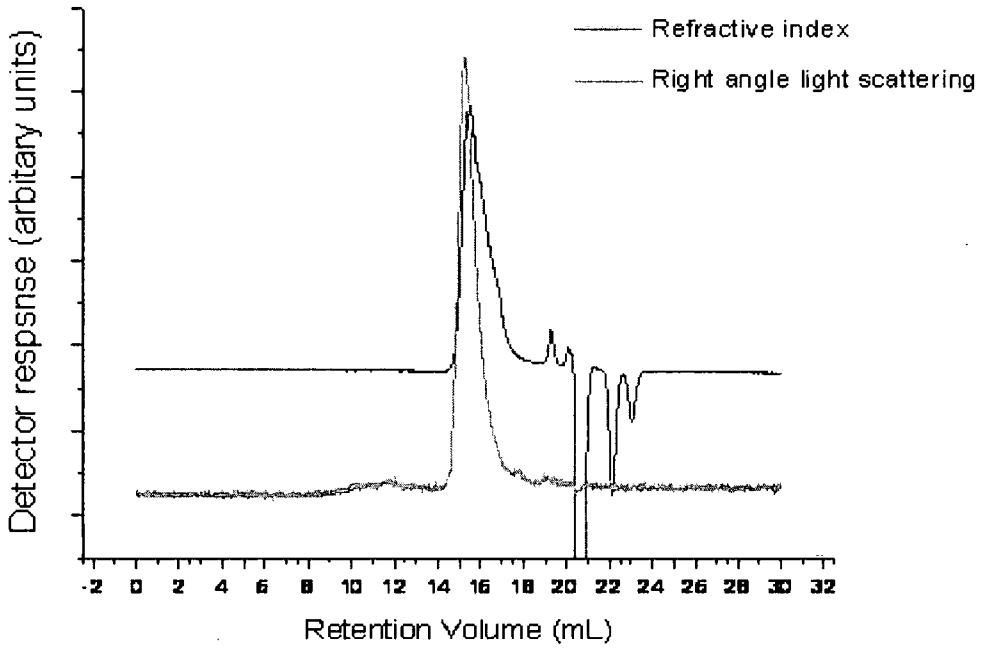

Figure 1 – THF SEC trace of poly(benzyl-L-threonine), M_n = 21600.

In all cases the polymerisation of the high purity Thr(Bzl)NCA was successfully initiated by addition of n-hexylamine. A single peak attributable to the polymer was observed in the SEC chromatograms with no low molecular weight material (other than unreacted monomer) present, (Figure 1). Increasing the feed ratio from 30:1 to 250:1 gave corresponding increases in the molecular weight of polymers formed, while the polydispersity indices remained below 1.4. The polymerisation data are summarised in Figure 2. Unlike when the lower purity monomers were used, there is no turbidity at any stage in the reaction.

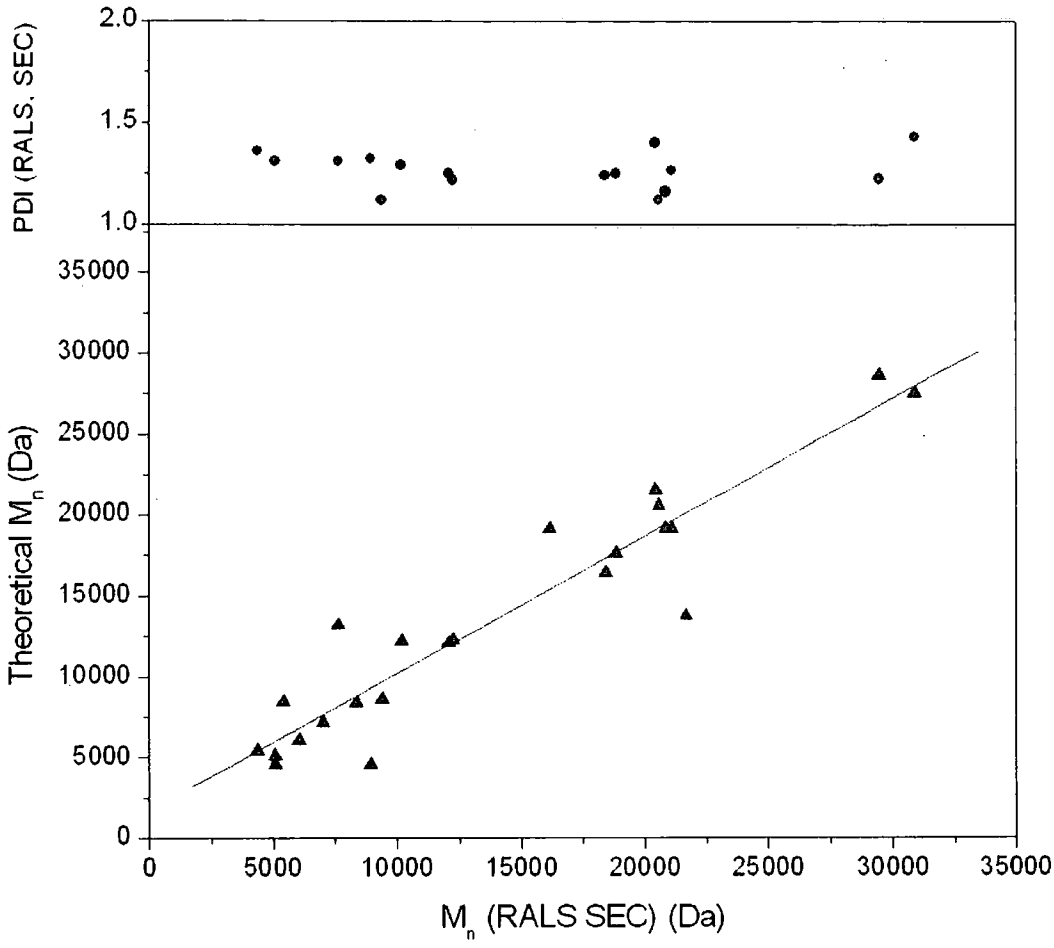

Figure 2. (Lower): Correlation between experimental and theoretical M_n determined by the feed ratio; (Upper): PDI of corresponding materials.

Utilisation of the aqueous extraction method obviously improved the level of control over the polymerisation of Thr(Bzl)NCA compared to monomers purified by the traditional routes. It was necessary to combine the increased purity with high vacuum techniques, as this is the only method which gives absolute control over the internal environment of the reaction vessel. It was thus possible to produce polymers with a high molecular weight (> 30,000 Da) without the need for a basic initiator, while still controlling the DP by stoichiometry. A monomodal distribution was obtained in the SEC traces and MALDI-tof, (Figures 3 and 4) suggesting that there

was a single polymerisation mechanism in operation without premature termination reactions, as opposed to the situation with the low purity NCAs which gave rise to multimodal distributions.

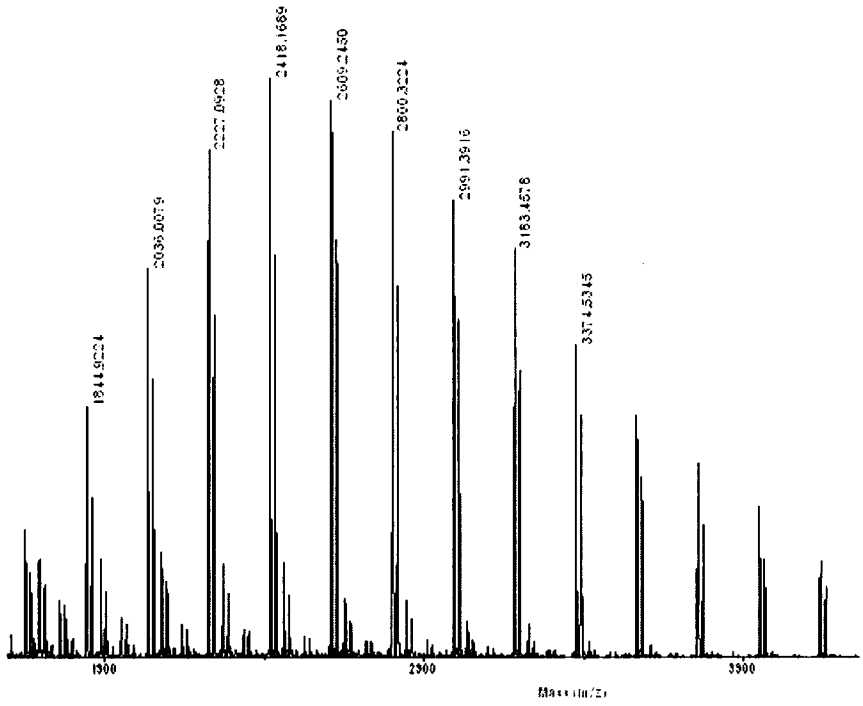

Figure 3. MADLI-TOF spectrum of low molecular weight poly(benzyl-L-threonine). Repeat unit = 191 Da

MALDI-Tof was used determine whether initiator was incorporated into all of the polymeric chains. This would indicate if the amine mechanism was operating exclusively. The higher molecular weight polymers did not 'fly' very well and gave poor results, so a low molecular weight polymer was used instead with a DP of 15, (Ca. 3 kDa).

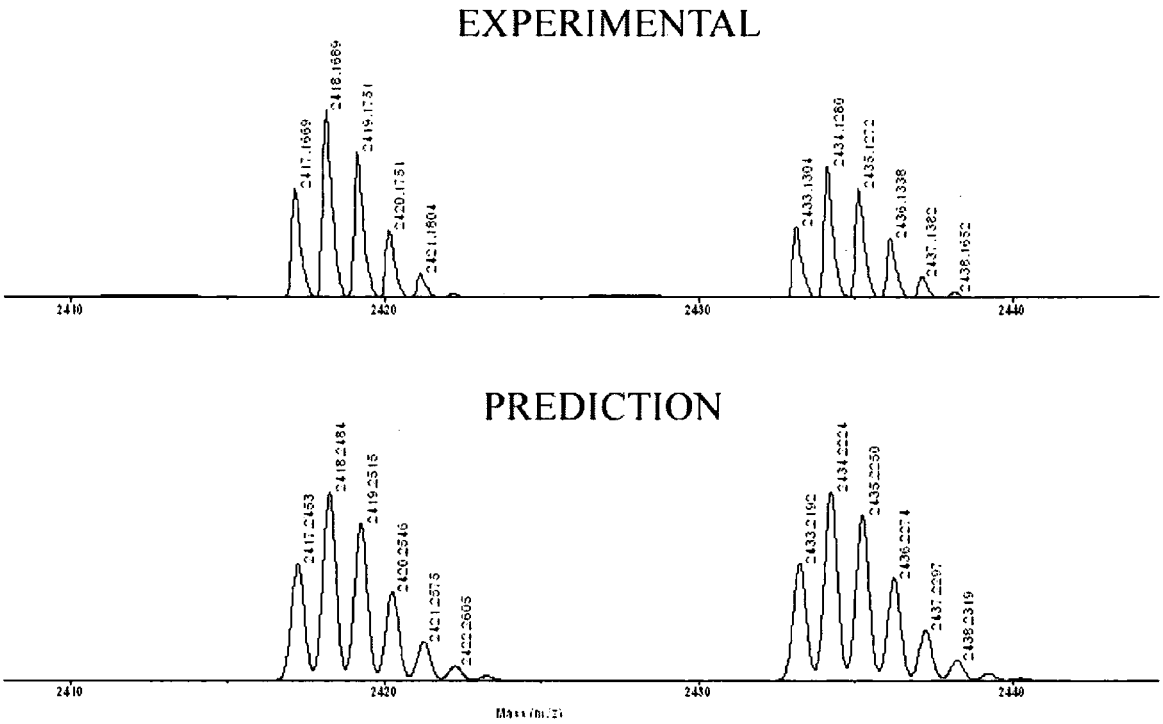

Figure 4. (Top) Expanded portion of MALDI-TOF spectrum of poly(benzyl-L-threonine). (Bottom) Predicted spectrum for poly(benzyl-L-threonine) incorporating $CH_3(CH_3)_5NH$ residue from initiator.

Figure 4 shows that the predicted spectrum matches exactly with that found, thus confirming that hexylamine was incorporated into each of the chains, and that the only repeat unit present has a mass of 191 Da: ie, a single (*O*-benzyl)-L-threonine unit. ^1H NMR also confirmed the presence of the end group but no attempt was made to asses the molecular weight as the peaks were both small and slightly obscured, which would introduce significant error.

3.2.3 POLYMER CHARACTERISATION

To determine the molecular weight and molecular weight distributions of the synthesised polymers, size exclusion chromatography (SEC) in combination with right angle laser light scattering (RALLS) was used. Extensive discussion of light scattering theory of this is not appropriate here, but is summarised below[39].

When light interacts with a molecule it is scattered. This scattered light has the same wavelength as the incident beam and is known as the Rayleigh scattering. Pure solvent also scatters light, so it is the excess light scattering caused by the solute which is measured. This excess light scattering is proportional to both the concentration of solute and its M_w. Polymeric materials scatter a sufficiently large excess, allowing them to be analysed by this method.

$$KC/R_\theta = 1/(M_w P_\theta) + 2A_2C \quad (1)$$

C is the concentration of the solution

A_2 is the second virial coefficient

K is an optical constant

P_θ is the particle scattering function, (angular dependence of scattering intensity)

R_θ is the excess Rayleigh ratio

The excess Rayleigh ratio is calculated from the amount of light scattered relative to a reference of the pure solvent and an instrument calibration using a known standard. P_θ is calculated online. To calculate M_w all that is needed is an accurate measure of the Rayleigh ratio (from the RALLS detector) and an accurate value of concentration. Concentration can be determined either by using volumetrically measured solutions of the polymer each time ensuring that no residual monomer

remains, or by an online method. This is achieved simply by using an online refractive index detector. Assuming a material has a constant refractive index increment (dn/dc) at all molecular weights (which is a reasonable assumption above a certain M_w) the concentration can easily be calculated. The value of dn/dc is normally obtained from tables of known values (such as can be found in the Polymer Handbook[40]). This value is specific to the solvent and temperature. No values are published for poly (*O*-benzyl-L-threonine) in any solvent thus we had to calculate dn/dc.

The integrated RI peak area is described by the following equation:

$$RI_{(area)} = \frac{RI_{(cal)}}{\eta_o} \bullet \frac{dn}{dc} \bullet V_{inj} \bullet C \quad (2)$$

The change in RI_{area} with concentration is thus:

$$\frac{\Delta RI_{area}}{\Delta C} = \frac{RI_{Cal}}{\eta_o} \bullet \frac{dn}{dc} \bullet V_{inj} \quad (3)$$

RI_{Cal}, η_o, and V_{Inj} are all known parameters so dn/dc is simply related to the slope of the plot of RI response against concentration.

The polymer used for this must be free of monomer, so that the concentration of polymer is known exactly. This was achieved by repeated precipitation into diethyl ether and water, then analysis by NMR to ensure no monomer persisted.

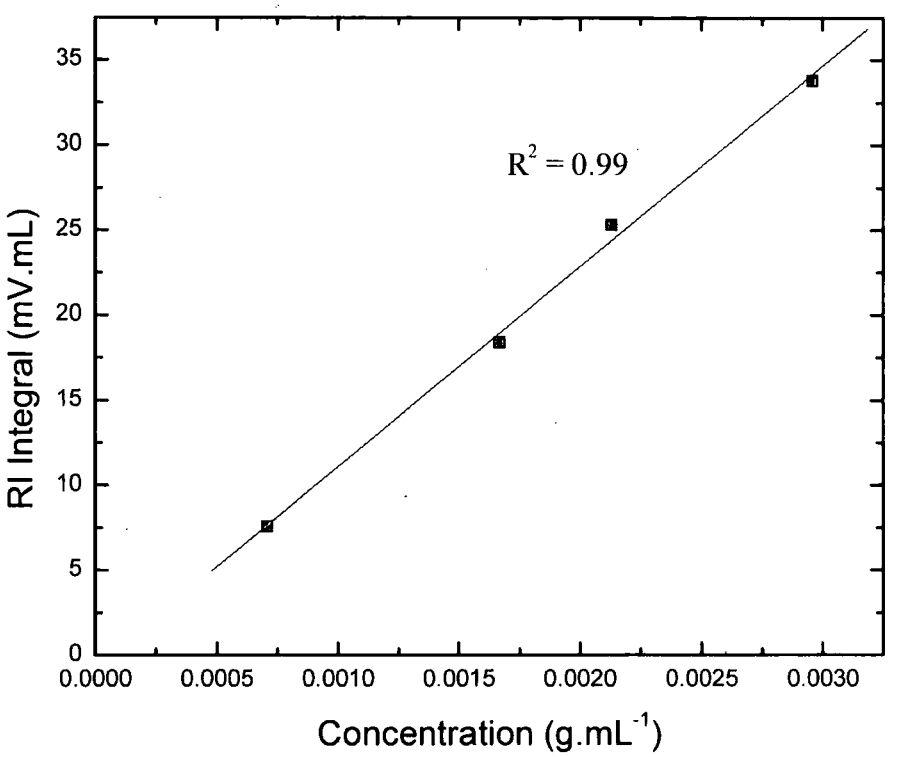

Figure 5. Change of refractive index integral with concentration of poly(benzyl-L-threonine) in THF. Measured online on SEC instrument

A good linear fit was obtained (Figure 5) between the RI response and concentration. Ideally, the extrapolated line of best fit should pass though the origin. This is not the case, probably due to impurities in the THF, particularly water absorbed from the atmosphere. When calculating the value of the slope the data obtained from the best fit regression were used, without forcing through the origin.

Table 5. Results of dn/dc determination of poly(benzyl-L-threonine) in THF

Polymer	**Slope (mV.mL^2/g)**	**dn/dc (mL/g)**
Poly-(Bzl)-L-threonine	11787	**0.1111**

An important observation to be made here is that the molecular weights calculated by RALLS using this value of dn/dc differed significantly from those

obtained by conventional calibration, using narrow polystyrene standards. The relationship is shown in Figure 6. The M_n calculated by RALLS is always larger than that from conventional calibration. The implication is that the hydrodynamic volume of poly-(benzyl)-L-threonine is smaller than that of polystyrene at similar molecular weights. This behaviour is consistent with the expectation that this polymer will form compact secondary structures rather than the random coil which is expected of polystyrene. The linear relationship between the two calculation methods is useful however when one needs to consider smaller polymers. As described above, the intensity of the light scattering signal is proportional to the molecular weight, meaning that low molecular weight polymers give less reliable data, if any significant signal at all. An approximation can be made to the true molecular weight from the conventional methods which only require an RI signal which is (relatively) insensitive to molecular weight.

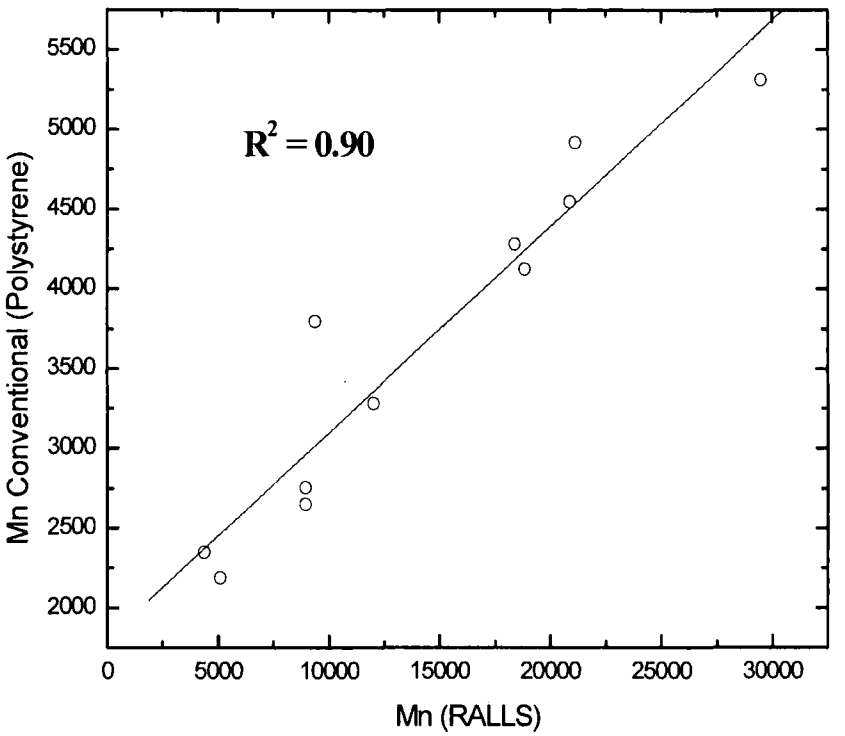

Figure 6. Plot of values of Mn obtain by RALLS verses those obtained from SEC with conventional calibration using polystyrene standards for poly(benzyl-L-threonine).

3.2.4 POLYMERISATION KINETICS

In a controlled polymerisation process, there should be no irreversible chain terminations reactions hence the number of active chain ends is constant during the course of reaction. If this criterion is fulfilled then the system should follow first order kinetics with respect to the chain ends.

The first order rate equation gives the following result:

$$\ln {M_0}/{M_t} = kt + C \quad (5)$$

Plotting $\ln(M_t/M_0)$ vs time will give a linear fit if the process follows first order kinetics . That is to say, the rate varies only with monomer concentration as the other reactants have constant concentration. A non linear fit suggests that other processes such as termination or chain transfer are occurring.

3.2.4.1 ONLINE NMR MONITORING OF NCA CONCENTRATION

The most convenient method for following vinyl polymerisations is by online ^{1}H NMR[41]. A tube can be sealed with a Young's tap or similar, and the reaction monitored by the disappearance of the vinyl protons between 5-6 ppm typically. This is particularly good for radical processes which can reach high conversion quickly (2-5 hrs), thus not using up expensive spectrometer time. In NCA polymerisation, the only proton peak which is specific to monomer conversion is the N-H. However, N-H peaks can be non-quantitative due to rapid exchange and hydrogen bonding interactions. To test the validity of NMR for online monitoring of Thr(Bzl)NCA a

series of proton spectra were collected with the concentration varied from 100 mg.mL^{-1} (typical polymerisation conditions) to 5 mg.mL^{-1}in $CDCl_3$. The spectra are shown in Figure 7.

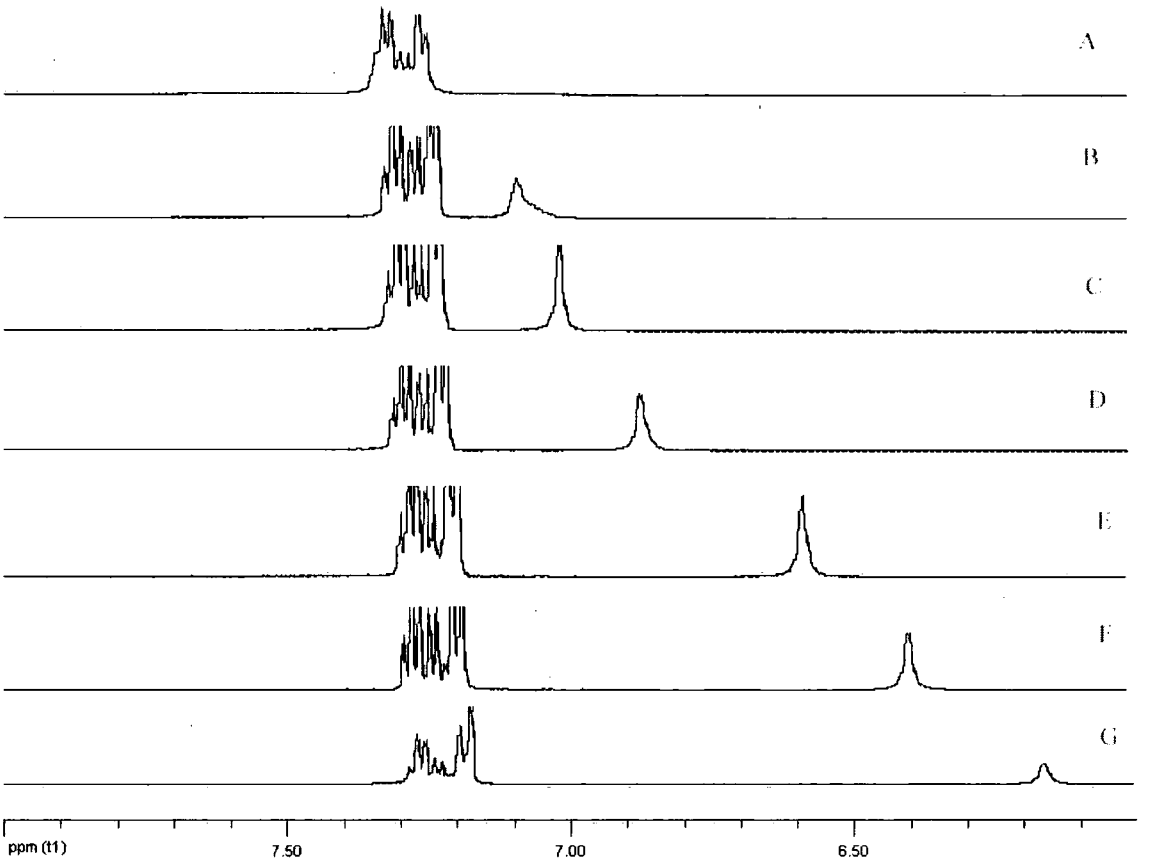

Figure 7. ^{1}H NMR spectra of Thr(Bzl) NCA in $CDCl_3$ taken at 25°C. Concentration (mg.mL^{-1}) A) 100; B) 71; C) 57; D) 36; E) 17; F) 11; G) 6.

When the NCA concentration is 100 mg.mL^{-1} the N-H peak is not resolved from the aromatic peaks of the benzyl protecting group (Figure 7, A), and as the concentration is reduced to 5 mg.mL^{-1} the peak has shifted approximately 2 ppm upfield. (Figure 7, G) A further complication is that the N-H peaks were not always well defined or quantitative. When the integral is compared to that of the β-methyl group, the N-H is found to vary from 0.6 to 0.98 protons, (Figure 8). To monitor successfully a polymerisation by NMR the observed peaks must be quantitative. To

this end, it was decided that NMR was not suitable for this polymerisation system. The variation in the integration of the N-H peaks was not due to H_2O contamination as dry $CDCl_3$ was used under a dry N_2 atmosphere when acquiring the spectra.

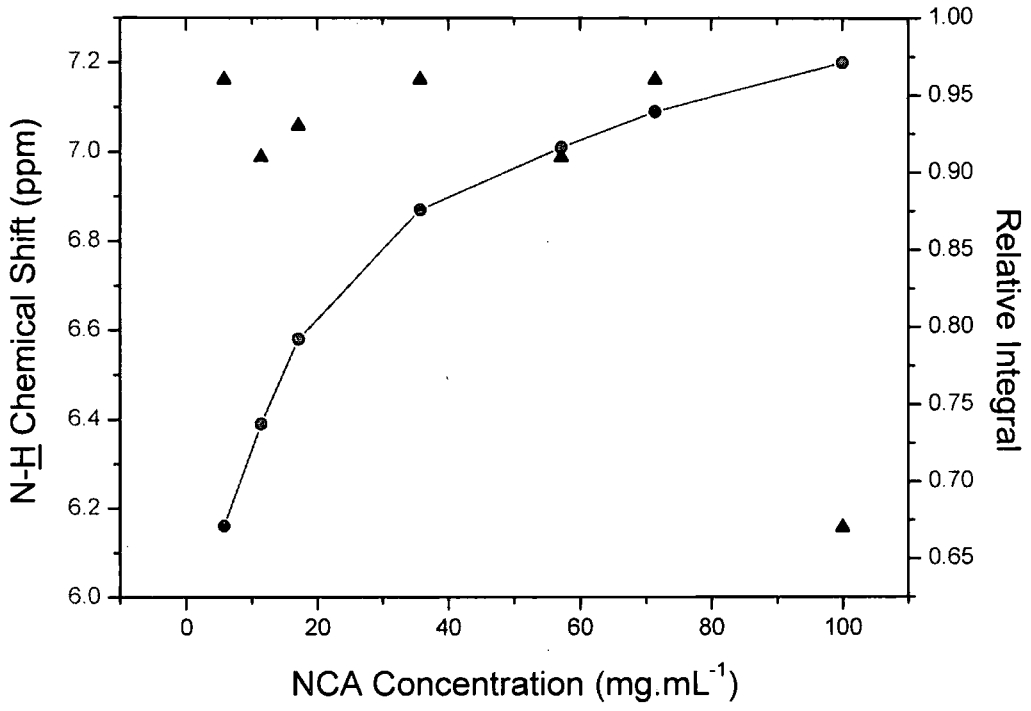

Figure 8. The chemical shift in ppm of the N-H peak (red circles) and the integrated area relative to the 3 β-methyl protons (blue triangles) against NCA concentration.

3.2.4.2 OFFLINE INFRARED SPECTROSCOPIC MONITORING OF NCA POLYMERISATION

Due to the demonstrated unreliability of NMR in analysis of amide protons, as discussed above, an alternative method was required to investigate the depletion of monomer during polymerisation. Infrared spectroscopy has been successfully used to monitor the polymerisation of vinyl monomers by anionic and free radical techniques[42]. The obvious caveat associated with this method is that it involves sampling or the use of a flow cell. Most polymerisation reactions are carried out under inert atmospheres, and in the case of anionic and ring opening polymerisation, in the complete absence of water to avoid chain termination and monomer degradation. It is impossible to rule out the introduction of contamination when withdrawing samples for analysis, and this must always be considered. *In situ* fibre optic probes, where available, have largely overcome this problem[43].

NCAs contain two distinct carbonyl groups which can be resolved from each other in the infrared region of 1750 – 1880 cm^{-1}. The IR spectrum of Thr(Bzl) NCA is shown in Figure 9. The amide carbonyl disappears as CO_2 is expelled during the polymerisation, and the ester carbonyl shifts to lower wavenumber (~1650 cm^{-1}) when it is incorporated as an amide bond. Both can therefore potentially be monitored to determine monomer concentration.

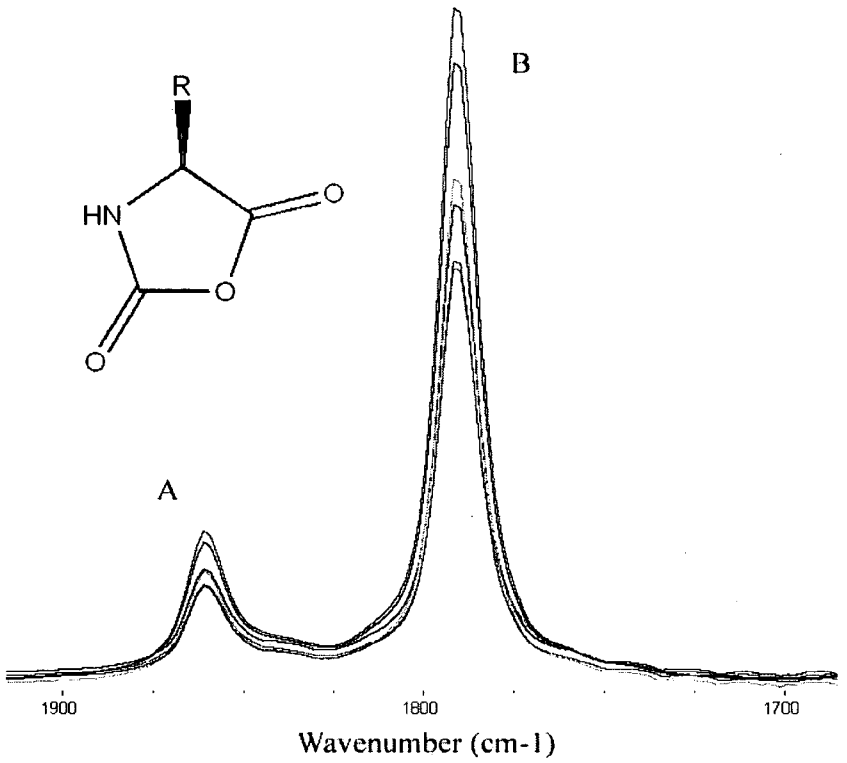

Figure 9. Depletion of anhydride stretches of Thr(Bzl)NCA with decreasing concentration. A is the amide carbonyl (blue) and B is the ester carbonyl (red).

It was again necessary to asses the reliability of this method using a series of control solutions of known concentration. Both the carbonyl peaks areas were measured, and plotted against concentration in Figure 10. As can be seen, there is a linear relationship between concentration and absorbance for both the carbonyl peaks. The wavenumber at which the signal is seen, is also unaffected by concentration.

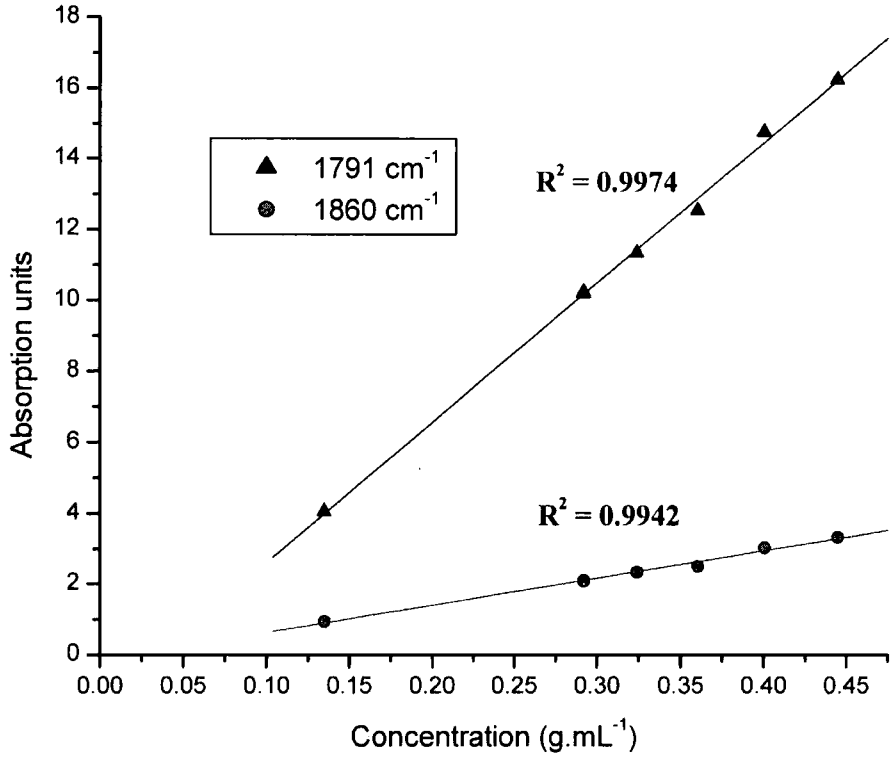

Figure 10. Dependence of the intensity of IR absorption of the carbonyl groups in Thr(Bzl) NCA with concentration

The absorption at 1790 cm^{-1} is significantly larger thus making it more suitable for following reactions, particularly at high conversion when the monomer concentration will be low. Unfortunately this strong absorption was found to be too strong in some cases, and the absorption was beyond the range of the IR spectrometer, meaning that the weaker, but still quantitative band at 1860 cm^{-1} was used.

Upon considering this evidence, it was decided that the IR method would be used for the kinetic investigations rather than NMR, despite the serious concerns over the introduction of impurities with each sample drawn. All efforts were made to reduce this, as described below and in the experimental.

3.2.4.3 RESULTS AND DISCUSSION

A series of polymerisation reactions were monitored by the depletion of the amide carbonyl stretch with conversion. Samples were drawn from a Schlenk tube fitted with a septum, by gas-tight syringe. The needle was flame dried before use, and the syringe body stored in a desiccator, under vacuum until required. (Figure 11)

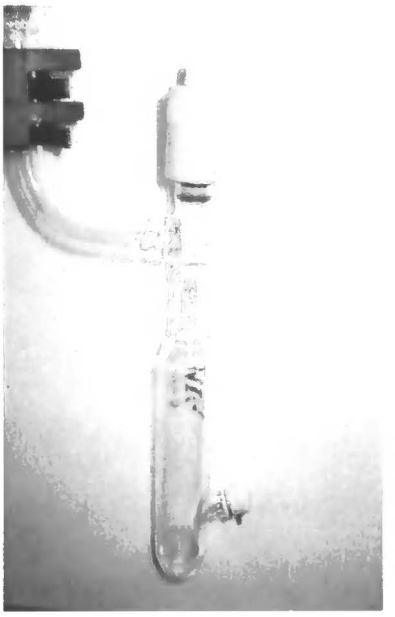

Figure 11. Photograph of Schlenk tube fitted with a septum for withdrawing samples for IR analysis.

Conversion was measured relative to the t=0 sample. This was drawn before any initiator was added, and the monomer conversion at all further times were calculated using the following equation:

$$\% \quad conversion = {}^{A_t}\!/_{A_0} \times 100 \quad (6)$$

The same baseline was defined for all samples based on the t=0 sample. It was not necessary to calculate an absolute value for $[M]_t$ as only the ratio of $[M]_t : [M]_0$ is required:

1st order rate equation:

$$\ln {[M]_0}/{[M]_t} = kt + C \quad (7)$$

Absorbance (A) is proportional to concentration $[M]_t$ k = proportionality constant.

$$\begin{aligned} A &\propto [M]_t \\ A &= k[M]_t \end{aligned} \quad (8)$$

Considering the ratio $[M]_t/[M]_0$, and substituting.

$$\begin{aligned} {[M]_0}/{[M]_t} &= {A_0 / k}/{A_t / k} \\ {[M]_0}/{[M]_t} &= {A_0}/{A_t} \end{aligned} \quad (9)$$

Thus only the total absorbance (in this case the integral) needs to be measured

$$\ln {A_0}/{A_t} = kt + C \quad (10)$$

The first order plots arising from this are shown below:

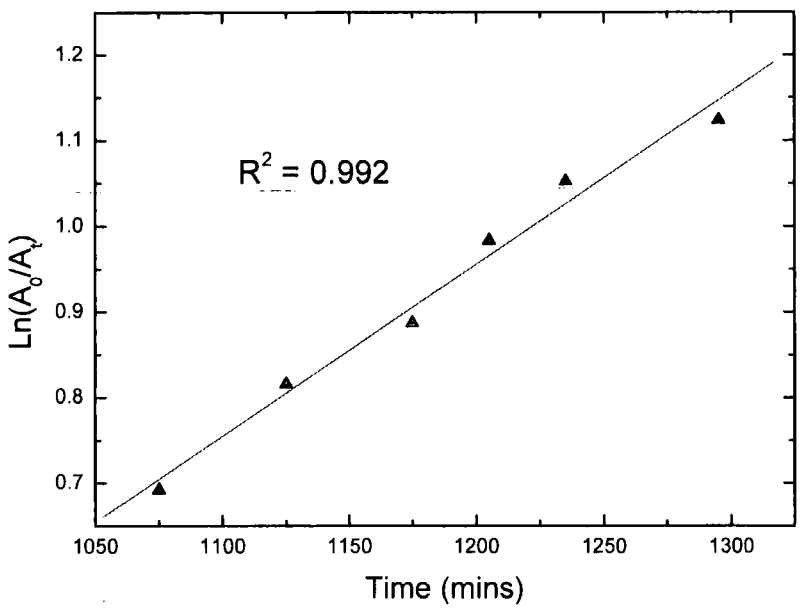

Figure 12. Polymerisation of Thr(Bzl)NCA monitored by offline IR. [M]:[I] = 50; 10 % (wt) in THF; 35°C; N_2 atmosphere

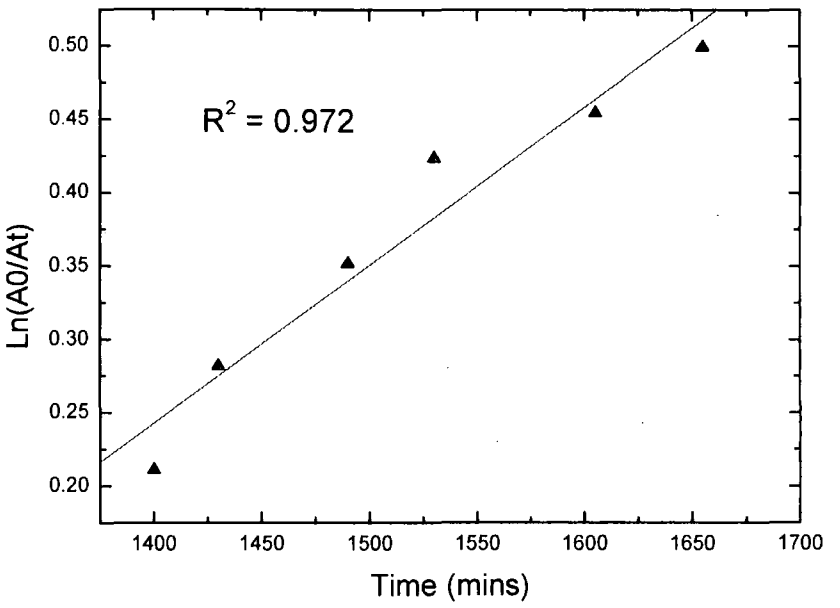

Figure 13. Polymerisation of Thr(Bzl)NCA monitored by offline IR. [M]:[I] = 60; 10 % (wt) in THF; 35°C; N_2 atmosphere.

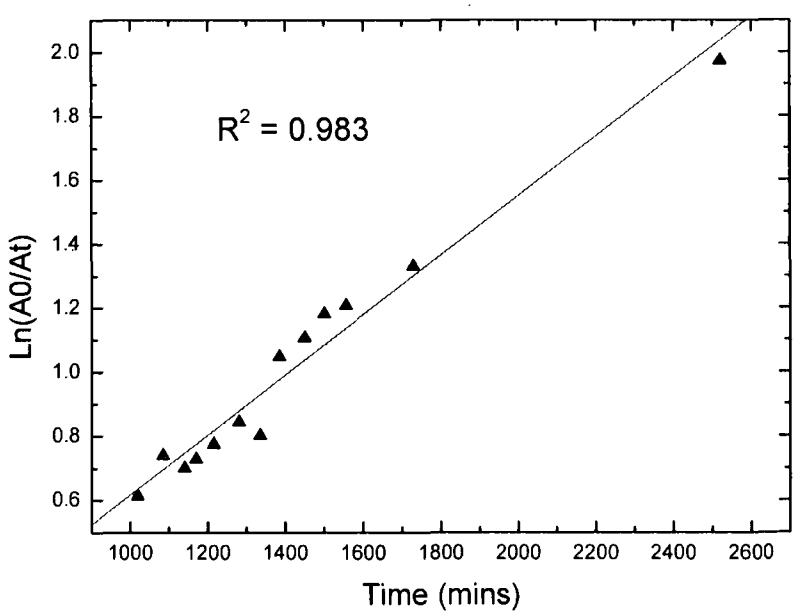

Figure 14. Polymerisation of Thr(Bzl)NCA monitored by offline IR. [M]:[I] = 75; 10 % (wt) in THF; 35°C; N_2 atmosphere.

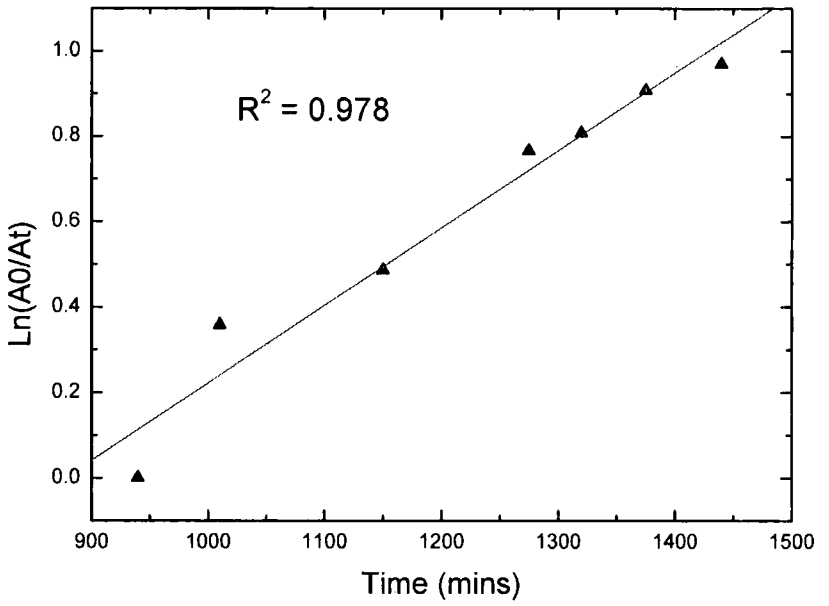

Figure 15. Polymerisation of Thr(Bzl)NCA monitored by offline IR. [M]:[I] = 80; 10 % (wt) in THF; 35°C; N_2 atmosphere.

Table 6. Summary of results of kinetic investigation of polymerisation of Thr(Bzl) NCA

Experiment	Conc. NCA (M)	[M]:[I]	Observed rate constant (min^{-1})
1 (Fig 11)	0.384	50	0.00201
2 (Fig 12)	0.377	60	0.00108
3 (Fig 14)	0.391	75	0.00093
4 (Fig 15)	0.327	80	0.00180

For each experiment shown in Table 6 a linear relationship between $\ln(A_0/A_t)$ and time was observed indicating that the number of active chain ends remained constant. No attempt was made to extrapolate the true rate constants for this system. To obtain these the total volume of solvent added would need to be measured accurately. The solvent was distilled into the Schlenk tube, and the total volume was not calculated, (although they were all tentatively the same volume having been filled

to the same predetermined mark). The ratio of the initiator to monomer in each case was known, allowing for the first order plots to be constructed.

Each of the kinetic plots shown begins at t > 1000 min. This is due to the observation of two different rate constants displayed in Figure 16. A long inhibition period can not be attributed to impurities as anything which inhibited the polymerisation (by interaction with amine end group) would do so irreversibly, and quantitative initiation would not be observed. This inhibition period has been observed previously in other kinetic investigations of NCA polymerisation[14]. The most likely reason is that, at low conversions, the less soluble β-sheet structures form. This reduces the rate initially until the chain ends become mobile enough to reach maximum reactivity.

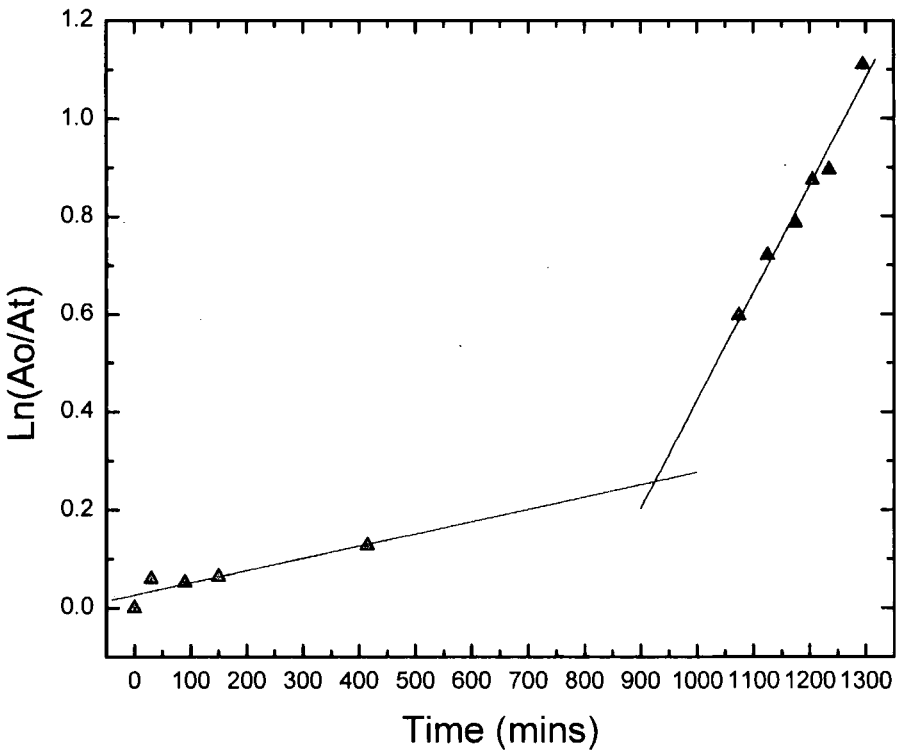

Figure 16. First order kinetic plot of polymerisation of Thr(bzl)NCA from t = 0 mins. [M]:[I] = 50; 10 % (wt) in THF; 35°C; N_2 atmosphere.

The intercept of the two linear regions, shown in Figure 16, corresponds to 25% conversion which is equivalent to a DP of 12.5 (as the target DP was 50). This agrees with previous observations that above 12 units homo poly (amino acids) become more soluble[36] accounting for the observed increase in the reaction rate.

3.2.5 EVOLUTION OF M_N WITH CONVERSION

A further criterion for a controlled polymerisation is that M_n evolves linearly with conversion. To determine this, it was necessary to remove samples from the reaction mixture again and analyse by SEC. The RI detector was used to determine the concentration of polymer and monomer at a given time. The molecular weights were determined by conventional calibration and are shown below.

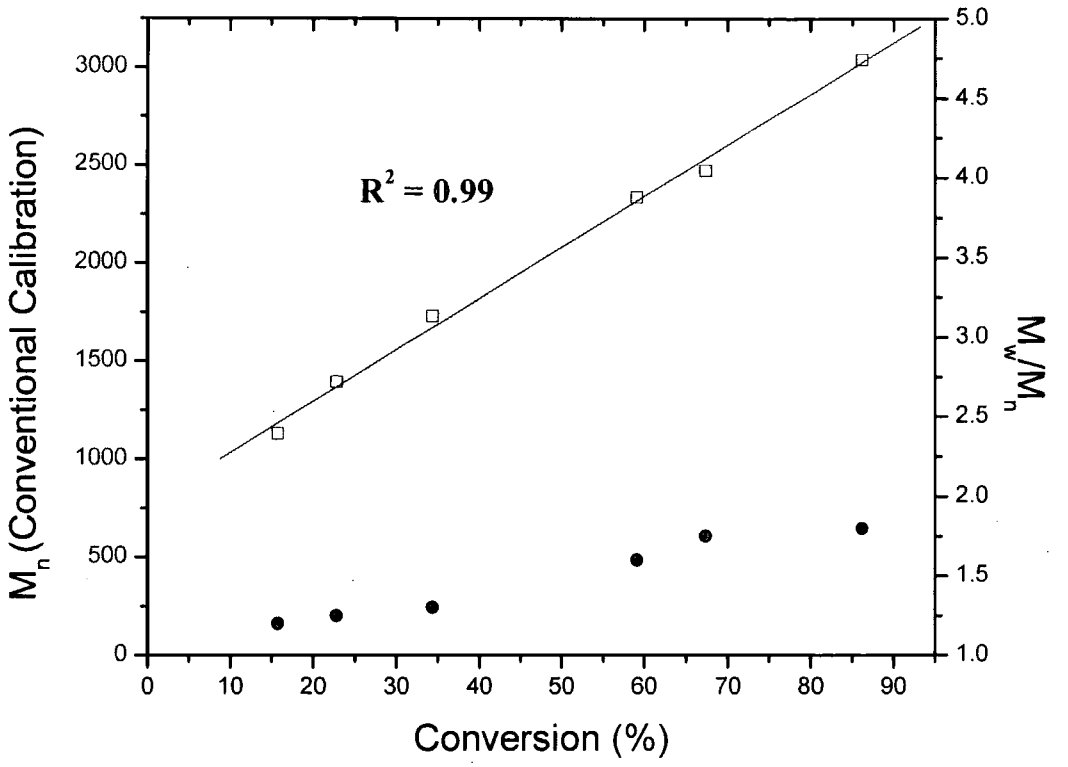

Figure 17. Evolution of M_n with conversion for polymerisation of Thr(Bzl)NCA. 10 % (wt); [M]:[I] = 100; n-hexylamine initiation; 35°C.

Figure 17 illustrates the excellent correlation between M_n and conversion, even up to 85% conversion (last sampled data point). The line of best fit does not pass through zero because conventional calibration was used. As discussed in the previous section, poly-(benzyl)-L-threonine does not have similar elution behaviour to polystyrene. Normally, this is overcome by the use of light scattering, but is not applicable here: in the early stages of the polymerisation the molecular weight is too low to obtain a sufficiently strong signal from the RALLS detector. Earlier experiments indicated a linear relationship between the two calibrations, so the results from the conventional method are proportional, if not absolute. The molecular weight of the final polymer by RALLS (18.4 kDa) agreed with that predicted by the feed

ratio (19.1 kDa). The polydispersity index increased with conversion, which is the opposite of what is expected for other controlled polymerisations, where higher PDI's are found at the initial stages. This was simply due to inherent problems of sampling from the reaction, resulting in some contamination being introduced, and the erosion of the rubber septa.

3.2.6 RE-INITIATION OF POLY-(BENZYL)-L-THREONINE

The kinetic and molecular weight data indicated that this polymerisation system was indeed controlled under the conditions used. As such the end groups of the polymer should still be well defined and of equal reactivity: that is to say, they retain their primary amine functionality, and can be thought of as being 'living'[44]. This is assessed by the ability to reinitiate polymerisation by the addition of further monomer to give chain extension. The presence of any residual low molecular weight polymer would indicate that some chain termination reactions have occurred. A sample was drawn from the initial polymerisation once it was completed, then a further aliquot of NCA added to the reaction vessel. SEC was used to judge if chain extension had occurred.

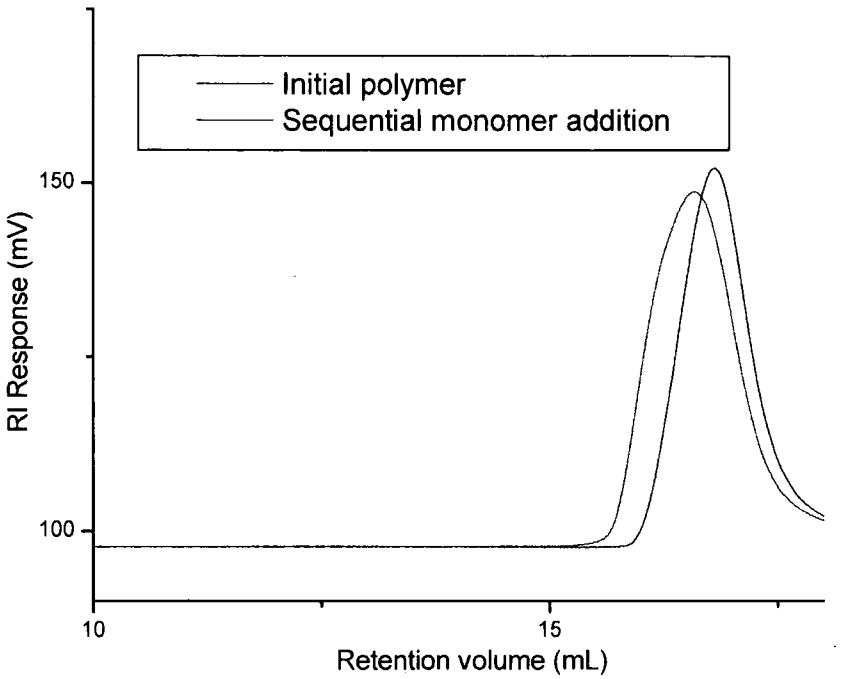

Figure 18. SEC refractive index traces showing chain extension by sequential monomer addition. Blue: Mn = 3330. Red: Mn = 5500. Conditions, 1st block: 10 % (wt); Initial [M]:[I] =20; n-hexylamine initiation; 35°C, 42 hrs. 2nd monomer addition: [M]:[I] = 30; 35°C; 48 hrs.

As can be seen in figure 18, chain extension occurred following addition of further monomer. The final polymer had a PDI of 1.16, as calculated by RALLS. This is probably an underestimate due to it being at the limit of the RALLS sensitivity. Conventional calibration gives a PDI of 1.3 which is more realistic. The important feature is that it is monomodal without any evidence of low molecular weight polymer contamination, (this is hard to judge as the two traces overlap, however if any of the initial polymer did remain a non symmetric distribution would have been obtained). This clearly indicates that under the reaction conditions described the end groups of the polymer can be considered to be living.

3.3 CONCLUSIONS

The effect of impurities on the polymerisation of Thr(Bzl) NCA resulting from the preparation procedure has been investigated. NCAs which were only purified by repeated crystallisations often failed to initiate even with strongly basic initiators. When initiation did occur, materials which were multimodal, with low molecular weight contaminants and low levels of conversion were obtained. This was shown to be solvent independent. By changing the purification procedure to include an aqueous wash to remove acidic impurities, and conducting the polymerisation under high vacuum conditions as is typically used for anionic ring opening polymerisation it was shown that high conversions and well defined materials with DPs up to 200 were obtainable. A key feature was the use of anhydrous THF as the solvent in place of the more commonly used DMF, which is difficult to handle and requires specially-made apparatus if controlled polymerisation is to be observed. Kinetic analysis by offline infrared spectroscopy demonstrated that the polymerisation followed first order kinetics, following an initial inhibition period associated with secondary structure formation, and that the molecular weight evolved linearly with conversion. Finally, the livingness of the end groups was demonstrated by a chain extension experiment.

This evidence demonstrates that controlled polymerisation of an NCA is possible without the need for either difficult to handle organometallic initiators or extreme purification and polymerisation conditions in conjunction with harsh polar solvents. It should be noted that this method does not produce materials with as narrow PDIs as the other two, nor has it yet been applied to the synthesis of controlled architectures, but it does provide a way of making predictably sized poly(amino acid), which is accessible to all chemists.

3.4 EXPERIMENTAL

GENERAL

All NCAs were synthesised as described in Chapter 2. They were used immediately following synthesis and purification, not being stored for longer than 3 hours and below -10°C. *n*-Hexylamine (>99.5%, H_2O<0.2%) was purchased from Fluka. THF and DCM (<99.5%) were purchased from Fischer Scientific and dried by passage through two alumina columns using an Innovative Technology Inc. solvent purification system and stored under N_2. THF was further dried over sodium/benzophenone complex with at least 3 freeze-thaw cycles, until the purple colouration persisted. Dimethyl acetamide (anhydrous <0.005% H_2O) was purchased from Aldrich. Further purification was achieved by drying over 3A molecular sieves for 24 hours. Hexane (Fischer Scientific >99%) was dried over 3A molecular sieves. 3A molecular sieves (Aldrich) were activated in an oven at 200°C before use. All other chemicals were used as received. NMR-spectra were recorded with a Varian-Inova 500 spectrometer, operating at 500MHz (^1H) or at 125 MHz (^{13}C); results of HSQC and COSY correlation studies have been used in order to assign the observed signals to the hydrogen and carbon atoms of the compound. Alternatively ^1H and ^{13}C spectra were acquired with a Brucker Advance-400 operating at 400MHz and 100MHz respectively. MALDI-TOF spectra were collected on an Applied Biosystems Voyager DE. Gel permeation chromatography was undertaken using THF as the eluent. 100μL of solution (agitated overnight to ensure complete dissolution) was injected at a flow rate of 1.00 $mL.min^{-1}$ by a Viscoteck SEC autochanger module. A Viscoteck TDA 301 unit with triple detection (right angle laser scattering at 670nm,

differential refractometer and viscometer) was used. dn/dc Values were calculated online for each polymer. Analyses were undertaken using OmniSEC 4.0 software. Infrared spectroscopy was conducted on a Nicolet Nexus FT-IR as a KBr disc. Liquid samples were analysed by direct injection of the reaction medium into a liquid cell with KBr windows. Omnic 5.1a (Nicolet) was used to analyse the data obtained.

Poly(O-benzyl-L-threonine) – (PBLThr)

Thr(Bzl)NCA (0.20 g, 0.85 mmol) was dissolved in 3 mL of dry DCM, and injected into a Schlenk tube fitted with a Young's tap and 9mm rubber septa already under vacuum. The DCM was removed under vacuum and the NCA allowed to dry under vacuum for a further 2 hours. THF (3mL) was vacuum distilled into the vessel to give an approximately 10 % (wt) solution. The tube was then immersed in an oil bath thermostated at 35°C, and stirred to dissolution. n-Hexyl amine (0.08mL, 0.2 M) was added via syringe into the tube and allowed to stir for 4 days.

Following this time a 100µl sample was withdrawn for SEC analysis, and the remainder of the reaction was poured into a 10-fold excess of diethyl ether with stirring, and the white powder was collected by filtration. Further purification was achieved by re -dissolving in THF and precipitating into a 10-fold excess of water. Yield 0.11 g, 70%.

^{1}H NMR ($CDCl_3$) δ_{ppm}; 0.93 (3H, H^5), 3.77 (1H, H^5), 4.1 – 4.8 (3H, $H^3 + H^{6a} + H^{6b}$), 7.09 -7.25 (5H, H^8)

^{13}C NMR δ_{ppm}; 17 (C^5), 57 (C^3), 71 (C^6), 75 (C^5), 127.2 and 128.2 (C^8), 138.3 (C^7), 169 (C^2)

IR (KBr disc) cm^{-1}: 3290 (N-H), 2973 (C-H), 1637, (C=O)

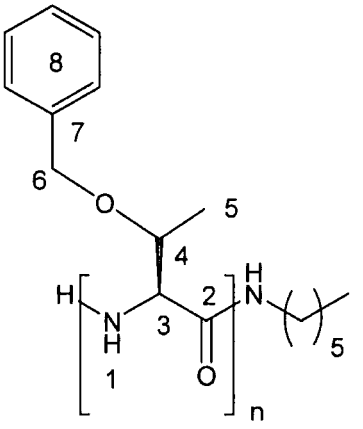

Chain extension of Poly(O-benzyl-L-threonine)

The initial polymer was grown in the same manner as described above (0.2 g, 0.85 mmol). After 3 days a 100 μL sample was drawn for SEC analysis. Thr(Bzl)NCA (0.1g, 4.26 mmol) prepared as described in Chapter 2 was added to another Schlenk tube as a DCM solution and concentrated to dryness on a high vacuum line for 2 hours. Approximately 1 mL of THF was then distilled into the flask, and it backfilled with dry N_2. Using a flame dried syringe this monomer was injected in a single portion to the polymerisation vessel and stirred at 35°C for a further 4 days. 100 μL was drawn for SEC analysis and the remainder precipitated into a large excess of diethyl ether to yield a white powder, collected by filtration. Yield 0.15 g, 60%.

3.5 BIBLIOGRAPHIC REFERENCES

(1) Kricheldorf, H. R. In *Alpha amino acid-N-CarboxyAnhydrides and Related Materials*; Springer-Verlag: New York, 1987.

(2) Fuller, W. D.; Cohen, M. P.; Shabankareh, M.; Blair, R. K. *J. Am. Chem. Soc.* **1990**, *112*, 7414-7416.

(3) Sim, T. B.; Rapoport, H. *J. Org. Chem.* **1999**, *64*, 2532-2536.

(4) Leban, J. J.; Colson, K. L. *J. Org. Chem.* **1996**, *61*, 228-231.

(5) Xue, C.-B.; Naider, F. *J. Org. Chem.* **1993**, *58*, 350-355.

(6) Kricheldof, H. R. *Angew. Chem. Int. Ed.* **2006**, *45*, 5752-5784.

(7) Hanby, W. E.; Waley, S. G.; Watson, J. *J. Chem. Soc.* **1950**, 3009-3013.

(8) Bloom, S. M.; Fasman G. D; De-Loze, C.; Blout, E. R. *J. Am. Chem. Soc.* **1962**, *84*, 458-463.

(9) Blout, E. R.; Idelson, M. *J. Am. Chem. Soc.* **1962**, *78*, 497-498.

(10) Barrett, G. C.; Elmore, D. T. *Amino Acids and Peptides*; Cambridge University Press, 1998.

(11) Deming, T. J. *J. Pol. Sci. Part A: Pol. Chem.* **2000**, *38*, 3011-3018.

(12) Blout, E. R.; Karlson, R. H. *J. Am. Chem. Soc.* **1956**, *78*, 941.

(13) Bamford, C. H.; Block, H. *J. Chem. Soc* **1961**, 4992.

(14) Ovsiannikova, A.; Rudkovskaya, G. D.; Vlasov, H. *Makromol. Chem.* **1986**, *187*, 2351-2356.

(15) Elias, H. G.; El-Sabbah, M. B. *Makromol. Chem.* **1981**, *182*, 1629-1640.

(16) Kricheldof, H. R.; Muller, D.; Stulz, J. *Makromol. Chem.* **1983**, *184*, 1407-1421.

(17) Plasson, R.; Biron, J. P.; Cottet, H.; Commeyras, A.; Taillades, J. *J. Chromatography A* **2002**, *952*, 239-248.

(18) Vayaboury, W.; Gianni, O.; Cottet, H.; Deratani, A.; Schue, F. *Macromol. Rapid. Commun.* **2004**, *25*, 1221-1224.

(19) Deming, T. J. *Nature* **1997**, *390*, 386-389.

(20) Yamashita, S.; Tani, H. *Macromolecules* **1974**, *7*, 406-409.

(21) Deming, T. J. *J. Am. Chem. Soc.* **1997**, *119*, 2759-2760.

(22) Deming, T. J.; Curtin, S. A. *J. Am. Chem. Soc.* **2000**, *122*, 5710-5717.

(23) Deming, T. J. *Polymer Preprints* **2000**, *41*, 386-387.

(24) Goodwin, A. A.; Bu, X.; Deming, T. J. *J. Organomet. Chem.* **1999**, *159*, 111-114.

(25) Siedel, S. W.; Deming, T. J. *Macromolecules* **2003**, *36*, 969-972.

(26) Brzezinska, K. R.; Curtin, S. A.; Deming, T. J. *Macromolecules* **2002**, *35*, 2970-2976.

(27) Brzezinska, K. R.; Deming, T. J. *Macromol. Biosci.* **2004**, *4*, 566-569.

(28) Brzezinska, K. R.; Deming, T. J. *Macromolecules* **2001**, *34*, 4348.

(29) Bhaw-Luximon, A.; Jhurry, D.; Belleney, J.; Goury, V. *Macromolecules* **2003**, *36*, 977-982.

(30) Goury, V.; Jhurry, D.; Bhaw-Luximon, A.; Novak, B. M.; Belleney, J. *Biomacromolecules* **2005**, *6*, 1987-1991.

(31) Dimitrov, I.; Schlaad, H. *Chem. Commun.* **2003**, 2944-2945.

(32) Lutz, J.-F.; Schutt, D.; Kubowicz, S. *Macromol. Rapid. Commun.* **2005**, *26*, 23-28.

(33) Nakamura, R.; Aoi, K.; Okada, M. *Macromol. Rapid. Commun.* **2006**, *27*, 1725-1732.

(34) Poche, D.; Moore, M. J.; Bowles, J. L. *Syn. Comm.* **1999**, *29*, 843-854.

(35) Aliferis, T.; Iatrou, H.; Hadjichristidis. N *Biomacromolecules* **2004**, *5*, 1653-1556.

(36) Kricheldof, H. R.; Von Lossow, C.; Schwarz, G. *Macromol. Chem. Phys.* **2004**, *205*, 918-924.

(37) Simo, C.; Cottet, H.; Vayaboury, W.; Gianni, O.; Pelzing, M.; Cifuentes, A. *Anal. Chem.* **2004**, *76*, 335-344.

(38) Hadjichristidis, N.; Iatrou, H.; Pispas, S.; Pitsikalis, M. *J. Pol. Sci. Part A: Pol. Chem.* **2000**, *38*, 3211-3234.

(39) Fernyhough, C. M.; Young, R. N.; Ryan, A. J.; Hutchings, L. R. *Polymer* **2006**, *47*, 3455-3463.

(40) *Polymer Handbook*; 4th ed.; John Wiley and Sons, 1999.

(41) Lagrille, O.; Cameron, N. R.; Lovell, P. A.; Blanchard, R.; Goeta, A. E.; Koch, R. *J. Pol. Sci. Part A: Pol. Chem.* **2006**, *44*, 1926-1940.

(42) Long, T. E.; Liu, H. Y.; Schell, B. A.; Teegarden, D. M.; Uerz, D. S. *Macromolecules* **1993**, *26*, 6237-6242.

(43) Darcos, V.; Monge, S.; Haddleton, D. M. *J. Pol. Sci. Part A: Pol. Chem.* **2004**, *42*, 4933-4940.

(44) Swarc, M.; Levy, M.; Milkovich, R. *J. Am. Chem. Soc.* **1956**, *78*, 2656-2657.

CHAPTER 4

SYNTHESIS AND CHARACTERISATION OF WELL DEFINED BLOCK COPOLYPEPTIDES

4.1 INTRODUCTION

The first synthesis of block copolymers was described by Swarc *et al*[1] in 1956 and they utilised anionic polymerisation of vinyl monomers. Under rigorously dry conditions, the anionic end groups remained active ('living'), such that addition of further monomer resulted in chain extension. This has since been applied to a wide variety of vinyl and cyclic monomers to create materials of defined architecture[2]. As was discussed in Chapter 3, NCA polymerisation has traditionally been blighted by the lack of control of the reaction, resulting in multimodal distributions and incomplete monomer conversion[3]. Selective precipitation or column chromatography was required to remove homopolymer contaminants[4] and in order to synthesis polymers of defined architecture, it was necessary to fractionate the mixture to obtain a narrow distribution of chain lengths. This is in stark contrast to radical vinyl polymerisations which, in the last 10 years have received much attention with regard to controlled polymerisation methods including RAFT[5] (reversible addition fragmentation and transfer), ATRP[6] (atom transfer radical polymerisation) and NMP[7] (nitroxide mediated polymerisation). The first successful method for synthesising block copolypeptides without isolation and purification of the homopolymer, was by Deming in 1997[8††] using zero-valent transition metal initiators, particularly those based on nickel and cobalt[9]. These have been applied to a wide range[10,11] of NCAs. Another transition metal system based upon aluminium-schiff base complexes[12] has been used to produce block copolymers of methyl glutamate and leucine NCAs by sequential monomer addition[13]. Unfortunately the only evidence for the diblock's architecture was based upon ^{13}C NMR and no GPC data were provided, casting

†† See chapter 3 for discussion of this method

doubts over whether the material was truly two individual blocks, or composed of some alternating regions. An intriguing report has been made, claiming that poly(L-glutamtic) acid has been used to make block copolymers with (γ-benzyl)-L-glutamate NCA[14]. This result seems remarkable, as NCAs are not tolerant of carboxylic acid functionalities. Quantitative yields were also reported, but again no GPC data were supplied. Mention here should be made of the work of Schlaad and coworkers[15], who showed that ammonium chloride terminated polystyrene macroinitiators could polymerise NCAs to give hybrid block copolymers with extremely narrow molecular weight distributions. This has been applied to a range of macroinitiators including poly(styrene)[16], PEG[17] and poly(oxazoline)[18], but has not yet been used for the synthesis of poly(vinyl)-block-poly(peptide)-block-poly(peptide)s yet. This may be due to the observation of inflated molecular weights at high conversion, attributed to incomplete initiation[15]. The residual macroinitator was removed by selective precipitation, which would not be possible when used with block copolypeptide macroinitiators as both blocks would have similar solubility. Simply using an amino terminated macroinitiator also allows the growth of a single peptide block in a reasonably controlled manner[19-23], but again no diblock peptides have been synthesised in this manner. There is evidence that the amine end groups remain active upon reducing the polymerisation temperature to 0°C preventing unwanted side reactions, which may allow for controlled polymerisation[24]. The final method of note is that described in 2004 by Hadjichristidis *et al.*[25] By applying rigorous high vacuum techniques to purify all the monomers, initiators and solvents it was possible to prevent any chain termination reactions, resulting in polymers with living amine end groups which can reinitiate polymerisation upon addition of further monomer. This

has been applied to the preparation of a series of well defined di- and tri-block co-polypeptides[26,27] and even star-branched polypeptides[28].

4.2 RESULTS AND DISCUSSION

Chapter 3 described how Thr(Bzl) NCA could be polymerised in a controlled fashion, including the observation that the addition of a second aliquot of monomer resulted in chain extension. To determine if this polymerisation system was applicable to other NCAs we chose to extend this to include (γ-benzyl)-L-glutamic acid (BLG) and (ε-Boc)-L-lysine (LysBoc) NCA, which have been used previously in the literature, and when the protecting groups are removed give either anionic or cationic side-group functionality.

4.2.1 HOMOPOLYMERISATION OF NCAs

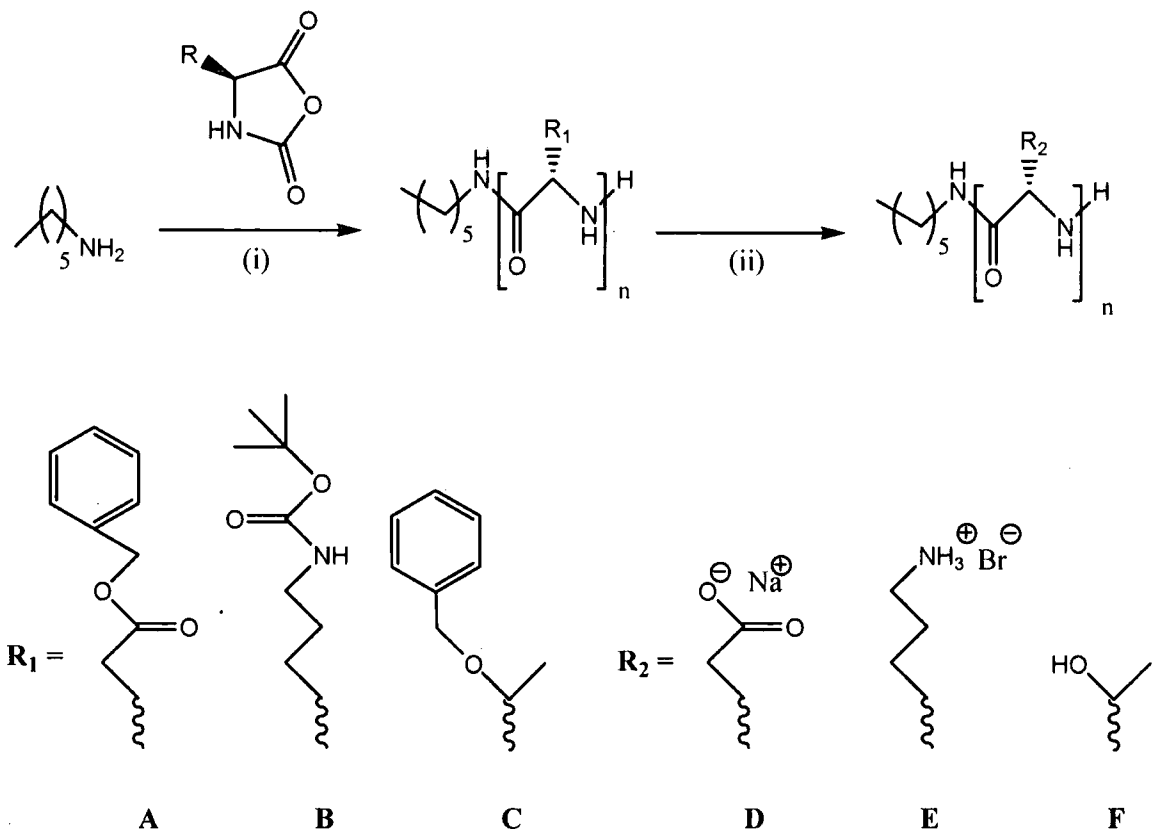

Scheme 1. Polymerisation of NCAs by n-hexylamine followed by protecting group removal. Conditions. (i) THF or DMAc; 35°C; 3 days; (ii) R_1 = A/B, HBr (2.5 equiv)/TFA; R_1 = C, Pd/C (10%) HCO_2H/DMF; N_2, 16 hrs.

n-Hexylamine was chosen as the initiator as it had shown in Chapter 3 that it gave well-defined materials when used in conjunction with high purity monomers and high vacuum conditions. BLG NCA was polymerised in THF at 40°C. The obtained molecular weights agreed well with those predicted by monomer : initiator ratios. LysBoc NCA displayed lower solubility in THF than the other NCAs used, requiring elevated temperatures > 50°C to maintain a homogeneous reaction mixture. Upon changing the solvent to DMAc a homogenous mixture was observed at all temperatures and the resulting polypeptides were sufficiently soluble in THF for SEC analysis. For polymers obtained from both monomers PDI values below 1.4 were

found. The values obtained by SEC for PLysBoc were elevated compared to the predicted values.

Table 1. Polymerisation of BLG NCA by n-hexylamine.

Run N°	[M]:[I]	$M_{n,SEC}$ (kDa)	$M_{n,Theo}$ (kDa)	Conv (%)	PDI
1	50	3.8	5.0	45	1.27
2	75	15.2	16.7	>95	1.21
3	100	19.0	22.3	>95	1.23
4	150	35.5	33.4	>95	1.30

Conditions: Monomer concentration 10 % (wt); THF; under vacuum (< 0.1mbar); 35°C; 4 days.

Table 2. Polymerisation of LysBocNCA by n-hexylamine

Run N°	[M]:[I]	$M_{n,SEC}$ (kDa)	$M_{n,Theo}$ (kDa)	Conv (%)	PDI
1	50	13.5	9.1	80	1.37
2	75	17.1	16.0	>95	1.27
3	100	31.1	23.1	>95	1.34

Conditions: Monomer concentration 10 % (wt); THF; under vacuum (< 0.1mbar); 35°C; 4 days.

SEC analysis was conducted as in Chapter 3, using RALLS to calculate molecular weight. The dn/dc values were calculated in exactly same manner by varying the concentration of pure polymer and recording the change in RI response. The plots of RI response verses concentration are shown below:

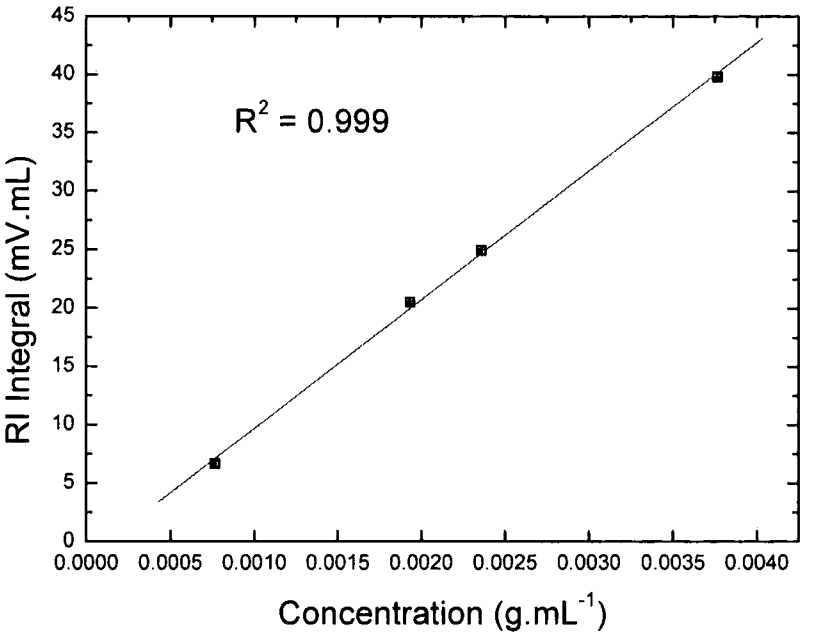

Figure 1. Change in refractive index integral with concentration for poly(γ-benzyl-L-glutamate), determined in THF; 30°C

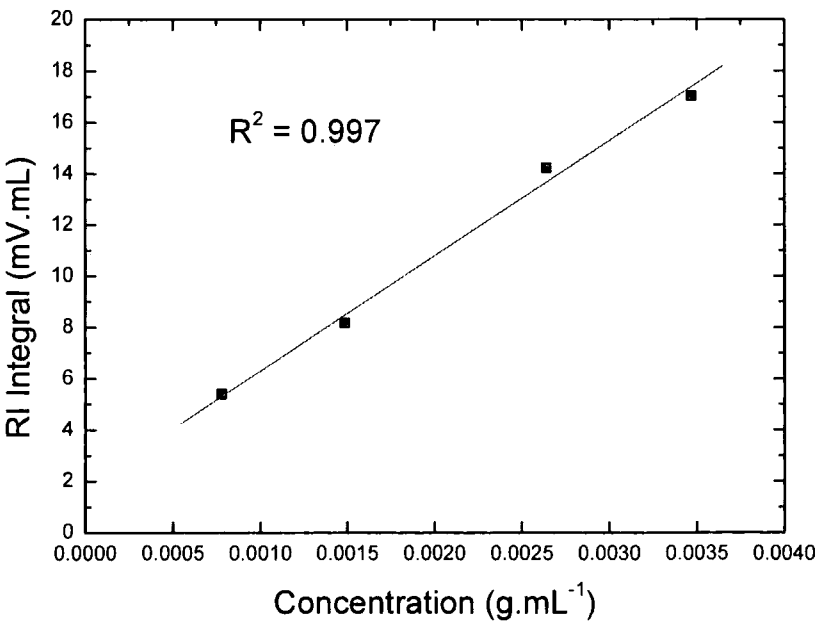

Figure 2. Change in refractive index integral with concentration for poly(ε-*N*-Boc-L-Lysine), determined in THF; 30°C

Table 3. Summary of the calculated values for dn/dc

		dn/dc (mL/g)	
Polymer	**Slope (mV.mL^2/g)**	**Experimental[a]**	**Literature[b][29]**
Poly (*O*-Bzl-L-glutamate)	10527	**0.1023**	**0.124**
Poly (*N*-Boc-L-lysine)	5179.5	**0.0503**	- [c]

(a) THF; (b) dioxane; (C) no data available

The experimental value for dn/dc of PBLG in THF agreed well with the literature value in the similar solvent dioxane. (Table 3) No value for PLysBoc has previously been reported, to the best of our knowledge. ^{1}H NMR analysis confirmed that the protecting groups had not been displaced during polymerisation or workup. Conversion was estimated by SEC. ^{1}H NMR was not used to estimate the molecular weight due to overlap of the relevant peaks with the polymeric backbone. PBLG has been analysed by SEC previously showing that its secondary structure (α-helix) would not give erroneous molecular weights[30]. Homo-polymerisation of L-Alanine NCA was attempted in both THF and DMAc, but only gave rise to insoluble materials and was not pursued further. The results shown here appear to suggest that the reaction conditions employed lead to well defined materials, as long as all the reactants display good solubility characteristics.

4.2.1.1 SIDE CHAIN DEPROTECTION

The high reactivity of NCAs to nucleophilic functionality necessitated that protecting groups were used in their synthesis and polymerisation. The protecting groups were chosen on the basis of their facile cleavage[31] and work-up, to give water soluble polymers which were required for the work in Chapter 6.

Cleavage of the benzyl ester and Boc, protecting groups was achieved by using 2 equivalents of HBr in trifluoroacetic acid. PBLG is more commonly deprotected by the use of KOH (or similar) in THF. We found that this gave rise to precipitation of the polymer, resulting in non-quantitative cleavage, even in the more polar solvent DMF. TFA on the other hand, is an excellent solvent for peptides, and in conjunction with HBr led to deprotection in less than one hour, reducing the possibility of racemisation or chain scission. The Boc group of PLysBoc was also removed quantitatively using these conditions. Following dialysis against ultra-pure water and freeze drying, the polymers were analysed by ^{1}H and ^{13}C NMR. Quantitative removal of the benzyl ester protecting group from PBLG was judged by the absence of both aromatic and benzylic peaks in the ^{1}H and ^{13}C NMR spectra in Figure 3 and 4 respectively.

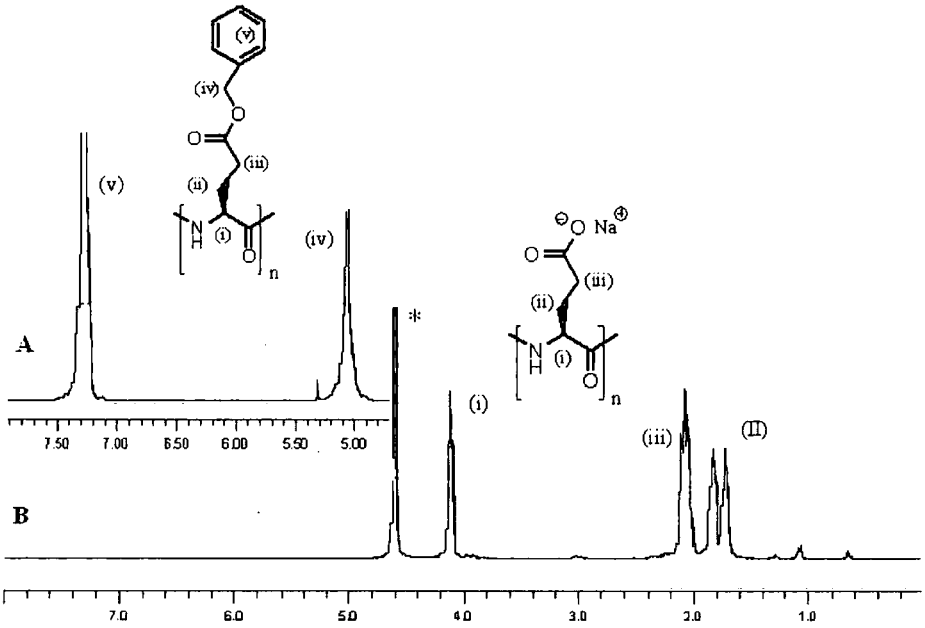

Figure 3. ^{1}H NMR spectra: A: poly(γ-benzyl-L-glutamate) aromatic region; B: poly(L-glutamic acid) without any evidence of aromatic peaks. Residual solvent peak (HOD)

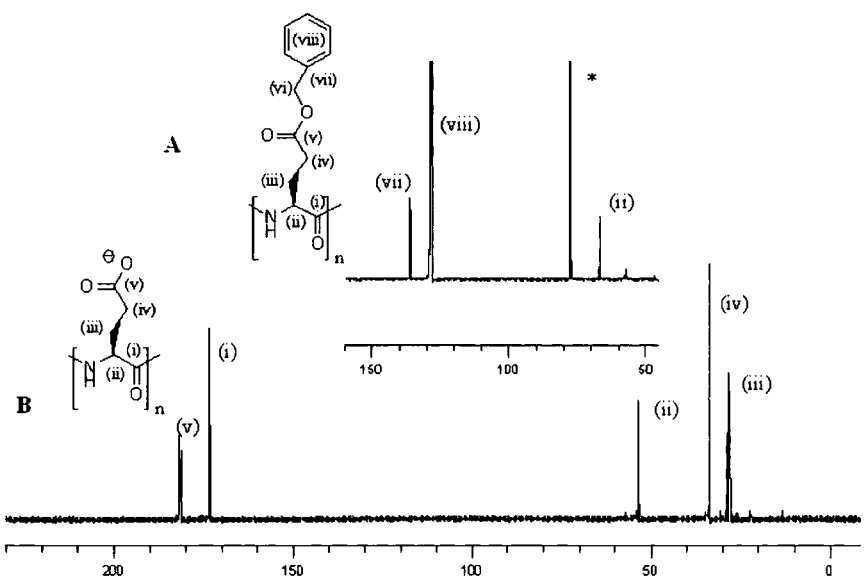

Figure 4. ^{13}C NMR Spectrum: (A): Poly(γ-benzyl-L-glutamate) with key resonances indicated. (B): Poly(L-glutamic acid) showing no protecting group residues.

^{1}H NMR interpretation for PLysBoc was made difficult by the ^{t}Bu peaks (from

Boc group) which were broad and obscured some of the CH_2 groups of the lysine residue preventing resolution of the individual peaks. Following deprotection the CH_2 groups of PLys were resolved from each other, without the presence of the large Boc group, (Figure 5). ^{13}C NMR analysis of PLysBoc (Figure 6) showed a peak at 150 ppm relating to the carbonyl functionality of the Boc group, resolved from that of the amide carbonyl (170 ppm). Following treatment with HBr/TFA the Boc carbonyl peak disappeared, while the amide remained.

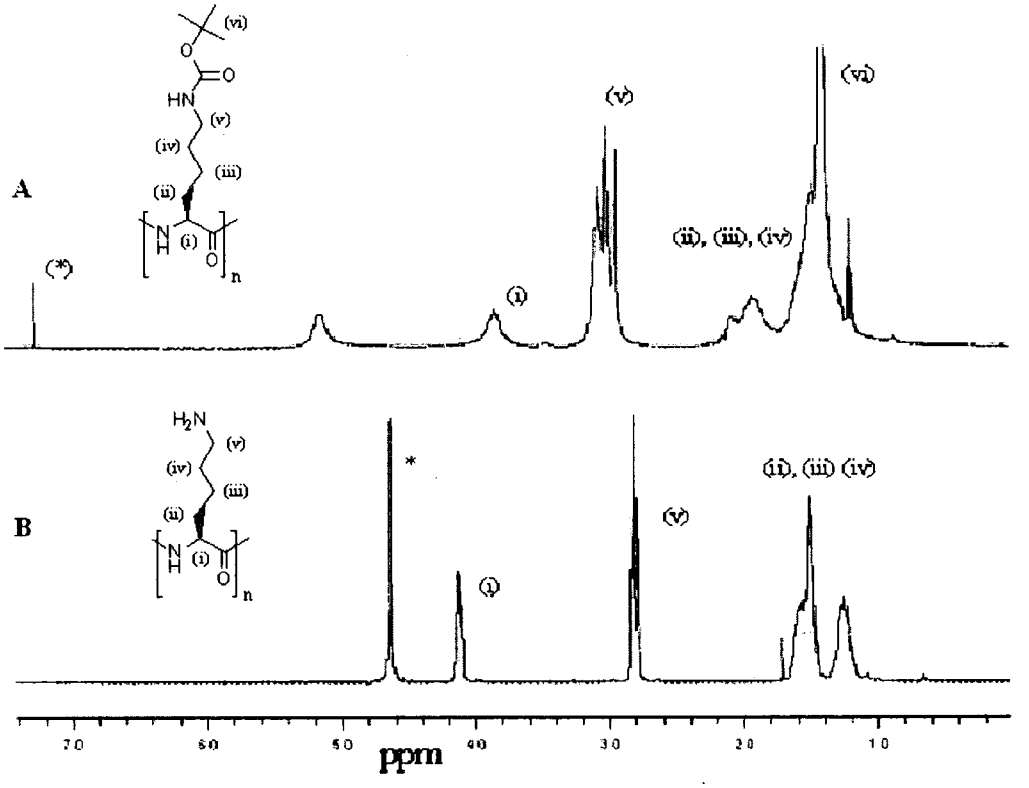

Figure 5. ^1H NMR spectrum Top: PLysBoc. Large, broad peak ~1.2 ppm of Boc can be seen. Bottom: PLys. CH_2 peaks are resolved without Boc Me obstructing. * = residual solvent peak, A: $C\underline{H}Cl_3$ B: $\underline{H}OD$

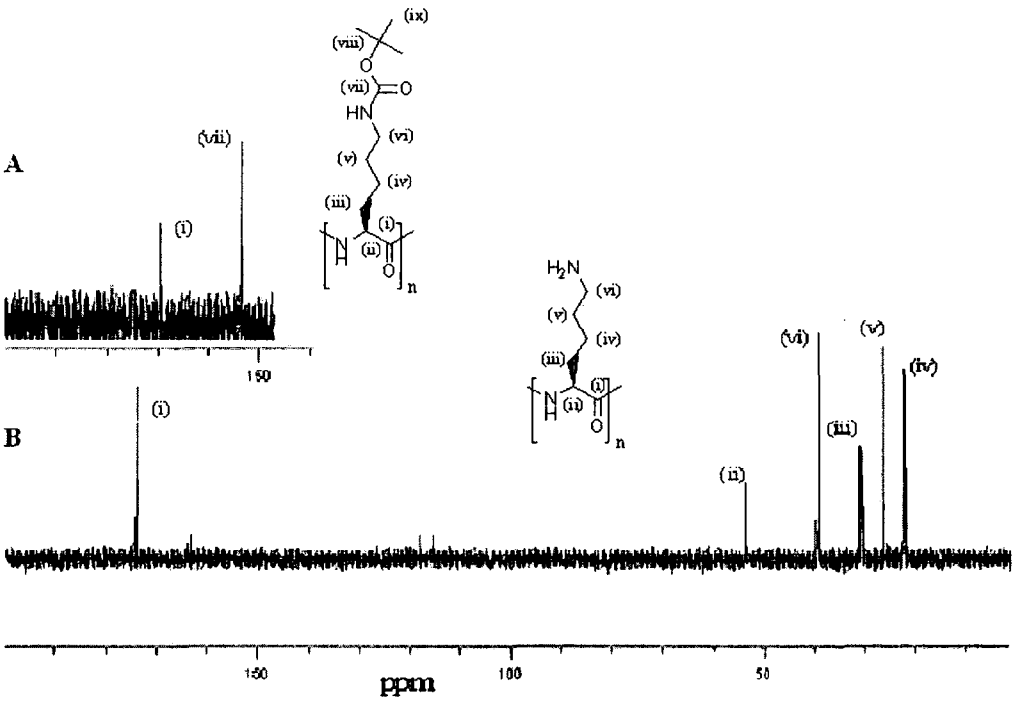

Figure 6. ^{13}C Spectra: A: Poly(ε-Boc-L-lysine) showing the carbonyl peak of Boc group. B: poly(l-lysine) without the Boc protecting group

PLG and PLys gave monomodal distributions in the aqueous SEC profile, proving that the conditions were mild enough to prevent any chain scission.

A different strategy was required to remove the protecting groups from PBThr. Benzyl ethers can be cleaved by the HBr/TFA reagent as used above, by bromination of the aromatic ring followed by hydrolysis of the ether[32]. Extended reaction times are required (>24 hours) to achieved full deprotection which would likely lead to cleavage of some of the amide bonds and racemisation[33]. Hydrogenation is the more common method for benzyl group removal[34], owing to the high conversions, selectivity and mild conditions. We chose to use catalytic transfer hydrogenation[35], where H_2 is generated *in situ*. This has obvious safety and handling benefits. Many reagents are available to generate the H_2 including cyclohexene[36], sodium

hypophosphite[37] and alcohols[38]. To avoid decomposition of the peptide backbone we required a system which was both high yielding and selective, without the need for elevated temperatures. This was achieved by the use of formic acid with palladium on carbon (10%)[39]. Formic acid is a far better solvent for peptides than cyclohexene, allowing a large excess of the H_2 donor to be present (30%). Following reaction overnight, the isolated polymer generated from this was found to be insoluble in boiling water. Initially this was attributed to a failed or incomplete deprotection reaction. Changing the catalyst system to $Pd(Ac)_2$ and $Pd(CaCO_3)$ also gave the same results. A search of the literature gave conflicting information regarding the solubility of poly(L-threonine). CD studies have been successfully conducted in aqueous solution[40], but other reports suggest this could be due to the presence of some D-isomers in the chain increasing the random coil character which is more soluble than the β-sheets[41]. NMR analysis of the resulting polymer was enabled by dissolution in D_2O with the addition of TFA-d (20%). The proton spectrum in Figure 7 shows clearly that the benzyl groups were removed quantitatively by the absence of aromatic resonances at around 7 ppm and benzylic at 5 ppm. No ^{13}C spectra were obtained as only very small concentrations of the polymer were dissolved. It was not possible to determine if any chain scission has occurred as SEC was not possible. We expect this not to be the case because: (i) literature suggests that these conditions do not degrade short peptide sequences. (ii) shorter peptide sequences or amino acid degradation products would have been water soluble, but this was not seen.

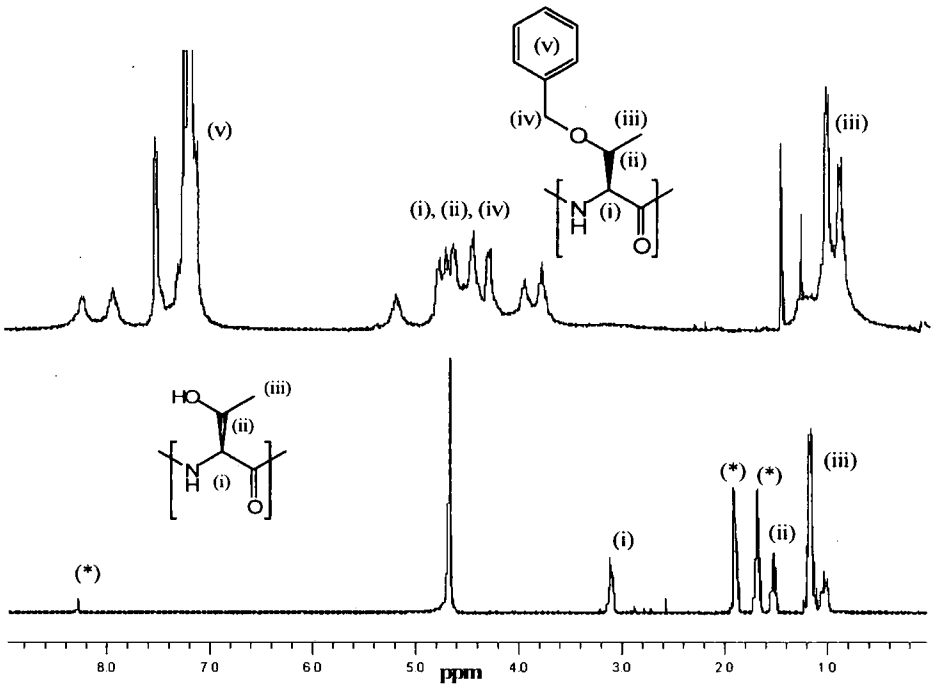

Figure 7. ^{1}H NMR spectrum showing PBThr (top) and PThr (bottom). Key resonances are indicated. * Indicates residual DMF.

4.2.2 BLOCK COPOLYMER SYNTHESIS

Encouraged by the successful polymerisation of BLG and LysBoc NCAs and the demonstrated 'living' character of the PBThr end groups we attempted to synthesise diblock copolypeptides by the sequential monomer addition method[25].

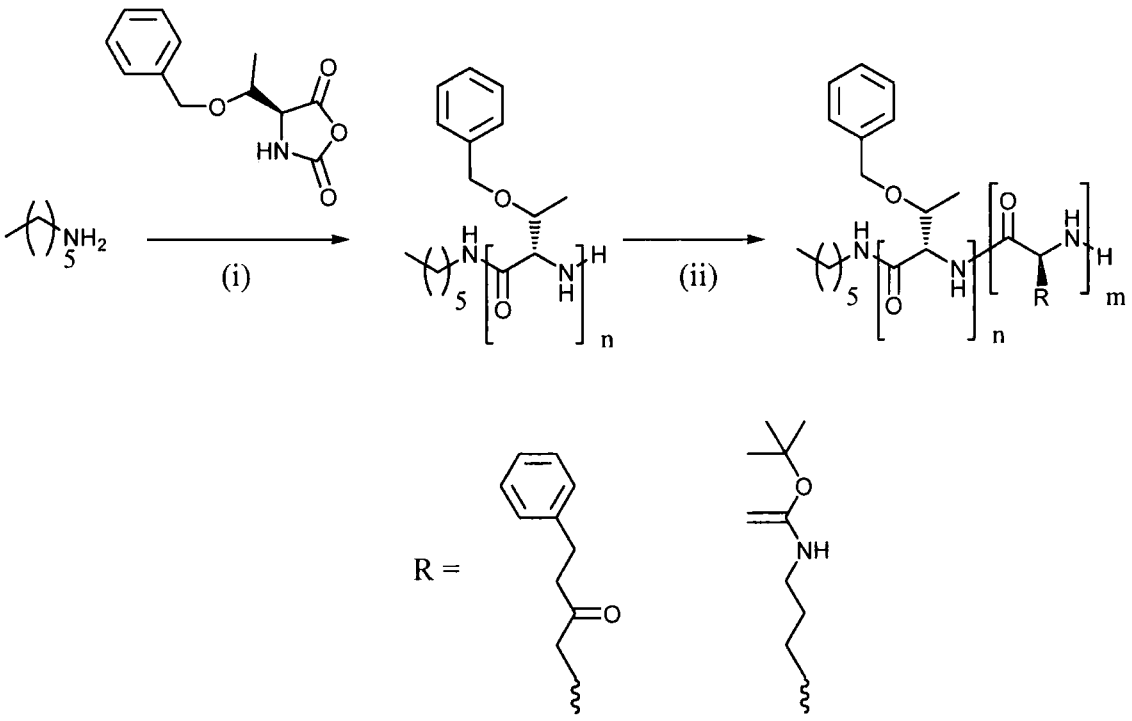

Scheme 2. Synthesis of block copolymers by sequential addition of NCAs to poly(*O*-benzyl-L-threonine) macroinitiator. Conditions: (i) [M] = 10 % (wt); DMAc; vacuum (<0.1mbar); 3 days; 40°C, (ii) BLG orLysBoc NCA; 4 days; 40°C.

As THF was a suitable solvent for polymerisation of both Thr(Bzl) and BLG NCA it was the first solvent investigated. PBThr was synthesised and a sample removed for SEC analysis, confirming that no monomer remained, and then an aliquot of the second monomer was added. This resulted in the solution becoming turbid followed by precipitation. THF SEC analysis, shown in Figure 8, of the soluble fractions showed residual homopolymer, plus a small amount of high molecular weight polymer assumed to be the di-block.

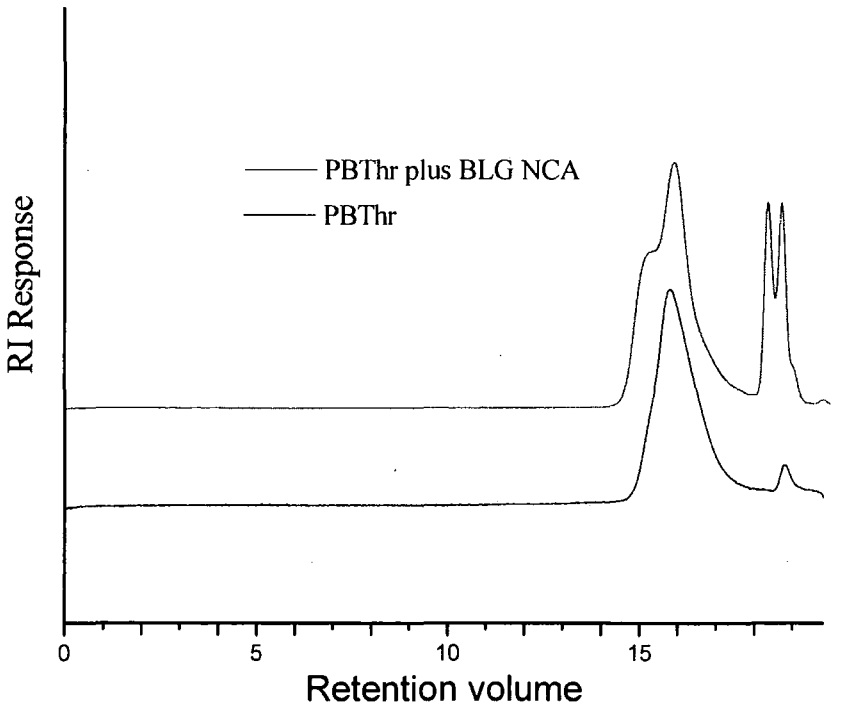

Figure 8. SEC trace for chain extension of PBLThr by BLG NCA in THF. Macroinitiator Mn = 11 kDa, PDI = 1.25

Initiation was clearly not quantitative and there is a large amount of excess monomer remaining. This suggests that the block copolymers display lower solubility in THF than the two constituent homopolymers. It is not uncommon for polypeptides to aggregate in non polar solvents, so the reaction solvent was changed to *N,N*-dimethyl acetamide (DMAc). This was chosen instead of the more commonly used DMF in response to poor results that had been obtained for the homopolymerisation of ThrBzl NCA, which was discussed in Chapter 3. DMAc does not have a labile proton, and is thus less prone to decomposition, but this still can occur to some degree. It was dried over 3Å molecular sieves[42] without distillation, as elevated temperatures would promote decomposition giving dimethyl amine, a good NCA initiator.

Using DMAc, the first block to be grown (PBThr) proceeded to high conversion and gave predictable molecular weights and reasonably narrow distributions (<1.4), showing it was a suitable solvent for this process. Following addition of BLG NCA, the reaction mixture remained homogenous. The same observation was true when LysBoc NCA was added as the second monomer. SEC in DMF showed an increase in molecular weight following the addition of both types of monomer. Figure 9 shows a SEC trace for each NCA type. In both the examples shown there is no residual macroinitiator, and the resulting block copolymer has a symmetrical distribution. Calculation of the molecular weight of the second block was not possible by RALLS, as the block copolymers will not necessarily have a constant value of dn/dc. Conventional calibration is also unsuitable owing to the significant structural differences between the polypeptides and polystyrene or PEG standards. To circumvent this, the first block was analysed by SEC in THF to determine the molecular weight. ^{1}H NMR (Figures 10 and 11) could then be used to determine the relative length of the second block to the first, and thus calculate the number of repeat units and overall M_n. These results are summarised in Table 4.

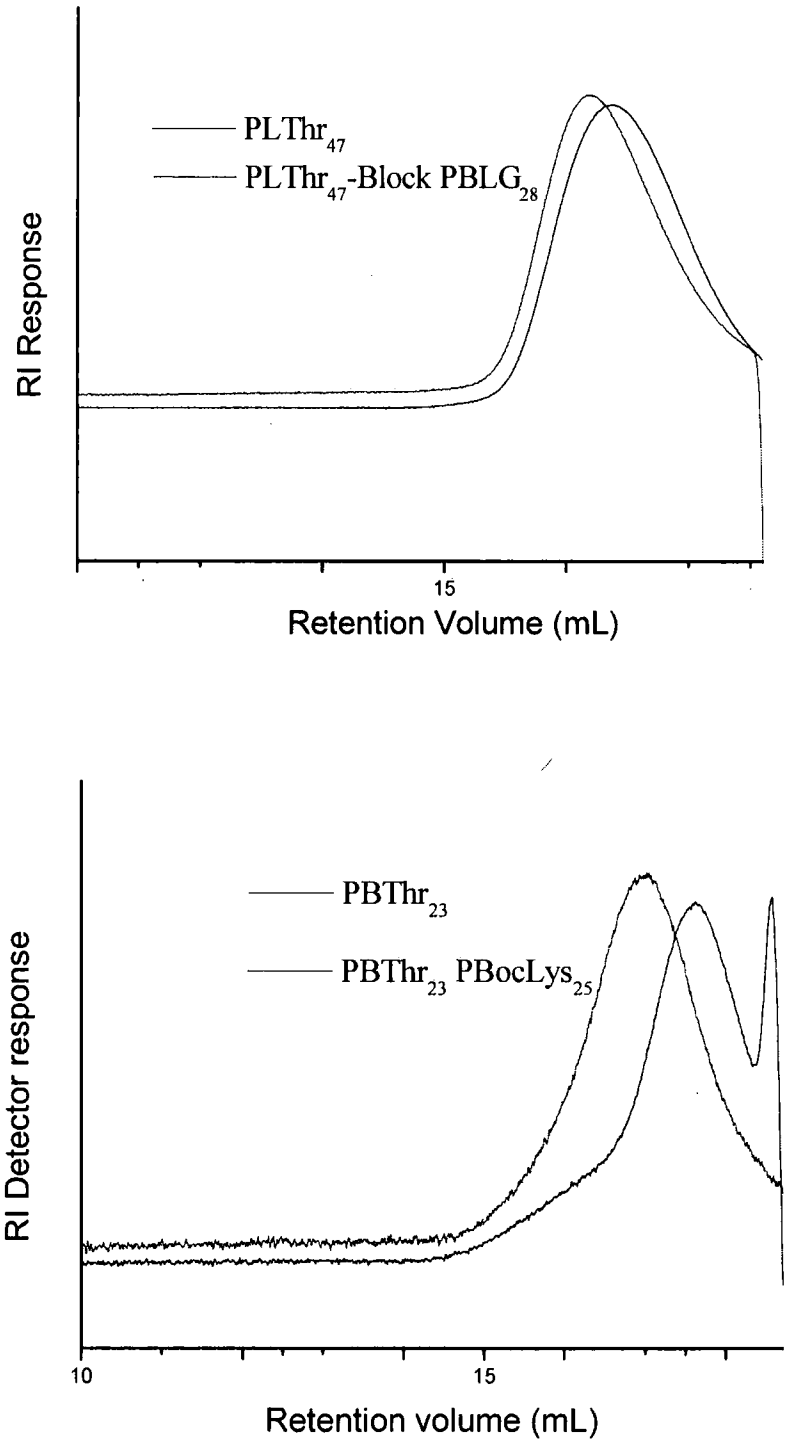

Figure 9 . SEC (DMF) traces showing chain extension of PBThr by sequential addition of BLG NCA (top) and LysBoc NCA (bottom).

Table 4. Chain extension of PBThr by addition of BLG NCA (top) and LysBoc NCA (bottom) in DMAc

	1st Block		2nd Block (BLG)			Copolymer	
Run No	**DP $_{SEC}$ [(a)]**	**PDI**	**[M]:[I]**	**DP_{NMR}**	**M_n [(b)]**	**PDI_{SEC}**	**N_{SEC},M_{NMR}**
P156	47	1.32	45	28	15500	1.60	47,28
P157	26	1.32	40	22	10200	1.47	26,22
P158	50	1.33	25	20	14500	1.71	50,20
P197	16	1.45	20	16	6800	1.54	16,16

	1st Block		2nd Block (LysBoc)			Copolymer	
Run No	**DP_{SEC} [(a)]**	**PDI**	**[M]:[I]**	**DP_{NMR}**	**M_n [(b)]**	**PDI_{SEC}**	**N_{SEC},M_{NMR}**
P160	16	1.20	23	19	7300	1.47	16,19
P163	46	1.38	20	18	12800	1.54	46,18
P195	20	1.38	25	22	8870	1.60	20,22
P196	20	1.41	50	46	14300	1.60	20,46

(a) Determined in THF by RALLS, dn/dc = 0.11 mL. g^{-1}; (b) calculated from sum of 1st block by SEC and 2nd by NMR

Increasing the ratio of [monomer]:[macroinitiator] gave a corresponding increase in DP for the second block. In all cases there was an increase in the polydispersity index following re-initiation, indicating some loss of control. All the distributions were monomodal, proving the absence of any competing initiation or termination processes. The broadening of the PDI can be attributed to the inherent difficulties of adding a further highly reactive species to the reaction. Typically, with anionic polymerisation, the second monomer (eg styrene, butadiene)[43] would be distilled in, ensuring the purity of monomers and maintaining the high vacuum

environment. The use of syringes and septa in our case will have resulted in a non–pristine environment, allowing some decomposition of the NCA to occur, and accounting for the reduced DP of the second block relative to the feed ratio.

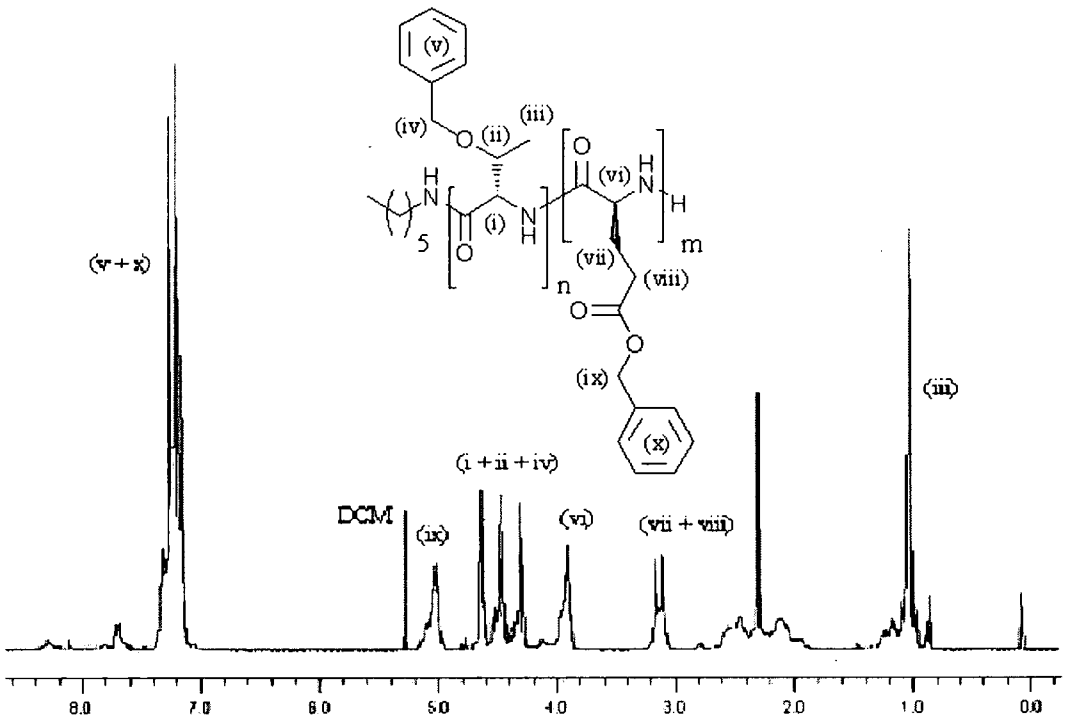

Figure 10. ^{1}H NMR spectrum of poly(BThr $_{47}$ -block-BLG$_{27}$). Solvent DCM/TFA-d(5%)

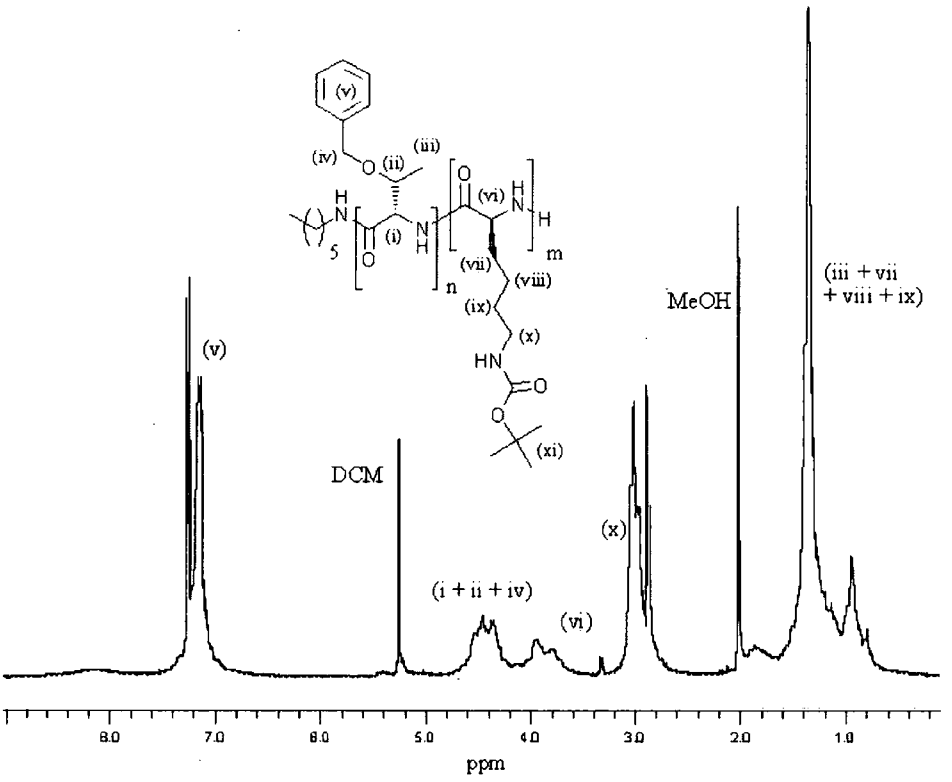

Figure 11. ^{1}H NMR spectrum of poly(BThr$_{16}$–block-LysBoc$_{19}$). Solvent $CDCl_3$/MeOH-d_4 (5%)

The homopolymerisation of alanine NCA failed due to its insolubility at low DPs, so we reasoned that polymerisation may be possible by using a solubilising macroinitiator, such as PEG-NH_2[44]. The same result was obtained as with the homopolymer, with precipitation occurring with 5 hours of monomer addition. No attempts were made to characterise this material.

An important observation was made during the NMR analysis of the block copolymers. In the common NMR solvent $CDCl_3$, gelation was observed during their preparation. To obtain liquid samples suitable for analysis we found that addition of approximately 5-10 % TFA-d was required for poly(BThr-block-BLG) and in the case of poly(BThr-block-LysBoc), 5-10 % MeOH-d_4. Both of these are known to disrupt H-bonding in peptides. TFA was preferable as it does not have any overlapping signals in the region of 0 – 7.5 ppm in the ^{1}H NMR, which are of interest. The acid

sensitive Boc group can not be used with TFA, hence the choice of MeOH. The gelation behaviour is investigated further in Chapter 5.

4.3 CONCLUSIONS

Following on from the results of Chapter 3, we first showed that BLG and LysBoc NCAs can be polymerised in a controlled fashion without the need for transition metal catalysts or meticulous high vacuum techniques. The resulting well defined homo-polymers were quantitatively deprotected without any chain scission occurring. This resulted in a diverse set of polypeptides bearing either a neutral, cationic or anionic side group. All the polymers were characterised by NMR and SEC, with the exception of poly(L-threonine) which was insoluble in most solvents. Having polymerised these monomers we then made use of the 'living' end groups of PBThr to initiate a second monomer of BLG or LysBoc NCA. For this to be possible, the first block grown must reach high conversion (>95%) to ensure that each block is homogenous. Using this sequential method, control over the composition of both blocks was obtained. The diblock copolymers were not as well defined as the homo polymers, with polydispersity indices around 1.5. They were however monomodal, indicating structural if not chain length homogeneity within the polymers. This is the first example of poly(benzyl-L-threonine) being combined into a block copolymer, and one of only a handful of reports of the controlled synthesis of block-co-polypeptides by NCA polymerisation. By removing the requirement for transition metal catalysis, the work up is facile and there are no concerns over the biological significances of residual metal species. This relatively simple methodology should be compatible with a wide range of NCA monomers.

4.4 EXPERIMENTAL

4.4.1 GENERAL

All NCAs were synthesised as described in Chapter 2. They were used immediately following synthesis and purification, not being stored for longer than 3 hours and below -10°C. *n*-Hexylamine (>99.5%, H_2O<0.2%) was purchased from Fluka. THF and DCM (<99.5%) were purchased from Fischer Scientific and dried by passage through two alumina columns using an Innovative Technology Inc. solvent purification system and stored under N_2. THF was further dried over sodium/benzophenone complex with at least 3 freeze-thaw cycles, until the purple colouration persisted. Dimethyl acetamide (anhydrous <0.005% H_2O) was purchased from Aldrich. Further purification was achieved by drying over 3A molecular sieves for 24 hours. Hexane (Fischer Scientific >99%) was dried over 3A molecular sieves. 3A molecular sieves (Aldrich) were activated in an oven at 200°C before use. All other chemicals were used as received. NMR spectroscopy (^1H, and COSY) was determined at 400MHz or (^{13}C) at 100MHz using a Brucker Avance-400. Alternatively this was conducted (^1H and COSY) at 500MHz and (^{13}C) 125MhHz on a Varian Inova-500 spectrometer. Alternatively Varian Inova-500 COSY and HSQC correlation studies were used to assign the observed signals to the carbon and hydrogen atoms of the compounds. MALDI-TOF spectra were collected on an Applied Biosystems Voyager DE. Gel permeation chromatography was undertaken using THF as the eluent. 100μL of solution (agitated overnight to ensure complete dissolution) was injected at a flow rate of 1.00 $mL.min^{-1}$ by a Viscoteck SEC autochanger module. A Viscoteck TDA 301 unit with triple detection (right angle

laser scattering at 670nm, differential refractometer and viscometer) was used. dn/dc Values were calculated online for each polymer. Analyses were undertaken using OmniSEC 4.0 software. Infrared spectroscopy was conducted on a Nicolet Nexus FT-IR as a KBr disc. Liquid samples were analysed by direct injection of the reaction medium into a liquid cell with KBr windows. Omnic 5.1a (Nicolet) was used to analyse the data obtained.

4.4.2 POLYMER SYNTHESIS

Poly(γ-benzyl-L-glutamate) (PBLG)

BLG NCA (0.20 g, 0.75 mmol) was dissolved into 3 mL of dry DCM, and injected into a Schlenk tube fitted with a Young's tap and a 9mm rubber septum already under vacuum. The DCM was removed under vacuum and the NCA allowed to dry under vacuum for a further 2 hours. THF (3mL) was vacuum distilled into the vessel to give an approximately 10 % (wt). The tube was then immersed in an oil bath thermostated at 35°C, and stirred to dissolution. n-Hexylamine (0.08mL, 0.2 M solution) was added via syringe into the tube and allowed to stir for 4 days.

Following this time a 100μl sample was withdrawn for SEC analysis, and the remainder of the reaction was poured into a 10 fold excess of diethyl ether with stirring, and the white powder collected by filtration. Further purification was achieved by re -dissolving in THF and precipitating into a 10 fold excess of water. Yield 0.13 g, 75%.

^{1}H NMR ($CDCl_3$) δ_{ppm}; 7.19 – 7.29 (5H, H^9), 5.04 (2H, H^7), 3.94 (1H, H^3), 2.60 (2H, H^5), 2.28 (2H, H^4)

^{13}C NMR δ_{ppm}; 175 (C^2), 172 (C^6), 136 (C^8), 128.0 and 128.4 (C^9), 66 (C^7), 57 (C^3), 31 (C^5), 25 (C^4),

IR (KBr disc) cm^{-1}: 3296 (N-H), 2955 (C-H), 1734 (Aromatic C-C), 1651 (Amide C=O)

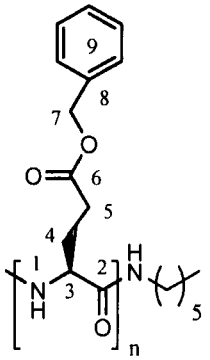

Poly(ε-*N*-butoxy carbonyl-L-lysine) (PLysBoc)

The same procedure was used as with the polymerisation of BLG NCA with DMAc as the solvent in place of THF. LysBoc NCA (0.2g, 7.35mmol); n-hexylamine (0.08mL, 0.2M solution). Yield 0.114g, 68%.

^{1}H NMR ($CDCl_3$) δ_{ppm}; 1.37 (13H, H^{11} + H^5 + H^6), 1.86 (2H, H^4), 3.02 (2H, H^7), 5.14 (1H, H^3), 8.21 (1H, H^8),

^{13}C NMR δ_{ppm}; 21.5 (C^5), 28.5 (C^{11}), 29.7 (C^4), 30.1 (C^6), 40.5 (C^7), 65.8 (C^3), 78.7 (C^{10}), 156.1 (C^9), 170.7 (C^2),

IR (KBr disc) cm^{-1}: 3292 (N-H), 2960 (C-H), 1695 (^{t}Boc C=O), 1651 (Amide C=O)

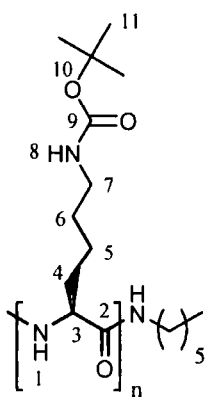

Poly(L-glutamic acid) sodium salt (PLG)

PBLG (250 mg, 1.16 mmol repeating unit) was dissolved in 1 mL of trifluroacetic acid. HBr (33% in acetic acid) (0.54 mL, 2.9 mmol) was added dropwise under N_2 and stirred at room temperature for 1 hour. The solution was then precipitated into a 30 fold excess of diethyl ether. The solid was washed (2 x 10 mL) with diethyl ether, then dissolved in 2 mL of 0.5M aqueous NaOH solution and dialysed against distilled water. The polymer was obtained as a white solid by freeze drying. Yield 145 mg, 72%.

^{1}H NMR ($CDCl_3$) δ_{ppm}; 0.65 (H^8), 1.07, 1.29, 3.06 (H^7), 1.72 (1H, H^{4a}), 1.83 (1H, H^{4b}), 2.07 (2H, H^5), 4.11 (1H, H^3)

^{13}C NMR δ_{ppm}; 28.2 (C^4), 33.7 (C^5), 53.6 (C^3), 173.6 (C^2), 181.6 (C^6)

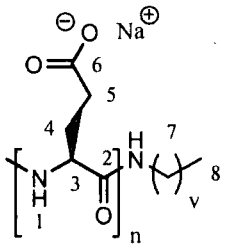

Poly(L-lysine) HBr salt (PLLys)

PLysBoc (160 mg, 0.66 mmol repeating unit) was dissolved in 1 mL of trifluroacetic acid. HBr (33% in acetic acid) (0.54 mL, 2.9 mmol) was added dropwise under N_2 and stirred at room temperature for 1 hour. The solution was then precipitated into a 30 fold excess of diethyl ether. The obtained solid was washed (2 x 10 mL) with diethyl ether, then dissolved in distilled water and dialysed against distilled water. The polymer was obtained as a white solid by freeze drying. Yield 120 mg, 82%.

^{1}H NMR ($CDCl_3$) δ_{ppm}; 1.20 – 2.82 (6H, $H^4 + H^5 + H^6$), 2.81 (1H,H^7), 4.11 (1H, H^3)

^{13}C NMR δ_{ppm}; 22.3 (C^5), 26.5 (C^6), 30.7 (C^4), 39.3(C^7), 53.5 (C^3), 173.7 (C^2)

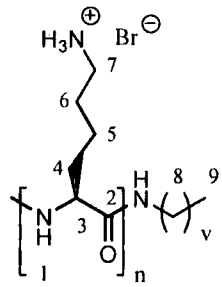

Poly(L-threonine) (PThr)

PBThr (0.2g, 1.05 mmol repeat unit) was dissolved in 2 mL of DMF, and HCO_2H was added dropwise until the solution became slightly turbid (0.8mL) under N_2. Pd/C (10%) (0.2 g) was added in a single portion under N_2, and the reaction stirred at room temperature overnight. The reaction was diluted with DMF (3 mL) then centrifuged to remove Pd/C. The resulting cloudy solution was precipitated into 100 mL of cold Et_2O and the grey solid obtained by filtration. Yield 0.04 g, 33%.

^{1}H NMR (D_2O/TFA-d) δ_{ppm}; 1.17 (3H, H^3), 1.54 (1H, H^2), 3.10 (1H, H^1)

^{13}C NMR (D_2O/TFA-d) δ_{ppm} : Peaks too weak due to low solubility. See text

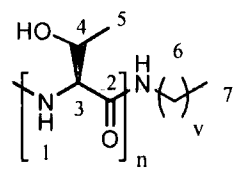

4.5 BIBLIOGRAPHIC REFERENCES

(1) Swarc, M.; Levy, M.; Milkovich, R. *J. Am. Chem. Soc.* **1956**, *78*, 2656-2657.

(2) Hadjichristidis, N. *J. Pol. Sci. Part A: Pol. Chem.* **1999**, *37*, 857-871.

(3) Deming, T. J. *Adv. Pol. Sci.* **2006**, *202*, 1-18.

(4) Hayahsi, T.; Walton, A. G.; Anderson, J. M. *Macromolecules* **1977**, *10*, 346-351.

(5) Moad, G.; Chiefari, J.; Chong, Y. K.; Krstine, J.; Mayadunne, R. R. A.; Postma, A.; Rizzardo, E.; Thang, S. H. *Polym. Int.* **2000**, *49*, 993-101.

(6) Matyjaszewski, K.; Xia, J. *Chem. Rev.* **2001**, *101*, 2921-2990.

(7) Hawker, C. J.; Bosman, A. W.; Harth, E. *Chem. Rev.* **2001**, *101*, 3661-3688.

(8) Deming, T. J. *Nature* **1997**, *390*, 386-389.

(9) Deming, T. J.; Curtin, S. A. *J. Am. Chem. Soc.* **2000**, *122*, 5710-5717.

(10) Euliss, L. E.; Bartl, M. H.; Stucky, G. D. *J. Cryst. Growth* **2006**, *286*, 424-430.

(11) Deming, T. J. *J. Pol. Sci. Part A: Pol. Chem.* **2000**, *38*, 3011-3018.

(12) Bhaw-Luximon, A.; Jhurry, D.; Belleney, J.; Goury, V. *Macromolecules* **2003**, *36*, 977-982.

(13) Goury, V.; Jhurry, D.; Bhaw-Luximon, A.; Novak, B. M.; Belleney, J. *Biomacromolecules* **2005**, *6*, 1987-1991.

(14) Higashi, N.; Jkoga, T.; Niwa, M. *Langmuir* **2000**, *16*, 3482-3486.

(15) Dimitrov, I.; Schlaad, H. *Chem. Commun.* **2003**, 2944-2945.

(16) Ludwigs, S.; Krausch, G.; Reiter, G.; Losik, M.; Antonietti, M.; Schlaad, H. *Macromolecules* **2005**, *38*, 7532-7535.

(17) Lutz, J.-F.; Schutt, D.; Kubowicz, S. *Macromol. Rapid. Commun.* **2005**, *26*, 23-28.

(18) Meyer, M.; Schlaad, H. *Macromolecules* **2006**, *39*, 3967-3970.

(19) Choen, J.-B.; Jeong, Y.-I.; Cho, C.-S. *Polymer* **1999**, *40*, 2041-2050.

(20) Cho, I.; Kim, J.-B.; Jung, H.-J. *Polymer* **2003**, *44*, 5497-5500.

(21) Checot, F.; Lecommandoux, S.; Klok, H.-A.; Gnanou, Y. *Eur. Phys. J., E* **2003**, *10*, 25-35.

(22) Lee, H.-F.; Sheu, H.-S.; Jeng, U.-S.; Huang, C.-F.; Chang, F.-C. *Macromolecules* **2005**, *38*, 6551-6558.

(23) Klok, H.-A.; Rodriguez-Hernandez, J.; Becker, S.; Mullen, K. *J. Pol. Sci. Part A: Pol. Chem.* **2001**, *29*, 1572-1583.

(24) Vayaboury, W.; Gianni, O.; Cottet, H.; Deratani, A.; Schue, F. *Macromol. Rapid. Commun.* **2004**, *25*, 1221-1224.

(25) Aliferis, T.; Iatrou, H.; Hadjichristidis. N *Biomacromolecules* **2004**, *5*, 1653-1556.

(26) Papadopoulos, P.; Floudas, G.; Schnell, I.; Aliferis, T.; Iatrou, H.; Hadjichristidis, N. *Biomacromolecules* **2005**, *6*, 2352-2361.

(27) Hanski, S.; Houbenov, N.; Ruokolainen, J.; Chondronicola, D.; Iatrou, H.; Hadjichristidis, N.; Ikkala, O. *Biomacromolecules* **2006**, *7*, 3379-3384.

(28) Aliferis, T.; Iatrou, H.; Hadjichristidis, N. *J. Pol. Sci. Part A: Pol.Chem.* **2005**, *43*, 4670-4673.

(29) *Polymer Handbook*; 4th ed.; John Wiley and Sons, 1999.

(30) Temyanko, E.; Russo, P. S.; Ricks, H. *Macromolecules* **2001**, *34*, 582-586.

(31) Rodriguez-Hernandez, J.; Klok, H.-A. *J. Pol. Sci. Part. A: Pol. Chem.* **2003**, *41*, 1167-1187.

(32) Claydon, J.; Greeves, N.; Warren, S.; Wothers, P. *Organic Chemistry*; 1st ed.; Oxford University Press. UK, 2001.

(33) Bohak, Z.; Katchalski, E. *Biochemistry* **1963**, *2*, 228-237.

(34) Sanda, F.; Kamatani, J.; Endo, T. *Macromolecules* **2001**, *34*, 1564-1569.

(35) Brieger, G.; Nestrick, T. J. *Chem. Rev.* **1974**, *74*, 567-580.

(36) Hanessian, S.; Liak, T. J.; Vanasse, B. *Synthesis* **1981**, 396-397.

(37) Li, J.; Wang, S.; Cripino, G. A.; Tenhuisen, K.; Singh, A.; Grosso, J. A. *Tet. Lett.* **2003**, *44*, 4041-4043.

(38) Cruzado, M. C.; Martin-Lomas, M. *Tet. Lett* **1986**, *27*, 2497-2500.

(39) ElAmin, B.; Anatharamaiah, G. M.; Royer, G. P.; Means, G. E. *J. Org. Chem.* **1979**, *44*, 3442-3444.

(40) Kubota, S.; Fasman, G. D. *Biopolymers* **1975**, *14*, 605-631.

(41) Deming, T. J. *J. Pol. Sci. Part.A: Pol. Chem.* **2000**, *38*, 3011-3018.

(42) Chrapava, S.; Tourad, D.; Rosenau, T.; Potthast, A.; Kunz, W. *Phys. Chem. Chem. Phys* **2003**, *5*, 1842-1847.

(43) Hadkichristidis, N.; Pitsikalis, M.; Pispas, S.; Iatrou, H. *Chem. Rev.* **2001**, *101*, 3747-3792.

(44) Rathore, O.; Sogah, D. Y. *J. Am. Chem. Soc.* **2001**, *123*, 5231-5239.

CHAPTER 5

ORGANOGELATION BEHAVIOUR OF BLOCK COPOLYPEPTIDES: PROPERTIES AND MECHANISM

5.1 INTRODUCTION

Molecular self-assembly has recently been drawing huge amounts of attention in the development of supramolecular structures and materials[1]: those held together by non/covalent interactions such as Van der Waals and H-bonding. The inspiration for these structures is taken from nature which utilises self-assembly of molecular scale objects to give macroscopic assemblies. Most synthetic polymeric materials can not form permanent 3-dimensional objects due to their irregular, random coil conformations. However, there are some cases where polymers do form rigid structures in solution[2,3]. Poly(γ-benzyl-L-glutamate), PBLG, for instance forms a stable α-helix in many organic solvents[4]. Above a critical concentration gelation is observed[5]. This behaviour has been attributed to phase separation as chain-chain entanglements can not form[6]. Microscopic phase separation increases the concentration of PBLG locally, and liquid crystalline alignment occurs. Formation of a network of fibres stabilised by dipolar π- π interactions physically immobilises the solvent matrix. This has led to significant interest in rod-coil block copolymers. The rigid rod segments can align together to give highly ordered solid state structures[7] shown in Figure 1. π-Conjugated polymers and oligomers, which have found applications in OLEDs[8] and as molecular wires[9], form rigid rods in the solid[7] and solution state[10]. These stacking interactions have been exploited as assembling motifs when incorporated as a block-co-polymer segment with a solublising unit such as PEG. PEG_{110}-block-oligo(phenylene vinylene)$_8$-block-PEG_{110} polymers assemble into long cylindrical micelles where the phenylene-vinylene rods stack within a corona of PEG[11]. Reducing the length of the phenylene-vinylene to three units, with a sufficiently long PEG chain results in gel formation, stabilised by lamellar packing of

the OPV units[12] when each PEG unit is fully hydrated with 4.6 molecules of water. Other conjugated polymers including poly(thiophene) block copolymers also display this behaviour[13].

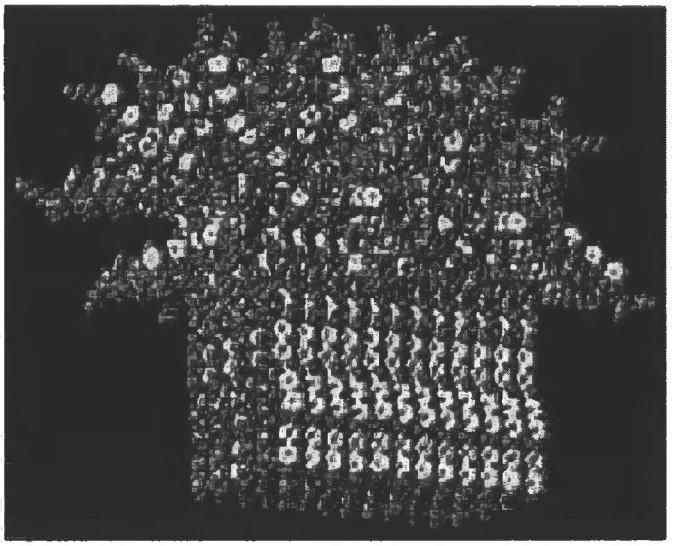

Figure 1. Schematic illustration of rod-coil block copolymer packing directed by rod-rod alignment.[14]

The onset of gelation in dilute solutions of these polymers is of particular interest as templates for nanostructured materials[15] or even for the restoration of artworks by immobilising organic solvents[16]. The underlying mechanism for gel formation is attributed to formation of a networked scaffold[17] (Figure 2) which can immobilise the solvent, even at low concentrations of the gellant. Gelation can also be induced in star shaped polymers where one block is incompatible with the solvent[18] (in linear diblock copolymers one may expect micelles or similar[19]) or by addition of charged endgroups to give end-to-end interactions[20].

Nature provides much of the inspiration for self assembled materials, the most famous being the DNA double helix[21]. In addition to this motif β-sheets and α-helices formed by polypeptides[22], which can then self organise into elegant tertiary and

quaternary[23] structures including enzymes and carbohydrate binding lectins[24], are similarly employed. Gelation systems based upon peptide sequences, and their rigid secondary structures, have been utilised extensively[25,26]. A particular driver is to understand the formation of amyloid fibrils which are associated with Alzheimer's and Parkinson's diseases[27]. Tirrel *et al.*[28] showed that ABA triblock structures of a flexible poly-electrolyte flanking a leucine zipper[29] core could reversibly self assemble by association of the 'zipper' regions. The elastin derived peptide sequence VPGVG has also been shown to be able to aggregate when incorporated into a polymer[30], but gelation has not been reported to date.

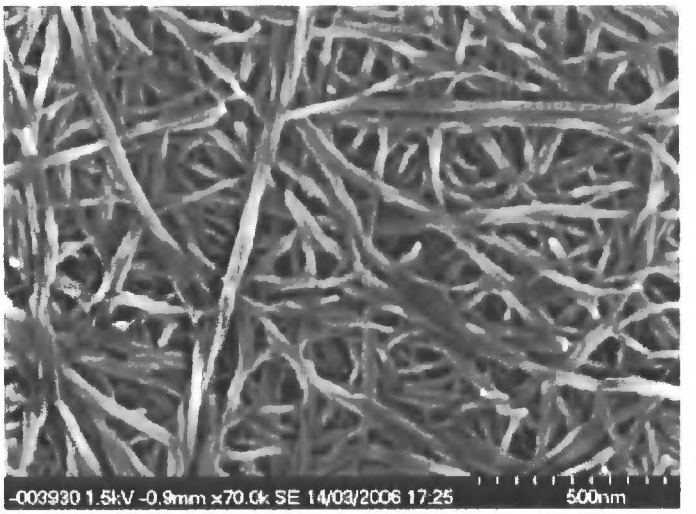

Figure 2. SEM of dried down gel fibres formed by self assembly of a low molecular weight organogelator[31].

The self assembly properties of β-sheet peptide sequences[32-34], especially those which have been inserted between two PEG blocks, have been the focus of intense research. Poly(L-alanine) oligomers with PEG flanking groups form self assembled structures in the solid state, in which poly(L-alanine) rich regions are produced by the formation of antiparallel β-sheets[35]. Klok and co-workers have used amphiphilic β-strand forming peptides conjugated to PEG[36], and shown that they assemble into

antiparallel β-sheets, which can then assemble into fibres[37] by lamella stacking in both the melt and solution state. By using a peptide which forms intra-chain antiparallel β-sheets, stacking only occurs in one direction giving molecularly thick ribbon structures[38].

Deming and co-workers have utilised controlled polymerisation of *N*-carboxy anhydrides[39] (as opposed to solid phase synthesis or bio-engineering) to produce polypeptides with defined structural motifs. By incorporating poly(L-valine) and poly(L-leucine), which give β-sheet and α-helical conformations respectively, with a poly-electrolyte block, hydrogels could be formed at concentrations below 1 % (wt).[40] Interestingly this work showed that α-helices are also suitable packing motifs for gelation, as shown in Figure 3.

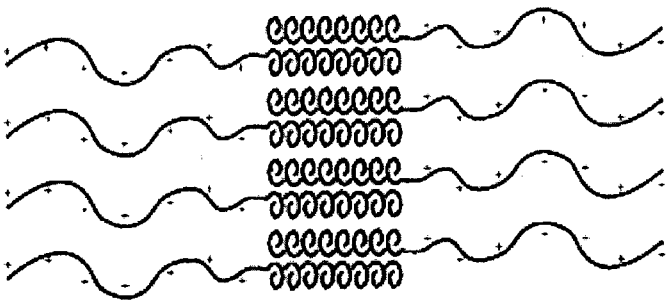

Figure 3. Assembly of poly(L-leucine)-block-poly(L-lysine) by antiparallel arrangement of helicies, insulated by water soluble, polyelectrolye blocks.

More recently Manners *et al.* showed that poly(γ-benzyl-L-glutamic acid) (PBLG), copolymers containing a random coil[41] or dendritic block[42] self assemble in a similar fashion, with antiparallel alignment of α-helices. The mechanism is essentially the same as that presented above, as the PBLG is insoluble in the solvent, toluene. The supramolecular ribbons can be viewed by AFM, and result in an entangled network, providing rigidity and hence organogelation. Increasing the size of the

assembling block gave a corresponding decrease in the minimum gelation concentration, attributable to more efficient packing. ‡‡

‡‡ PBLG has also been used extensively as the rod unit in rod-coil polymers described earlier. These systems did not give gelation unless mentioned, so were outside of the scope of this introduction.

5.2 RESULTS AND DISCUSSION

During the analysis of the block copolypeptides described in Chapter 4, it was observed that thermo-reversible gelation occurred in the common NMR solvents $CDCl_3$ and CD_2Cl_2. This was surprising, as the constituent homopolypeptides were soluble in these solvents, without any observed gelation at concentrations above 200 $mg.mL^{-1}$. To assess the gelation abilities of the block-co-polypeptides we first screened a range of solvents for solubility. Heating or sonication was required in most cases. The results of this are shown in Table 1, below.

Table 1. Solubility test for P(BLThr$_{47}$-BLG$_{28}$) at 1 wt%

Solvent	Soluble*
THF	X
Dioxane	X
DMF	✓
DMAc	✓
$CHCl_3$	✓
DCM	✓
TCE	✓
Benzyl Alcohol	✓
TFA	✓

*** Judged by formation of optically transparent solutions**

The diblock polymer was soluble in all the three chlorinated solvents which were tested, along with benzyl alcohol. TFA, DMAc and DMF which are all known as excellent solvents for peptides also readily dissolved the block-co-polymer.

Surprisingly, THF and dioxane could not dissolve the polymer even with heating and sonication. Homopolymers of the individual blocks are very soluble (>200mg.mL^{-1}) in both of these solvents at room temperature.

To evaluate the gel forming properties, simple inversion tests were used. Briefly a sample of block co-polymer was transferred to a vial with solvent and sonicated for 30 minutes then left to stand for 1 hour. The vial was then inverted and allowed to stand for 1 hour. If no flow was observed it was defined as being a gel. Table 2 shows the results of the inversion tests which began with solutions of concentrations of 8 wt % which were then diluted until the minimum gelation concentration was found. This was only undertaken for DCM and $CHCl_3$. Gelation was also observed in tetrachloroethane.

Table 2. Composition of block-co-polypeptides, and their minimum gelation concentration as determined by inversion tests

				Min. Gel Conc. (wt %)[c]	
Entry	**PBThr[a]**	**PBLG[b]**	**PLysBoc[b]**	**DCM**	**$CHCl_3$**
P156	47	28		4	4
P157	26	22		4	4
P158	50	25		4	3
P197	16	16		-	-
P160	16		19	-	-
P163	46		18	5	5
P195	20		22	3	-
P196	20		46	4	6

(a) Determined by RALS SEC in THF. (b) Calculated by ^{1}H NMR relative to PBThr block. (c) Minimum gelation concentration: tested in 1 wt % increments. (-) indicates no gelation was observed at up to 8 wt % concentration.

Figure 4 shows photographs of $PBThr_{47}$-$PBLG_{28}$ at 4 wt% concentration. All the gels are clear and able to support their own weight for extended periods (observed to last for over 1 week).

Figure 4. Photographs of $PBThr_{47}PBLG_{28}$ at 4 wt % concentration in different chlorinated solvents. Samples have been inverted for 1 hour previously

When the concentration of the polymers was reduced below their critical concentration a viscous liquid instead formed and upon lowering the concentration further a free flowing liquid was obtained; (Figure 5).

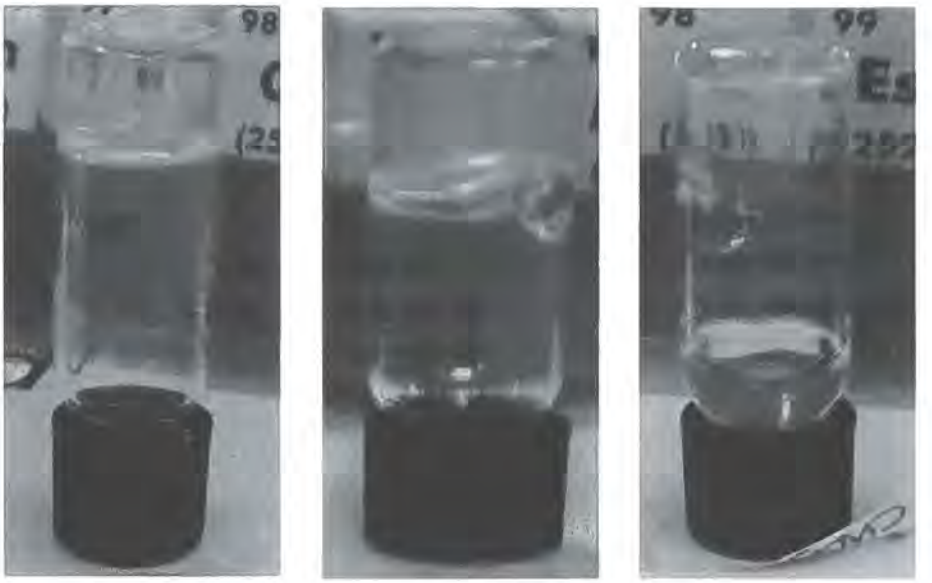

Figure 5. $PBThr_{23}PLysBoc_{18}$ in $CHCl_3$ at various concentrations, showing transition from gel (far left) to viscous liquid (middle) to free flowing liquid (right)

The different copolymers containing a PBLG block gelated DCM and $CHCl_3$ similarly, with the exception of the best gelator $PBThr_{50}PBLG_{25}$ which could gelate $CHCl_3$ down to 3 wt% concentration as opposed to 4 wt % for the others. Polymers containing a PLysBoc segment gelated DCM at lower concentrations than in $CHCl_3$. The di-blocks with the shortest PBThr block (DP = 16) failed to gelate either $CHCl_3$ or DCM. In comparison the diblock with the longest PBThr (DP = 50) segment was the strongest gelator. This suggests that the PBLThr block plays a key role.

Polymeric gelators typically have amphiphilic character, allowing for a self assembly process whereby solvent is excluded from the insoluble region, or regions where chains can associate by electrostatic, hydrogen bonding or entanglment. For instance polypeptides have been used to make hydrogels where one segment has a rigid hydrophobic structure, and the other is a polyelectrolyte[40]. The homopolymers from which our block copolymers are derived from are all soluble in the solvents in which gelation has been induced: TCE, $CHCl_3$ and DCM, making the gelation

behaviour completely unexpected. Mixtures of the two homopolymers in solution do not result in gelation; neither do solutions of the individual homopolymers. It has been commented[43] that block copolypeptides containing an L-glycine block form gels in DMF, due to the highly insoluble nature of the polyglycine, which is in contrast to the soluble nature of both the blocks in our system.

All the gelation systems we investigated displayed irreversible loss of structure by addition of hydrogen bond breaking co-solvents: methanol for PLysBoc and TFA for PBLG containing copolymers. This process made it possible for NMR analyses to be conducted in chlorinated solvents. The gels were also observed to be thermo-reversible. At 4 wt %, $PBThr_{47}$-$PBLG_{28}$ was stable to heating to 35°C, but when the temperature was increased to 40°C, the gel broke down to give a free flowing liquid. Upon standing and allowing to cool to ambient temperature a clear gel reformed. This process was repeated 5 times, with gelation occurring following each heating period.

The first step taken in explaining the above behaviours was to visualise the structures which support the gel.

5.3 ORGANOGEL STRUCTURE AND MORPHOLOGY

For gelation to occur in the dilute concentration range, it was apparent that a network of some sort must be forming, stabilising the solution. In the case of a 4 wt % solution in $CHCl_3$ of a 10 kDa each chain is gelating over 6000 molecules of solvent! To our surprise the dried down gels, shown in Figure 6, had a network structure which was clearly visible by optical microscopy.

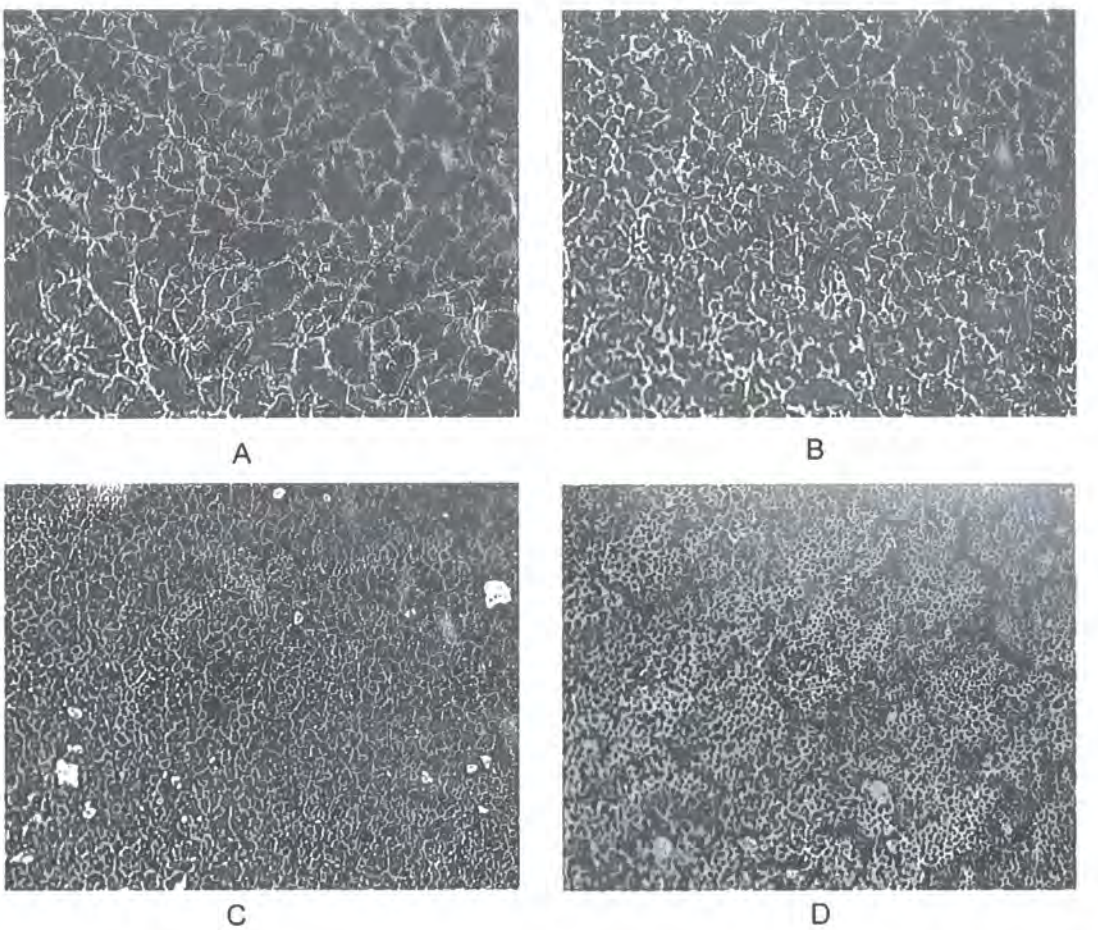

Figure 6. Optical micrographs of dried gel samples cast onto glass from 0.1mg.mL DCM solution. Width of images = 250 μm. A = $PBThr_{26}$-$PBLG_{22}$, B = $PBThr_{50}$-$PBLG_{25}$, C = $PBThr_{20}$-$PLysBoc_{22}$, D = $PBThr_{46}$-$PLysBoc_{18}$.

The size and morphology of these networks varied from one polymer to another. The sizes of the fibres are in the region of 1-3 microns as measured from these photographs, though the values are not really reliable, as this is at the diffraction limit of optical microscopy. The copolymers which failed to induce gelation in any solvent also produced these networked structures when dried down. In Figure 6 a range of morphologies are shown. A and B show extended, dendritic features. C and D appear to have smaller fibres resulting in a porous appearance.

To circumvent the diffraction limit problem, environmental scanning electron microscopy (ESEM) was employed. The images obtained in the presence of H_2O vapour had very poor resolution, and the underlying structures were not clearly visible. We found that coating with gold and using standard SEM mode gave superior results (Figure 7).

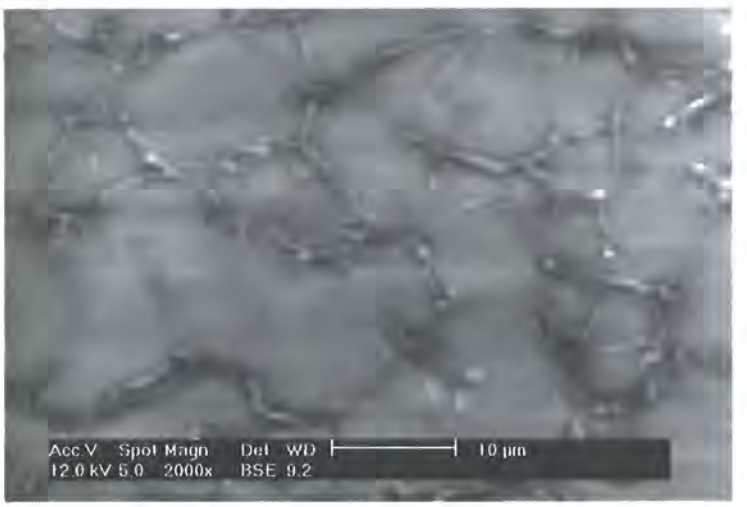

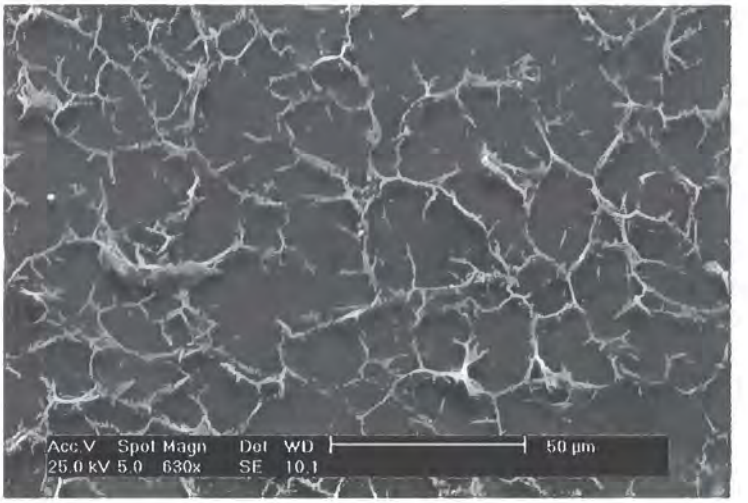

Figure 7. (E)SEM micrographs of $PBThr_{26}$-$PBLG_{22}$. Top in ESEM mode with H_2O vapour. Bottom high-vacuum SEM mode following gold coating

As in the optical images, a fibrous network is clearly present. It appears there are entanglement points where many fibres meet together, which are essential to retain the network rigidity. Although all the samples displayed a network structure, the morphology of these varied. $PBThr_{26}$-$PBLG_{22}$ shown in Figure 7 displays a highly branched, almost dendritic morphology. Significantly, increasing the size of the PBThr block to give $PBThr_{50}PBLG_{25}$ resulted in a different morphology, in Figure 8.

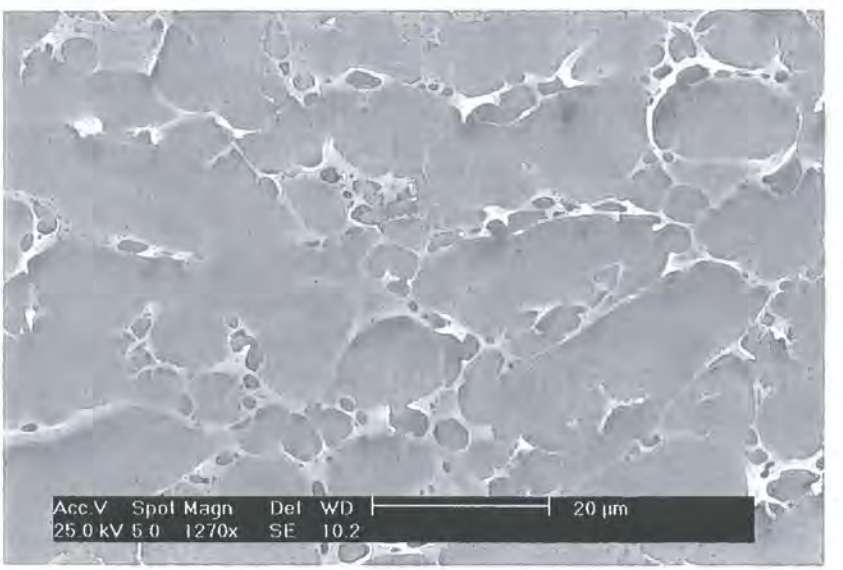

Figure 8. $PBThr_{50}$-$PBLG_{25}$

The structure comprises similar networked fibres. Surprisingly, along the fibres pores were visible. Shortening both blocks to $PBThr_{16}$-$PBLG_{16}$ (which did not give gelation) encouraged the porous morphology giving an appearance akin to the highly porous polyHIPE[44] cross linked-materials shown in Figure 9.

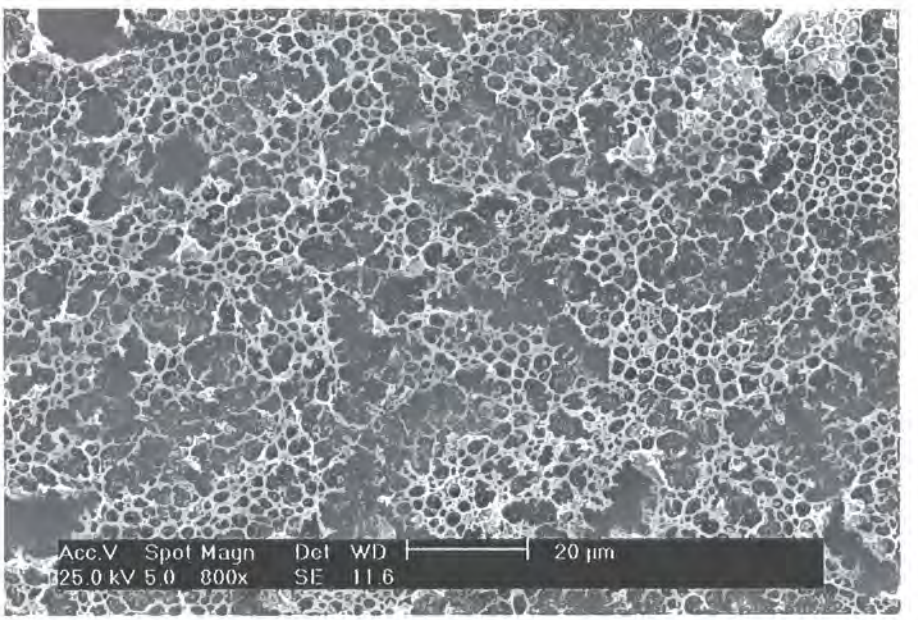

Figure 9. SEM showing porous structure obtained from $PBThr_{16}PLysBoc_{16}$

This morphology was not expected. Gel forming polymers tend to form long fibrous assemblies which entangle. In Figure 10, at higher magnification the structure still appears to be porous, rather than layered assemblies of fibres.

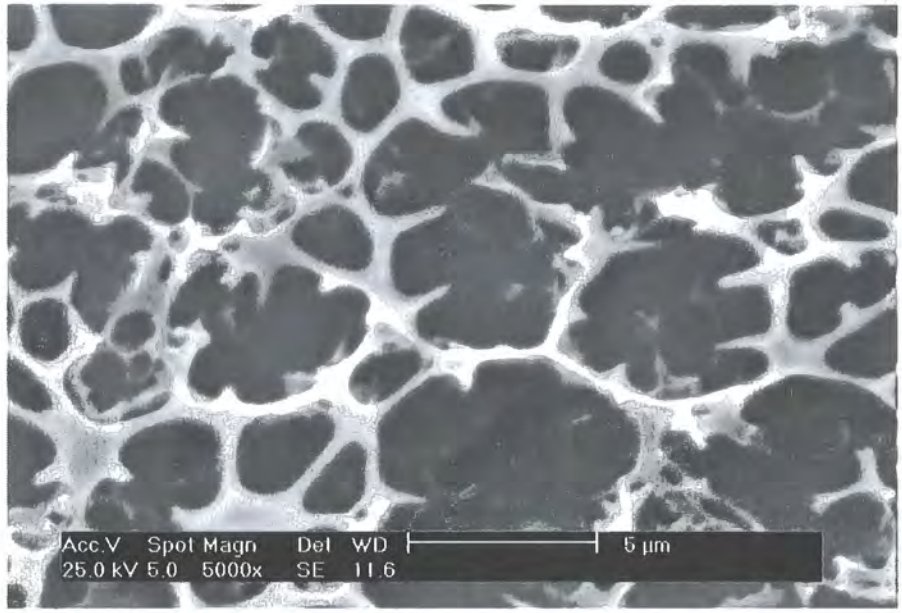

Figure 10. High magnification ESEM of $PBThr_{16}PLysBoc_{16}$

This structural phenomena was not unique to this one polymer. More examples are shown below (Figure 11).

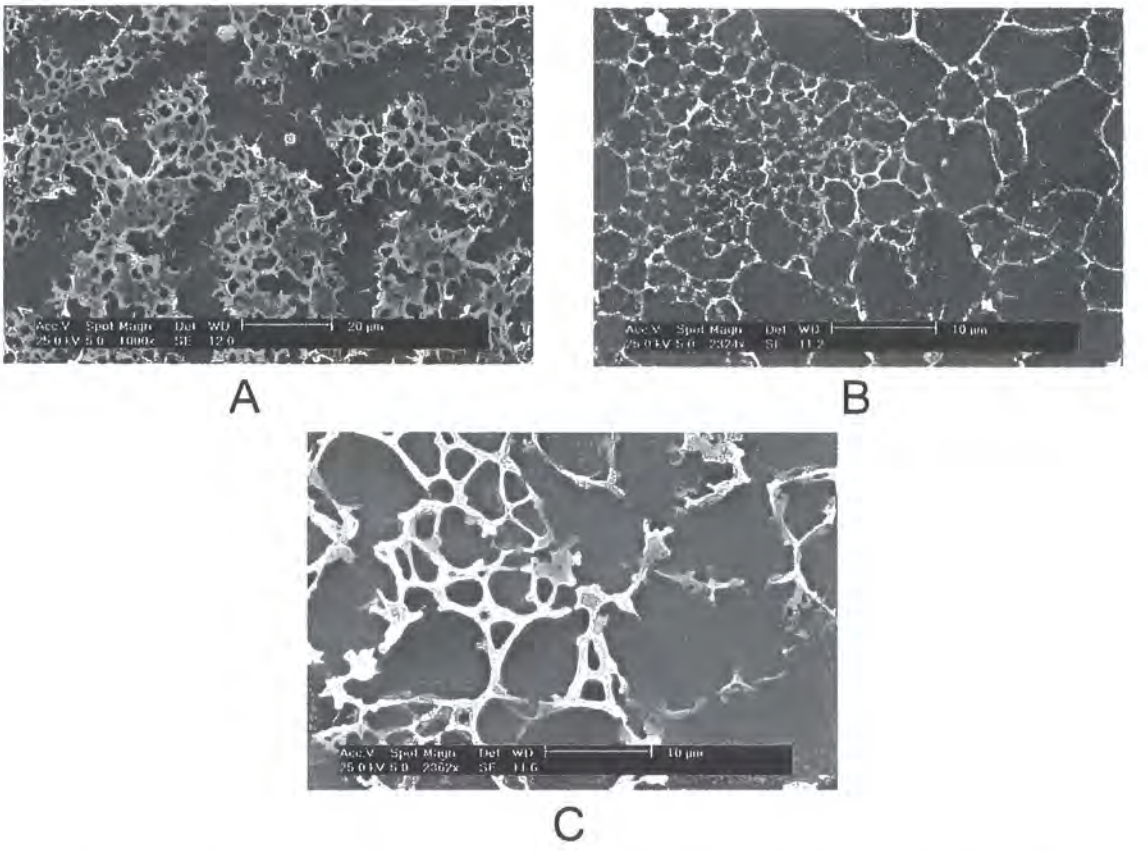

Figure 11. Examples of porous structures from drying down polymers. A = $PBThr_{46}PLysBoc_{18}$, B = $PBThr_{20}$-$PLysBoc_{46}$, C = $PBThr_{16}PBLG_{16}$

Both morphologies also appear for polymers containing PBocLys. $PBThr_{20}$-$PLysBoc_{22}$ in Figure 12.A appears to be porous, but closer examination (B), shows that it is overlaying fibres that give this appearance. The morphological features and average fibre sizes are summarised in Table 3.

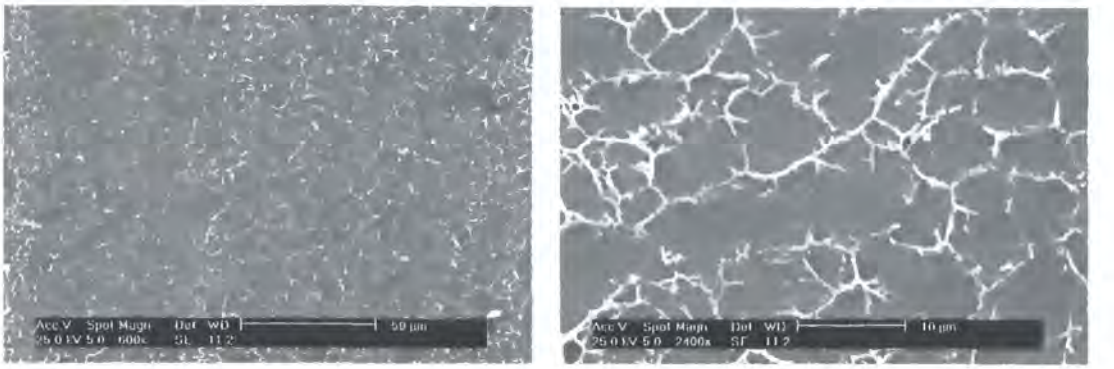

Figure 12. $PBThr_{20}$- $PLysBoc_{22}$. Picture A can be misinterpreted as having a porous morphology, but higher magnification resolves overlaying dendritic fibres.

Table 3. Summary of morphological characteristic of dried down gel samples determined by SEM.

Polymer	Ratio A:B[(a)]	Fibre width (μm)[(b)]	Morphology
$PBThr_{47}PBLG_{28}$	1.68	1.31	Dendritic network
$PBThr_{26}PBLG_{22}$	1.18	1.45	Dendritic network
$PBThr_{50}PBLG_{25}$	2	1.10	Network of porous fibres
$PBThr_{16}PBLG_{16}$	1	0.61	Porous
$PBThr_{16}PLysBoc_{19}$	0.84	0.58	Highly porous
$PBThr_{46}PLysBoc_{18}$	2.55	0.67	Porous. Large aggregates
$PBThr_{20}PLysBoc_{22}$	0.91	0.62	Dendritic network
$PBThr_{20}PLysBoc_{46}$	0.43	0.37	Highly porous

(a) $DP_{BThr}/DP_{2nd\ Block}$ (b) Average of 10 points from SEM images

Table 3 shows a relationship between the ratio of PBThr to the helical block and the average width of the fibres formed. The length ratio of one block to the other does not seem to influence the mean fibre width. The morphology appears to be independent of fibre size and the ratio of helix to sheet. Similar features were obtained from a series of castings of each sample, though the effect of concentration and

casting procedure was not investigated. Thus, this should be regarded as only an observation of the morphology rather than a critical study into the relationship between it and the composition of the constituent polymers.

The dried down gels were also examined by atomic force microscopy, AFM. This is not normally used for investigating structures so large, which requires a large area to be scanned increasing the chances of any features being damaged or affected by the AFM tip. It was however possible to visualise the points where individual fibres intersect. One of these is shown in Figure 13.

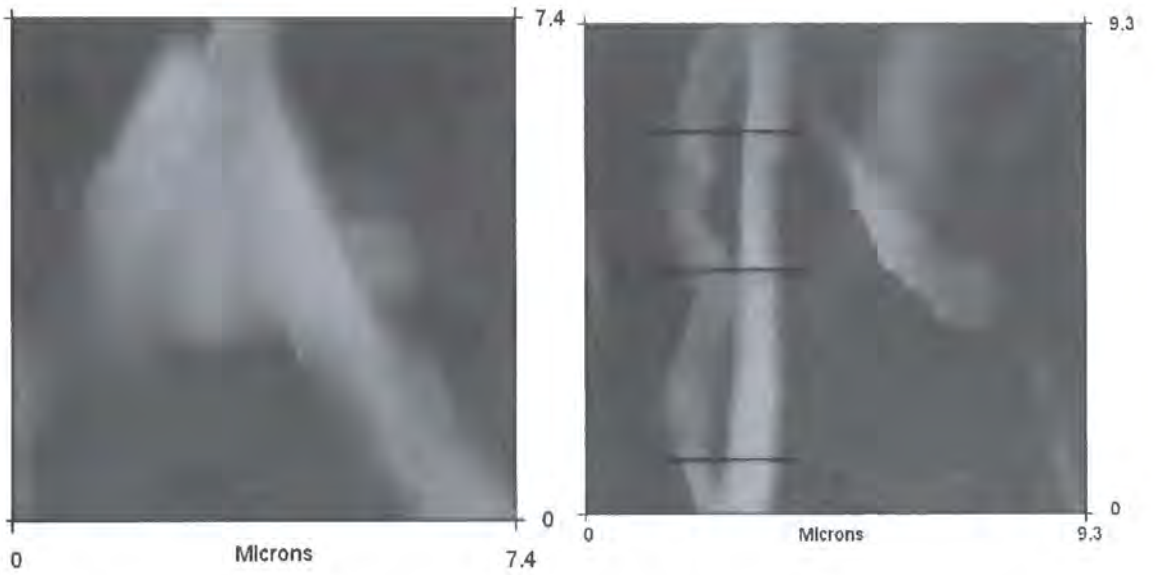

Figure 13. AFM Height image of dried down $PBThr_{47}$-$PBLG_{28}$. Left shows an entanglement point for three fibres. Right shows two different fibres side by side, with the appearance of some twisted character. Horizontal lines represent cross sections shown in Figure 14.

The width of these fibres is between 1.3 and 1.6 μm, in agreement with the values obtained by SEM, reported in Table 3. The fibres appear to have some twisted character to them. Using the image in Figure 13, right, it is possible to examine the height of individual fibres. Figure 14 shows three cross sections taken across both the fibres at three points. The two fibres have different sizes, but surprisingly, each individual fibre appears to have a constant height profile along its long axis.

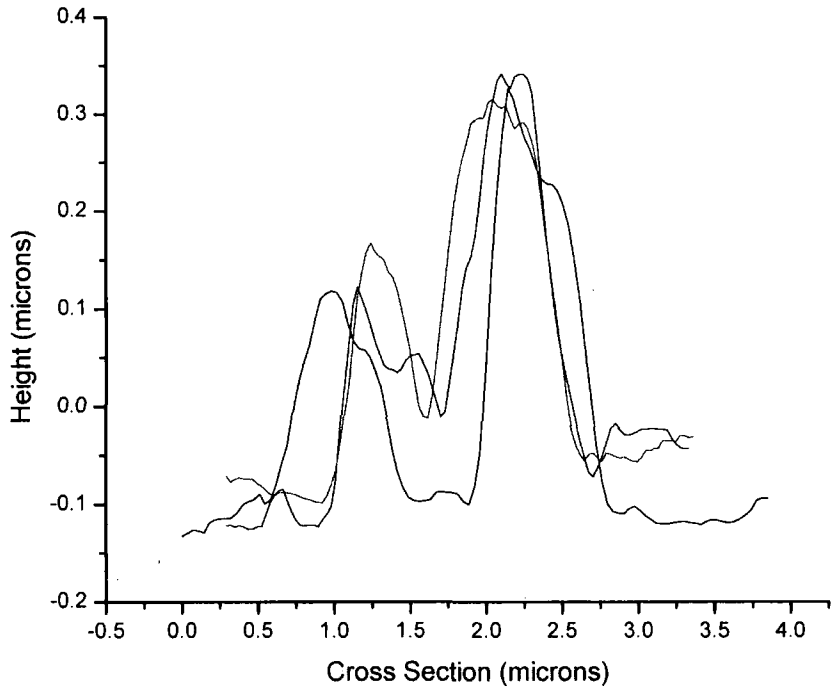

Figure 14. Height profiles of cross sections through fibre of $PBThr_{48}$-$PBLG_{28}$ taken from Figure 13 (right)

The larger fibre has a height roughly twice (300 nm) that of the smaller fibre (150 nm). This agrees well with the SEM observations that not all the fibres are of equal size. Individual fibres showed consistent heights over tens of microns but a range of heights can be seen between different fibres. A possible explanation is that the larger features could be assembled from smaller ones. By reducing the concentration of the solutions which were cast from 0.1 $mg.mL^{-1}$ to approximately 0.02 $mg.mL^{-1}$ it was possible to decrease the amount of entanglements and view the morphology of individual fibres. To our surprise the fibres formed micron-scale right handed helical aggregates. These structures are typically found on far smaller length scales and are composed of chiral building blocks. The helical fibres are over 20 microns in length which we believe to have not been seen previously on this scale.

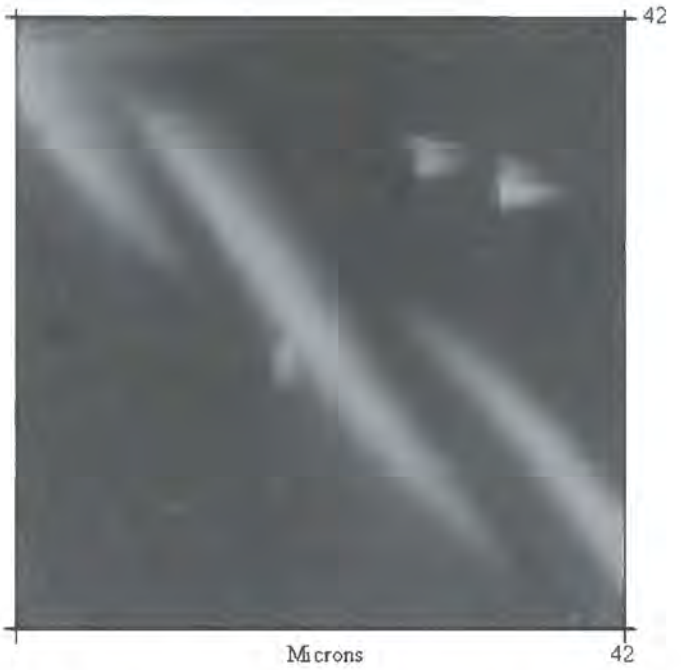

Figure 15. AFM height image of $PBThr_{48}PBLG_{28}$. Example of the twisted helical structures formed from dilute solution casting, 0.02mg.ml^{-1}.

From the evidence presented here, it would seem that the large structures which were visible in the optical and ESEM micrographs are constructed of smaller features. To explain these phenomena the structure of the block copolymers must be fully understood, particularly their secondary structures which are responsible for many self assembly processes.

5.3.1 BLOCK COPOLYPEPTIDE SECONDARY STRUCTURE

Infrared spectroscopy has been used for over 50 years to probe the structure of peptides owing to the subtle differences arising from the hydrogen bonding interactions in random coils, α-helices and β-sheets. PBLG has been investigated

extensively in reference to its well defined α-helical conformation in organic solvents. In general α-helices are more soluble than β-sheets, demonstrated well in the case of poly-L-alanine which can form both structures[45]. The most commonly investigated region of the infrared spectrum in this respect is the so-called amide I region (Table 4).

Table 4. Characteristic wavenumbers (cm^{-1}) of infrared bands associated with secondary structure motifs of homo-polypeptides

Band	α-Helix	β-Sheet	Disordered
Amide A	3293 (II)	3283 (⊥)	
Amide I	1650 (II)	1630 (⊥)	1656
		1685 (II)	
Amide II	1546 (⊥)	1530 (II)	1535
Amide V	615 (⊥)	700 (⊥)	650

(II) Indicates a parallel, and (⊥) a perpendicular stretch.

The amide I regions of the homopolymers in DCM are shown in Figure 16. The amide I peak at 1652 cm^{-1} for PBLG and PLysBoc is characteristic of their expected α-helices. PBThr also has a peak in a similar region at 1647 cm^{-1}. It is unlikely that a homopolymer containing L-threonine would form a helix, as this amino acid is predicted[46] to be helix breaking and β-sheets promoting. A peak in this region could also be interpreted as being a random coil. Upon changing to the solid state there is no difference in the spectrum for PBLG which retains its helical structure, and displays the same peak at 1653 cm^{-1}. PBThr conversely shows a shift to lower wavenumber relative to what is seen in solution. The amide I peak is found at 1630 cm^{-1}, which is characteristic of a β-sheet.

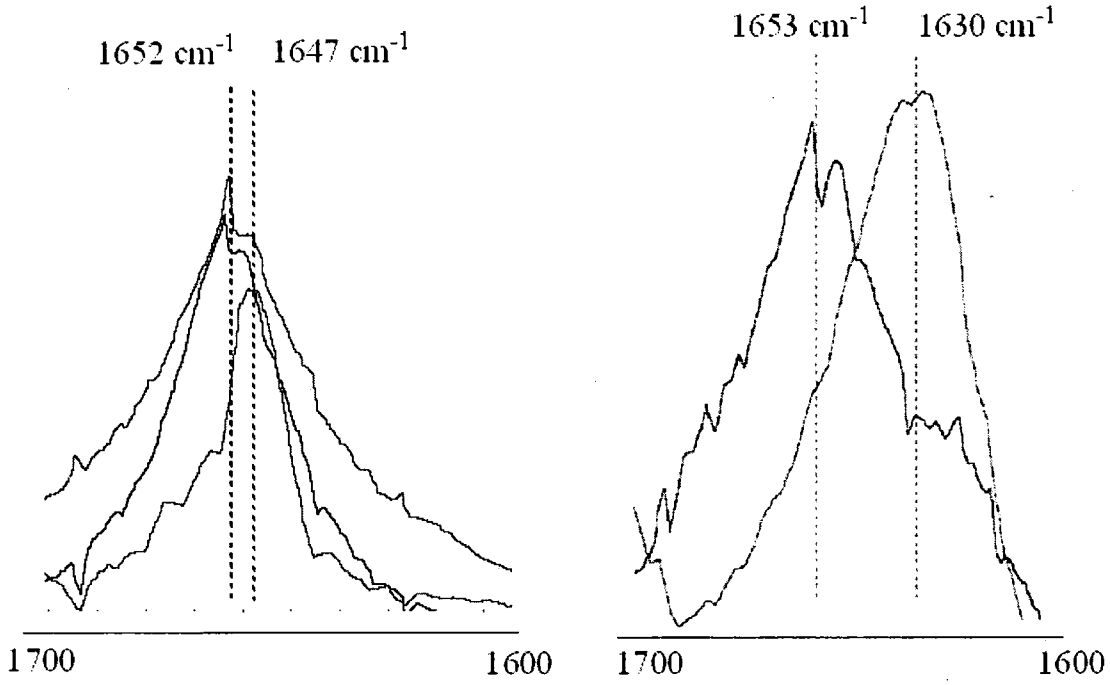

Figure 16. Infrared spectra of homopolymers. Left: (in DCM) green = PLysBoc; blue = PBLG; red = PBThr. Right: (solid state) blue = PBLG; red = PBThr.

It is now possible to explore the structure of the block copolymers and compare them to their parent homopolymers. This was undertaken at dilute concentrations, well below that at which gelation occurs for each sample. Figure 17 shows the amide I region for $PBThr_{26}PBLG_{22}$ in DCM. The peak at 1653 cm^{-1} is identical to that observed in the homo PBLG and can be assigned as its α-helical amide stretch. A second peak at lower wavenumber is also present (1627 cm^{-1}) indicative of a β-sheet. It was not possible to analyse the amide II region (which gives information about β-sheets) due to aromatic vibrations from the protecting groups.

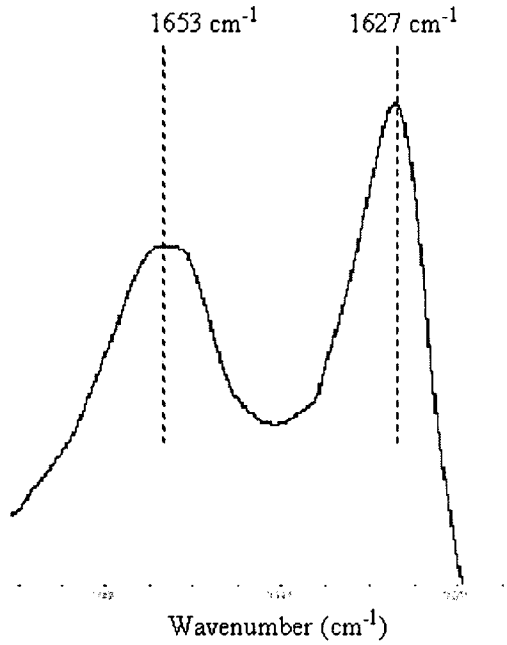

Figure 17. Infrared spectrum of $PBThr_{26}PBLG_{22}$, obtained in DCM.

The same peaks were present in all the block co-polymers, including those containing PLysBoc. Of the three amino acids used here only L-threonine has any tendency to form sheets. Accordingly the peak at 1627 cm^{-1} is assigned as PBThr in the β-sheet conformation, which is significantly different from the random coil seen in solution for the homopolymer, but in agreement with its solid state conformation.

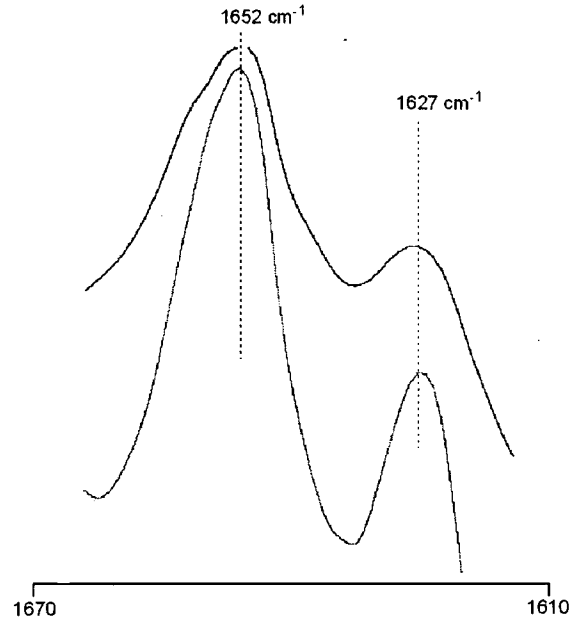

Figure 18. IR spectra of $PBThr_{20}PLysBoc_{46}$ in benzyl alcohol (red) and methanol (blue).

As mentioned earlier, it is normally required for a polymeric gelation system to contain at least one block which is incompatible with the solvent. The parent homopolymers used here clearly do not obey this rule. The IR results show a change in secondary structure of the PBThr block when going from homopolymer (random coil) to block-copolymer (β-sheet) giving a peak equivalent to what is seen in the solid state. The conclusion which can be drawn from this is that, when the PBThr is incorporated with a helix-forming block, it assumes a more rigid β-sheet conformation, which is far less soluble than the coil adopted by the homopolymer. Stabilisation of β-sheet peptides by conjugation to PEG has been observed[47]. This provides the requisite feature of amphiphilicity thus explaining the onset of gelation, if not the origin of this structural reorganisation. Upon changing the solvent from DCM to benzyl alcohol, or addition of methanol, systems in which no gelation was seen, there was little change in the IR spectra (Figure 18) suggesting that both secondary structures remained though a quantitative analysis of the sheet and helix

content was not possible. Addition of methanol to PBLG or PLysBoc homopolypeptides did not produce any changes in the amide I peak. (Data not shown)

5.3.2 MECHANISM OF SELF-ASSEMBLY

Considering the evidence shown so far, it is apparent that a self-assembly process is occurring, resulting in the long fibres which support the gel solution, as opposed to micellisation which may be expected for amphiphilic block copolymers. The process must also involve hydrogen bonding, as shown by the gel-disrupting effect of methanol and TFA. To probe the 3 dimensional structures of the gels, wide angle X-ray scattering (WAXS) was utilised. Samples of the dried-down gels revealed diffraction patterns, indicating that ordered structures are present. An example is shown in Figure 19.

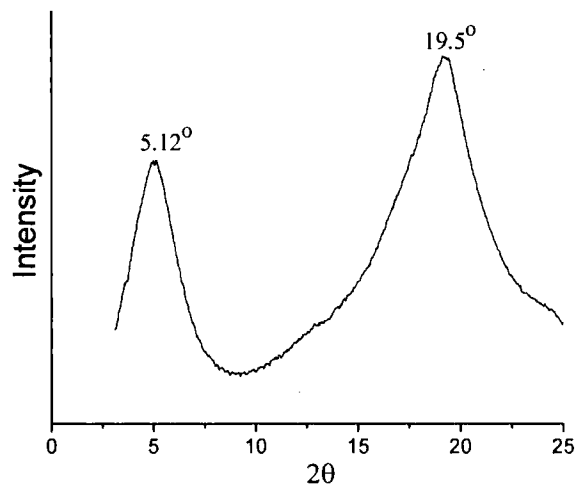

Figure 19. WAXS pattern for $PBThr_{46}PlysBoc_{18}$.

Table 5. Results from WAXS investigation of dried down gels

Sample	2θ	d spacing	Assignment
$PBThr_{50}$-$PBLG_{25}$	19.5	4.55 Å	Anti-parallel β-sheet
	5.12	16.0 Å	Inter-sheet spacing
$PBThr_{46}PLysBoc_{18}$	19.5	4.55 Å	Anti-parallel β-sheet
	5.12	16.9 Å	Inter-sheet spacing

$PBThr_{50}$-$PBLG_{25}$ showed a peak at $2\theta = 19.5^{\circ}$, which corresponds to a d-spacing of 4.55 Å. This has been observed as the interchain separation for the antiparallel β-sheet of poly(L-alanylglycine) in the orthorhombic unit cell[48]. Identical patterns were seen in the PLysBoc-containing polymer, showing that the secondary structure of the PBThr is maintained by two different helical co-blocks. A further reflection was seen corresponding to a d spacing of 15 Å. In the nano-scale assembly of a PEG-block-β-strand peptide-block-PEG a d spacing of 12.7 Å was attributed to a lamella type ordering[36]. A similar mechanism can be proposed for this system, but with a larger separation between lamella due to the sterically large benzyl protected side chains. This would result in the growth of a ribbon in the direction of the lamella stacking. A schematic representation of this is shown in Figure 20.

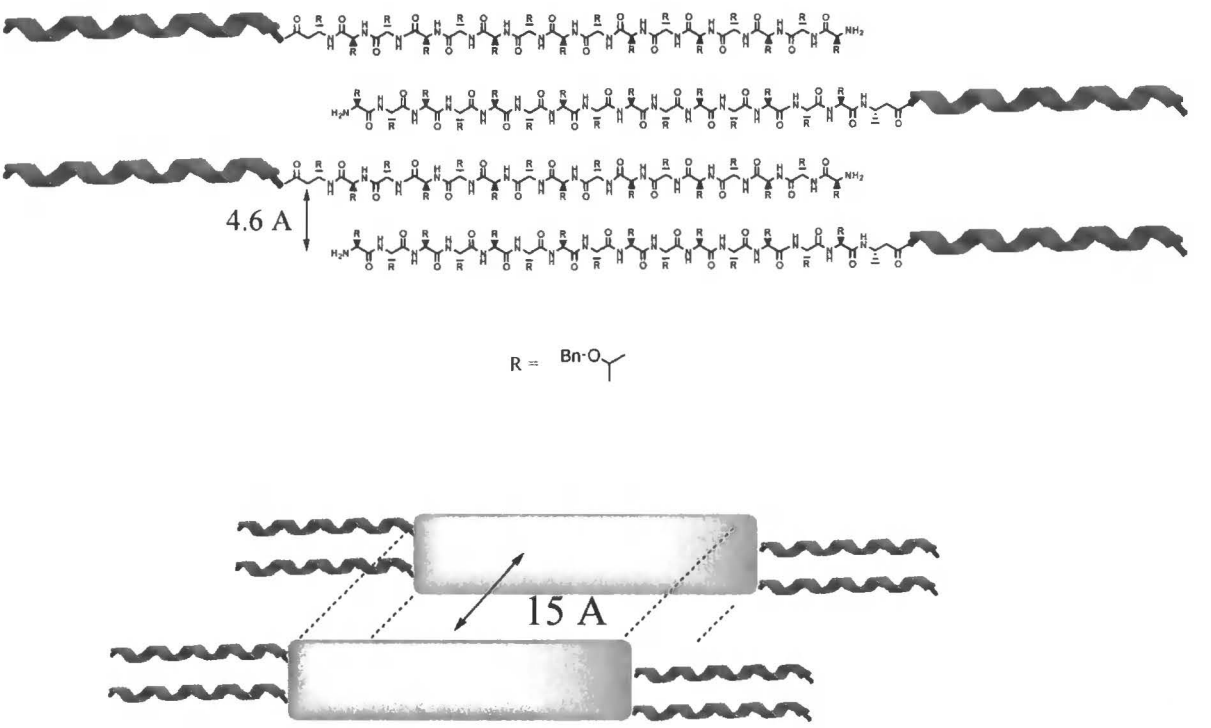

Figure 20. Proposed mode of self assembly for the case of $PBThr_{16}PBLG_{16}$. Top:. antiparallel arrangement of sheet segments with an interchain spacing of 4.6 Å as determined by WAXS. Below: lamella ordering of sheets, separated by 15 Å.

There are other examples of similar structures in the literature, but they all contain a random coil polymeric block, such as PEG as the 'insulating' outer layer. In this case a rigid rod protrudes from stacked lamella, which has not been previously described. The schematic shown in Figure 20 suggests that the PBLG rods are aligned in an ordered, parallel fashion. However, the most favourable alignment of PBLG (due to the dipole moment) is antiparallel, which may also contribute to the increased separation between lamellae. SAXS investigations did not reveal any further information, probably reflecting the relatively wide distribution of chain lengths. This does not affect the WAXS profile as it can only see inter-chain spacing. A SAXS reflection would be necessary to confirm unambiguously this structure.

This mechanism does not explain why such large, micron sized features are seen. There is clearly at least one higher level of assembly. Twisting induced by the

chiral nature of the constituent units is normally used to explain why fibres (and gels) are formed, as opposed to uncontrolled aggregation, and precipitation[49]. Indeed, helical superstructures were seen which raises the possibility that a series of hierarchically ordered structures may be contributing to the fibre formation, which have been previously described and are shown in Figure 21.

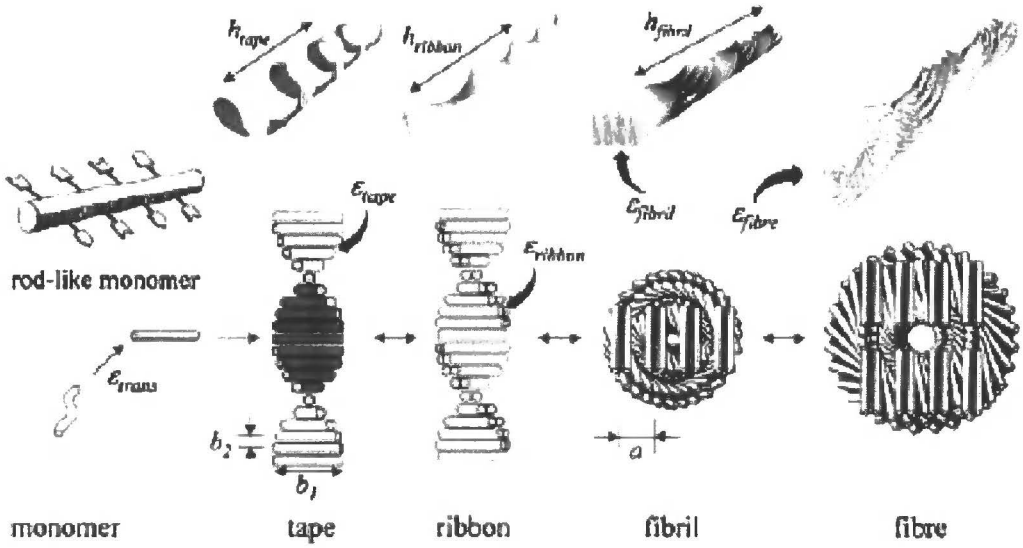

Figure 21. Assembly of rod-like monomeric units into hierarchally order structures[49].

If this model was used to describe the system presented here, then the rod-like monomer would be the sheet-assembled unit shown in figure 20. Twist would be induced by the chiral nature of the amino acids, giving a self assembled tape. Associated to give the large ribbons, fibrils and fibres would then follow giving the macro-scale features which have been observed. It should be noted that this is only a speculated mechanism and more data is required to designate the process occurring, but it does help explain the large, micron sized twists. If this mechanism is correct, then the different morphologies seen in the ESEM micrographs will be caused by the entanglement of the fibres and the different morphologies perhaps representative of the drying down process.

5.4 CONCLUSIONS

Here we have described for the first time the self assembly of rod-sheet block copolypeptides into (sub)micron sized fibres. The assembly is driven by alignment of β-sheets into lamellae, which can then stack to give a long axis. Uniquely, these structures have helical rods protruding from the ribbons, in comparison to the known sheet-coil polymers which have a random coil insulating layer. These ribbons then assemble to give higher order structures resulting in the large fibres which have been observed by microscopy. These fibres vary in width and length within a sample, probably reflecting the non-monodisperse nature of the constituent diblock copolypeptides. It was possible to view the helical assemblies which form the fibres by SEM. Analysis of the secondary structures of the homopolymers by infrared spectroscopy showed that, upon conjugation to a helical block, poly(benzyl-L-threonine) assumes its solid state β-sheet structure, as opposed to the random coil seen in solution. This then acts as a structure-directing rigid unit, allowing the molecule to assemble in a lamella fashion, with an insulating layer of helical poly(peptide). In order to confirm unambiguously the structures postulated here, SAXS data are required. A mono-disperse polypeptide may be required for this, which could be obtained by solid phase methods, as the peptides involved are all relatively short. As a consequence of this fibrous network formation, solutions of the block

copolypeptides form thermoreversible gels, which are disrupted upon addition of hydrogen bond-breaking solvents including methanol and TFA. The effect of molecular weight and composition was investigated. This system may prove to be a useful model for polypeptide gelation systems due to the highly soluble nature of both blocks, facilitating the synthesis.

5.5 EXPERIMENTAL

DCM (>99%), $CHCl_3$ (>99%) and benzyl alcohol (>98%) were purchased from Fischer Scientific UK. Methanol (HPLC grade) and trifluoroacetic acid (>98%) were purchased from Aldrich. Polymers were synthesised by the ring opening polymerisation of the appropriate NCA, as described in Chapter 4. Infrared spectra were collected using a liquid cell with KBr windows, path length = 0.1mm or as a KBr disc (5 wt %) on a Nicolet Nexus FT-IR. Optical, AFM and (E)SEM microscopy samples were prepared by dropping 50 μL of a 0.1 $mg.mL^{-1}$ solution of the polymer onto an appropriate surface and drying in the air overnight. AFM samples were prepared on freshly cleaved mica. ESEM samples were prepared on borosilicate glass slides, and coated with gold by vapour deposition where necessary. (E)SEM analyses were conducted on a Phillips FEI XL30 operating between 20-25 kV. AFM imaging was carried out in tapping mode on a Multimode Nanoscope IV (Digital Instruments, Santa Barbara, CA, USA), using etched silicon probes (Budget Sensors, BS-TAP300), with a spring constant, k = 40 N/m (Windsor Scientific, Slough, Berkshire, UK). Samples for WAXS and SAXS were prepared by taking a 6 wt% gelated solution of the polymer in DCM, and drying under a stream of nitrogen overnight. WAXS data were obtained on a Bruker D8, operating at 40kV using a copper-alpha source with a wavelength of 1.54 Å. SAXS data were collected on a Bruker Nanostar fitted with

Kratky SAXS camera operating at 40kV using a copper-alpha source with a wavelength of 1.54 Å. Digital photographs were taken using a Kodak DX 6340 at 3.1 megapixels. Molecular graphics images were created using Cambridgesoft, Chem 3D.

5.5 BIBLIOGRAPHIC REFERENCES

(1) Lehn, J.-M. *PNAS* **2002**, *99*, 4763-4768.

(2) Lee, H.-F.; Sheu, H.-S.; Jeng, U.-S.; Huang, C.-F.; Chang, F. C. *Macromolecules* **2005**, *38*, 6551-6558.

(3) Klok, H.-A.; Lecommandoux, S. *Adv. Mater.* **2001**, *13*, 1217-1229.

(4) Tadmor, R.; Khalfin, R. L.; Cohen, Y. *Langmuir* **2002**, *18*, 7146-7150.

(5) Doty, P.; Bradbury, J. H.; Holtzer, A. M. *J. Am. Chem. Soc* **1956**, *78*, 947-954.

(6) Yu, S. M.; Conticello, V. P.; Zhang, G.; Kayser, C.; Fournier, M. J.; Mason, T. L.; Tirrell, D. A. *Science* **1997**, *389*, 167-170.

(7) Lee, M.; Cho, B.-K.; Zin, W.-C. *Chem. Rev.* **2001**, *101*, 3869-3892.

(8) Friend, R. H. *Pure Appl. Chem.* **2001**, *73*, 425-430.

(9) Schenning, A. P. H. J.; Meijer, E. W. *Chem. Commun.* **2005**, 3245-3258.

(10) Hoeben, F. J. M.; Jonkheihm, P.; Meijer, E. W.; Schenning, A. P. H. J. *Chem. Rev.* **2005**, *105*, 1491-1546.

(11) Wang, H.; Wang, H. H.; Urban, V. S.; Littrell, K. C.; Thiyagarajan, P.; Yu, L. *J. Am. Chem. Soc* **2000**, *122*, 6855-6861.

(12) Hulvat, J. F.; Sofos, M.; Tajima, K.; Stupp, S. I. *J. Am. Chem. Soc.* **2005**, *127*, 366-372.

(13) Liu, J.; Sheina, E.; Kowalewski, T.; McCullough, R. D. *Angew. Chem. Int. Ed* **2002**, *41*, 329-332.

(14) Stupp, S. I.; Lebonheur, V.; Walker, K.; Li, L. S.; Huggins, K. E.; Keser, M.; Amstutz, A. *Science* **1997**, *276*, 384.

(15) Ray, S.; Das, A. K.; Banerjee, A. *Chem. Commun.* **2006**, 2816-2818.

(16) Carretti, E.; Dei, L.; Baglioni, P.; Weiss, R. G. *J. Am. Chem. Soc* **2003**, *125*, 5121-5129.

(17) George, S. J.; Ajayaghosh, A. *Chem. Eur. J* **2005**, *11*, 3217-3227.

(18) Li, Y.; Narain, R.; Ma, Y.; Lewis, A. L.; Armes, S. P. *Chem. Commun.* **2004**, 2746-2747.

(19) Rodriguez-Hernandez, J.; Checot, F.; Gnanou, Y.; Lecommandoux, S. *Prog. Polym. Sci.* **2005**, *30*, 691-724.

(20) Suzuki, M.; Owa, S.; Shirai, H.; Hanabusa, K. *Macromol. Rapid Commun.* **2005**, *26*, 803-807.

(21) MacGregor, E. A.; Green, C. T. *Polymers in Nature*; John Wiley and Sons: USA, 1980.

(22) Mart, R. J.; Osborne, R. D.; Stevens, M. M.; Ulijn, R. V. *Soft Matter* **2006**, *2*, 822-835.

(23) Vandermeulen, G. W. M.; Tziatzios, C.; Duncan, R.; Klok, H.-A. *Macromolecules* **2005**, *38*, 761-769.

(24) Ambrosi, M.; Cameron, N. R.; Davis, B. G. *Org. Biomol. Chem.* **2005**, *3*, 1593-1608.

(25) Schneider, J. P.; Pochan, D.; Ozbas, B.; Rajagopal, K.; Pakstis, L.; Kretsinger, J. *J. Am. Chem. Soc.* **2002**, *124*, 15030-15037.

(26) Gular, M. O.; Hsu, L.; Soukasene, S.; Harrington, D. A.; Hulvat, J. F.; Stupp, S. I. *Biomacromolecules* **2006**, *7*, 1855-1863.

(27) Kelly, J. W. *Curr. Opin. Struct. Biol* **1998**, *8*, 101-106.

(28) Petka, W.; Harden, J. L.; McGrath, K. P.; Wirtz, D.; Tirrell, D. A. *Science* **1998**, *281*, 389-392.

(29) Landschultz, W. H.; Johnson, P. F.; McKnight, S. L. *Science* **1988**, *240*, 1759-1764.

(30) Ayres, L.; Vos, M. R. J.; Adams, P. J. H. M.; Shklyarevskiy, I. O.; van Hest, J. C. M. *Macromolecules* **2003**, *36*, 5967-5973.

(31) Stanley, C. E.; Clarke, N.; Anderson, K. M.; Elder, J. A.; Lenthall, J. T.; Steed, J. W. *Chem. Commun.* **2006**, 3199-3201.

(32) Goeden-Wood, N. L.; Keasling, J. D.; Muller, S. J. *Macromolecules* **2003**, *36*, 2932-2938.

(33) Aggeli, A.; Bell, M.; Boden, N.; Keen, J. N.; Knowles, P. F.; McCleish, T. C. B.; Pitkeathly, M.; Radford, S. E. *Nature* **1997**, *386*, 259-262.

(34) Aggeli, A.; Bell, M.; Boden, N.; Carrick, L.; Strong, A. E. *Angew. Chem. Int. Ed.* **2003**, *42*, 5603-5606.

(35) Rathore, O.; Sogah, D. Y. *J. Am. Chem. Soc.* **2001**, *123*, 5231-5239.

(36) Rosler, A.; Klok, H.-A.; Hamley, I. W.; Castelletto, V.; Mykhaylyk, O. O. *Biomacromolecules* **2003**, *4*, 859-863.

(37) Hamley, I. W.; Ansari, I. A.; Castelletto, V.; Nuhn, H.; Rosler, A.; Klok, H.-A. *Biomacromolecules* **2005**, *6*, 1310-1315.

(38) Smeenk, J. M.; Otten, M. B. J.; Thies, J.; Tirrell, D. A.; Stunnenberg, H. G.; van Hest, J. C. M. *Angew. Chem. Int. Ed.* **2005**, *44*, 1968-1971.

(39) Deming, T. J. *Nature* **1997**, *390*, 386-389.

(40) Nowak, A. P.; Breedveld, V.; Pakstis, L.; Ozbas, B.; Pine, D. J.; Pochan, D.; Deming, T. J. *Nature* **2003**, *417*, 424-426.

(41) Kim, K. T.; Park, C.; Vandermeulen, G. W. M.; Rider, D. A.; Kim, C.; Winnik, M. A.; Manners, I. *Angew. Chem. Int. Ed* **2005**, *44*, 7964-7968.

(42) Kim, K. T.; Park, C.; Kim, C.; Winnik, M. A.; Manners, I. *Chem. Commun.* **2006**, 1372-1374.

(43) Papadopoulos, P.; Floudas, G.; Schnell, I.; Aliferis, T.; Iatrou, H.; Hadjichristidis, N. *Biomacromolecules* **2005**, *6*, 2352-2361.

(44) Cameron, N. R. *Polymer* **2005**, *46*, 1439-1449.

(45) Kricheldorf, H. R.; von Lossow, C.; Schwarz, G. *Macromol. Chem. Phys.* **2004**, *205*, 918-924.

(46) Barrett, G. C.; Elmore, D. T. *Amino Acids and Peptides*; 1st ed.; Cambridge University Press: Cambridge, 1998.

(47) Hamley, I. W.; Ansari, I. A.; Castelletto, V. *Biomacromolecules* **2005**, *6*, 1310-1315.

(48) Panich, A.; Matsuki, K.; Cantor, E. J.; Cooper, S. J.; Atkins, E. D. T.; Fournier, M. J.; Mason, T. L.; Tirrell, D. A. *Macromolecules* **1997**, *30*, 42-49.

(49) Aggeli, A.; Nyrkova, I. A.; Bell, M.; Harding, R.; Carrick, L.; B., M. T. C.; Semenov, A. N.; Boden, N. *Proc. Nat. Acad. Sci.* **2001**, *98*, 11857-11862.

CHAPTER 6

INHIBITION OF ICE CRYSTAL RECRYSTALLISATION BY POLYMERIC ADDITIVES

6.1 INTRODUCTION

Since antifreeze glycoproteins were discovered in the blood serum of Antarctic fish[1] they have attracted interest as additives in cryopreservation[2,3], cryomedicine[4], cell membrane diffusion moderators[5] and even in frozen foods[6,7]. Their three main effects are: non-colligative freezing point depression; dynamic ice shaping; and recrystallisation inhibition. The first two effects are closely related to the precise structure of the AFGP in solution and the carbohydrate moiety. A thorough investigation by Nishimura *et al*[8] concluded that the amino acid sequence and the presence of an *N*-acylated carbohydrate was essential to maintain the antifreeze activity, and related this to the secondary structures present as judged by CD spectroscopy. However, they did not consider recrystallisation inhibition properties as a marker of antifreeze activity. Consequently there has not been a complete study on the structural features required for this property. Briefly, recrystallisation inhibition is the effect of AFGPs (and related compounds) whereby the rate of growth of ice crystals, at subzero temperatures, is retarded or stopped. Without the AFGPs the larger ice crystals grow at the expense of smaller ones, resulting in a larger mean crystal size, shown in Figure 1.

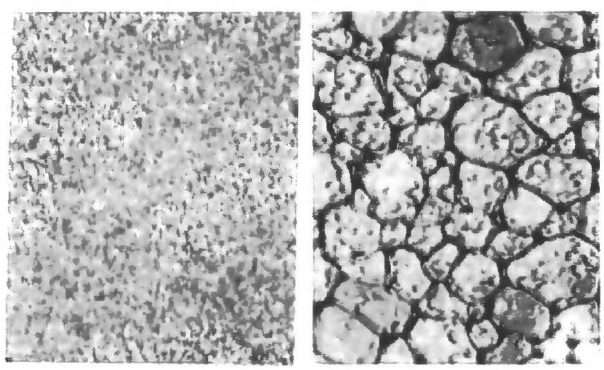

Figure 1. Micrographs of ice wafers with (left) and without (right) AFGP. The photo on the left clearly shows smaller ice crystals. Scales are identical in both images. (500μm width)

The most extensive work in this area has been conducted by the group of Robert Ben. Their first generation AFGP mimics showed some RI activity despite significant structural changes from native AFGP[9-11]. Firstly, the disaccharide linked to threonine was replaced with a monosaccharide, galactose, linked to a lysine residue, and the two alanines were substituted by glycine (Figure 2).

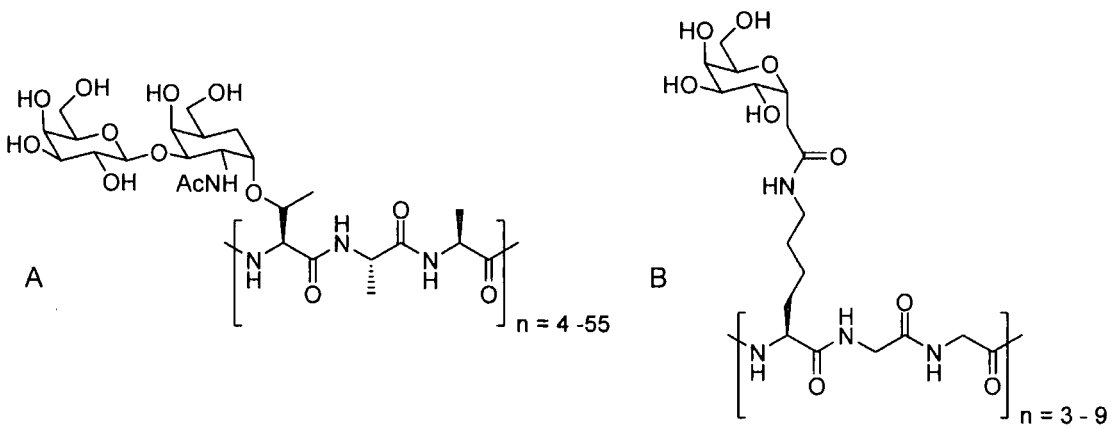

Figure 2. Tripeptide repeat units of A) native AFGP; B) first generation RI inhibitor of Ben *et al*[9].

These derivatives were only weekly active, approximately 80 X less so than AFGP 8, which is the least active of all the native AFGPs. Interestingly, they only showed weak dynamic ice shaping and thermal hysteresis effects, showing that it is possible to isolate the individual properties from one another. By exchanging the native *O*-glycosidic bond for a *C*- linkage, the stability of the materials to enzymatic and chemical degradation is improved[12]. The importance of the distance between the carbohydrate moiety and the peptide backbone was also probed by a second generation of RI inhibitors[13] (Figure 3). The shortest distance, of 2 CH_2 groups, gave the strongest RI activity, while 3 and 4 CH_2 groups produced a sharp decrease similar to the G1 peptides described above.

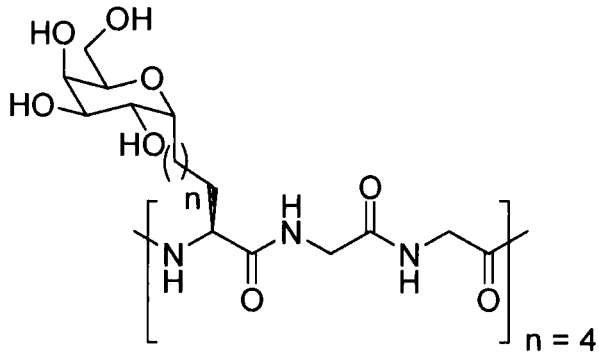

Figure 3. Second generation RI peptides with variable separation between backbone and carbohydrate

Perhaps the most remarkable, and only other example of an RI inhibitor is the structurally simple poly(vinyl alcohol), PVA. It does not possess either the polypeptide backbone or the carbohydrate moiety which conventional thought would suggest is essential for RI activity. In fact, PVA with a molecular weight of ~80 000 Da was as effective an RI inhibitor as AFGP 8 at equal molar concentrations[14], (This represents a 30x increase in mass concentration). Later studies[15,16] showed that PVA inhibited the same crystal faces, {1 0 1}, as the native AFGPs resulting in the appearance of pyramidal faces, previously only associated with AFGPs[17]. A very weak, but definite, thermal hysteresis of 0.037 K was also present. Capping of the hydroxyl groups reduced the RI and thermal hysteresis activity, as was seen with native AFGP. The most remarkable feature is PVA's lack of a rigid secondary structure, which is thought to be essential if a sufficiently hydrohobic face is to be presented following adsorption onto the ice crystal. Another class of poly-ol has recently been reported to influence the growth of ice. Poly(tartar amides)[18], Figure 4, which contain the rigid amide bonds found in peptides and multiple –OH functionalities, were shown to inhibit the growth of hexagonal ice by WAXS, and to alter the freezing process by DSC compared to water alone. No thermal hysteresis or quantitative RI assays were undertaken, preventing comparison to the afore-

mentioned systems. PEG-block-poly((hydroxyethyl)ethylene) can also influence the growth of hexagonal ice, and displays recrystallisation inhibition[19].

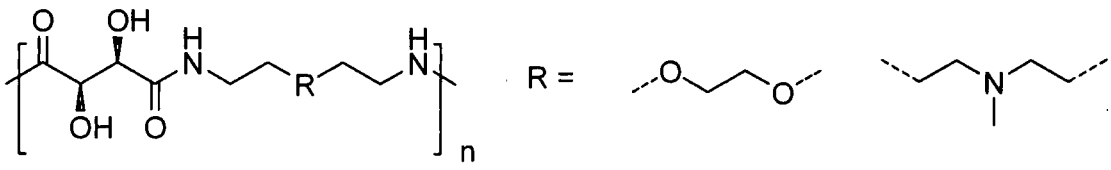

Figure 4. Poly(tartar amides) used as AFGP mimics. Mw ~ 7000 g.mol^{-1}

AFPs should also be mentioned briefly. Antifreeze peptides that display strong RI behaviour have been found in both nature and designed[20]. They all contain an ice binding hydrophilic face and a hydrophobic face which makes it energetically unfavourable for the addition of further water molecules. Modifications to remove the α-helicity from winter flounder AFP resulted in a loss of antifreeze activity[21], highlighting their relationship between secondary structure and activity for AFPs. Also, some of the proteins which display strong RI effects, do so without a significant thermal hysteresis gap[22]. AFPs contain various functional groups including carbohydrates, alcohols and amines, whereas AFGPs only contain OH (carbohydrate) groups. The common feature of AFPs is a well defined secondary structure, compared to AFGP analogues which are largely unstructured.

In summary, the structural features required for RI inhibition for both native AFGPs and their derivatives, and how this relates to AFPs are not yet known.

6.2 RESULTS AND DISCUSSION

To investigate which structural features are essential for recrystallisation inhibition by polymeric materials, a series of stepwise structural simplifications of native AFGPs were undertaken and the activity of the resulting compounds assayed. The polymers used are summarised below.

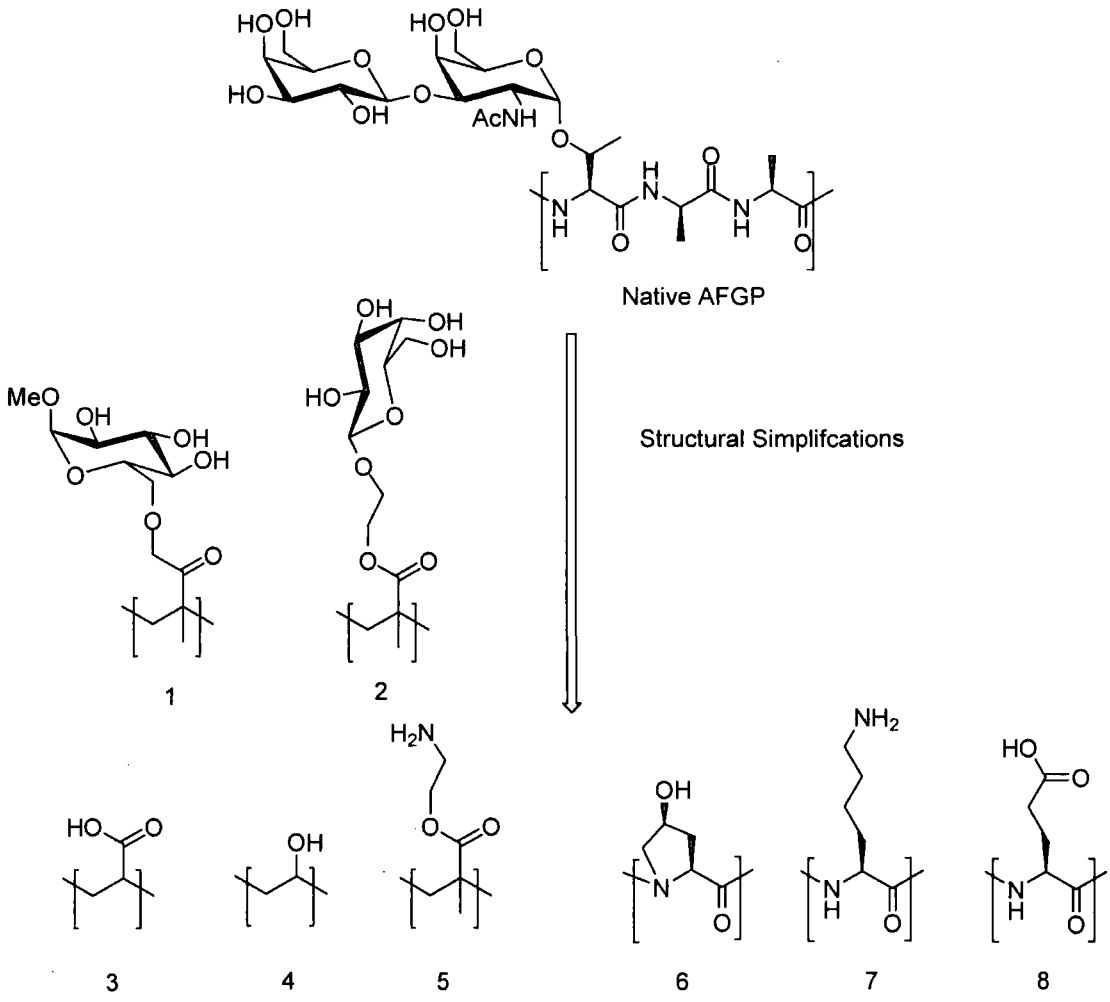

Figure 5. Summary of the polymers which are evaluated for recrystallisation inhibition in this section. 1) poly(methyl-6*O*-methacryloyl-α-D-glucopyranoside; 2) poly((β-D-galactosyloxy)ethyl methacrylate); 3) poly(acrylic acid); 4) poly(vinyl alcohol); 5) poly(ethylamino-methacrylate); 6) poly(hydroxyl-L-proline); 7) poly(L-lysine); 8) poly(L-glutamic acid)

The first tests undertaken were to establish the viability of using the splat test[23], to assess recrystallisation inhibition. This involves generating a polycrystalline wafer of an aqueous solution of the polymer being examined, by dropping 10 μL of the solution onto an aluminium sheet cooled with dry ice. The samples were allowed to anneal at -6°C for 30 minutes, before being photographed between crossed polarisers. The micrographs were examined to find the single largest crystal axis in any direction and recorded. The average largest grain size (LGS, μm) was calculated from 3 individual assays. Phosphate buffered saline was used as the solvent in all cases, so this is the null result, and as it was known from the literature that PVA strongly inhibits ice recrystallisation[14], it was used as the positive control

Table 1. Mean largest grain size measurements of PBS and PVA (Mw 85-146kDa), 5mg.mL^{-1}

	LGS 1	LGS 2	LGS 3	MLGS	½ Range
PBS	272.7	268.3	254.3	265.1	9.6
PVA	55.0	48.7	54.4	52.7	3.5

The deviation in the observed grain lengths were less than 10% in both cases. The image in Figure 6 clearly demonstrates the reduction in grain size associated with recrystallisation inhibition in the presence of PVA, compared to the reference solution of PBS. This method was thus employed as it allows for a value to be associated with the RI effect unlike some other methods in use[18,24].

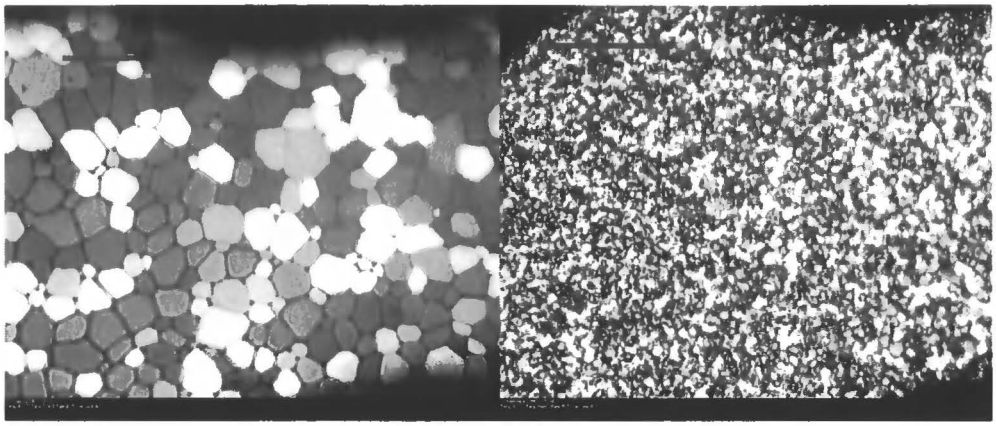

Figure 6. Optical micrographs viewed through crossed polarizers of 'splat' tested PBS (left) and PVA (100k). Scale bar = 500 μm. PVA was 5 mg.mL^{-1} in PBS. Samples annealed at -6°C for 30 minutes.

6.2.1 Influence of Side Chain Functionality on RI Properties

Encouraged by the strong RI activity of PVA we decided to probe the effects of different water soluble side chains along a vinyl derived backbone. The following polymers were used.

Table 2. Vinyl derived polymers used, and their characteristics.

Polymer	Mw[(a)]	Side Chain
Poly(acrylic acid)$_{54}$	5110	-CO_2OH
Poly(ethylamino methacrylate)	20 000	-$C(O)O(CH_2)_2NH_2$
Poly(vinyl alcohol)$_{2625}$	85 -146k	-OH
Poly(vinyl alcohol)$_{205}$	9000	-OH
Poly(vinyl alcohol)$_{80}$	3500	-OH
Poly(ethylene oxide)$_{225}$	10000	N/A (CH_2CH_2O) backbone

(a) M_w according to suppliers specifications

The polymers were chosen to allow the RI properties to be related to the charges on the side chains. PEO allows the influence of polymers without any H-bonding protons to be tested, and is isomeric to PVA. The results of the splat tests for these polymers are summarised in Figure 7.

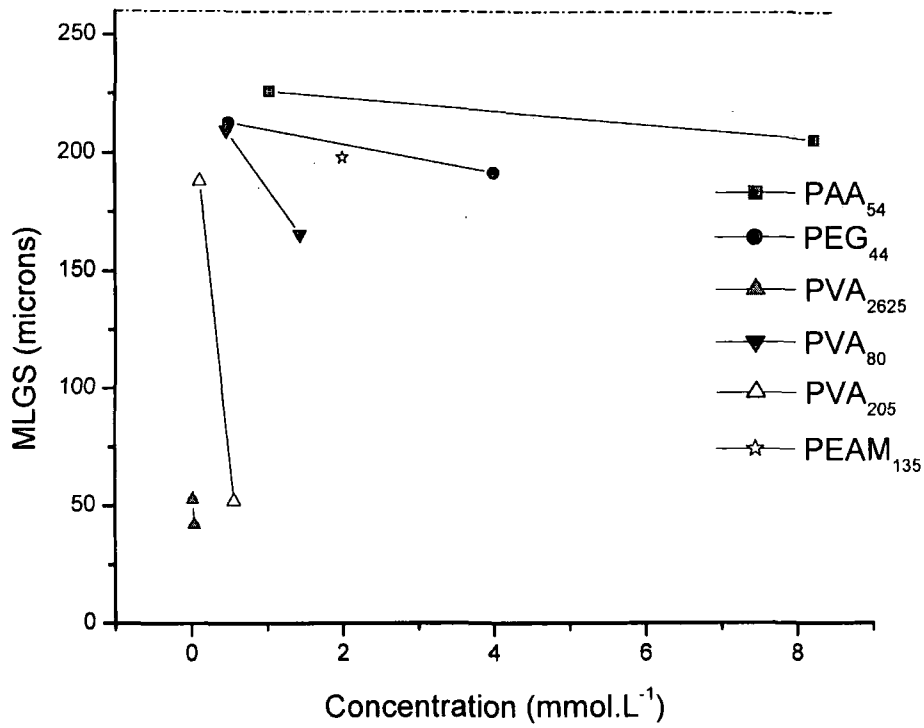

Figure 7. Mean largest grain sizes of various vinyl based polymers at different concentrations. Dashed line represents PBS. PEAM could not be used at higher concentrations due to gel formation.

Figure 7 shows the RI behaviour of the vinyl-based polymers at different chain lengths and concentrations. All three PVA chain lengths which were tested displayed RI behaviour, with PVA_{2625} and PVA_{205} both giving MLGS around 50 microns, which is the limit of detection by this method[§§]. At equal molar concentrations the high molecular weight PVA gave a stronger RI effect (smaller grains).

[§§] The thickness of the wafer generated by the splat test is approximately 50 microns which due to orientation considerations produce the MLGS lower limit.

To investigate the origin of the RI behaviour the polymer mass concentration is normalised to 5mg.mL^{-1}. In this situation the total number of PVA repeat units present is constant, ruling out any non-specific effects. This is plotted in Figure 8.

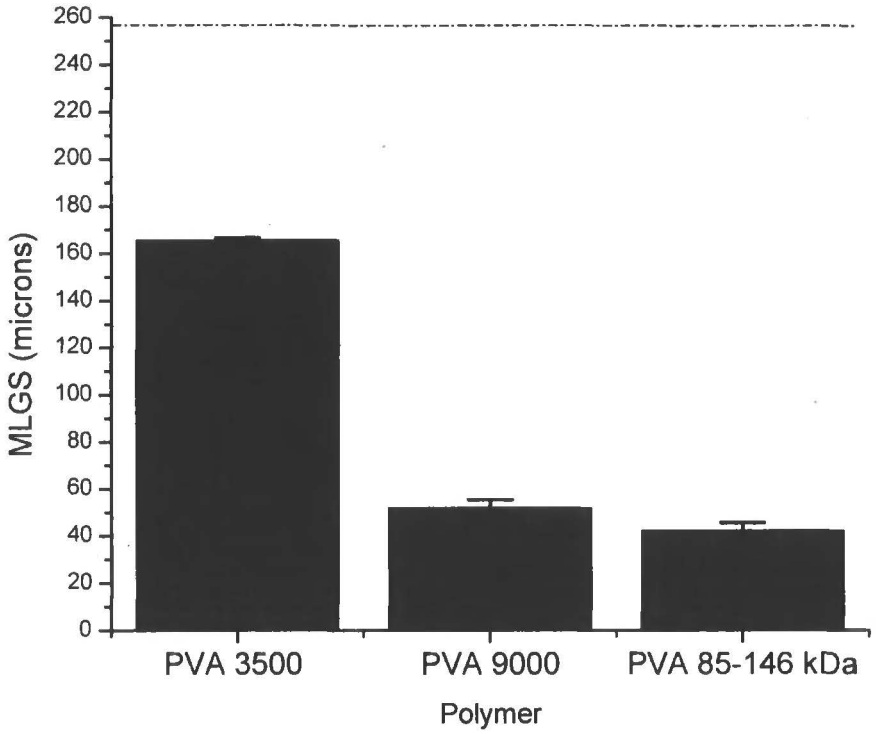

Figure 8. Variation in observed MLGS with chain in molecular weight of PVA, at a constant concentration of 5 mg.mL^{-1}. Dashed line indicates PBS.

A strong correlation between RI activity and molecular weight is observed in Figure 8. By analysing the data this way, it is possible to rule out any false positive results that might occur due to the high concentrations of side chains, when comparing polymers of different molecular weight, but at equal molar concentrations. It is not possible to determine whether the 85-146 kDa polymer can produce a stronger effect at this concentration than the 9000 Da polymer as 50 microns is the smallest size which can be defined in this test. Figure 7 does show that the higher molecular weight polymer retained its activity upon on dilution whereas the 9000 Da

polymer began to loose it. An important issue raised from this analysis is that both molar and mass concentrations should be considered when defining the activity of polymers tested. This is especially true when comparing polymers of different structure, where equal molar concentrations can result in markedly different mass concentrations.

The other polymers tested, PAA, PEAM and PEG all showed a small RI effect, in that they reduce the size of the crystals from 250 microns for PBS to around 200 microns in all cases. This does not appear to be a true RI effect, as PEG has previously been analysed and has been shown to have no activity. Increasing the concentration of PAA to 40 $mg.mL^{-1}$ (data not shown) did not give any significant decrease in the grain size. Importantly, upon dilution there was no large increase in the grain size as would be expected if they were showing RI activity. These effects could be attributed to the increased concentration of solutes in the case of the polymer electrolytes; (which were used as their salts). These observations are important to take into consideration when analysing other polymers, as any of them taken individually would give a false positive (if rather weak) effect.

To investigate the role of solutes on RI a $10mg.mL^{-1}$ solution of 1-*O*-methyl glucoside was analysed. The observed MLGS was 198 μm, a similar value to what was obtained for the polyelectrolytes, suggesting that additive effects due to increased numbers of solutes should be considered during interpretation of any results.

6.2.2 HOMO-POLYPEPTIDE RI PROPERTIES

The polypeptide backbone of native AFGP is likely to play a role in its RI activity, therefore it is prudent to investigate the RI properties of polypeptides with the same (or closely related) side chains as were present in the vinyl polymers, discussed in the previous section. A small range of polymers were synthesised from their corresponding *N*-carboxyanhydrides (Chapter 4). The polymers shown in Table 3 were used for this study.

Table 3. Polypeptide-based polymers used and their molecular characteristics

Polymer	M_n[(a)]	Side Chain
Poly(L-lysine)$_{50}$	7200	-$(CH_2)_4NH_2$
Poly(L-lysine)$_{110}$	14400	-$(CH_2)_4NH_2$
Poly(L-glutamic acid)$_{110}$	15950	-$(CH_2)_2CO_2H$
Poly(L-hydroxyproline)[(b)]	5676[(b)]	-OH

(a) M_w obtained from THF GPC of protected polymers; (b) Value from supplier.

Typical micrographs obtained from each polymer are shown in Figure 9 and the MLGS values are summarised in Figure10.

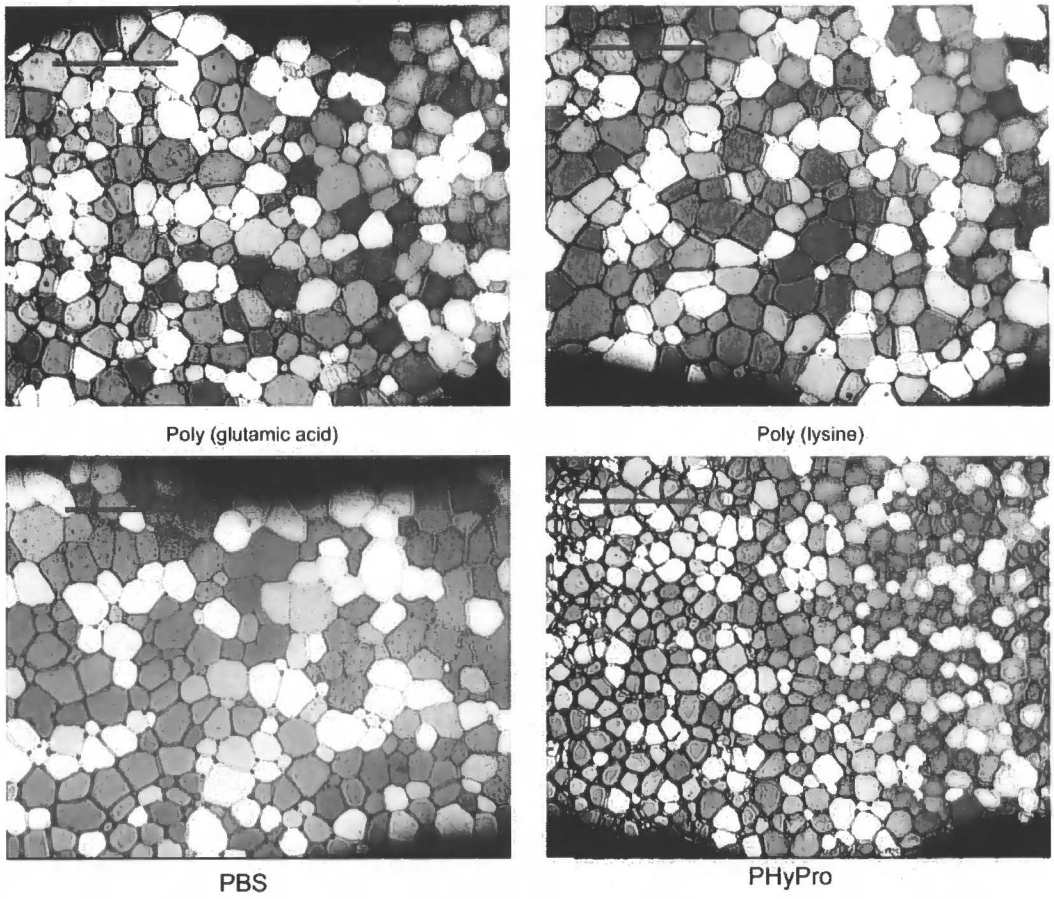

Figure 9. Optical micrographs of frozen polymer solutions at 40 mg.mL^{-1}. Scale bar = 500 µm.

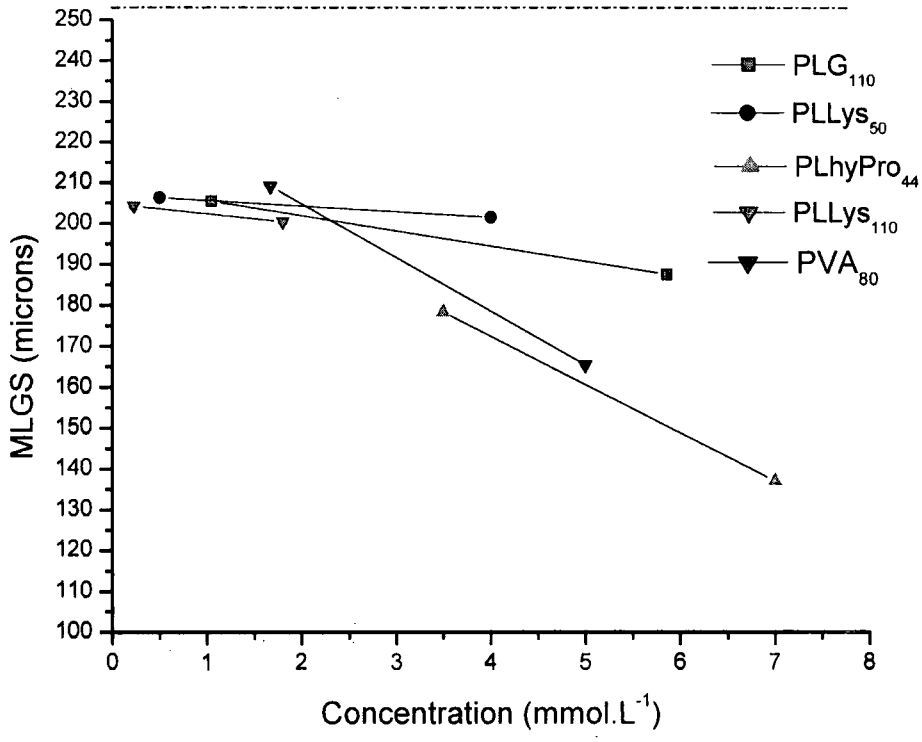

Figure 10. RI inhibition by peptide based polymers. Dashed line indicates PBS control

As for the vinyl polymers, a small RI effect was observed for all the polymers, reducing the MLGS from around 250 μm for PBS to 200 μm. The same reasoning, based upon polyelectrolyte concentration that was discussed in the previous section to explain this behaviour can be applied here. The polypeptides bearing charged side groups did not display any significant RI behaviour, even at concentrations of 40 $mg.mL^{-1}$. Conversely, the relatively low molecular weight poly(hydroxy-proline)$_{44}$ showed a reasonably strong RI effect. The observations confirm the previous results that charged side chains, as the water solublising component, do not result in any RI. Figure 10 also includes the data for PVA_{80} which has a similar molecular weight to the poly(hydroxy-proline) and surprisingly the observed RI activity of the two polymers is very similar. Poly(hydroxy-proline) is expected to have a polyproline

helical[25] secondary structure, but this does not give any significant increase in RI activity relative to the largely unstructured PVA. This is as remarkable as the PVA results; poly(hydroxy-proline) has a structure significantly different from that of native AFGP. The lack of activity for all the charged species proves that a rigid polypeptide backbone of defined primary structure is not an essential component for RI activity, but it may play a role in the increased RI activity of native AFGPs.*** No quantitative study using poly(hydroxyl-proline) has been previously described in the literature.

6.2.3 VINYL DERIVED GLYCOPOLYMER RI PROPERTIES

The strong recrystallisation inhibition observed with the simple polyols encouraged us to investigate whether vinyl derived-glyco polymers would be effective. The increased density of hydroxyl groups should facilitate stronger ice lattice binding, while the activity of PVA shows that a carbon-based backbone presents a sufficiently hydrophobic surface. Two structurally different glycopolymers, of controlled molecular weight, synthesised by aqueous RAFT polymerisation of the appropriate monomer were tested, (see Experimental section for further details).

*** It is again worth noting here that RI activity is distinct from the thermal hysteresis and dynamic ice shaping effects which are also associated with antifreeze proteins. The precise peptide structure and carbohydrate component both appear to be critical for these properties.

Table 4. Molecular characteristics of glycopolymers used in this study.

PMAMGlc			PGalEMA		
	M_n[(a)]	PDI		M_n	PDI
$PMAMGLc_{70}$	18000[(b)]	1.12	$PGalEMA_{50}$	12700[(a)]	1.3
$PMAMGlc_{144}$	37000[(a)]	1.05			
$PMAMGlc_{220}$	56500[(b)]	1.03			
$PMAMGlc_{405}$	10500[(a)]	1.24			

(a) Determined by aqueous GPC using RALS. (b) Determined by DMF GPC using RALS

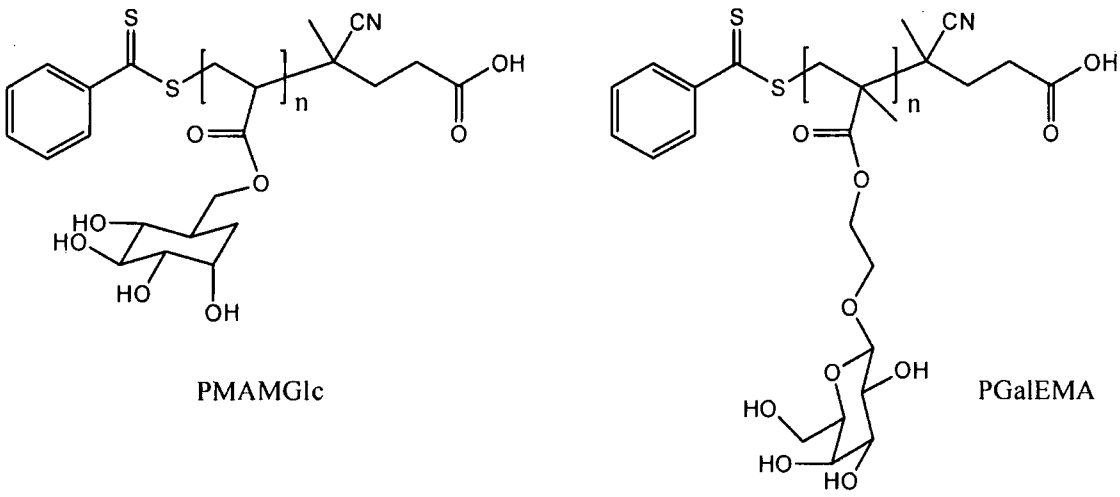

Figure 11. Structures of the glycopolymers tested, including the end groups derived from RAFT polymerisation. PMAMGlc = poly(methyl-6*O*-methacryloyl-α-D-glucopyranoside). PGalEMA = poly((β-D-galactosyloxy)ethyl methacrylate)

For these polymers, a high initial concentration corresponding to 40 $mg.mL^{-1}$ was used to ensure that any effects were as pronounced as possible, avoiding any false negative results arising from weak activity. The micrographs in Figure 12 show a PBS control alongside $PMAMGlc_{220}$ at $40mg.mL^{-1}$. The sample containing the polymer clearly shows a higher population of crystals, and hence a smaller grain size. There are also no single larger crystals in view, compared to the PBS which contains several significantly larger crystals.

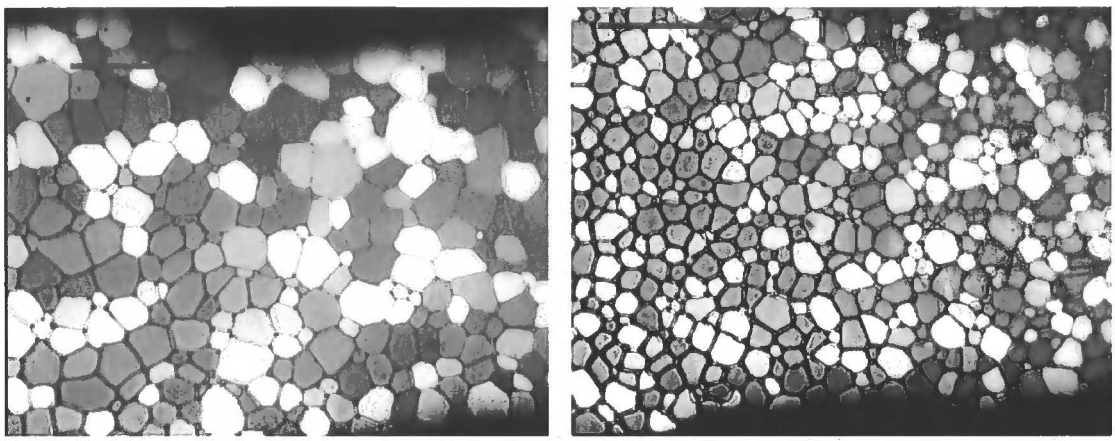

Figure 12. Optical micrograph of PBS (left) and PMAMGlc220 at 40 mg.mL^{-1}. Scale bar represents 500 μm.

To probe this apparent RI effect further different molecular weight glycopolymers were examined and the concentration reduced in a stepwise fashion. This helps determine if the RI effect is real, as it should show a strong dependence on the concentration of polymer.

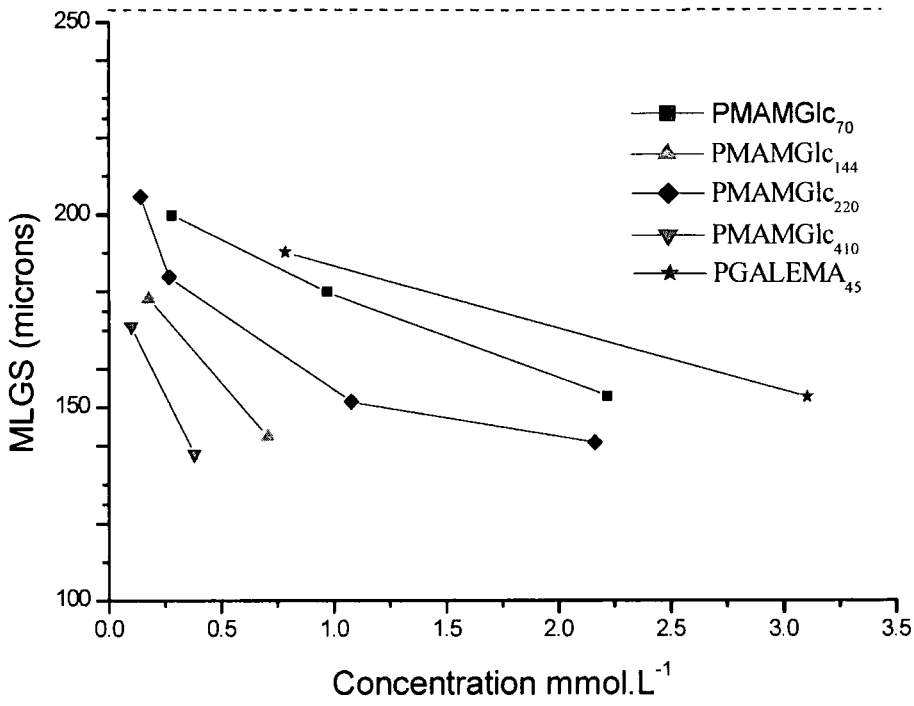

Figure 13. Graph showing the change in MLGS with concentration for the glycopolymers. Dashed line indicates PBS control

The data presented in Figure 13 show a strong correlation between both the concentration of the polymer solution and the molecular weight of the polymer with the observed MLGS. Both low molecular weight polymers ($PMAMGlc_{70}$ and $PGalEMA_{50}$) show similar behaviour suggesting that the stereochemistry of the carbohydrate may not be significant. The observed largest grain size of 138 μm for the most active glyco-polymer, $PMAMGlc_{405}$, at 0.44 $mmol.L^{-1}$ represents stronger activity than was observed for PVA_{80} (M_w = 3500) but weaker than PVA_{200} (M_w = 9000) at similar concentrations. Surprisingly, at the lower concentration of 0.11 $mmol.L^{-1}$, $PMAMGlc_{405}$ retains its (rather weak) RI activity to the same degree as PVA_{80}. It should be noted that the total mass of glycopolymer is far higher than the mass of PVA at equal concentrations. These observations are not due to colligative effects, as demonstrated by the fact that at equal molar concentrations the higher

molecular weight polymers are more active than the lower. It is, however, necessary to explore whether the RI is affected by the total amount of carbohydrate present in the solution: that is to see whether there are additive effects. This is done by comparing the results of the RI assays with polymers of equal mass concentration, rather than equal molar concentration. In this situation, the total number of repeat units is equal, and the effects of polymer chain length can be probed.

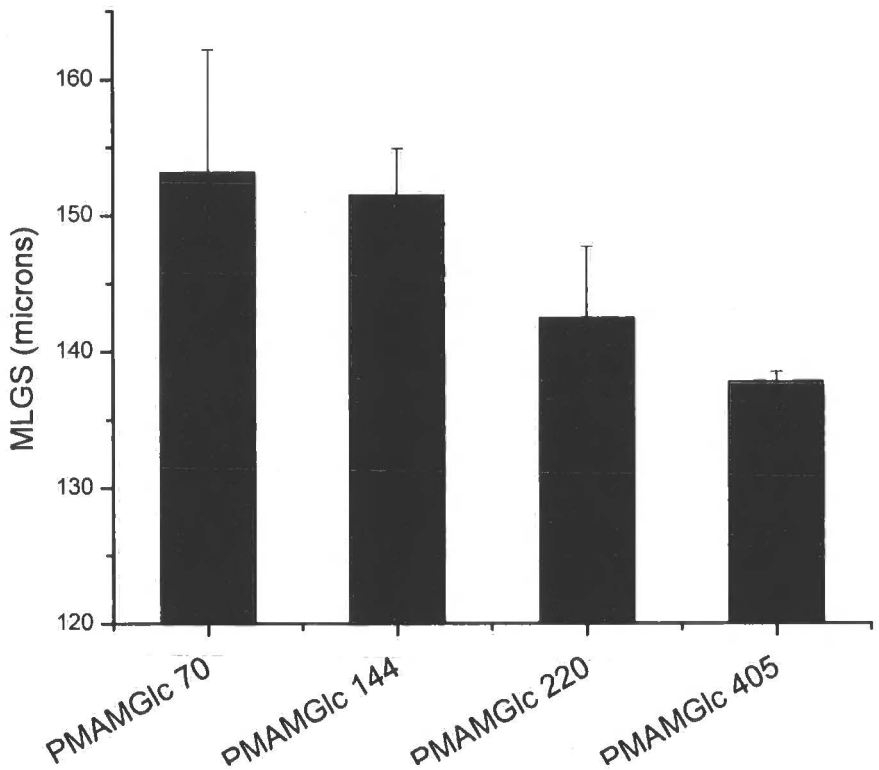

Figure 14. MLGS of PMAMGlc of varying molecular weight at a constant concentration of 40 mg.mL^{-1}. Error bars indicate the standard deviation.

In Figure 14, the results of the RI assay at 40 mg.mL^{-1} are shown, for 4 different molecular weights of PMAMGlc. There is a clear trend towards increasing activity (decreasing grain size) with an increase in the molecular weight of the polymer. As the total carbohydrate concentration is constant throughout this series the increase in activity can be directly attributed to the effect of increased chain length.

This result is remarkable considering the major structural differences between the glycopolymers and native AFGP. The activities which are observed are significantly lower than native AFGP. The smallest fraction, AFGP 8, is more active than these polymers even at concentrations as low as 10^{-3} mmol.L^{-1}.

It has been shown previously that for thermal hysteresis to be present in native AFGP, the hydroxyl groups are an essential feature – oxidation to carboxylic acids results in complete loss of activity[1]. Our results here show that RI activity is also dependent upon hydroxyl groups, rather than other water soluble motifs. An important consequence of this is that, when new glycosylated compounds are being assessed for RI effects the control samples should also contain an alcohol moiety, to determine if it is the backbone or the side chain which is contributing. Taking this into account we can consider the increased activity of PVA relative to our glycopolymers at various chain lengths. We would expect that an increased concentration of –OH groups in the glycopolymer would increase the strength of the ice binding relative to PVA, and consequently increase the RI activity. This is the opposite of what is observed. Previous work by Ben *et al*, indicates that a short distance between polypeptide backbone and the carbohydrate moiety in their AFGP mimics was crucial to maintain RI function. Increasing the separation from 2 CH_2 units to 4 resulted in a complete loss of RI activity. The separation from backbone to –OH in PVA is zero units, whereas in PMAMGlc it is 3 atoms, and in PGalEMA it is 5 atoms. This is shown schematically in Figure 15.

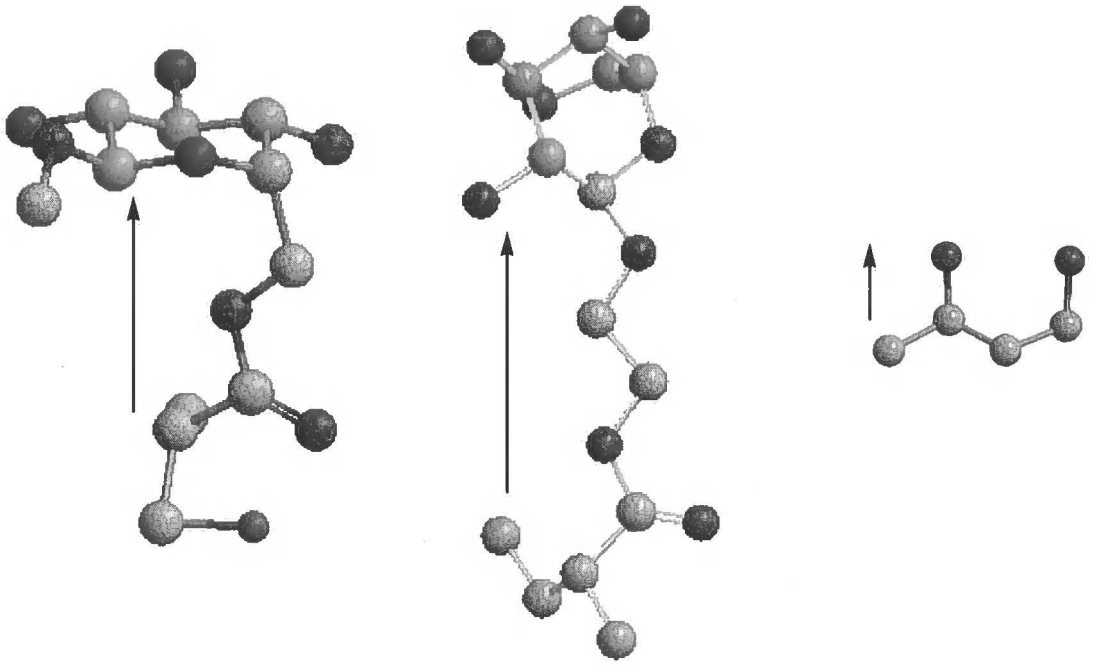

Figure 15. Schematic representation of a repeat unit of three different polymers. The arrows are intended to lead the eye, not represent an actual distance.

The images shown in Figure 5 demonstrate the increased separation from poly(vinyl) backbone to the hydrogen bonding units (OH, or sugar)[†††]. This would explain the reduced RI activity of the glycopolymers relative to PVA when the mode of action is assumed to follow the absorption-inhibition model. The short separation in PVA, would result in the hydrophobic poly(vinyl) backbone being presented close to the advancing ice front causing more effective inhibition. In the cases of the glycopolymers, the long, flexible linker would allow more backbone flexibility to avoid contact with the hydrophilic ice surface and thus effect less efficient inhibition. Comparisons with the conformation of native AFGP is hard, owing to the complex secondary structures assumed by peptides. Many of the AFPs have however been

[†††] The images were generated using Chem3D, as part of the ChemDraw package. Only a fully extended conformation is shown, and is not intended to represent a predicted or experimental conformation. For this reason no estimations of the actual distance have been made, and the arrows are there simply to highlight the point.

shown to present their hydrophilic residues along a single face of their rod-like helical structure, ensuring a large hydrophobic face is presented which gives them their astonishingly strong RI behaviour.

The activity of the glycopolymers was strongly linked to their molecular weight. The high molecular weight polymers (DP = 405) showed the highest activity, which were comparable to that of PVA at similar molar concentrations. This may be due to the increased binding of the polymer to ice relative to PVA by virtue of a higher concentration of hydroxyl groups. The increased binding would limit the freedom of movement of the backbone giving rise to the requisite hydrophobicity and hence RI.

6.3 CONCLUSIONS

This chapter describes the first study to investigate the structural features that are essential for recrystallisation inhibition activity by water soluble polymers. Firstly, the importance of the side chain was demonstrated, showing that hydroxyl groups are essential for any effect to be observed, and also that charged side chains completely negate any RI. The importance of having a rigid (planar amide bond) polypeptide backbone was also investigated and it was demonstrated that poly vinyl backbones are sufficient for the desired effect. During this work poly(hydroxy-proline) was investigated in a quantitative fashion for the first time, and shown to inhibit recrystallisation as well as PVA. A series of glycopolymers bearing either galactosyl or glucosyl moieties were found to have a weak, but significant, RI effect which increased with molecular weight, as found in native AFGP. This result is remarkable in that it is only the second non-peptidic compound, after PVA to display this effect, and the first to contain carbohydrates related to the native variants. By determining which features are essential for conservation of activity, we believe it will be possible to design new materials with stronger RI behaviour, without resorting to tedious and expensive solid phase peptide synthesis.

6.4 EXPERIMENTAL

Poly (L-glutamic acid) sodium salt and poly(L-lysine) HBr salt were synthesised as described in Chapter 3 from their corresponding NCAs. Glycopolymers were synthesised by the aqueous RAFT polymerisation[26] of their corresponding monomers by Mr Seb Spain, or Mr C Barker at the University of Durham. Poly(acrylic acid), poly(ethylene oxide) and poly(vinyl alcohol) were all purchased from Aldrich and dialysed against UHQ water (18 MΩ resistivity)

Phosphate buffered saline was made using pre-formulated tablets (Aldrich). One tablet was dissolved in 200 mL of ultra high quality water (UHQ), 18 MΩ resistively, to give a buffer with pH 7.4. Ice wafers were annealed on a Linkam THMS600 thermostated microscope stage using liquid nitrogen as the coolant. Splat tests were conducted according to the method of Knight *et al*[23]. A 10μL sample of polymer dissolved in PBS was dropped 1.5 metres down a hollow acrylic tube onto a piece of polished aluminium sat on dry ice. Upon hitting the aluminium, a wafer with diameter of approximately 10mm was formed instantaneously. The wafer was transferred using a chilled blade to a glass slide on the Linkam cool stage, and held at -6°C under N_2 for 30 minutes. A photograph was taken of the initial wafer to ensure that a polycrystalline sample had been obtained, and after 30 mintues through crossed polarisers at a resolution of 2 megapixels. ImageJ[27] was used to analyse the obtained images. A large number of the ice crystals (30+) were then measured to find the largest grain dimension. The average of this value from 3 individual wafers was calculated to give the mean largest grain size (MLGS). A schematic of the apparatus is shown below, (Figure 16).

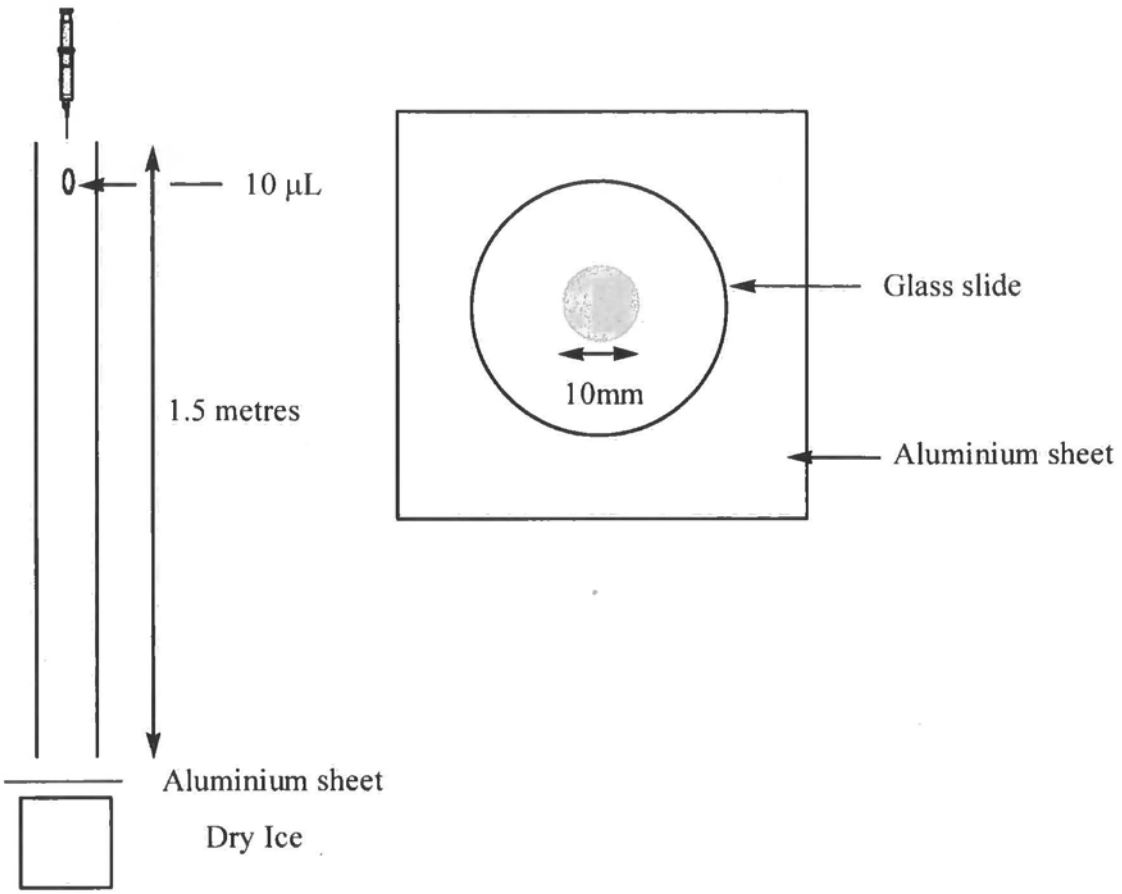

Figure 96. Schematic of the splat test apparatus

6.5 BIBLIOGRAPHIC REFERENCES

(1) Harding, M. M.; Anderberg, P. I.; Haymet, A. D. J. *Eur. J. Biochem.* **2003**, *270*, 1381-1392.

(2) Palasz, A. T.; Mapletoft, R. J. *Biotech. Adv.* **1996**, *14*, 127-149.

(3) Prathalingam, N. S.; Holt, W. V.; Revell, S. G.; Mirczuk, S.; Fleck, R. A.; Watson, P. F. *Theriogenology* **2006**, *66*, 1894-1900.

(4) Bouvet, V.; Ben, R. N. *Cell. Biochem. Biophys.* **2003**, *39*, 133-144.

(5) Inglis, S. R.; Turner, J. J.; Harding, M. M. *Current Protein and Peptide Science* **2006**, *7*, 509-522.

(6) Griffith, M.; Ewart, K. V. *Biotech. Adv.* **1995**, *13*, 375-402.

(7) Crevel, R. W. R.; Fedyk, J. K.; Spurgeon, M. J. *Food. Chem. Tox.* **2002**, *40*, 899-903.

(8) Tachibana, Y.; Fletcher, G. L.; Naoki, F.; Tsuda, S.; Monde, K.; Nishimura, S.-I. *Angew. Chem. Int. Ed* **2004**, *43*, 856-862.

(9) Eniade, A.; Purushotham, M.; Ben, R. N.; Wang, J. B.; Horwath, K. *Cell. Biochem. Biophys.* **2003**, *38*, 115-124.

(10) Eniade, A.; Murphy, A. V.; Landreau, G.; Ben, R. N. *Bioconjugate Chem.* **2001**, *12*, 817-823.

(11) Eniade, A.; Ben, R. N. *Biomacromol.* **2001**, *2*, 557-561.

(12) Ben, R. N.; Eniade, A.; Hauer, L. *Org. Lett.* **1999**, *1*, 1759-1762.

(13) Liu, S.; Ben, R. N. *Org. Lett.* **2005**, *7*, 2385-2388.

(14) Inada, T.; Lu, S.-S. *Crystal Growth and Design* **2003**, *3*, 747-752.

(15) Inada, T.; Lu, S.-S. *Chem. Phys. Lett.* **2004**, *394*, 361-365.

(16) Inada, T.; Modak, P. R. *Chem. Eng. Sci* **2006**, *61*, 3149-3158.

(17) Ewart, K. V.; Lin, Q.; Hew, C. L. *Cell. Mol. Life. Sci.* **1999**, *55*, 271-283.

(18) Yagci, Y. E.; Antonietti, M.; Borner, H. G. *Macromol. Rapid Commum.* **2006**, *27*, 1660-1664.

(19) Mastai, Y.; Rudloff, J.; Colfen, H.; Antonietti, M. *Chem. Phys. Chem* **2002**, *1*, 119-123.

(20) Zhang, W.; Laurson, R. A. *FEBS Letters* **1999**, *455*, 372-376.

(21) Houston, M. E.; Chao, H.; Hodges, R. S.; Sykes, B. D.; Kay, C. M.; Sonnichsen, F. D.; C, L. M.; L, D. P. *J. Biol. Chem.* **1998**, *273*, 11714-11718.

(22) Pudney, P. D. A.; Buckley, S. L.; Sidebottom, C. M.; Twigg, S. N.; M.-P, S.; Holt, C. B.; Roper, D.; Telford, J. H.; McArthur, A. J.; Lillford, P. J. *Arch. Biochem. Biophys.* **2003**, *410*, 238-245.

(23) Knight, C. A.; Hallet, J.; DeVries, A. L. *Cryobiology* **1988**, *25*, 55-60.

(24) Knight, C. A.; DeVries, A. L.; Oolman, L. D. *Nature* **1984**, *308*.

(25) Barrett.G.C; Elmore.D.T *Amino Acids and Peptides*; Cambridge University Press, 1998.

(26) Spain, S. G.; Albertin, L.; Cameron, N. R. *Chem. Commun.* **2006**, 4198-4200.

(27) Rasband, W. S.; Image J Version 1.37 ed.; National Institutes of Health: Bethesda, Maryland, USA, 1997-2006.

7. CONCLUSIONS AND SUMMARY

The objective of this Thesis was the synthesis and characterisation of well defined, novel poly(peptide) based materials, with particular attention paid towards using them to investigate the mechanism of recrystallisation inhibition by polymeric additives. The rationale behind this was discussed in Chapter 1.

In **Chapter 2** a new synthetic strategy was developed for glycosylated *N*-carboxyanhydrides. This involved starting from an *N*-Boc protected amino acid, which was glycosylated in a stereo-specific manner with an activated anomeric bromide. Iodine was used as the promoter in place of the highly toxic mercuric cyanide previously used in the literature. Subsequent deprotection and treatment with triphosgene led to the NCAs in improved yields. The use of an *N*-Boc protecting group expedited the synthesis as the side products were all gaseous and removed quantitatively. This methodology was applied to synthesise 4 different glycoNCAs.

I In **Chapter 3** it was shown that L-threonine(O-benzyl)-*N*-carboxyanhydride can be polymerised in a highly controlled fashion without resorting to organometallic catalysts or extremely controlled polymerisation environments by using the easily dried solvent THF in conjunction with high-purity monomers. The competing activated monomer mechanism was not observed. The effects of the purification procedure on the polymerisation were also investigated. The controlled/living character of this method was shown through kinetic analysis of the polymerisation by offline IR spectroscopy, GPC and the re-initiation of the polymerisation by sequential monomer addition.

Chapter 4 demonstrated the synthesis of block-copoly(peptides) containing poly(*O*-benzyl-L-threonine) and either poly(γ-benzyl-L-glutamate) or poly(ε-*N*-Boc-

L-lysine). This was achieved by polymerisation of the first block followed by addition of the second monomer. Characterisation of the resulting block-co-polymers was achieved by NMR and GPC analysis, which confirmed the structures, and revealed that monomodal distributions were obtained without contamination of homo-polymers.

In **Chapter 5** the thermoreversible organogelation properties of the block-co-poly(peptides) synthesised in Chapter 4 were investigated. The polymers gelated chlorinated solvents, which the homopolymers were soluble in. Analysis of the gels revealed an extended network of fibrous structures ranging in size from 0.3 to 2 microns, which is significantly larger than the size of the individual polymers. The assembly of the fibres was attributed to a change in the conformation of the poly(*O*-benzyl-L-threonine) block from largely unstructured coil to β-sheet upon conjugation to the second (α-helical) block. Wide angle X-ray scattering suggested that this assembly was driven by the lamella stacking of the β-sheets with insulated helices protruding from the structure. These could then act to direct formation of hierarchical structures, which were seen to contain some right-handed helices by AFM.

The ability of numerous water-soluble polymers to inhibit recrystallisation of ice was assessed in **Chapter 6**. Vinyl and poly(peptide) based polymers were investigated and it was observed that only those polymers bearing hydroxyl moieties displayed any recrystallisation inhibition at concentrations as high as 40 mg. ml^{-1}. The strongest inhibitor was shown to be high molecular weight poly(vinyl alcohol). A series of vinyl-based glycopolymers were finally tested. Surprisingly, they showed a small but measurable RI activity which increased with molecular weight. The activity was shown to be lower than PVA and poly(hydroxy-L-proline) of equivalent molecular weight. This demonstrated that it maybe possible to discover new

polymeric ice recrystallisation inhibitors which do not require a rigid peptide backbone by changing the density and distance of the hydroxyl groups from the backbone.

It is hoped that the work began in this Thesis can be applied to develop new and interesting peptide-based materials. The glycosylated NCAs will give rise to glyco(peptides) which may act as mimics of naturally occurring proteins, particularly the antifreeze glycoproteins. These conclusions are drawn from the data showing that simple poly-ols can inhibit ice recrystallisation, when the distance between the backbone and alcohol is minimised. These materials could have widespread application in medicine, organ-preservation, food storage and industrial cooling processes.

The organogelating peptides can also be studied to elucidate the dependence of chain length and composition of the two blocks on the strength of the gels and also upon the self assembled structures which were visualised. Particular interest could be found in determining origins of the conformational changes seen in the poly(*O*-benzyl-L-threonine) block and whether this is limited to helical peptides as the second block or if other, more flexible polymers were also used.

In summary, it is hoped that this body of work does not only contribute significant knowledge to the wider scientific community, but also provoke many more questions leading to further discoveries in the exciting areas of peptide self assembly, polymeric mimics of natural products and fundamental organic synthesis.

PUBLICATIONS AND PRESENTATIONS

Journal articles

- Spain, S. G., Gibson, M. I., Cameron, N. R., *Journal of Polymer Science, Part A: Polymer Chemistry*, **2007**, 45, 2059-2072. "Recent Advances in the Synthesis of Well-Defined Glycopolymers".

- Gibson, M. I., Hunt, G. J., Cameron, N. R., *Organic and Biomolecular Chemistry*, **2007**,. "Improved Synthesis of *O*-Linked, and First Synthesis of *S*-Linked, Carbohydrate Functionalised *N*-Carboxyanhydrides (GlycoNCAs)" **DOI**: 10.1039/b707563d

- Gibson, M. I., Cameron, N. R., "Organogelation of Sheet-Helix Diblock Copolypeptides", *In preparation*

- Gibson, M. I., Cameron, N. R., "Controlled Polymerisation of L-Threonine *N*-Carboxyanhydride, and the Synthesis of Block Copolypeptides", *In preparation*

- Gibson, M. I., Barker, C. A., Cameron, N. R., "Surprising Inhibition of Ice Recrystalisation by Synthetic Glycopolymers: Implications for Antifreeze Glycoprotein Mimetics", *In preparation*

Oral Presentations

- Gibson, M. I., Carbohydrates at the Chemical-Biological Interface, University of Liverpool 20/21 April 2006. "Synthesis and Characterisation of Glycosylated *N*-Carboxyanhydrides"

Poster Presentations

- 6/7 April 2004, Macro Group UK, Young Researchers Meeting; Sheffield University
- 4/9 July 2004, Macro 2004, World Polymer Congress; Paris, France
- 6/7/8 September 2004, UK polymer showcase; Wakefield
- 31 March/1st April 2005, Macro Group UK, Young Researchers Meeting; Sheffield University
- 24th June 2005. Macro Group UK meeting, Symposium for NR Cameron Young Researchers Medal; University of Liverpool
- 5th – 8th July 2005, Materials Chemistry 7 (MC 7), University of Edinburgh
- 5th-7th September 2005, UK polymer showcase; Wakefield
- 6th April 2006, RSC organic group meeting (North East) and Musgrave lecture; Durham University
- 23-28th July 2006, 23rd International Carbohydrate Symposium; Whistler, Canada
- 31st July – 3rd August 2006, Macro Group UK International Conference on Polymer Synthesis; Warwick University

Awards

- 2006 Final Year Postgraduate Presentation award, Department of Chemistry, University of Durham.

- Wiley Interscience Macro award for best poster presentation at Warwick International Conference on Polymer Synthesis, July 2006.